FINAL REPORT

MANNED SPACECRAFT ADVANCED DIGITAL TELEVISION COMPRESSION STUDY

VOLUME 1 TEXT

FOR:

N A S A Manned Spacecraft Center,
Houston, Texas,
Contract NAS 9-3429
26 April 1965

SARASOTA DIVISION EMR

FINAL REPORT

MANNED SPACECRAFT ADVANCED DIGITAL TELEVISION COMPRESSION STUDY

VOLUME 1 TEXT

FOR:

N A S A Manned Spacecraft Center,
Houston, Texas,
Contract NAS 9-3429
26 April 1965

SARASOTA DIVISION EMR

TECHNICAL CONTRIBUTORS

B. C. KING (PROJECT ENGINEER)

J. L. CAIN

J. K. FADELY

J. M. KNIGHT

A. E. PIEPER

G. L. RAGA

TABLE OF CONTENTS

TABLE OF CONTENTS (Cont' d.)

SECTION 1

INTRODUCTION

1.1 GENERAL

The information presented in this report represents the results of a seven-month investigation (combining theoretical and experimental approaches) into advanced digital television techniques having potential application to future manned spacecraft missions. The information is presented in two volumes. Text Volume I incorporates in Sections 2 through 5 the summary results of the various study tasks. Program conclusions and recommendations are given in Sections 6 and 7, respectively, and the detailed results of the study tasks appear in Appendices A through F. Volume II, the photographic volume, includes the pictorial results obtained in several of the supporting experimental areas.

1.2 PROGRAM SCOPE

The central theme throughout this entire program is digital video data compression, and the compression approaches studied assume several diverse forms when applied to different elements within the total television system.

The major program task, identified in the Statement of Work as Task I - Compression Technique Studies, is specifically concerned with the theoretical study and experimental investigation (as required) of four compression techniques having the potential of achieving gross data compressions of six to one relative six-bit PCM video. These techniques are:

- o Frame-to-frame coding
- o Area coding
- o N-dimensional processing
- o Linear-approximation coding

Three additional, related tasks also specified in the Statement of Work have been pursued in parallel with the principal compression study effort. These are:

- o Task II - Digital Communication Channel Analysis

- o Task III - Digital Color Television Investigations
- o Task IV - Digital TV Equipment and System Capability Improvement Studies

Task II is purely an analysis effort, while Tasks III and IV include both analysis and experimental efforts in achieving the study objectives.

Experimental support essential to the success of this overall study program was provided by the almost daily use of the experimental digital television system (EDITS) developed on a company-sponsored program during the past three years. The bulk of the statistical and pictorial data obtained in the Task I compression study area was obtained from the combined EDITS/ASI digital computer system. The design and checkout of the EDITS/ASI interface equipment was accomplished as a company-sponsored effort in direct support of this MSC study program. A description of this support hardware is given in Appendix A.

An additional company-sponsored effort related to the initial design work accomplished on the linear-approximation compression coding system is included in Appendix F in order to make this final report as complete as possible.

1.3 PROGRAM OBJECTIVES

As given in the Statement of Work, the overall objectives of this program have been:

- o To investigate the feasibility (and desirability)[a] of implementing for manned spacecraft applications the advanced digital TV techniques included in the study.
- o To estimate the performance to be expected by employing these techniques.
- o To carry the definition of the most promising techniques through the preliminary logical design stage, where applicable.
- o To recommend future promising courses of development in the above areas.

[a] Not directly stated, but implied.

SECTION 2

SUMMARY OF COMPRESSION-TECHNIQUE STUDIES

2.1 STUDY OBJECTIVE

The primary objective of this study task was to determine a technique which can achieve a gross average data compression of 6 to 1 relative to a 6-bit PCM video source, while producing a subjectively acceptable output picture.

2.2 SCOPE OF OVERALL COMPRESSION STUDY

Four general categories of promising data compression techniques were included in this study. They are:

- o Frame-to-frame coding
- o Area coding
- o N-Dimensional processing
- o Linear approximation

2.3 STUDY APPROACH

The general approach followed in investigating the compression techniques was as follows. First, a mathematical model was formulated for the technique and the average compression was calculated based on the entropy of the model. Next, if compression on the order of 6 to 1 were indicated from this analysis, the particular approach either was simulated directly on EDITS or on the ASI-210 computer (processing stored video frames obtained from EDITS) to obtain actual signal statistics. Then, if the calculated compression values based on these measured statistics approached 6 to 1, the computer simulation program was expanded to permit transmission of the compressed data back to EDITS for photographic recording, and subsequent subjective image evaluation.

2.4 INDIVIDUAL STUDY TASK SUMMARIES

2.4.1 Frame-to-Frame Coding

Scope

Three approaches to frame-to-frame coding were considered. These are:

Frame-difference coding (FDC)

Zero-difference frame coding (ZDFC)

Intraframe difference coding (IFDC)

Frame-Difference-Coding Study

In this technique, successive frames are compared and the amplitude and position data are transmitted to identify only those elements which do not have the same amplitude as the corresponding elements in the previous frame.

From the mathematical model derived for this coding method, it was determined that for 4-bit video encoding, 96.6% of the corresponding elements on successive frames must be identical in order to achieve a 6 to 1 gross average compression. Assuming no image movement, the corruptive effect of sensor noise alone was sufficient to require a 55-db video signal-to-noise ratio in order to maintain the required element redundancy. Therefore, due to excessively high sensor signal-to noise requirements plus the equally restrictive limitation on allowable image movement between frames, this technique was ruled out.

Zero-Difference Frame-Coding Study

In this method, successive frames are compared and a single, unique code word is transmitted if the two frames are identical.

The same limitations discussed in connection with the FDC approach apply here also (to an even greater degree since identical frames are being sought). Based on the mathematical model derived for the ZDFC method, if 100 consecutive 4-bit video frames are considered (of 256-line resolution), 83% of the frames must be identical in order to achieve a 6 to 1 compression. This assumes a unique code word of 60 bits. Therefore, based on these factors, this technique was eliminated from further consideration.

Intraframe-Difference-Coding Study

This approach combines a technique which achieves data compression within each given frame with the ZDFC method in an attempt to reduce the requirement on identical frames to a more manageable number. The intraframe compression was assumed to be 2 to 1; then, from the mathematical model it was found that 68 out of 100 successive frames (selected as a basis for the calculation) still must be identical to achieve a 6 to 1 compression. Therefore, this approach was similarly ruled out.

Conclusion

Frame-to-frame coding techniques do not meet the 6-to-1 compression goal due to the large amount of redundancy required between successive frames and to the impractibility of achieving this redundancy with operational TV systems.

2.4.2 Area Coding

Scope

Four coding methods, which utilize both horizontal and vertical correlation within a TV frame, were included in this study; each is an extension of the previous method. They are:

Flat Area Coding (FAC)

Huffman Area Coding (HAC)

Area Coding with Previous-Element Coding (ACPE'C)

Previous-Area Coding (PAC)

In addition, an area-coding computer simulation was performed to provide the necessary area-statistic data to permit calculation of FAC compression values.

Description of Area-Coding Techniques

In the FAC method, a video frame encoded to B bits per element is effectively divided into subrasters which are sequentially scanned. If all the elements in a given subraster area are of equal intensity, this area is encoded with (B + 1) bits. If any element within a given area is different, each element is encoded with (B + 1) bits. This assignment of the same number of bits to each event is known as flat coding.

The HAC method was studied as a possible means of increasing compression by efficiently encoding the area blocks corresponding to each quantizing level based on their probability of occurrence within a TV frame.

The ACPE'C method extends the efficient encoding concept to include those elements which are not within area blocks but do qualify as previous elements (PE's).

The PAC method further extends the efficient encoding concept to include adjacent area blocks which are of the same intensity by applying the previous element (PE) concept to previous (similar and adjacent) areas.

Selection of Best Area-Coding Techniques

Although the latter three efficient coding methods potentially offer some increase in compression relative to the FAC approach, the FAC approach was selected for more detailed study since it represents the best compromise between compression and implementation complexity.

Computer Simulation of FAC

A computer program based on the FAC technique was prepared and implemented in order to analyze selected frames of video data generated by EDITS. By means of this program, it is possible to determine the number of 2 x 2[a], 3 x 3, 4 x 4, or 5 x 5 area blocks in a given frame and from this, calculate the FAC compression.

Due primarily to the disorganizing effects of sensor noise, compression of video data encoded to 6 bits is quite low (an average of about 1.5 to 1). However, compression of 4-bit data is considerably greater. A compression ratio of 5 to 1 is obtained by encoding 5 x 5 size area blocks of 4-bit data representing a relatively low detail scene. Similar encoding of a higher detail scene produces a compression of 3.5 to 1 (both of these ratios are relative to 6-bit PCM video. If they are made relative to 4-bit PCM, there is a corresponding reduction in compression values).

Conclusions

Area coding, as typified by FAC, does not meet the 6-to-1 compression goal set for this study. However, for some applications it has a compression potential in excess of previously studied techniques.[b] Also, it is an information-preserving method, which may be of importance for certain applications.

2.4.3 N-Dimensional Processing

Scope

Three processing techniques having data compression potential were investigated in the study phase. They are:

Two-dimensional optical processing

One-dimensional digital processing

One-dimensional analog processing

---

[a] Two scan elements wide by two scan elements high

[b] Such as delta modulation, Roberts coding, PE coding, and run-length coding

The optical method is applied to the visual image in advance of the TV sensor, the digital method is applied to the video signal following analog-to-digital encoding, and the analog method is applied between the sensor and the analog-to-digital encoder.

Two-Dimensional Optical Processing

Two optical spatial filtering methods were analyzed, namely, the coherent illumination method and the incoherent illumination method. The objective of these analyses was to determine whether or not spatial filtering applied to the optical image could effect significant compressions, either independently or in conjunction with other compression techniques.

It was determined that sets of filters (for the coherent and incoherent cases) can be synthesized to provide a theoretical increase in data redundancy and thereby increase the effectiveness of certain other compression methods. However, practical considerations severely limit the effectiveness of the filtering process in a conventional television system. Here, sensor noise effects establish the upper limit on signal redundancy, virtually independently of the optical filtering action. For this reason, optical processing was ruled out as a potential compression technique for spacecraft video transmission.

One-Dimensional Digital Processing

For purposes of this study, digital processing assumes the specialized form of a technique identified as previous-element qualification and of an associated item of hardware, known as the Previous Element Qualifier (PEQ) unit. This equipment was developed and integrated into EDITS during this study program. The PEQ unit essentially performs a "noise-cleaning" function on the digital video output from the analog-to-digital encoder. This is accomplished by initially comparing the value of successive elements i and i + 1. If they are equal, i + 1 is identified and coded as a previous element (PE). If they are not equal, the value of element 1 + 2 is compared with the (stored) value of i. If i + 2 and i are equal, i + 1 is qualified as a PE. That is, it is assumed that the i + 1 value has been corrupted by noise. If i + 2 and i are not equal, the actual value of i + 1 is transmitted.

The PEQ action has the effect of increasing the signal redundancy, and thus the PE count, for a given video signal-to-noise ratio. It is not in itself a compression technique; however, when used in conjunction with a compression method, the resultant data compression is increased with negligible subjective degradation in picture quality attributable to the PEQ process. The percentage of increase in compression is a function of the operating video signal-to-noise ratio and the compression coding method employed. As one example, with PEC/Huffman 4-bit coding at 30 to 40-db signal-to-noise ratios, an average compression increase of 35 to 40% was obtained.

One-Dimensional Analog Processing

The simplest form of one-dimensional analog processing applied to a television system is a low-pass filter which is inserted immediately after the sensor. This filter acts to attenuate the higher-frequency video signal components including the sensor noise components, providing increased signal redundancy. Of course, this desired effect is accompanied by an undesired image "softening" effect.

The initial objective of this study task was to evaluate the trade-off between the above factors for a digital TV system. After additional study, however, it became evident that a pure digital TV system of the type represented by EDITS places certain restrictions on the application of low-pass filtering applied to the sensor output signal. This is due to the pulse-type nature of the sensor signal which results from the digital scanning process. Through previous analysis, it had been determined that there is an optimum video bandwidth related to the digital type video signal which provides a maximum video signal-to-noise ratio; this bandwidth is designed into EDITS. Thus, placement of a separate low-pass filter, to provide additional signal redundancy, is limited to the point in the system between the output of the sample-and-hold circuit and the input to the analog-to-digital converter.

A series of measurements were performed with this particular filter placement. Filter cutoff frequency was decreased in step fashion from the nominal video baseband frequency down to approximately 1/10 this value. The resulting increases in PE probability and decreases in subjective image quality were recorded and compared with similar measurements made with the PEQ system. This comparison showed that at higher video signal-to-noise ratios, PEQ is a more effective and desirable method and provides greater increases in PE than the specialized one-dimension analog filtering method for equivalent image qualities. At video signal-to-noise ratios nearer 20 db, the analog filtering method is judged superior to PEQ on the basis of slightly better picture quality (due to a more general softening of visible picture noise) for equal PE's.

Conclusions

None of the N-dimensional processing methods provides an independent data-compression capability.

Due to sensor noise-corrupting effects, optical filtering is not considered a promising supplementary compression technique.

One-dimensional analog processing has very limited usefulness for the pure digital TV application, due to restrictions placed on the location of the filter.

One-dimensional digital processing (1-DQ) shows promise of being an effective supplement to a primary compression method to provide increased data compression.

2.4.4 Linear Approximation

Scope

This study task encompassed the following areas of investigation:

A preliminary ASI-210 computer simulation of linear approximation applied to selected, single, video scan lines (with manual computation of the video data points and subsequent insertion into the computer).

An expanded and highly flexible ASI-210 computer simulation of linear approximation applied to entire frames of selected video data transmitted from EDITS. This included the capability for transmitting compressed video frames back to EDITS for photorecording and subsequent image analysis.

A format design analysis for linear approximation involving the determination of the optimum data coding and synchronization coding formats for a practical system.

Linear-Approximation Concept

This method operates on the principle of approximating the video waveform, corresponding to each TV scan line, with straight-line segments. The instantaneous amplitudes of these segments may deviate from the true values of the corresponding scanned elements to the degree allowed by the established error criteria. The basic information required to encode the data in this manner consists of the amplitudes and raster coordinates of the intersections (or vertices) of the line segments.

With this process, all waveform slopes may be encoded, as opposed to run-length coding methods (and variations thereof), which are restricted to the single, zero-slope-approximation condition. Thus, the large compression potential of linear approximation results from its ability to approximate all waveform slopes with straight line segments and to encode the segment identification data in an efficient manner for purposes of transmission.

Linear-Approximation Computer Simulation

Based on very encouraging results obtained in the initial computer program in which single video lines were processed, the expanded simulation program was designed and implemented to obtain full-frame compression and pictorial results. Considerable flexibility was provided in the choice of system parameters; namely:

Error band--Adjustable from ±1 to ±64 levels out of a possible 64 levels.

Errors outside the error band--Provision made to allow 0, 1, or 2 consecutive errors before terminating the line segment.

Truncation length--Adjustable in length to 16, 32, and 64 scan elements.

Four test objects, two representing fairly low-detail material and two representing fairly high-detail material, were selected for these measurements. The initial purpose of the simulation was to obtain compression values over a wide range of parameter combinations. This permitted the selection of the best parameter combinations from the standpoint of compression. Then, these selected compressed-video frames were transmitted to EDITS and pictures were recorded for subjective assessment purposes.

In summary, the computer simulation results show that subjectively acceptable pictures with average compressions of 6 to 1 are obtainable with linear approximation on the lower detail test scenes, and compressions of 4 to 1 are obtainable on the higher detail test scenes.

Format Design for Linear Approximation

This analysis was concerned with the selection of an optimum error-correction code which can be combined with the linear approximation data words to achieve an acceptably low error probability in the presence of expected levels of communication channel noise. The analysis further was concerned with the selection of strong horizontal and vertical synchronization words which would enable the system to achieve and maintain synchronization at bit error probabilities which produce significant degradation in data word accuracy and thus in picture fidelity (to assure that synchronization stability does not limit system performance).

Assuming a 256-line-resolution frame, the linear-approximation data segments of 16-elements maximum length can be defined by a 6-bit code representing the vertex amplitude plus an 8-bit code representing the absolute position of the vertex (a total of 14 bits). Alternatively, a 10-bit code word can be employed in which 6 bits still represent the amplitude, but only 4 bits are required to denote Δx, the number of elements between vertices. Both of these methods are subject to considerable error in the presence of channel noise; however, the 10-bit data code permits the errors along a line to propagate and thus is more susceptible to degradation.

By using an error-correcting code to transmit these data bits, a significant improvement in error probability can be achieved. This study shows that the Hamming (14, 10) error-correcting code is one of the shortest suitable for this purpose of transmitting the linear-approximation data bits. In this case, the data word consists of the 10 bits as described above, and the additional 4 bits are check bits which will provide correction of all single errors in transmission. Of the data formats investigated, the Hamming (14, 10) code was selected on the basis of achieving the highest net compression[a] for the linear approximation system. With the criterion

a Compared with other linear approximation data-transmission methods considered, it requires the minimum transmitter power to satisfy a given data error criterion.

of one scan line per frame in error, the selected Hamming code permits transmission at a bit-error probability of 1.5×10^{-3}.

Linear approximation synchronization presents certain unique problems due to the variable number of data words (representing segments) which may occur within a scan line and within a complete frame. For this reason, the normal PCM check and lock mode strategies cannot be employed. The selected linear-approximation synchronization scheme employs a 42-bit synchronization code pattern at the end of each scan line and at the end of each frame of video. The probability of achieving line and frame synchronization during the first received line and frame, respectively, is calculated to be 0.99991 under search-mode operation. Even higher probabilities result in the lock-mode operation.

Conclusions

Linear-approximation coding has the demonstrated capability of achieving gross average data compression of 6 to 1 on certain representative classes of test subjects, thus satisfying the original compression goal established for the overall study. Effective error correction is bought at the expense of some decrease in compression. Using the Hamming (14, 10) code, the gross compression must be divided by a factor of 1.4 to arrive at the net average compression. Therefore, for a 6 to 1 gross compression the resulting net compression is 4.3 to 1.

SECTION 3

SUMMARY OF DIGITAL COMMUNICATION CHANNEL ANALYSIS

3.1 STUDY OBJECTIVE

The objective of this portion of the program was to investigate the properties of modulation systems with respect to utilizing them with particular compressed digital TV techniques to optimize overall system performance.

3.2 STUDY SCOPE

The study scope included a survey of existing digital binary, N-ary, and hybrid systems; consideration of rf bandwidth-reduction techniques to determine if some customized variant of the above modulation methods would permit the transmission of four bits per cycle of bandwidth occupancy; and a general parametric study of digital modulation methods.

3.3 STUDY APPROACH

A survey and analysis of some 40 digital modulation papers and two books was conducted, with 20 of the papers being selected as sufficiently representative of the field for inclusion in an annotated table included in Appendix C. These papers encompass 24 identifiable modulation systems. Most of the papers expressed modulation performance on the basis of bit-error probability versus signal-to-noise ratio, or more precisely, signal-energy-per-bit to noise-spectral-density ratio. The question of bandwidth occupancy was left largely untouched, most analyses implicitly assuming a transmitted spectra determined by the transmission of ideal pulses. For those papers which did supply information relating bits per cycle versus signal-to-noise ratio, the information was plotted with C/W as a function of S/N. This plot gives a general feel for the "possible" as compared with the Shannon ideal for several systems.

As the survey progressed it became evident that there exists many practical constraints imposed largely by the channel, such as nongaussian impulse noise and differential delay distortion, which render impossible a good choice of modulation method based solely on a set of design curves relating bits per cycle to signal-to-noise ratio. Also, several of the referenced papers contain generalized modulation-comparison charts. Accordingly, no further effort was devoted to producing a set of "generalized" design curves. The remainder of effort was spent on devising and calculating the bit-error performance of a rather specific four-bit-per-cycle MODEM.

The four-bit-per-cycle MODEM decided upon employs four-level, coherently detected, amplitude-shift keying (ASK) simultaneously on two-phase orthogonal carriers. This choice yields 16 signal states (four bits) per signaling interval, and a derivation in Appendix C shows a bandwidth occupancy (also defined) of one cycle per signaling interval. Thus, the goal of four bits per cycle is attained. It is also explained in Appendix C why this system is preferred to coherent ASK single sideband, which also theoretically has the same four-bit per cycle capability.

The particular choice of four bits per cycle was based upon two facts: that analog TV transmission packs two analog picture elements per cycle using incoherently detected AM vestigial side-band modulation, and that digital compression systems are available which can send one picture element for an average cost of two bits. Thus, a digital TV system employing compression to two bits per picture element and a MODEM packing four bits per cycle would occupy a bandwidth no wider than that occupied by an equivalent analog TV system. Even with these constraints, it was expected that the compressed digital TV system would offer a significant power saving over the analog system.

3.4 CONCLUSIONS

The conclusions of this section are that it is possible to fit a compressed digital TV signal into an equivalent analog bandwidth at a 10-db power saving; that such a system will require a signal-to-noise ratio of approximately 20 db; and that such a MODEM, operating at four bits per cycle, is feasible.

SECTION 4

SUMMARY OF DIGITAL COLOR-TELEVISION INVESTIGATIONS

4.1 STUDY OBJECTIVES

The objectives of this study task were (1) to investigate color TV methods applicable to digital TV processing, with particular emphasis on achieving compression of the digital color data, and (2) to select and define the most promising color TV approaches for satisfying future MSC requirements.

4.2 STUDY SCOPE

This investigation was divided into two principal task areas, namely, (1) the study effort and (2) the experimental color TV support effort. The study effort included the following subtasks:

- o The study of basic colorimetry as related to color television.
- o The review of past and present color television techniques.
- o The determination of probable MSC color television functions and typical operating parameters.
- o The determination of ground rules for the application of color TV to MSC missions.
- o The selection and definition of the most promising system approaches for satisfying MSC requirements.

The experimental support effort included the following subtasks:

- o Modification of the EDITS system for color reproduction.
- o Preliminary full-color frame-sequential recording and subsequent color picture assessment.
- o Gamma measurement and adjustment
- o Final color reproduction and fidelity assessment
- o Measurement of primary color signal statistics and compression potential

4.3 COLOR TV STUDY RESULTS

Early in the program, based on a review of various references dealing with the colorimetric [a] aspects of color TV, the decision was made to restrict this study to the investigation of the three-primary (red, green, and blue, qualitatively speaking,) color TV system category. The two-color systems were ruled out on the basis of having too restrictive a gamut of reproducible colors.

The analog systems of interest in this study transmit the three colorimetric properties of the scene (hue, saturation, and brightness) [b] in one of three ways: (1) by simultaneous transmission of the R, G, and B signals, or linear transformations of these signals (as is done in the U.S. commercial broadcast NTSC system; (2) by sequential transmission of the R, G, and B signals; or (3) by a combination of the above methods, herein termed simultaneous/-sequential (or hybrid) transmission.

The basic characteristics of the various systems(both past and present) included in these categories were studied to gain an understanding of the advantages and disadvantages of each system in the primary application for which it was designed. Since the majority of color television development effort has centered around commercial broadcast usage, the overriding, common operational restriction was found to be the "monochrome TV compatibility" requirement. In every case, the adherence to monochrome TV scanning standards and rf-channel bandwidth allocations has resulted in some moderate-to-serious compromises in system performance during less-than-optimum transmission conditions.

Based on a review of available literature dealing with the anticipated image data-transmission requirements for future NASA orbiting research laboratory programs, two probable color-TV functions evolved. These are (1) real-time biomedical monitoring (typically a 300 TV line, 10-to-15 frame per-second system), and (2) non-real-time, or single-frame, image data transmission (typically 500 TV lines resolution) for the transmission of high-definition, full-color pictorial data of a static nature.

Concurrently with this literature survey, ground rules were established relating to the application of color TV systems (including digital color versions) to MSC missions. The key factor in this ground-rule listing was the elimination of the "monochrome TV compatibility" requirement for spacecraft color-TV systems.

By applying this extra degree of freedom to the present analog color-TV system designs, the developmental French SECAM (hybrid-type) system, with modifi-

---

[a] Colorimetry is defined as the science of measurement and specification of color.

[b] Hue and saturation collectively are termed "chrominance."

cations,[a] was determined to be the best choice for the real-time monitoring function. A digital version of the SECAM system also was studied, and--although offering high-quality performance--was rated second to the modified analog SECAM method because of its greater complexity.

Although the non-real-time function could be accomplished by use of the SECAM system, a significantly simpler approach would be to use a frame-sequential color-TV system, (If the real-time system were already in the spacecraft and available and if transmission bandwidth were not a serious consideration, then this simplicity factor may not be valid.) The simplicity advantage of this method is a result of the R, G, B primary-color sampling method employed. Due to the low sample rate involved, a rotating, R, G, B filter disc accomplishes the color switching, and only a single TV camera (and a single TV display with a similar synchronized disc) is required for full-color singal generation. This compares with a minimum of three TV cameras required for the SECAM system with its significantly greater equipment complexity, weight, size, and power requirements. The choice of digital or analog implementation for the frame-sequential method revolved around a question of the required fidelity of the received color data. Since the R, G, and B frames each carry high-resolution luminance data in addition to the lower-acuity chrominance data, it is essential to maintain precise color image registration on the receiver display. This implies extremely accurate time-base stability for each of the sequential color frames. A properly designed digital TV system inherently provides excellent time-base stability, independently of spacecraft or ground video recorder instabilities, on an element-to-element as well as line-to-line and frame-to-frame basis; therefore, the frame-sequential digital method was selected for the second function.

4.4 COLOR TV EXPERIMENTAL SUPPORT EFFORT

All of the experimental, color TV work was accomplished on EDITS, which was suitably modified to reproduce full-color, digital frame-sequential recordings. The color-recording medium employed Polarcolor film, due primarily to its rapid (60-second) development time. In these particular recordings, sequential R, G, B color sampling was accomplished manually. This involved placing pairs of Kodak Wratten type R, G, B color separation filters (in turn) in front of the TV camera and the film camera, having previously established the correct color balance for the camera/illumination source combination and

[a]The principal modification involves moving the chrominance FM subcarrier well outside the luminance passband to eliminate crossmodulation of the luminance and chrominance signals and to permit transmission of full-amplitude chrominance data to improve the signal-to-noise performance of the chrominance channel.

for the TV display/Polarcolor film combination by adjusting the relative R, G, and B exposure values.

Following an initial series of test reproductions, refinements were made in the equipment set-up and operating procedures to achieve a reasonable dynamic recording range and accurate registration of the sequential images. Then, two series of final color reproductions were made of two test objects covering a reasonably wide range of pictorial characteristics in terms of the image detail and chrominance values represented. Digital coding methods included in these series were: 6-bit PCM, 4-bit PCM, 3-bit PCM, 3/4 Roberts coding, and 2-bit delta modulation.

Relative to image fidelity assessment, the 6-bit PCM renditions are the best, and they were used as standards of comparison in both series. Four-bit PCM fidelity was judged almost equivalent to 6 bit.[a] The 3-bit photographs exhibit the effects of coarse quantization, producing brightness contouring and chrominance errors. The 3/4 Roberts coding method does a very effective job of eliminating the basic 3-bit quantization errors at the expense of a moderate increase in fine-grain noise. The 2-bit delta reproductions appear generally "softer" than the other renditions, due to its limited step function response. Also, delta produces a very objectionable hue error following dark-to-light transitions. This effect, also attributable to limited step-function response, shows up as a smear following such transitions.

The final color-TV experimental task involved the measurement of previous element (PE) statistics on frames of R, G, and B video data. Statistics were taken on video signals produced with 6-bit PCM, 4-bit PCM, 3-bit PCM, and 3/4 Roberts coding, and at video signal-to-noise ratios of 40 db, 30 db, and 20 db.

From these measurements it was determined that in the general case, PE statistics are only secondarily influenced by the variations in image content among the R, G, and B frames. The controlling factor on PE statistics is sensor noise. Based on these measurements, it was calculated that previous element coding (PEC) of 3/4 Roberts signals would result in a maximum gross compression of 3 to 1 relative to 6-bit PCM. Since the basic 3/4 Roberts system provides a net compression of 2 to 1, it is doubtful that PEC coding could be justified because of the additional complexity involved.

[a]The brightness contouring normally expected on 4-bit pictures was almost nonexistent. This is due to the sequential R, G, B recording process, which effectively increases the number of quantizing levels to well above the 16 observed on a single-color recording.

4.5 CONCLUSIONS

- The modified analog SECAM system best satisfies the requirements established for a real-time color-TV system.

- The digital frame-sequential system best satisfies the requirements established for a non-real-time color-TV system.

- 3/4 Roberts coding, providing a 2 to 1 net compression relative to 6-bit PCM, is the best choice for a compression-coding technique to be applied to the digital frame-sequential system.

- For equal values of frame-sequential data compression, PCM and its derivatives are superior to delta modulation in terms of reproduced image fidelities.

SECTION 5

SUMMARY OF DIGITAL TV EQUIPMENT AND SYSTEM CAPABILITY IMPROVEMENT STUDIES

5.1 STUDY OBJECTIVE

The principal objective of this task was to study and recommend components and equipment design techniques suitable for use on future high-performance MSC television systems.

5.2 STUDY SCOPE

Four subtask areas were included in this section--

- Investigation of the operational aspects of monochrome digital TV for MSC application
- Investigation of digital television sensor requirements
- Investigation of digital television scanning techniques
- Development of a high-speed Roberts coding simulator

5.3 INDIVIDUAL STUDY-TASK SUMMARIES

5.3.1 Operational Aspects of Monochrome Digital TV for MSC Applications

A survey of the available literature dealing with anticipated monochrome television operation and equipment requirements for future MSC missions served as the primary basis of this study task. From this survey, it was determined that spacecraft television for initial NASA Orbiting Research Laboratory missions can be grouped into two categories; (1) transmission-type TV, primarily used for remote, real-time, frame dual monitoring and behavioral assessment purposes; and (2) closed-circuit TV, used for various monitoring functions in and about the spacecraft.

The unique operational characteristics noted with respect to the transmission-type system is the wide variation in minimum acceptable TV resolutions specified for the various monitoring functions. While a certain test may call for a resolution of 500 TV lines, another function may be adequately monitored at one-third this resolution or less. For constant-frame rates (nominally 10 to 15 per second), this represents approximately a 10-to-1 variation in required transmitted data rate, and this probably is not the lowest acceptable limit.

Where transmission efficiency is a significant factor, such as on projected ORL missions of long duration, digital TV can serve an important role. The equipment can be readily designed to incorporate a large degree of operational flexibility (in terms of resolutions, frame rates, and quantizations). In order to realize this potential increase in system efficiency, the transmission link also must incorporate operational flexibility. If the receiver bandwidth is optimized for each data rate, a reduction in data rate will permit a corresponding reduction in transmitter power to maintain a fixed receiver signal-to-noise.

It was concluded, therefore, that digital TV equipment can fulfill an important function in future MSC missions where equipment operating flexibility combined with high data accuracy and high operational stability are important considerations.

5.3.2 Digital Television Sensor Investigation

At the outset of this study program, it was believed that a pure digital TV system, such as EDITS, might impose unique requirements on TV sensors due to the digitally indexed nature of the scans employed. However, based on the results of digital scanning studies performed during this program (and discussed in paragraph 5.3.3), it was concluded that digital TV equipment designs are not restricted to a particular class of TV sensors (such as electrostatic deflection types). Instead, digital TV sensor selection will be based on the same operational and physical requirements and constraints which apply to analog TV equipment.

5.3.3 Digital TV Sensor Scanning Investigation

This task was made up of two parts; first the experimental investigation of methods to improve the performance of the all-electrostatic vidicons used in EDITS, and second, the study of important magnetic deflection circuit parameters applicable to digital TV equipment.

In the electrostatic deflection area, the initial problem was that of being unable to simultaneously achieve satisfactory center, edge, and corner resolutions together with a satisfactory shading characteristic when using the Westinghouse WX-4384 electrostatic vidicon.

In order to perform the color-TV experiments, it was necessary to change to a Westinghouse WX-4915 electrostatic vidicon early in the program. At this time, a detailed vidicon alignment procedure was instituted, and the combination of these changes made it possible to achieve the desired sensor performance. Therefore, it was concluded that the initially experienced problem was not basic to the EDITS System, but was peculiar to the earlier vidicon type and/or to the earlier alignment method employed.

With respect to the magnetic digital deflection study, the initial area of concern was related to the performance of magnetic-deflection-circuits when required to operate at the element rate of a pure digital system. Since the self-resonant frequency of the yoke is the limiting factor in deflection-circuit bandwidth, several manufactures were contacted to determine the operating characteristics of typical high-speed yokes. Data were obtained on one unit having a self-resonant frequency of 2.1 Mc. Based on rise-time criteria developed in the study, it was determined that this standard yoke would be satisfactory for element scanning rates up to 400 kc (the nominal rate of EDITS is 100 kc).

For higher element rates, an alternate technique is recommended. This involves the use of a high-frequency "tickler" coil in conjunction with a standard yoke. The "tickler" coil would require very few turns, since it functions only to deflect the beam on incremental distance, while the standard yoke provides the main deflection fields. Based on these techniques, it was concluded that magnetic scanning is feasible for digital TV equipment operating over a wide range of scan rates.

5.3.4 High-Speed Roberts Coding Simulator

This unit was developed to demonstrate the subjective image fidelity obtainable with a representative high-speed digital coding method when employed to encode off-the-air commercial television signals. The Roberts coding method was selected for the purpose and, based on previous study results, 3-bit PCM plus 4-bit Roberts pseudorandom noise (identified as 3/4 Roberts) were chosen as the desired coding parameters.

A portable television set is used to provide the standard analog video signals and for image display. The simulator is designed to permit rapid switching between the standard analog mode, the straight 3-bit PCM mode, and the 3/4 Roberts coding mode for subjective-comparison purposes.

The pseudonoise generator operating at a 10-Mc clock rate is constructed from Motorola MECL integrated circuits. Three-bit PCM encoding is simulated by applying the analog video signal (with or without Roberts noise) to seven parallel threshold circuits, each consisting of a Schmitt trigger, AND gate, and storage flip-flop. These threshold circuits effectively quantize the video to eight levels. Their outputs, sampled at the 10-Mc clock rate, are summed by a resistive ladder and are fed back to the TV set for display.

The results obtained with this simulator unit have been very instructive, particularly in the assessment of the effectiveness of Roberts noise to minimize 3-bit brightness contouring. In general, the higher the video signal-to-noise ratio, the greater the effectiveness of (and need for) the Roberts noise in improving basic 3-bit PCM fidelity. However, under the highest signal-to-noise conditions, the analog picture fidelity is superior to 3/4 Roberts fidelity due to the greater noise content of the Roberts picture. At approximately 20-db S/N,

the basic transmission channel noise overshadows all digital coding effects, making it difficult to distinguish between the analog and the two digital coding methods.

SECTION 6

STUDY PROGRAM CONCLUSIONS

6.1 INTRODUCTION

Because of the compartmented nature of this program, these summary conclusions are presented separately for each major study task area. More detailed conclusions are presented in the individual report sections.

6.2 COMPRESSION TECHNIQUES STUDY

- From the standpoint of compression potential, linear approximation is clearly superior to the other coding techniques considered in this study.
- Linear approximation yields gross compressions on the order of 4 to 1 for complex pictures and 6 to 1 for simpler pictures.
- Linear approximation can be constructed immediately at a 100-kc picture element rate, based on current EMR design experience.

6.3 DIGITAL COMMUNICATION CHANNEL ANALYSIS

- A 4 bits per cycle modulation-demodulation (MODEM) system is feasible.
- It requires approximately 20 db signal-to-noise ratio for satisfactory operation.
- It can fit a 2 bits-per-picture-element digital television signal into an equivalent analog bandwidth at a 10 db power saving.

6.4 DIGITAL COLOR TV INVESTIGATION

- **A modified, analog SECAM color television system is the best choice for live spacecraft television transmission.**
- **A digital, sequential-frame color television system is the best choice for still, or document-transmission, spacecraft television.**
- **Of the color digital systems studied, PCM and its derivatives are, for equal sample density, definitely superior to delta modulation in terms of resolution and color fringing.**

6.5 DIGITAL TV EQUIPMENT AND SYSTEM CAPABILITY STUDIES

- Current operating and adjustment procedures allow optimum digital operation of the WX 4915 electostatic vidicon.
- Digital TV can work equally well with electrostatic and magnetic deflection image tubes.
- 3/4 Roberts pseudorandom noise coding yields a demonstrably workable high speed compressed digital TV system.

SECTION 7

RECOMMENDATIONS

Based on the demonstrated data compression capability of the computer-simulated linear approximation coding technique, the primary recommendation resulting from this study lies in the compression area. Significant results also were obtained in the other major task areas, and useful equipment construction is now possible in each. However, specific follow-on recommendations in these areas will depend on specific MSC requirements in these areas.

It is recommended that a linear-approximation program about one year in length be initiated to procure linear-approximation coder hardware suitable for laboratory performance evaluation. This equipment should incorporate operational flexibility permitting variation of all significant coding parameters. Based on the design work reported on in Appendix F, EMR has specific, current knowledge of linear-approximation circuits required to produce practical hardware. This hardware will be capable of operation within the current transistor state of the art at a 100-kc element rate.

The recommended course of action allows MSC to achieve experimentally the optimum trade-offs between compression, sensor signal-to-noise ratio, channel bit error rate, and subjective image fidelity for different classes of test subjects.

APPENDIX A

EXPERIMENTAL SUPPORT EQUIPMENT

APPENDIX A

TABLE OF CONTENTS

SECTION 1

INTRODUCTION

The experimental phases of the data compression and digital color television studies were heavily supported throughout the MSC study program by the EMR Experimental Digital Television System (EDITS). Also, the basic EDITS capability was considerably expanded under company sponsorship during this program to permit EDITS video data to be processed on an ASI-210 digital computer. This provided realistic simulations of digital compression coding techniques which were under active investigation in the MSC program.

Since a considerable portion of the succeeding appendices deal directly with the results obtained on EDITS and on the EDITS/ASI-210 interfaced system, the following sections of this appendix are devoted to describing the operating characteristics, functions, and general capabilities of this equipment.

SECTION 2

EDITS SYSTEM

2.1 BASIC FUNCTION

The EDITS system is designed primarily as a laboratory tool to investigate statistical and pictorial characteristics associated with various digital television processing techniques. Its operating video coding capability includes:

1. One-, two-, three-, four-, five-, and six-bit PCM
2. Roberts (any combination of PCM and Roberts-bits up to seven bits total, except the 0-7 combination)
3. PEC/Huffman
4. Two-bit delta
5. EDITS/ASI-210 digital computer interface, providing the capability to computer-simulate an additional wide range of coding techniques (see Section 3)

2.2 PHYSICAL CHARACTERISTICS

The electronic equipment comprising EDITS, with the exception of the TV camera proper is rack mounted as shown in Figure A.2-1. The basic electronic system element is the plug-in module, a considerable number of which are standard DEC (Digital Equipment Corp., Maynard, Mass.) logic units. Figure A.2-2 shows a view of the TV camera unit, mounted in the light-shield housing viewing the test fixture which mounts and illuminates the input-test photographic data.

2.3 INPUT/OUTPUT EQUIPMENT CHARACTERISTICS

Input/output equipment characteristics are as follows:

Sensor	Westinghouse one-inch all-electrostatic vidicon, Type WX-4915 (slow-scan type), rated limiting resolution - 500 TV lines in center, and 350 TV lines in corners.
TV Display	Tektronix Type RM503, 5-inch all-electrostatic CRT with P4 phosphor. Rated limiting resolution - approximately 350 to 400 TV lines.

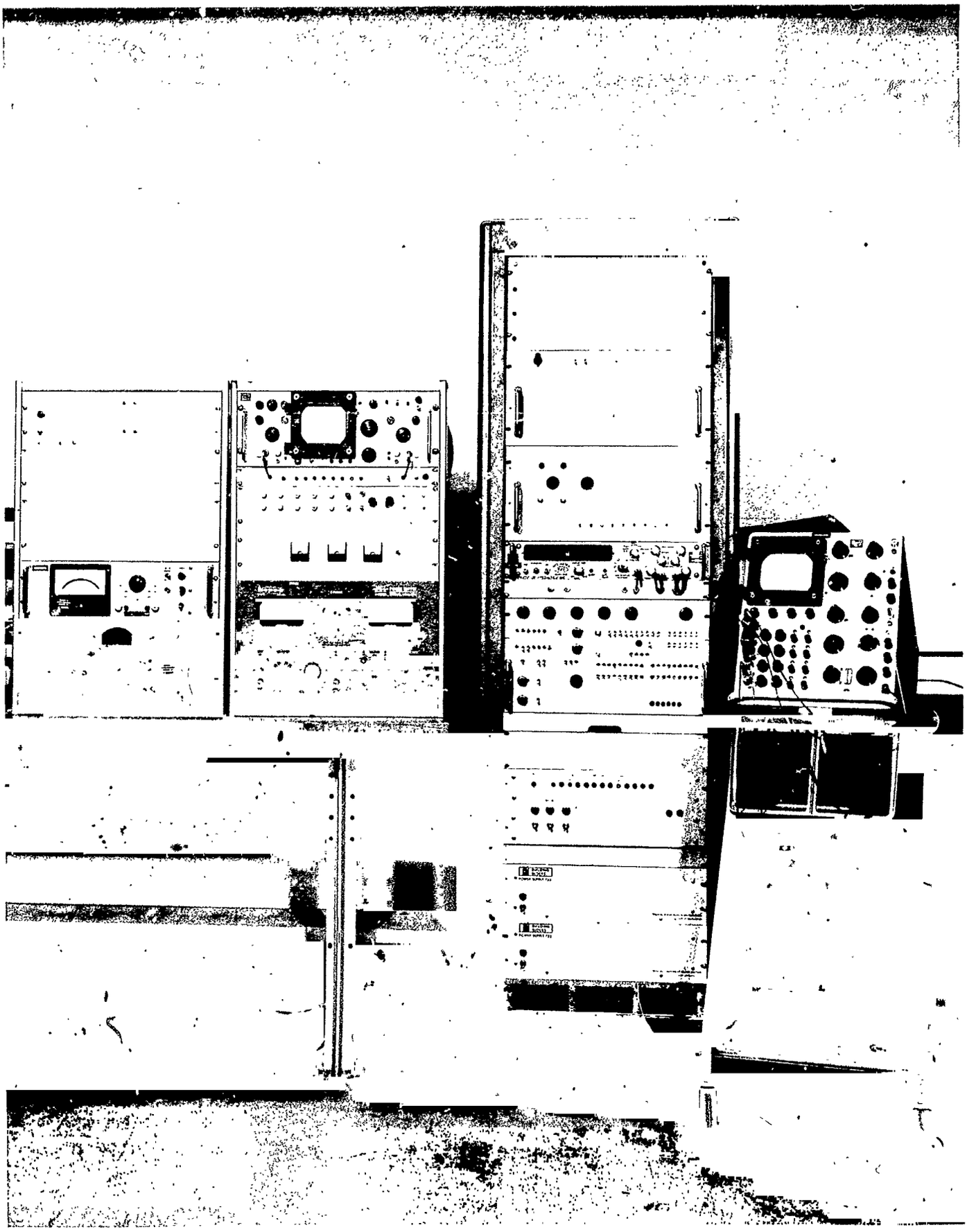

FIGURE A.2-1

EDITS ELECTRONIC EQUIPMENT

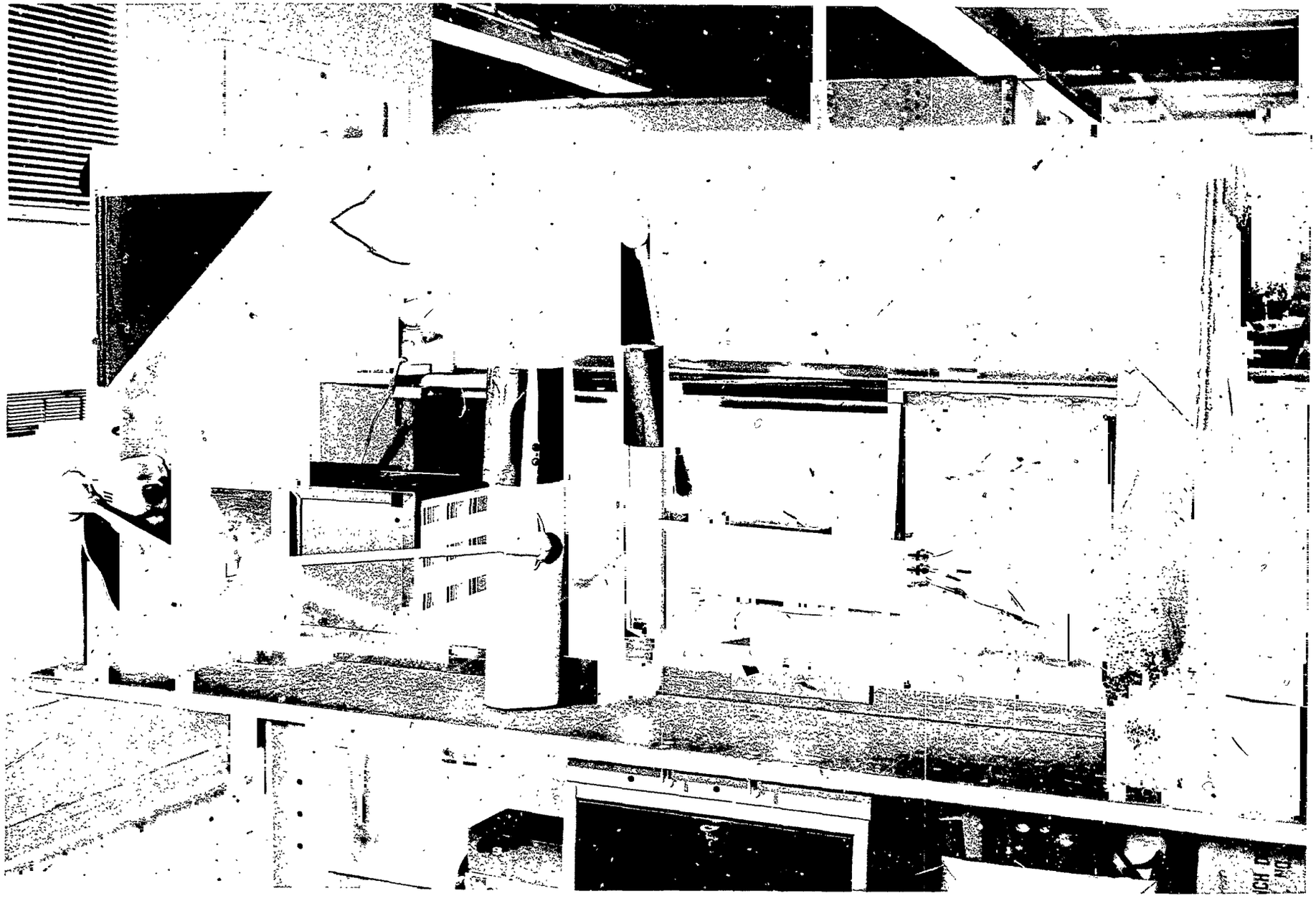

FIGURE A.2-2

THE EDITS CAMERA AND TARGET EQUIPMENT

Display Recorder	Polaroid camera - Employs Speed/Type 47 film for Monochrome TV recording. Employs Polocolor Type 48 for color TV recording (see Appendix D).

2.4 SYSTEM OPERATING CHARACTERISTICS (NORMAL MODE)

System operating characteristics are as follows:

Scan elements/line	128, 256, or 512 (horizontal and vertical), selectable
Frame periods	0.16, 0.66 or 2.6 second, respectively
Frame rates	6, 1.5 or 0.4/seconds, respectively
Element period	10 microseconds
Scan type and format	Horizontal and vertical stairstep scan with square format
Digital encoding	1 to 6 bits. Element sampling rate - 100 kc

2.5 SIGNAL STATISTICAL MEASUREMENT CAPABILITY

Signal statistical measurement capabilities include:

1. First Order--number of times a scan element of a given level occurs within a selected period. This period is selectable by means of gate switching, from a total frame or line period to a fractional frame or line.

2. Second Order--number of times a given element level follows another given element within a selected period.

3. Run Length (RL)--number of times a given element level successively repeats within a selected period.

4. Previous Element (PE)--number of times within a selected period that adjacent elements along a horizontal line have equal levels.

5. Not Previous Element (1-PE)--number of times within a selected period that adjacent horizontal elements do not have equal levels.

6. Previous Line (PL)--number of times within a selected period that matching levels occur on vertically adjacent elements (which are not PE elements).

2.6 NOISE-SIMULATION CAPABILITY

1. Channel (digital) Noise--P_e from $10^{-\infty}$ to 5×10^{-1}. Noise source is a General Radio Random Noise Generator Type 1390-BR plus adjustable threshold and sampling circuitry.

2. Sensor (analog) Noise--S/N from greater than 40 db (limited by vidicon/preamplifier combination) to 15 db (lower if desired).

2.7 NOISE REDUCTION CAPABILITY

Incorporates a Previous Element Qualifier (PEQ) unit to perform this function (see Appendix B, Section 4).

2.8 TEST CHART/TEST PHOTO ILLUMINATION MONOCHROME

1. Front--incident illumination is approximately 150 foot candles. Daylight fluorescent lamps.

2. Back--screen brightness is approximately 250 foot lamberts. Daylight fluorescent lamps.

3. Front Only--3200° Kelvin incandescent lamps (for color reproductions)

2.9 TYPICAL VIDICON EXPOSURE

Using normal 25- or 50-mm lens at an aperature of f/8 (effective), and operating at 256-element scan condition, typical photocathode highlight exposure is approximately 0.3 foot-candle-seconds.

2.10 BLOCK DIAGRAM

Figure A.2-3 is a simplified block diagram of the EDITS system. This diagram depicts the various functions listed in the above section.

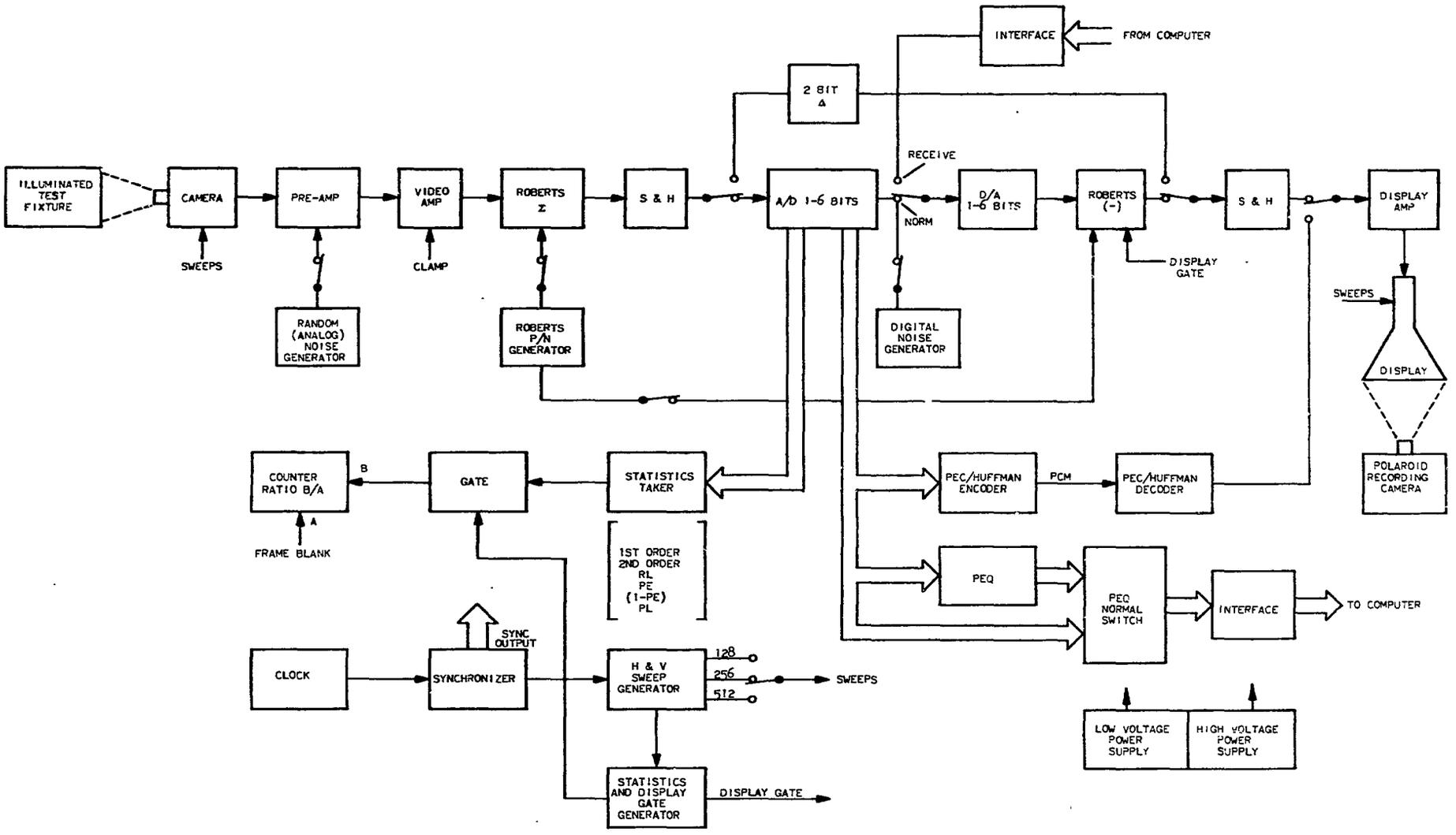

FIGURE A. 2-3

EDITS BLOCK DIAGRAM

SECTION 3

EDITS/ASI-210 DIGITAL COMPUTER INTERFACE

3.1 INTRODUCTION

To facilitate the investigation of picture parameters and the simulation of complex compression techniques, interface equipment was developed and incorporated into EDITS during the course of this study program to allow digital processing of the scanned video data. The system is also capable of transmitting to EDITS from the computer either the original input video data or the processed data, where it is photographed for subjective evaluation.

3.2 PHYSICAL CHARACTERISTICS

Physically the interface unit shown in Figure A.3-1 is 22-inches wide, 18-inches deep and 32-inches high, and occupies approximately 7 cubic feet in a corner of the computer laboratory. The circuitry is housed in a cabinet which has been outfitted with ASI-style indicators and push-button controls. The unit has been designed with maintenance and reliability in mind. A 167-foot cable assembly, consisting of 19 individual coaxial cables and an intercom cable, join EDITS and the interface.

3.3 INTERFACE SYSTEM OPERATION

The interface permits control of the Input/Output (I/O) section of the computer to be transferred to the EDITS area and also provides the facility for making the timing of EDITS and the ASI-210 compatible.

The EDITS/ASI interface general block diagram, shown in Figure A.3-2, is composed of the following functional blocks: Initial Call, ED Control, Timing, Data Transfer Logic, Data Exchange, and Termination Logic. When control of the computer is desired by EDITS, one of the two call lines is raised at the EDITS location depending on whether an input or an output of data is required. A signal on either call-line initiates the following action by the Initial Call block: drops the READY line to EDITS, switches a flip-flop to its proper state to indicate whether an input or an output call has been raised, generates an inhibit level to prevent the receipt of any further calls until the initial call has been completely processed, and transmits a level to the computer indicating that EDITS has requested a priority interrupt. When the ASI-210 receives the signal that EDITS has requested a priority interrupt, it will jump the interrupt scanner to begin its search of the priority addresses. The interface logic will respond to one of two of these addresses which in turn will cause a priority interrupt command to be transmitted and stop the scanner at the desired address. The program in the

FIGURE A. 3-1

INTERFACE UNIT

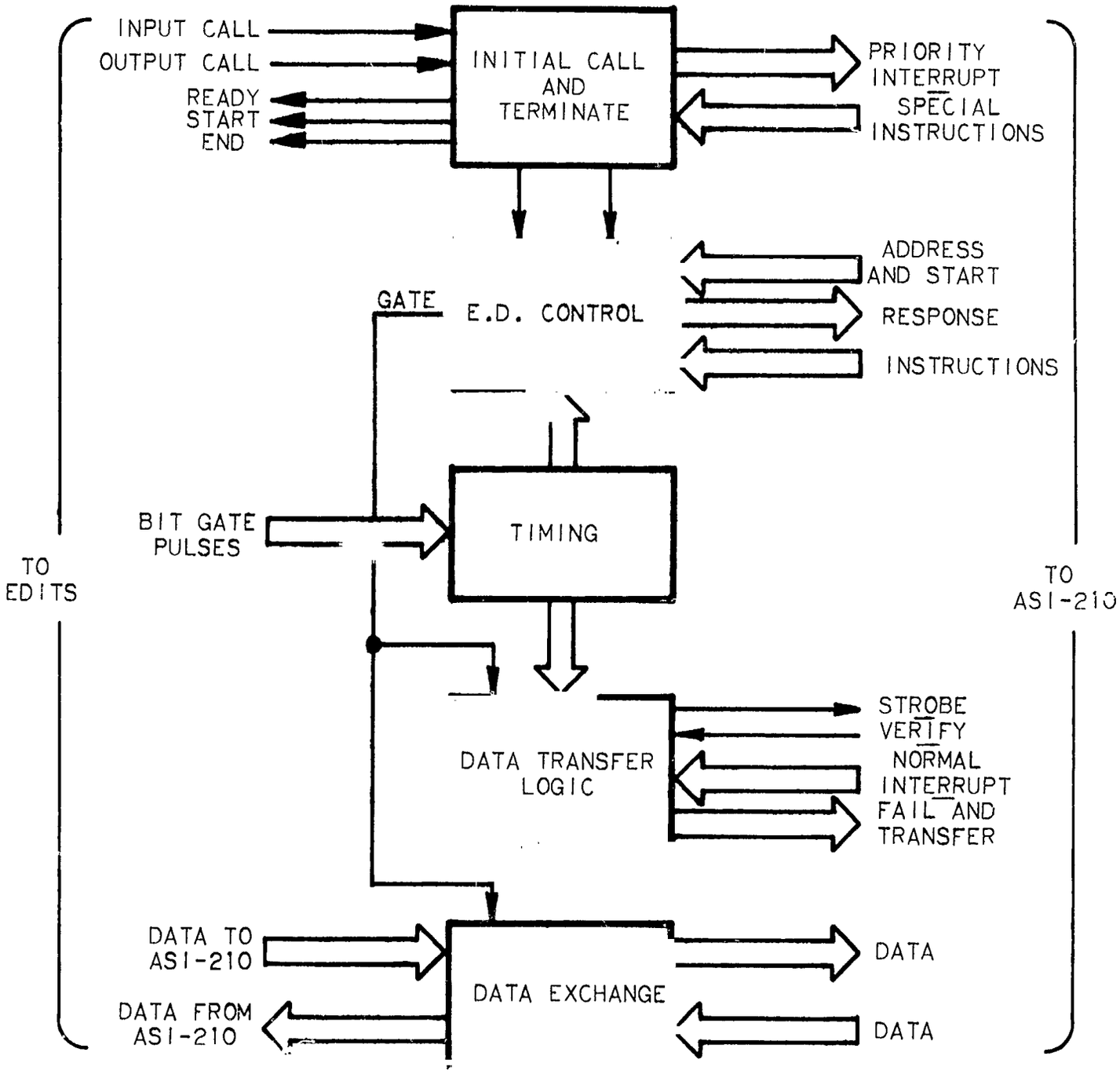

FIGURE A. 3-2

EDITS/ASI-210 INTERFACE BASIC BLOCK DIAGRAM

ASI-210 is arranged to jump to either the input or output routine depending upon which priority address has been recognized.

The ED Control section determines if the status of the computer is such that control can be given to EDITS. When in the course of the assembly language program, an External Device Instruction (EXD) is raised, the unique address of the interface will be placed on the address lines and recognized by the interface. There follows an integration of logic to determine the BUSY status of the interface logic, assembly registers, and interrupt logic. If all is in order, an ED START pulse is transmitted which sets the BUSY routine flip-flop in the interface thereby transferring I/O control to EDITS. At this time, a number of lines to the computer are raised to clear the assembly register and to indicate the mode and direction of transmission required. When this has been accomplished, a signal START will be sent to EDITS to permit transmission of the first picture element.

The receipt of a BIT GATE pulse from EDITS will start, within the Timing Circuit, an internal clock which provides a series of four timing pulses to stop the interface logic. The fourth pulse in this series turns off the clock.

Within the Data Transfer Logic block all active interface control logic is common both to input and output modes of transmission with reversal accomplished by passive logic to minimize circuitry. When data is being exchanged, a strobe flip-flop is set and a strobe pulse is transmitted to the ASI-210 indicating a request for data exchange. Upon receipt of this pulse, the computer I/O will gate the six data lines to or from an appropriate position in the assembly register (depending whether an input or an output call has been initiated) and send back a VERIFY pulse to the interface. This pulse will clear the strobe flip-flop and the logic will await the next BIT GATE pulse from EDITS. Successive pulses will transfer the remaining picture elements in the same manner until the 21-bit assembly register if filled. At this time the I/O will initiate a memory reference. The VERIFY line will remain up until the storage has been completed. This represents an inhibit condition to the interface clock to prevent further strobes until the assembly register has been cleared. The transfer will then resume.

The timing for a group of seven elements within a scan line is shown in Figure A.3-3; seven elements making a cycle, since seven elements having six bits each constitutes two computer 21-bit words (the 21-bit word being a basic characteristic of the ASI-210). The EDITS timing is slowed down from a basic rate of 100 kc to 50 kc to allow a steady rate of data transfer. The horizontal blanking period of EDITS also has been extended to permit the computer to relocate the data from core memory to magnetic tape at the end of each line.

The Data Exchange consists of gated receivers (pulse shapers) and transmitters (line drivers) to transfer data directly on twelve lines between EDITS and the interface. Six of these lines are for input to the computer and six are for output to EDITS.

The number of frames to be transferred is determined by the computer program. The Termination Logic signals EDITS at the end of each line and at the end of the

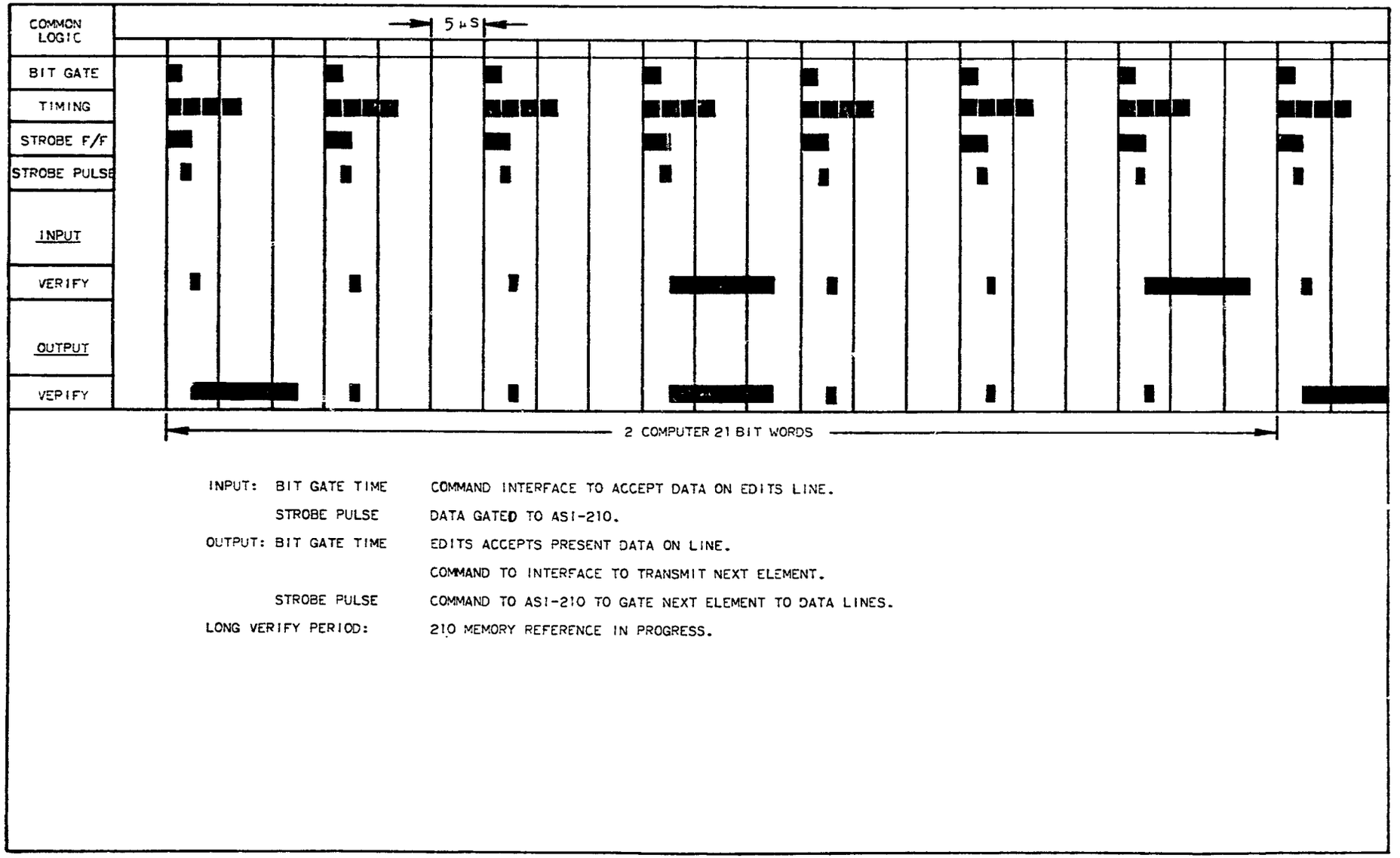

FIGURE A. 3-3

EDITS/ASI-210 INTERFACE GENERAL TIMING DIAGRAM

last line of the last frame to be transferred. Following the receipt (or transmission) of the last element of a line, a command is given to the interface which will clear the BUSY routine. The normal ED interrupt is thereby generated as a command to release control of the I/O. The computer program then processes the data or calls for magnetic tape operation. When the desired number of frames have been transmitted and processed, a signal is sent to EDITS indicating the end of the program. At this time the inhibit to the CALL lines is lifted thus permitting the receipt of the next initial call.

3.4 APPLICATIONS OF THE EDITS/ASI INTERFACE

With an EDITS picture on tape, the possibilities for picture compression or picture processing are limited only by ingenuity and by available computer running time. The computer has been used on this study program to simulate linear approximation coding and decoding and to calculate the resulting compression ratios. The output video data resulting from the computer processing operation is recorded on the magnetic tape in a manner similar to the recording of the input video data. Therefore, both the input video frames and the output (processed) frames may be recalled and photographically recorded on EDITS for subjective comparison purposes (see Appendix B, Section 5--Linear Approximation). The computer also was used to obtain area statistics on selected video frames. These statistics were determined for area sizes of 2x2, 3x3, 4x4, and 5x5 element areas for both six-bit and four-bit quantization. In addition to performing these measurements, the computer also was programmed to calculate the compressions which could be achieved by employing a selected area coding technique. These results are contained in Area Coding, Appendix B, Section 3.

Figure A. 3P-1 shows representative EDITS video frames (6-bit coding) which have been transmitted to the computer, formatted, stored, and retransmitted to EDITS as original 6-bit frames.[a] This photographic group demonstrates that there is no degradation resulting from the basic signal transmission, storage, and retransmission processes.

[a] Figure numbers containing P refer to photographs in Volume II of this report.

APPENDIX B

COMPRESSION TECHNIQUE STUDIES

APPENDIX B

TABLE OF CONTENTS

APPENDIX B (Cont'd.)

TABLE OF CONTENTS

SECTION 1

INTRODUCTION

The goal of the compression task was to determine a compression technique with a 6:1 or greater gross average compression relative to 6-bit PCM. The techniques investigated were: (1) frame-to-frame coding; (2) area coding; (3) n-dimensional processing; and (4) linear approximation.

These techniques were analyzed in the following general manner. A mathematical model was formulated for each technique and the gross average compression was calculated from the entropy of the model. If this limiting value of the desired statistics indicated that a compression in the order of 6:1 was possible, the system was either simuiated on EDITS or on the ASI-210 digital computer (processing stored video frames obtained from EDITS). Practical constraints of a real-life operating system then were considered and if these were not insurmountable, the technique would be qualified as one which would achieve a gross average compression of 6:1.

SECTION 2

FRAME-TO-FRAME CODING ANALYSIS

2.1 INTRODUCTION

The preliminary analysis of frame-to-frame coding indicated that techniques could be conceived that would in theory achieve a 6:1 compression. Three approaches to frame-to-frame coding will be analyzed. This first approach is to compare successive frames and transmit the intensity and location of those elements in the successive frames that do not have the same intensity as the corresponding elements in the previous frame. This approach will be referred to as frame-difference coding (FDC). The second approach is to compare successive frames and transmit a single unique code word if all the corresponding elements in two successive frames have the same intensity. This approach will be referred to as zero-difference frame coding (ZDFC). The third approach to frame-to-frame coding is to combine intraframe coding with some form of frame-to-frame coding. This approach would combine a technique such as linear-approximation coding with the zero difference frame coding technique. Each of these approaches will be analyzed to determine whether in theory they have the potential of achieving a 6:1 gross average compression. If the techniques do have the potential, practical constraints will be imposed to determine whether the techniques will be computer simulated or whether circuitry has to be constructed to obtain the necessary statistics to evaluate the particular techniques.

2.2 FRAME-DIFFERENCE CODING

For this particular technique, it is necessary to determine the number of elements in successive frames that must have the same intensity. Assume that the video is quantized to N bits and the raster is composed of m^2 elements. The successive frames are compared and if element X_{ij} in frame F_{j+1} does not have the same intensity as the corresponding element Y_{ij} in frame F_j, the magnitude of X_{ij} with its coordinates i and j are transmitted.

For the m x m raster, $\log_2 m^2 = 2M$ bits are required to specify the location of X_{ij} and N bits are required to specify the intensity. Therefore, for each element X_{ij} that is different, 2M + N bits are transmitted. If P(D) represents the probability of obtaining the difference signal, the gross average frame difference compression is then given by:

$$\overline{FDC} = \frac{N}{(2M + N)\,P(D)} \qquad (1)$$

If the symbol P(S) represents the probability that S elements in a frame are exactly like the corresponding elements in the previous frame, it is given by P(S) = 1-P(D). Therefore, Equation 1 can be rewritten in terms of P(S) and is:

$$\overline{FDC} = \frac{N}{(2M + N)\left[1-P(S)\right]} \qquad (2)$$

If N = 6 and m = 256, the gross average-frame-difference compression as a function of P(S) can be plotted and is given in Figure B.2-1. From the curve it is seen that in order to achieve large compressions, that P(S) must approach unity.

Onepossible manner to obtain this is by thresholding the difference signal; that is, compare element X_{ij} and Y_{ij} and if $|Y_{ij}-X_{ij}| \leq T$, consider that the two signals are identical. This relationship can be stated alternately, that is, compare corresponding elements in successive frames and do not transmit the element unless it is significantly different than the corresponding element in the previous frame. This requires a carefully controlled subjective experiment to determine T.

Before considering this aspect, consider Figure B.2-1 again. In order to achieve a 6:1 gross average compression with T = O for 4-bit quantization, 96.6% of the corresponding elements in successive frames must be identical. In the 256 by 256 raster, this means that the new information in successive frames is limited to only 562 elements. This imposes rather severe restrictions on the signal-to-noise requirements in the system. For four-bit quantization, with the assumption that the elements between successive frames are statistically independent and the noise has a gaussian distribution, the required signal-to-noise in the sensor can be calculated. Figure B.2-2 plots the sensor signal-to-noise ratio required as a function of P(S) for the above assumptions.[a] At P(S) = 0.966,the required sensor signal-to-noise ratio is 55.2 db. This is not possible with current state-of-the-art sensors. At 6-bit quantization the required signal-to-noise ratio is in excess of 55.2 db. One manner in which this value could be reduced is by a coding technique that encodes to three bits, and subjectively produces pictures at 3-bit coding which are equivalent to 6-bit quantization. However, even with 3-bit coding and making the compression relative to 6 bits, the desired sensor signal-to-noise ratio is 44 db, still in excess of what one can normally achieve. Even at this

[a]EMR, Final Report--Manned Spacecraft Advanced Television Study, Contract NAS 9-991, 31 July 1963.

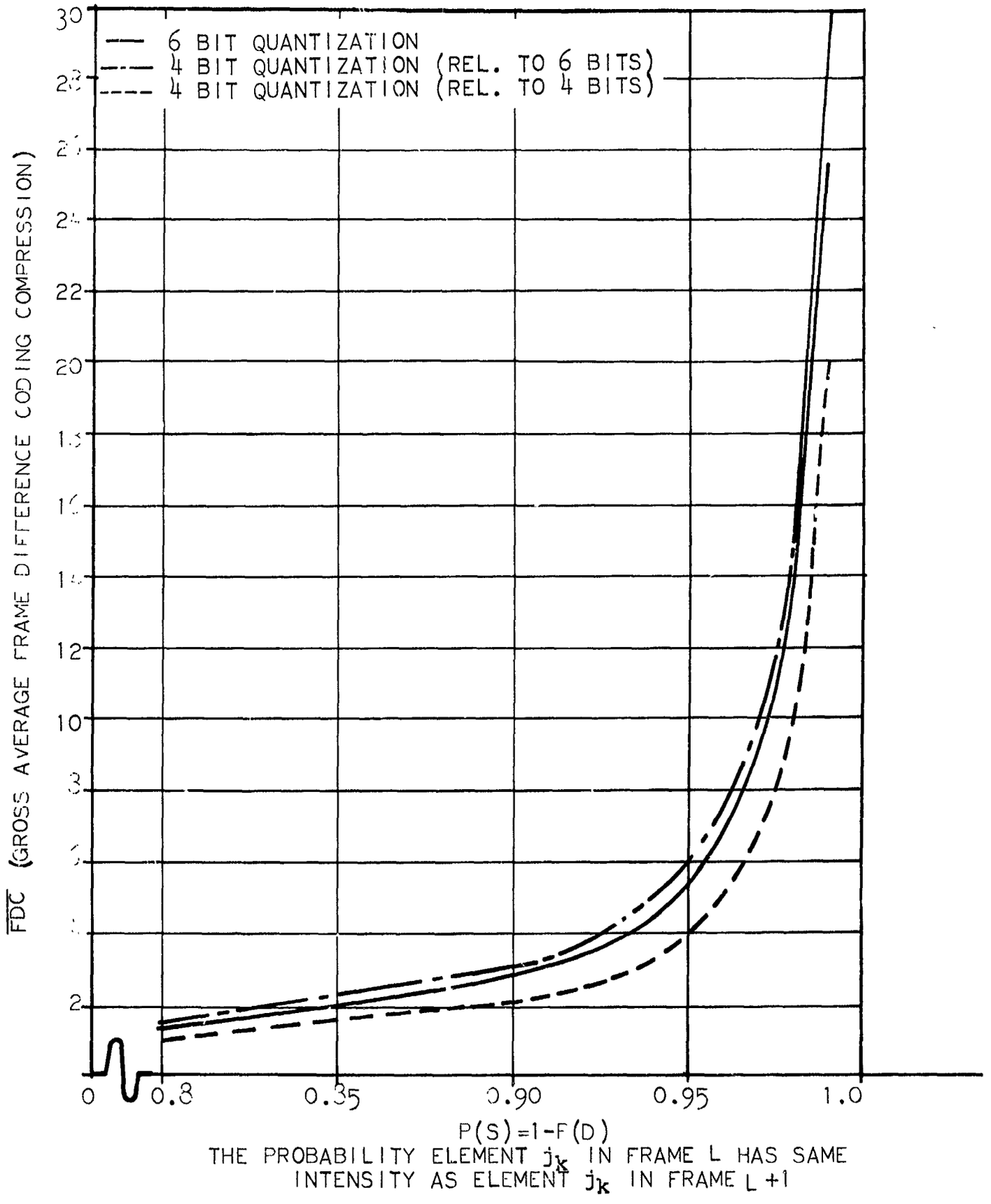

FIGURE B.2-1

GROSS AVERAGE FRAME DIFFERENCE CODING COMPRESSION AS A FUNCTION OF P(S) FOR 256 X 256 RESOLUTION PARAMETER IN THE QUANTIZATION

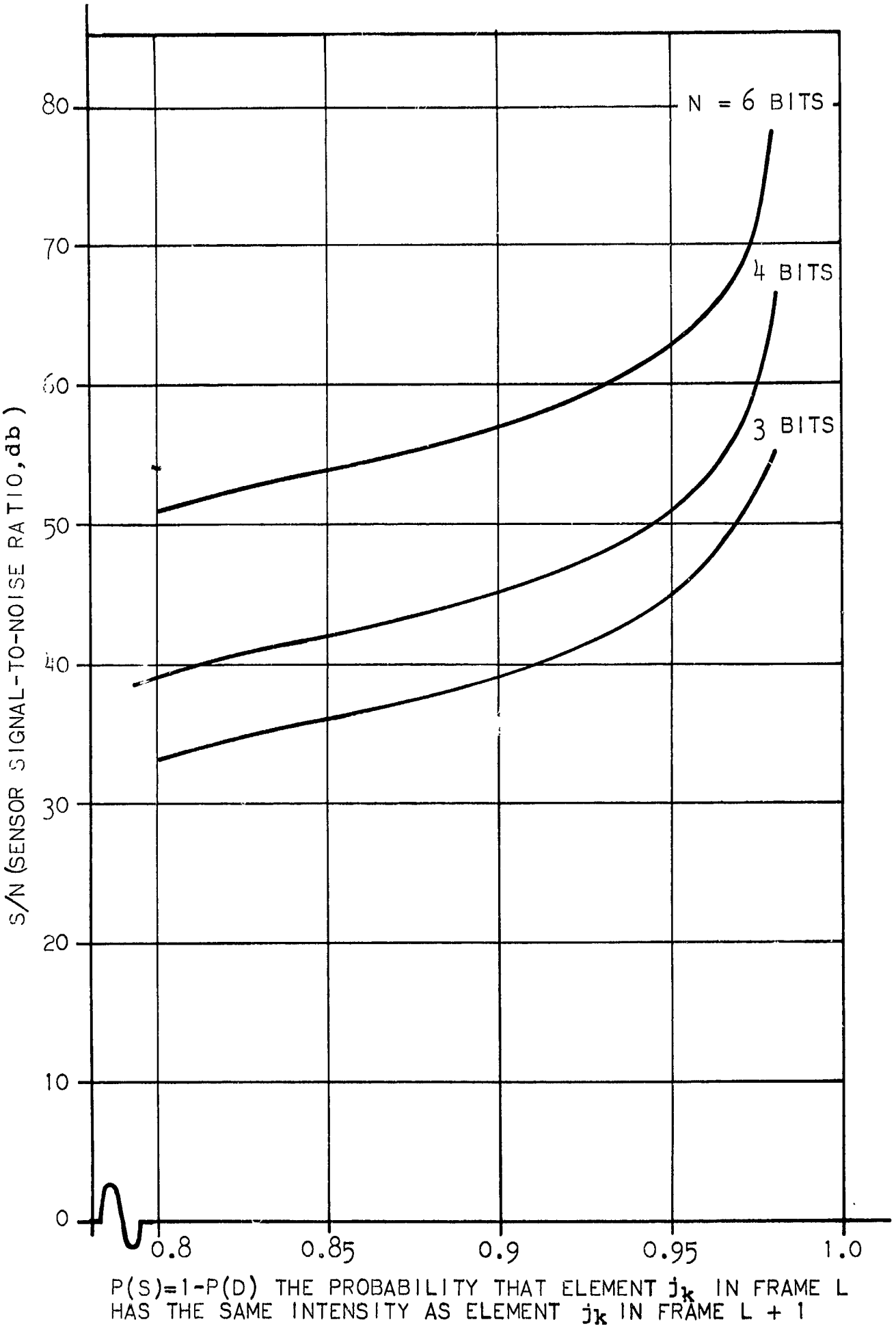

FIGURE B.2-2

SENSOR SIGNAL-TO-NOISE RATIO AS A FUNCTION OF
P(S) FOR A NOISY A/D CONVERTER

value of sensor signal-to-noise ratio, only 3,277 elements can change between frames. When considering that any movement whatsoever, however so slight, will cause many elements to change, it is extremely doubtful that frame-difference coding could ever achieve the desired compression. Therefore, based on current state-of-the-art sensors and "motion-carrying" element restrictions, frame-difference coding can be eliminated from further consideration. With this approach eliminated, the next step is to consider the case of zero-difference frame-coding.

2.3 ZERO-DIFFERENCE FRAME CODING

Assume that the signal is quantized to N bits, has m x m resolution, and f frames are to be compared. The coding algorithm compares two successive frames, and a single code word is transmitted if they are identical. Assume that this code word is composed of F bits. On a single-frame basis the compression is Nm^2/F. If N = 4, m = 256, and F = 64, there is a compression of 4000:1 if the two frames are alike. This may appear to be the answer to compression; however, this is not the case since it is not the single-frame compression value that must be calculated, but the long-term average compression over many frames. For this case, the gross average zero difference frame-coding compression is given by:

$$\overline{ZDFC} = \frac{Nm^2 f}{Fa + N(f-a)\,m^2} \tag{1}$$

Where a is the number of frames that are exactly alike. For N = 6 bits, F = 60 bits, f = 100 frames, the approximate gross average $\overline{ZDFC}$ compression becomes,

$$\overline{ZDFC} \cong \frac{1}{1 - 0.01a} \tag{2}$$

Figure B.2-3 is a plot of this curve; in order to achieve a 6:1 gross average compression, 83 frames (or 83%) must be exactly alike. If this percentage of frames must be identical, evidently the frame rate is too high. It is assumed that the techniques are for space applications, where the frame rate will be initially minimized. Therefore, it appears that this approach to frame-to-frame coding will not achieve the desired compression. The final approach to be considered in the frame-to-frame coding analysis is that of combining frame-to-frame coding with intraframe coding.

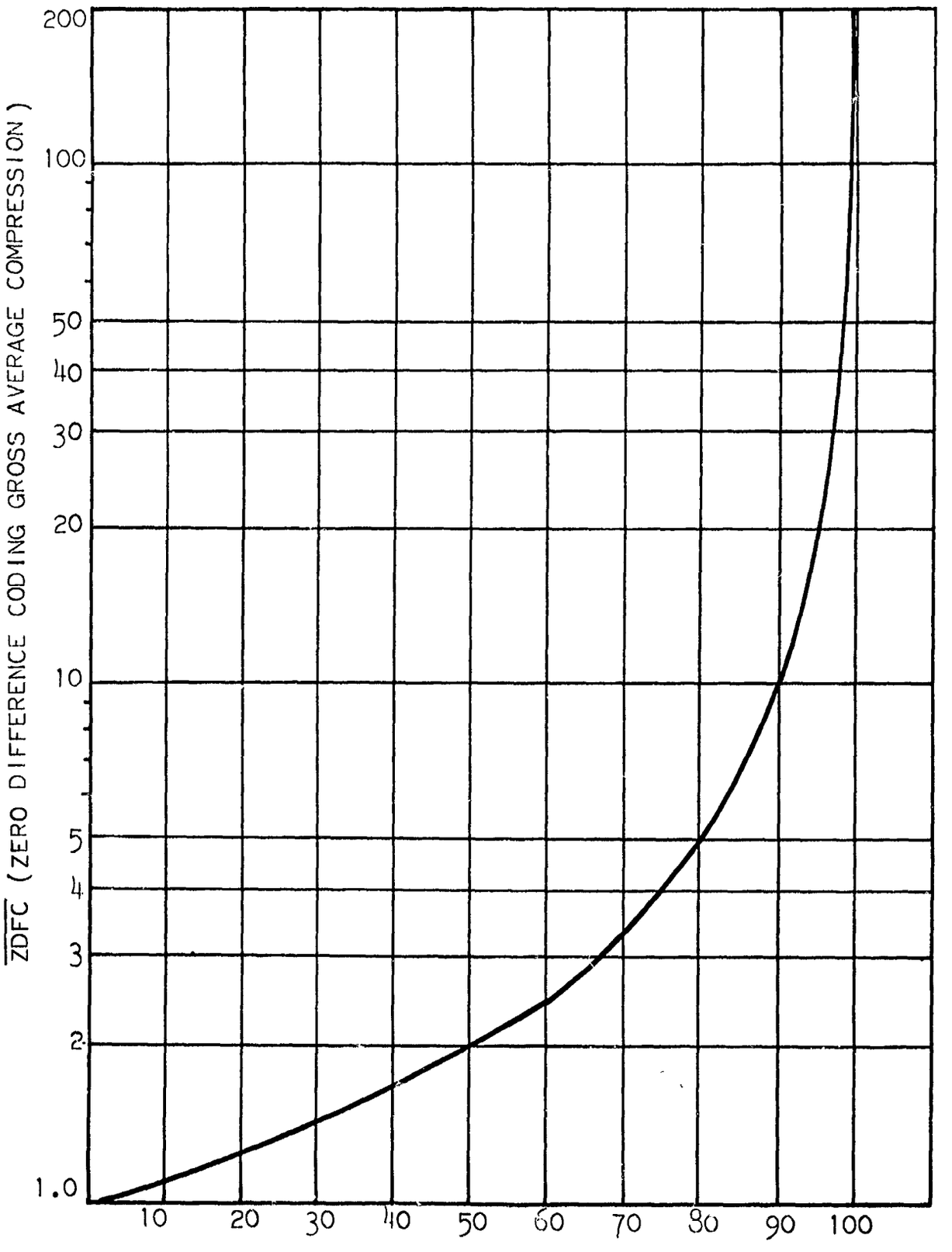

FIGURE B.2-3

ZERO-FRAME DIFFERENCE GROSS AVERAGE COMPRESSION AS A FUNCTION OF THE NUMBER OF IDENTICAL FRAMES OUT OF 100

2.4 INTRAFRAME AND FRAME-TO-FRAME CODING

In this particular approach to frame-to-frame coding, it is assumed that on an intraframe basis a gross average compression of $\overline{CA}$ is possible and successive frames are compared; if they are identical, a single code word is transmitted. The formula for compression from Equation 2 of Section 2.3 is modified by $\overline{CA}$ and the intraframe-coding compression is:

$$IFC = \frac{Nm^2 f}{Fa + \frac{N}{\overline{CA}} (f - a) m^2} \tag{1}$$

For F = 60, m = 256, N = 4, and f = 100,

$$IFC = \frac{f\overline{CA}}{f - a}$$

Figure B.2-4 plots $\overline{IFC}$ compression as a function of A parametric in the gross average compression for the single frames.

An examination of Figure B.2-4 reveals that, given a gross average compression on an intraframe basis of X:1, to double the compression using IFC requires that 50% of the 100 total frames be identically alike. Combining intraframe coding with a gross average compression of 2:1 with the zero-difference frame-coding technique, to obtain a gross average compression of 6:1 requires that 68% of the frames be identical. This appears to be a rather stringent requirement if the frame rate had been minimized initially.

2.5 CONCLUSIONS

From Figure B.2-1, B.2-3, and B.2-4, it is apparent that extremely large values of compression theoretically could be achieved by frame-to-frame coding. However, when the amount of redundancy necessary to achieve this compression is considered, practical limitations prevent these large values compression from being achieved. If an excessively high frame rate is transmitted in actual practice, then it would be possible to obtain compression by frame-to-frame coding, but at an extremely high cost of implementing the technique. However, it will be assumed that the frame rate has been minimized for space applications of digital television; therefore, frame-to-frame coding will be eliminated from further consideration as a potential compression system for the current study.

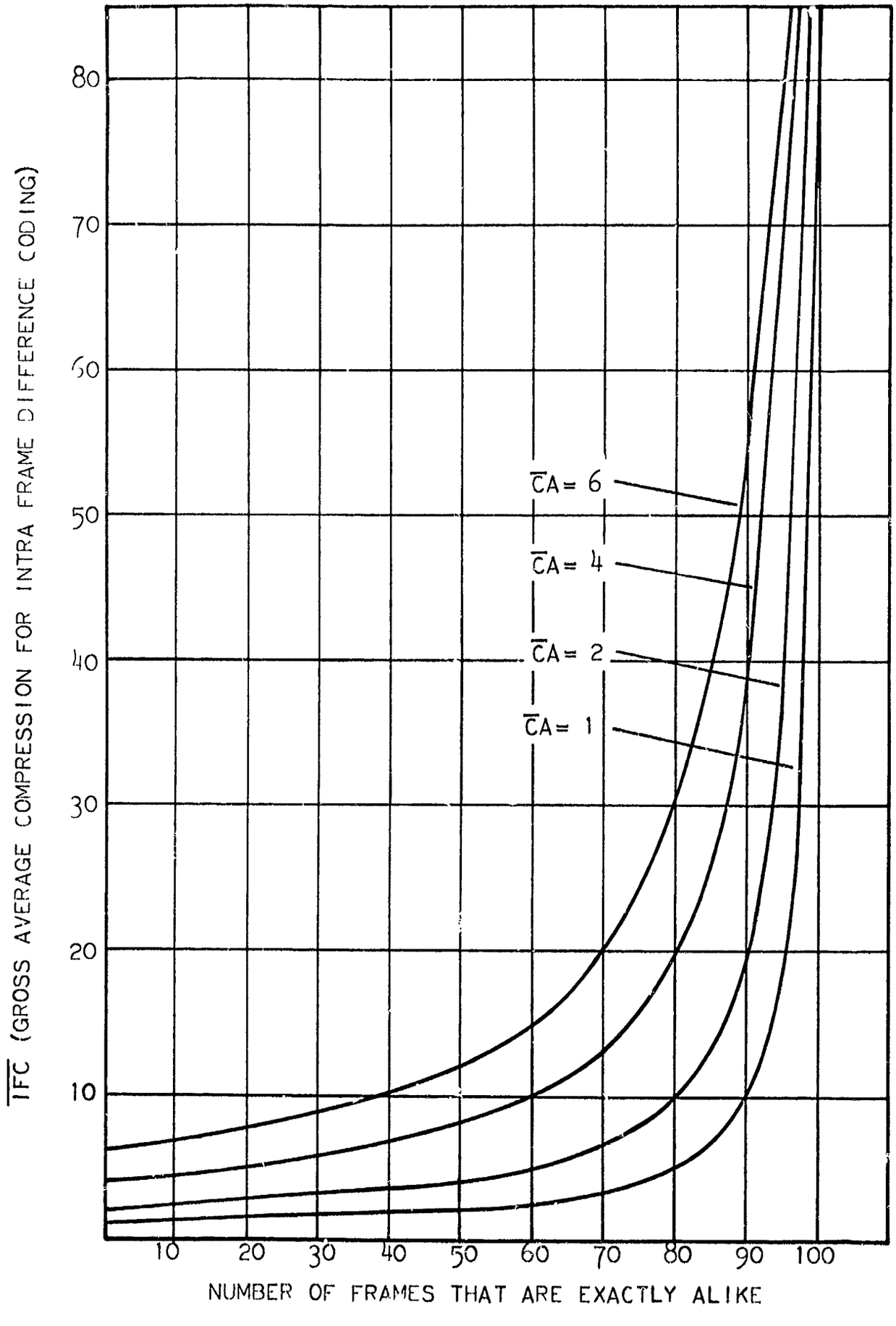

FIGURE B. 2-4

INTRAFRAME DIFFERENCE CODING AS A FUNCTION OF NUMBER OF IDENTICAL FRAMES PARAMETRIC IN THE GROSS AVERAGE COMPRESSION FOR INDIVIDUAL FRAMES

SECTION 3

AREA CODING

3.1 INTRODUCTION

To utilize both the horizontal and vertical correlation efficiently in a television frame, it is necessary to employ some form of area coding. A statistic necessary to determine the efficiency of several approaches to area coding is P(A), the probability of obtaining an area in which all the elements in the area have the same intensity. P(A) will be referred to as the block area statistics. Basic mathematical models will be developed to determine the efficiency of various approaches to area coding.

Before preliminary area statistics are given, a mathematical model for one area compression technique will be given. This will show that the technique of area coding could in theory achieve a high compression ratio. The model assumes that the television frame is composed of E elements per line, L lines per frame, and each element is quantized to B bits per element. The total number of bits to specify a frame is ELB bits per frame. If it is assumed that the frame is subdivided into subframes composed of a block of FM elements where F and M represent the number of elements per area, the simplest area-coding technique would be to sequentially scan the frame on a subraster basis and encode the FM elements with (B + 1) bits if all the elements have the same intensity. If any one of the FM elements in the block is of different intensity, each element in the block is encoded to (B + 1) bits. The average area compression is then given by

$$\overline{FAC} = \frac{BEL}{(B + 1)\left[EL + A\,(1 - FM)\right]}, \tag{1}$$

where A is the total number of FM areas in the frame.

In addition to the Flat-Area Coding (FAC) model that was developed, three additional mathematical models were developed, each one being a logical extension of the previous mathematical model. These models are: (1) Huffman Area Coding (HAC), where the areas and remaining elements are encoded with the Huffman Code based on the probabilities of occurrence of the events; (2) Area Coding with Previous Element Coding (ACPE'C), where those elements not in a coded area are previous-element encoded, while the areas and 1-PE (not PE) Area Coding (PAC), where successive areas of the same intensity are PA coded while the remaining elements and (1-PA) areas are encoded under the assumption of a flat probability distribution.

The basic definitions for each model will be presented along with the appropriate compression formulas. By utilizing (1) the compression formulas, (2) previous EDITS statistics, (3) photographic-simulated area properties of the individual

levels, and (4) a computer simulation, it is possible to draw certain conclusions from the models regarding the potential of area coding.

3.2 FLAT-AREA CODING

Flat-area coding assumes that the frame is composed of fixed geometric areas of constant intensity and quantized elements not in the areas. Each of these events is assumed to occur with the same probability and therefore each is encoded with a fixed-word-length code word. The basic formulas necessary to specify this model will be presented along with the compression model.

For FAC, the probability of an area block of level j, $P(A_j)$, is given by

$$P(A_j) = \frac{A_j}{\sum_{j=1}^{n} A_j + \sum_{j=1}^{n} L_j}, \tag{2}$$

where A_j represents the L_j number of area blocks of level j which occur in a television frame and L_j represents the number of elements, not in an area block, of level j which occur per television frame. The probability of an element of level j which is outside an area block, $P(L_j)$, and the probability of an area block of any level, P(A), are given in a similar manner by

$$P(L_j) = \frac{L_j}{\sum_{j=1}^{n} A_j + \sum_{j=1}^{n} L_j}, \text{ and} \tag{3}$$

$$P(A) = \frac{\sum_{j=1}^{n} A_j}{\sum_{j=1}^{n} A_j + \sum_{j=1}^{n} L_j}. \tag{4}$$

The total number of elements in a frame composed of E elements per television line and L lines per frame is given by

$$\sum_{j=1}^{n} L_j + F \cdot M \sum_{j=1}^{n} A_j = E \cdot L, \tag{5}$$

where F·M is the number of elements in an area block. With these fundamental equations, the general area compression ratio, $\overline{FAC}$, for FAC is

$$\overline{FAC} = \frac{B\left[(FM - 1)\cdot P(A) + 1\right]}{\sum_{j=1}^{n}\left[P(L_j)\ N_j + P(A_j)\ B_j\right]}, \qquad (6)^a$$

where the compression is relative to a B bit PCM source. In Equation 6, N_j is the number of code bits for an element of level j which is not within an area block and B_j is the number of code bits for an area block of level j.

If L_j and A_j are assumed to be equally likely, the code words will contain N + 1 bits, where N is the number of quantization bits. If 3-bit quantization is used, the compression formula relative to a 6-bit basic system becomes

$$\overline{FAC} = \frac{6\left[(F \cdot M - 1)\cdot P(A) + 1\right]}{4\sum_{j=1}^{8}\left[P(L_j) + P(A_j)\right]} . \qquad (7)$$

Since the sum of the probabilities is unity, the final expression for three-bit quantization FAC compression becomes

$$\overline{FAC} = 1.5\,(F\cdot M - 1)\cdot P(A) + 1.5. \qquad (8)$$

The graphs of $\overline{FAC}$ versus P(A) for 2 x 2, 3 x 3, 4 x 4, and 5 x 5 area blocks for 3-bit and 4-bit quantization are given in Figures B.3-1 and B.3-2, respectively.

3.3 HUFFMAN AREA CODING

HAC encodes the previous events with an optimum code to increase the compression. To determine the effect of HAC on compression for a nonuniform distribution, the area blocks were assumed to have a gaussian distribution and the elements not within area blocks to have a uniform distribution. Two distributions were used; one with P(A) = 0.5 and the other with P(A) = 0.3. The compression obtained by the use of HAC from Equation 6 with 3-bit quantization is shown for both 3 x 3 and 2 x 2 area blocks for the assumed distribution by individual points on Figure B.3-1. Since only a small increase in compression was obtained by the use of Huffman coding, the increase in complexity does not warrant considering optimal encoding of the areas and (1 - PE') elements; therefore, a uniform distribution for these events will be considered for ACPE'C and PAC.

---

[a] Equation 6 is also the general expression for HAC.

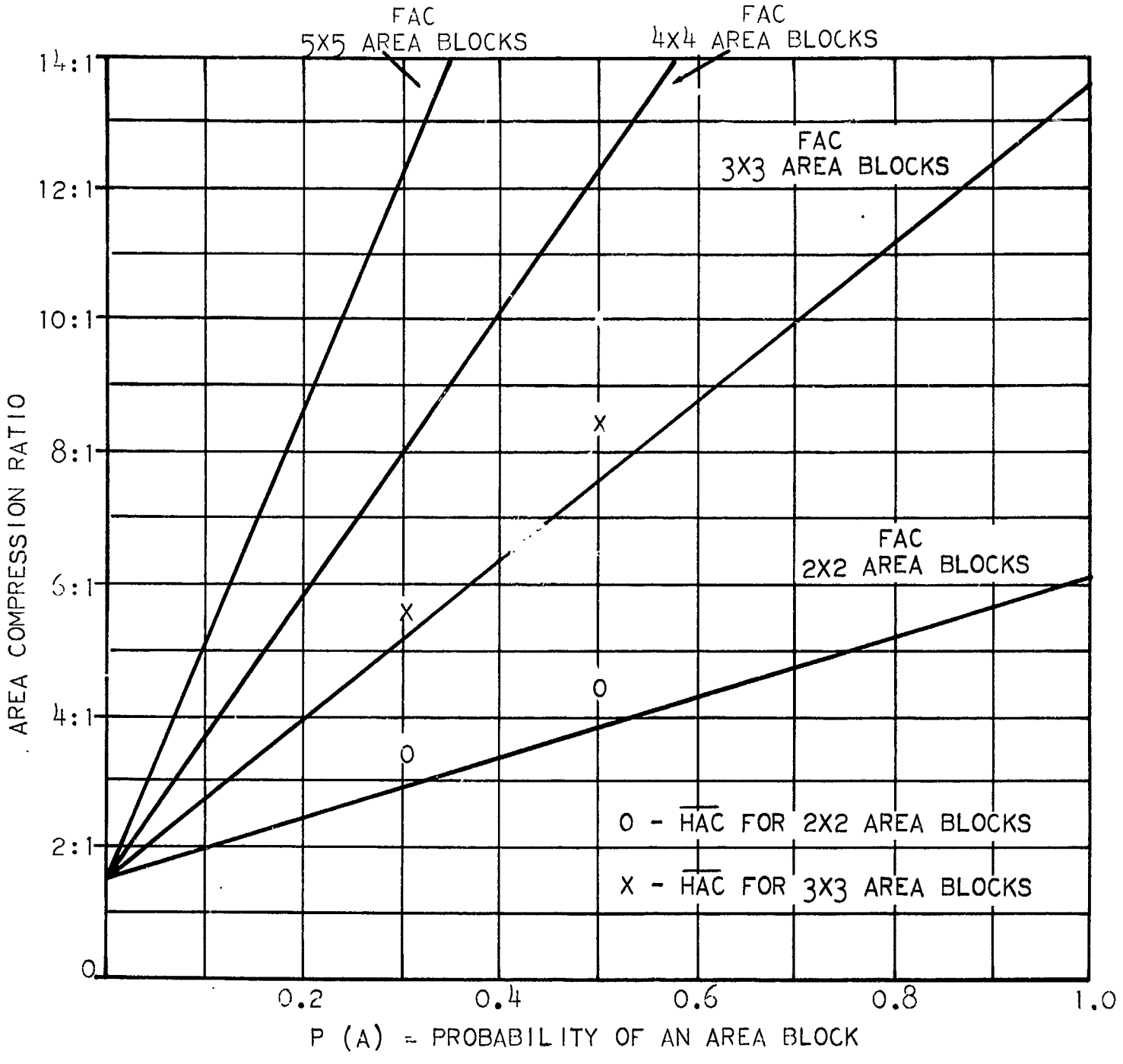

FIGURE B.3-1

COMPRESSION RATIO VERSUS P(A) FOR
FAC AND HAC FOR 3-BIT QUANTIZATION

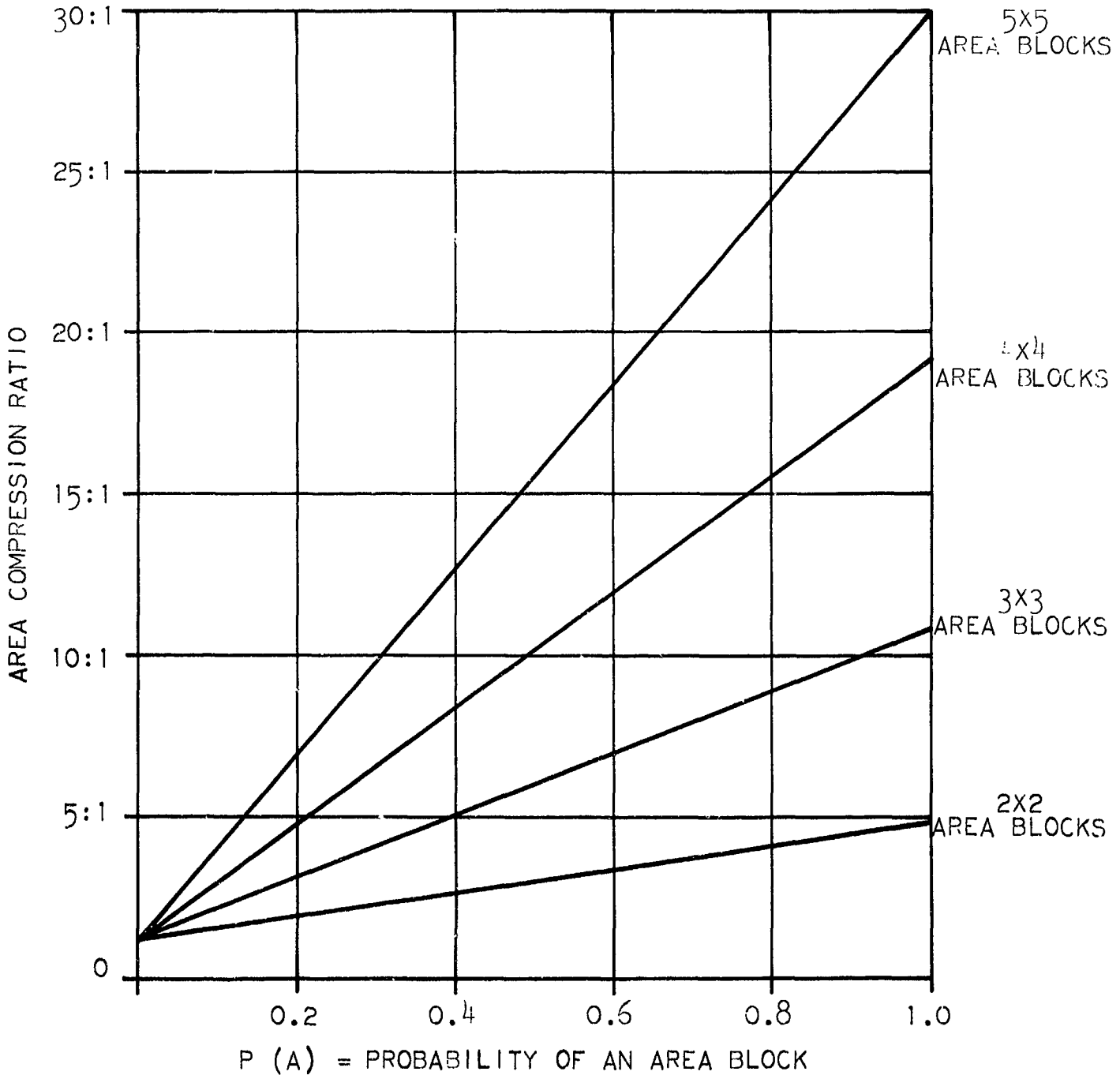

FIGURE B.3-2

FAC COMPRESSION RATIO AS A FUNCTION OF P(A) FOR 4-BIT QUANTIZATION

3.4 AREA CODING WITH PREVIOUS-ELEMENT CODING (ACPE' C)

Following the coding of area blocks and individual elements not within an area block, the next order of complexity in compression models is to code, in addition to area blocks and individual elements, those elements which are not within an area block but do qualify as previous elements. For ACPE' C the probability of an area block of level j is now given as

$$P(A_j) = \frac{A_j}{\sum_{j=1}^{n} A_j + \sum_{j=1}^{n} L'_j + PE'} \tag{9}$$

where L'_j represents the number of elements of level j in a television frame which are not within an area block and do not qualify as previous elements and PE' is the number of elements in a television frame which are not within an area block but do qualify as previous elements. The probability of an element of level j which is not within an area block or qualified as a previous element, $P(L'_j)$; the probability of a previous element not in an area block, P(PE'); and P(A) are given likewise as

$$P(L'_j) = \frac{L_j}{\sum_{j=1}^{n} A_j + \sum_{j=1}^{n} L'_j + PE'}, \tag{10}$$

$$P(PE') = \frac{PE'}{\sum_{j=1}^{n} A_j + \sum_{j=1}^{n} L'_j + PE'}, \text{ and} \tag{11}$$

$$P(A) = \frac{\sum_{j=1}^{n} A_j}{\sum_{j=1}^{n} A_j + \sum_{j=1}^{n} L'_j + PE'}. \tag{12}$$

The total number of elements in a television frame for ACPE' C becomes

$$\sum_{j=1}^{n} L'_j + F \cdot M \sum_{j=1}^{n} A_j + PE' = E \cdot L. \tag{13}$$

From these basic equations, the general formula for the compression ratio of ACPE' C can be derived to be

$$\overline{\text{ACPE' C}} = \frac{B\left[(FM - 1) \cdot P(A) + 1\right]}{\sum_{j=1}^{n} \left[P(L'_j)\, N'_j + P(A_j)\, B_j\right] + P(PE')D} \tag{14}$$

where the compression is relative to a B-bit PCM source and N'_j represents the number of code bits for an element of level j which is not in an area block or qualified as a previous element and D is the number of code bits for a previous element not within an area block.

Consider the case of 3-bit quantization and assume that PE' is the most probable event which is assigned a 1-bit code word. Further assume that A_j and L'_j are equally likely and assigned 5-bit code words, 5-bit words being needed to preserve the prefix property. For these assumptions, the compression ratio formula relative to a 6-bit source reduces to

$$\overline{\text{ACPE' C}} = \frac{6\left[(F \cdot M - 1) \cdot P(A) + 1\right]}{5 - 4\,P(PE')}. \tag{15}$$

Figure B.3-3 shows $\overline{\text{ACPE' C}}$ versus P(A) for 3-bit quantization and 3 x 3 area blocks for the ACPE' C mathematical model. A comparison of FAC and ACPE' C systems indicates that a choice of which system to investigate further can be made only after statistics have been obtained.

3.5 PREVIOUS-AREA CODING (PAC)

Previous area coding involves the coding of area blocks, elements not within an area block, and those area blocks which have the same level as the previous adjacent-area block. By coding these previous area blocks, it is theoretically possible to obtain a larger compression ratio than is possible by coding previous elements not within area blocks.

For PAC the probability of an area block of level j which is not a previous-area block, $P(A'_j)$ is given as

$$P(A'_j) = \frac{A'_j}{\sum_{j=1}^{n} A'_j + \sum_{j=1}^{n} L_j + \overline{PA}}; \tag{16}$$

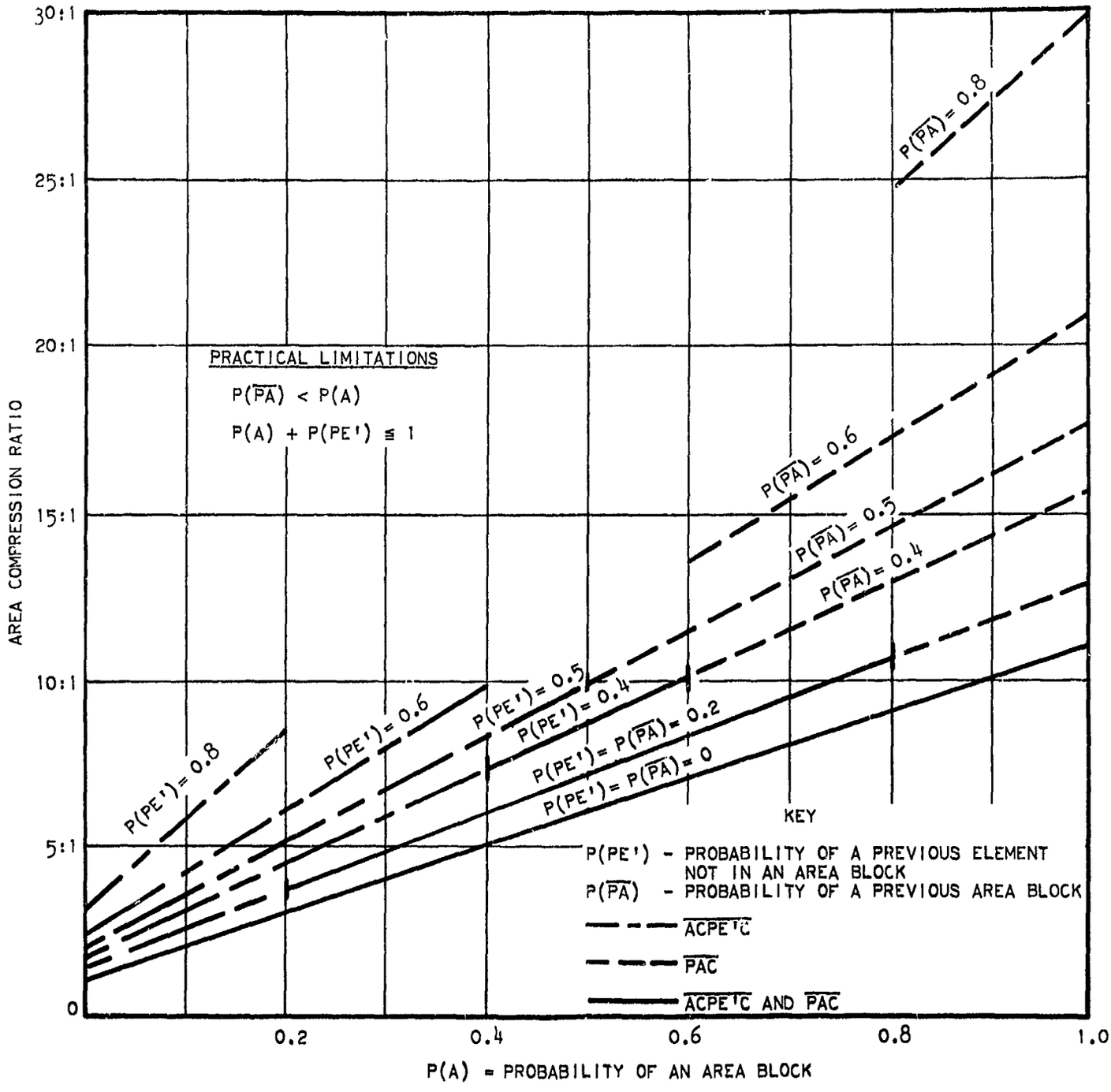

FIGURE B.3-3

COMPRESSION RATIO VERSUS PROBABILITY OF AN AREA BLOCK FOR ACPE'C AND PAC FOR 3-BIT QUANTIZATION AND 3 x 3 AREA BLOCKS

where A'_j represents the number of area blocks of level j in a television frame which are not previous areas and $\overline{PA}$ is the number of area blocks in a television frame which have the same level as the previous adjacent-area block. The probability of an element of level j not within an area block; the probability of a previous area block, $P(\overline{PA})$; and the probability of an area block of any level are given as

$$P(L_j) = \frac{L_j}{\sum_{j=1}^{n} A'_j + \sum_{j=1}^{n} L_j + \overline{PA}}, \tag{17}$$

$$P(\overline{PA}) = \frac{\overline{PA}}{\sum_{j=1}^{n} A'_j + \sum_{j=1}^{n} L_j + \overline{PA}}, \text{ and} \tag{18}$$

$$P(A) = \frac{\sum_{j=1}^{n} A'_j + \overline{PA}}{\sum_{j=1}^{n} A'_j + \sum_{j=1}^{n} L_j + \overline{PA}}. \tag{19}$$

For previous area coding, the total number of elements in a frame is given by

$$\sum_{j=1}^{n} L_j + F \cdot M \sum_{j=1}^{n} A'_j + FM \cdot \overline{PA} = E \cdot L. \tag{20}$$

The use of these relationships yields the compression ratio of PAC to be

$$\overline{PAC} = \frac{6\left[(F \cdot M - 1)\, P(A) + 1\right]}{\sum_{j=1}^{n} P(L_j)\, N_j + \sum_{j=1}^{n} P(A'_j)\, B'_j + P(\overline{PA})K}. \tag{21}$$

relative to a 6-bit PCM source, B'_j is the number of code bits for an area block of level j which is not a previous area block, and K is the number of code bits for a previous area block.

Consider the case of 3-bit quantization and assume that the most probable event is the occurrence of a previous area block, and therefore, assign it a 1-bit code word. Further assume that A'_j and L_j are equally likely and assign 5-bit code words to these events. For this case, the compression-ratio formula simplifies to

$$\overline{PAC} = \frac{6\left[(F \cdot M - 1)\, P(A) + 1\right]}{5 - 4\, P(\overline{PA})}. \qquad (22)$$

This expression for PAC compression is of the same form as that for ACPE'C with P(PE') being replaced by $P(\overline{PA})$. Figure B.3-3 gives $\overline{PAC}$ versus P(A) for 3-bit quantization and 3 x 3 area blocks for the PAC compression model. From Figure B.3-3, it can be seen that P(A) must be greater than 0.5 in order for $\overline{PAC}$ to exceed $\overline{ACPE'C}$. Consider the highly improbable case of a picture in which all previous elements are contained within area blocks. The average previous-element probability, P(PE), for 3-bit quantization and a 40-db signal-to-noise ratio is approximately 0.8. For this particular picture, further assume the very optimistic value of 0.9 for P(PE). The number of 3 x 3 area blocks per television frame for a frame where E = L = 256 is given as

$$\frac{E \cdot L\, P(PE)}{3 \times 3} = \frac{(256)^2\,(0.9)}{9} = 6550 \text{ area blocks.}$$

This leaves

$$(256)^2 - 9(6550) = 6550 \text{ elements,}$$

which must be coded as $L'_{j'}$s or PE''s. This results in a P(A) of

$$P(A) = \frac{6550}{6550 + 6550} = 0.5$$

for this special case. Since P(A) just equals the 0.5 boundary for this specialized example, it does not appear that this boundary could be exceeded for a typical real-life picture. For this reason previous-area coding should no longer be considered for the compression of picture information; PAC may be worth further investigation in connection with facsimile transmission.

3.6 AREA-CODING SIMULATION

Based on the mathematical models, it is apparent that certain forms of area coding have the potential of achieving 6:1 or larger compression. This, coupled with recent work by Nishikawa[a] (where he indicates that the average area size for 3-bit pictures is 54 elements), would lead one to believe that area coding will succeed in obtaining the desired compression goal. Unfortunately, the average area size quoted was not based on a sequential fixed geometric scan, and consequently the value cannot be related to compression as previously described. Furthermore, it becomes apparent that the total number of areas is limited by a real-life sensor such as a vidicon. Hence, it was decided to obtain preliminary area statistics from EDITS by a photographic simulation of area coding and then later to simulate the promising techniques on the ASI-210 Digital Computer.

[a]Nishikawa, S., Massa, R. J., and Mott-Smith, J. C., "Area Properties of Television Pictures," Physical Sciences Research Papers No. 23, Air Force Cambridge Research Laboratories, AFCRL-64-478, June, 1964.

The following experimental procedure was employed to obtain preliminary area statistics: EDITS was used to photographically produce quantized video-amplitude plane pictures of two test photos, Astronaut Cooper and the MIT girl. These quantized video-amplitude plane pictures display only those elements which are of a preselected level. By taking one picture for each intensity level and manually counting the areas and elements, the statistics needed to calculate the compression ratio for the various compression models could be obtained.

The first test subject used was the photograph of Astronaut Cooper. It was felt that if this detailed scene could produce a sufficient number of area blocks to result in a 6:1 compression ratio, the outlook for area coding would be promising. The first set of quantized video-amplitude plane pictures were taken using 3/4 Roberts coding; 3-bit quantization was used since the probability of getting an area block would be greater than if more quantized levels were used and Roberts noise was added to improve the picture quality (minimize brightness contouring effects). The results of the video-amplitude plane pictures were disappointing in that the Roberts noise acted as anticipated and tended to break up uniform regions to the point that few area blocks existed. After a cursory examination of the pictures, it was decided that it would be useless to count the existing areas manually.

Quantized video-amplitude plane pictures were then taken on the Cooper picture for 3-bit PCM. This resulted in the regions being more organized, and therefore a larger number of area blocks existed. Although the number of area blocks increased with 3-bit PCM, the annoying contouring also increased. The photographs for the 3-bit PCM and 3/4 Roberts areas are shown in Figure B.3P-1 through B.3P-4.[a]

From these results it appears that satisfactory compression could not be obtained by applying area coding to a detailed picture. To determine the possibility of using area coding on a more uniform scene, quantized video-amplitude plane pictures were taken for the MIT girl picture using 3/4 Roberts only. Although these results were more encouraging than those of Cooper for 3/4 Roberts, regions which would normally be of the same intensity were broken up by the Roberts noise to the extent that a manual count of area blocks was not merited.

3.7 AREA-STATISTICS-TAKER DESIGN

The preliminary circuit design was completed on a subsystem for EDITS which would permit the desired statistics to be taken. This subsystem would be placed after the PEQ system, thereby permitting areas of both PCM and PCM-PEQ[b] transmission to be studied. The system is designed to compare the nine

[a] Figure numbers containing P refer to photographs in Volume II of this report.

[b] See paragraph 4.2 of this Appendix.

elements of a 3 x 3 area (or 4 elements of a 2 x 2 area) in a nonoverlapping block manner as shown in Figure B. 3-4. If the nine elements of Area A (or four elements of Area A-1) are all of the same level, the area is counted; if one or more of the nine (four) elements is of a different level, the entire block is discarded. The system then compares the nine elements of Area B (or four elements of Area B-1) and the elements of each of the succeeding nine (or four) element blocks in the same manner as for Area A (or Area A-1)

The basic principle of operation of the circuit is that if there are N elements of the same level in a row, there will be N-1 pairs of adjacent elements of the same level. By comparing adjacent elements of a row and counting the number of pairs of adjacent elements which are alike, N elements in a row can be checked for equality by using only two registers.

For the following operational discussion, refer to the sequence timing diagram, Figure B. 3-5, and the area-statistics taker block diagram, Figure B. 3-6. This explanation is for 3 x 3 area blocks; the operation is much the same for 2 x 2 area blocks. It is assumed that a block within the interior of the picture is about to be tested; the elements of this area block are numbered as shown in Figure B. 3-7. Elements 8 and 7 are presently in Registers A and B, respectively; elements 5 and 4 are in Registers C and D, respectively; and elements 2 and 1 are in Registers E and F, respectively. The elements stored in Registers A and B are compared and, if equal, the pair counter receives a pulse upon the occurrence of Display Gate No. 2. On Display Gate No. 1, the contents of Register A are shifted into Register B and element 9 is read into Register A. Elements 8 and 9 are then compared and, if equal, the pair counter is again pulsed when Display Gate No. 2 occurs; if either pair of elements are unequal, the pair counter will not reach the count of two, which is necessary for the AND gate to be satisfied. The same comparison and counting technique is simultaneously employed on elements 1, 2, and 3 by means of Registers E and F and elements 4, 5, and 6 by Registers C and D. The delay lines result in the elements in Registers A and C and the elements in Registers C and E being separated by one line of video data; this enables the elements of the three successively scanned lines of the picture to be compared and counted simultaneously. The comparators between Registers B and D and between Registers D and F are necessary to ensure that equality among the elements exists between lines. The level of the area block is specified by the level switches.

The picture is grouped into 3 x 3 area blocks by the use of two counters. The horizontal set counter divides the picture vertically into sets of three elements; this is done by the counters yielding a negative level for two counts and a zero level for one count. The negative level satisfies the AND gates and allows equal elements to be counted; the zero level inhibits the AND gates and thereby separates adjacent elements of adjacent-area blocks. The picture is divided horizontally by the line counter, which has a negative output level every third line. The statistics taker will receive a pulse when sampled (thereby noting that a nine-element area block of the proper level has been detected) if (1) all three pair counters have reached the proper count of two, (2) the between line

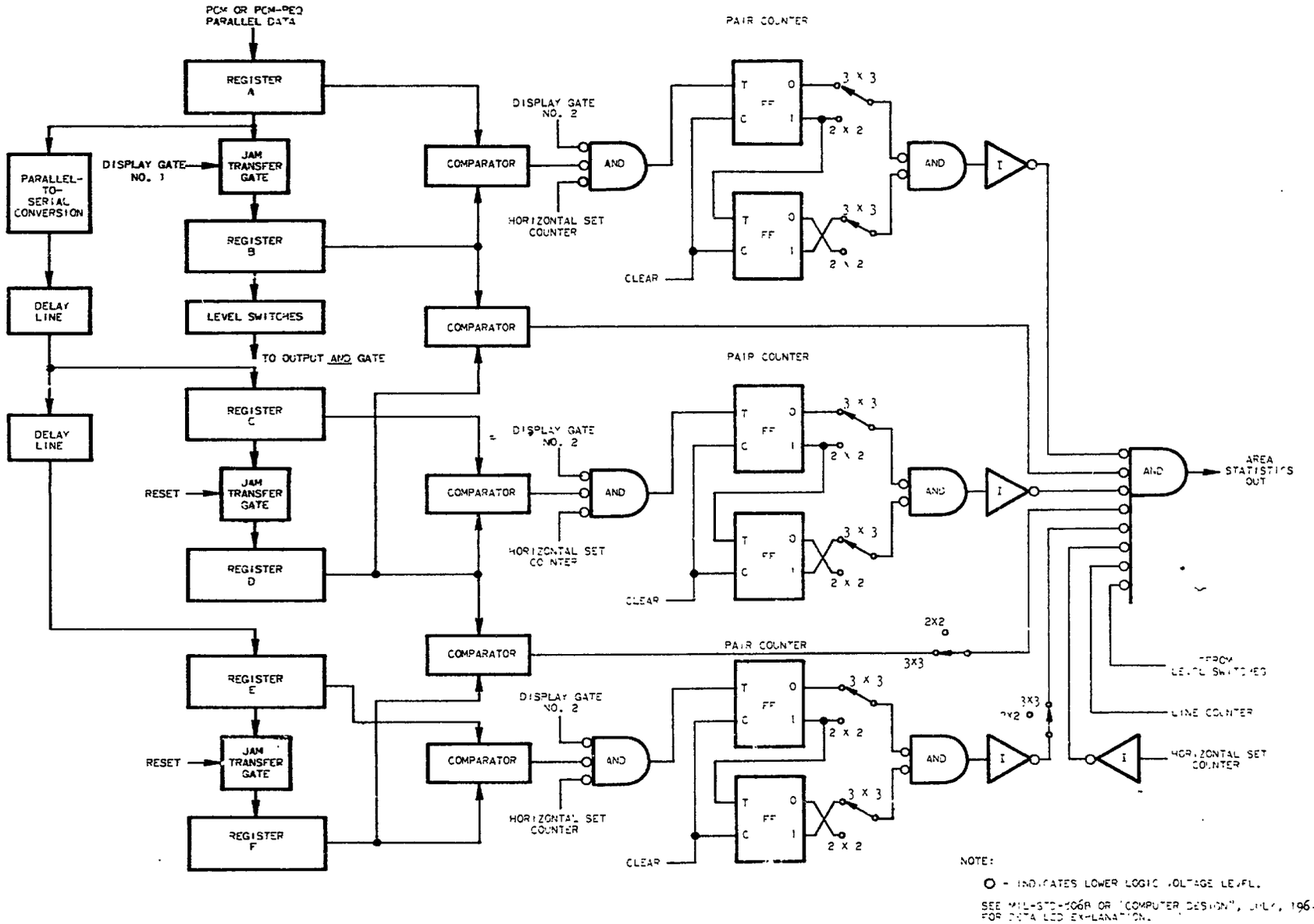

FIGURE B. 3-6

AREA STATISTICS-TAKER BLOCK DIAGRAM

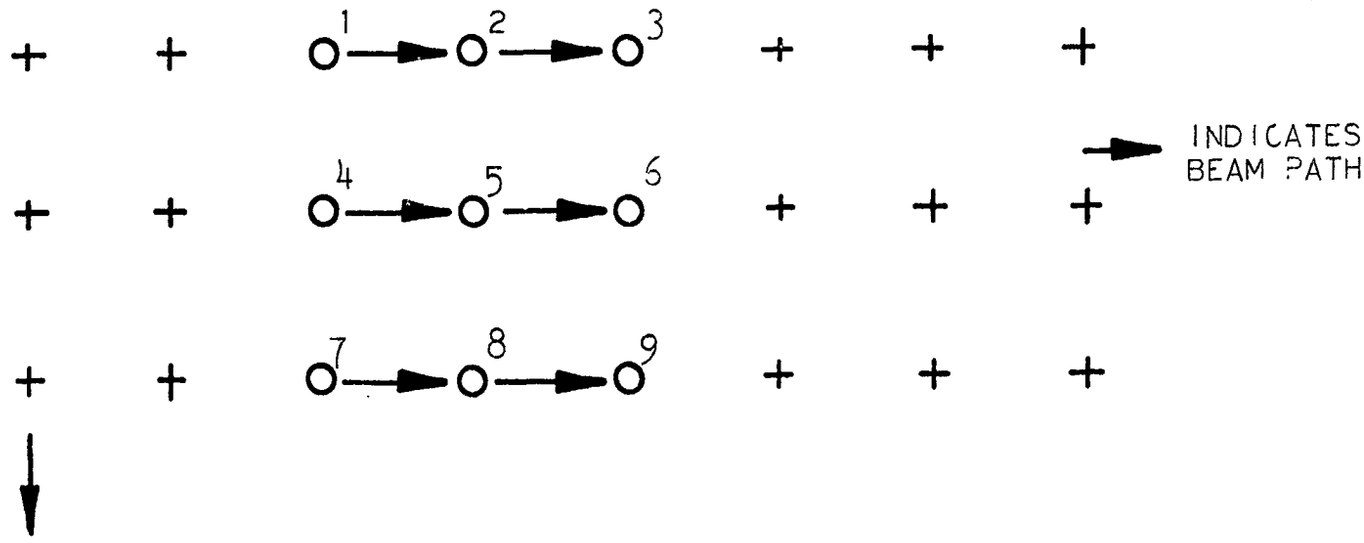

FIGURE B.3-7

AREA BLOCK NUMBERING

comparators and the level switches are satisfied, (3) the horizontal set counter has reached the third count, and (4) the line counter is negative.

The 3 x 3 area counter is easily converted to a 2 x 2 area counter by the use of switches. To obtain 2 x 2 area statistics, the pair counters are set to be satisfied by a count of one, the horizontal set counter alternates negative and zero levels, the line counter is negative on every second line, and the excess between line comparator and pair counter are disconnected from the output AND gate.

3.8 COMPUTER SIMULATION OF AREA CODING

Although it was initially assumed that the necessary area statistics would be taken on EDITS by use of the area-statistics taker, it was decided upon completion of the ASI-EDITS interface that the additional flexibility gained by the interface would not warrant completion of the statistics taker. A computer program was written which would analyze a frame of data and determine the number of 2 x 2, 3 x 3, 4 x 4, and 5 x 5 area blocks in the sequentially scanned frame and calculate the compression, using flat area coding. Flat-area-coding compression was calculated since, of the four techniques analyzed, it represented the best compromise between compression and complexity. The data analyzed can be quantized to 1 through 6 bits per element and P(A) can be obtained for the four block area sizes and the corresponding compression calculated. Four test objects were scanned on EDITS and placed on magnetic tape for computer processing. Each picture was quantized to 6 and 4 bits per element. These photographs, given in Volume II, Section B.3P are (1) the Gemini capsule, (2) the Apollo mock-up, (3) the close-up view of astronaut Cooper, and (4) the MIT girl picture. To determine the efficiency of the FAC technique, P(A) was obtained for the four pictures with the four area sizes for 6-bit and 4-bit quantization and is given in Figures B.3-8 and B.3-9, respectively.

The FAC compression can then be plotted and is given in Figure B.3-10 relative to 6 bits. If nonlinear amplification such as preemphasis and deemphasis is used and 4-bit quantization is employed, area coding with 5 x 5 area blocks could result in a 5:1 compression for Gemini-type scenes and 3.5:1 compression for Cooper-type scenes. Although this represents an information-preserving technique, the desired goal of 6:1 was not achieved with even the coarser quantization. For 6-bit quantization FAC results in compressions of 1.5:1, which is well below the desired 6:1 goal. To determine further the efficiency of area coding, the 4-bit data compression was made relative to 4-bit quantization, and compressions of 3.5:1 for Gemini type scenes and 2.3:1 for Cooper type scenes were computed. This approaches the 1-bit-per-element goal, but subjectively the quality of 4-bit data is not equivalent to the 6-bit source. Figure B.3-11 plots the compression as a function of the area block size for the four scenes.

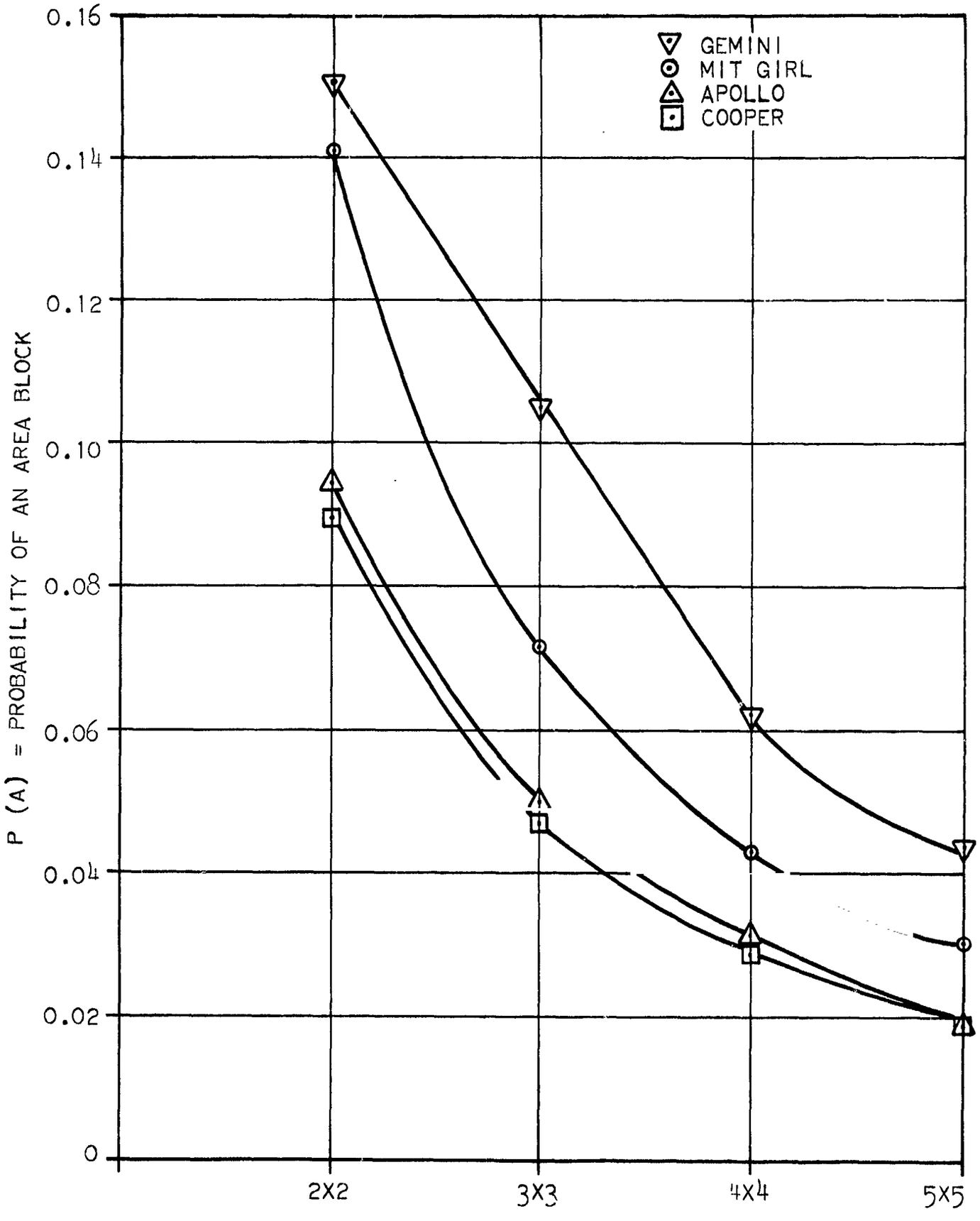

FIGURE B.3-8

P(A) VERSUS AREA BLOCK FOR 6-BIT QUANTIZATION

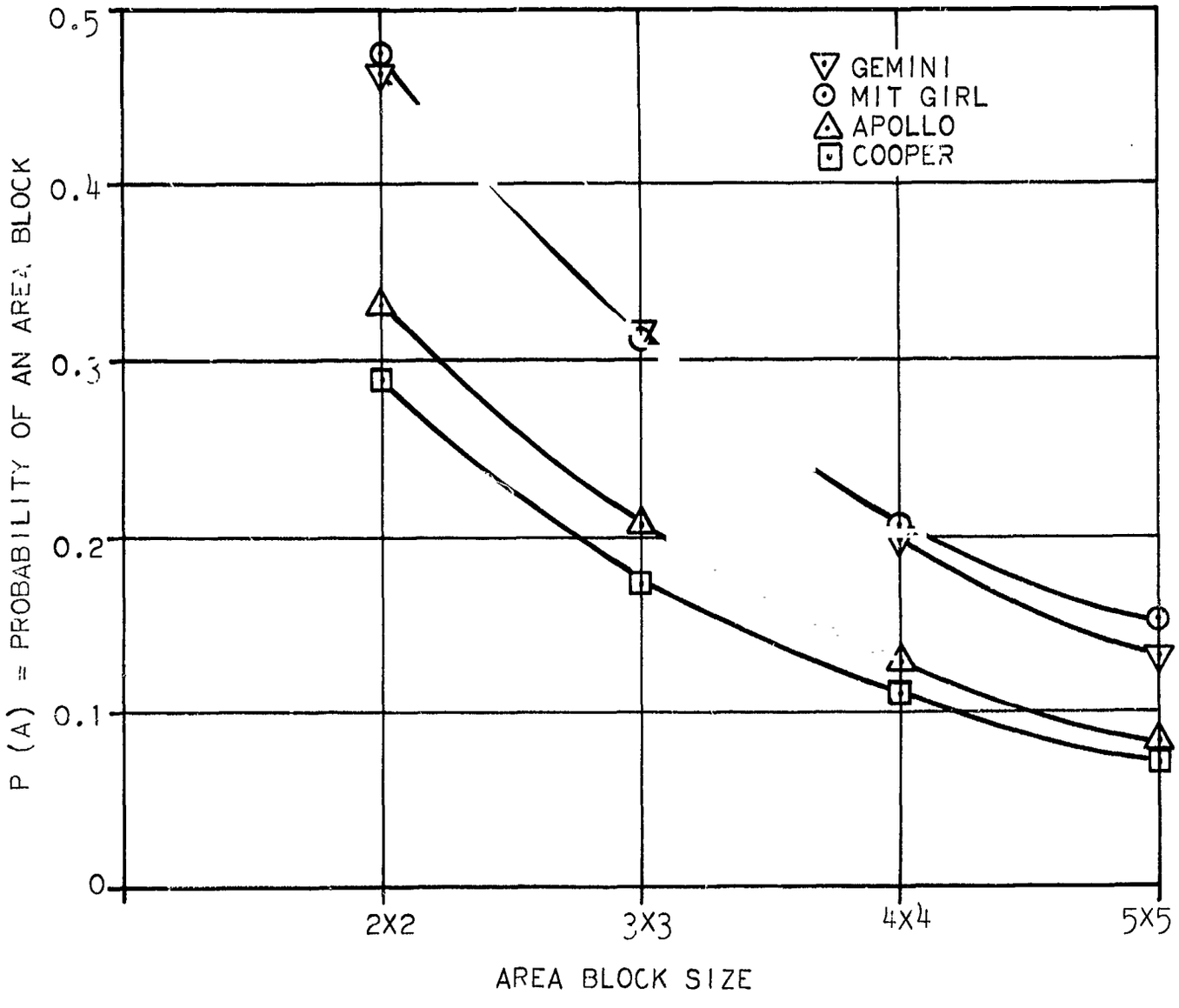

FIGURE B.3-9

P(A) VERSUS SIZE AREA BLOCK FOR 4-BIT QUANTIZATION

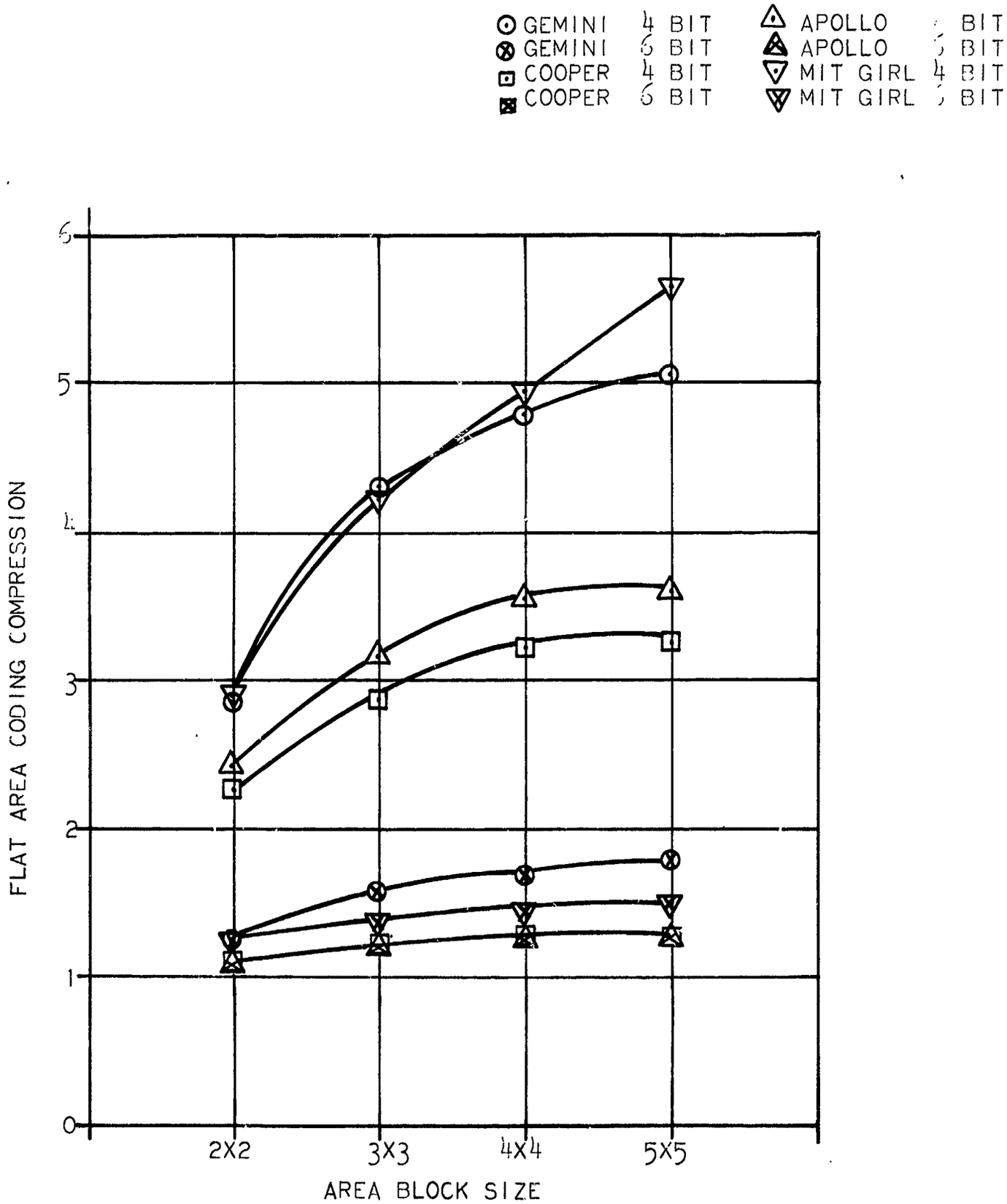

FIGURE B. 3-10

FAC COMPRESSION AS A FUNCTION OF AREA SIZE RELATIVE TO 6 BITS

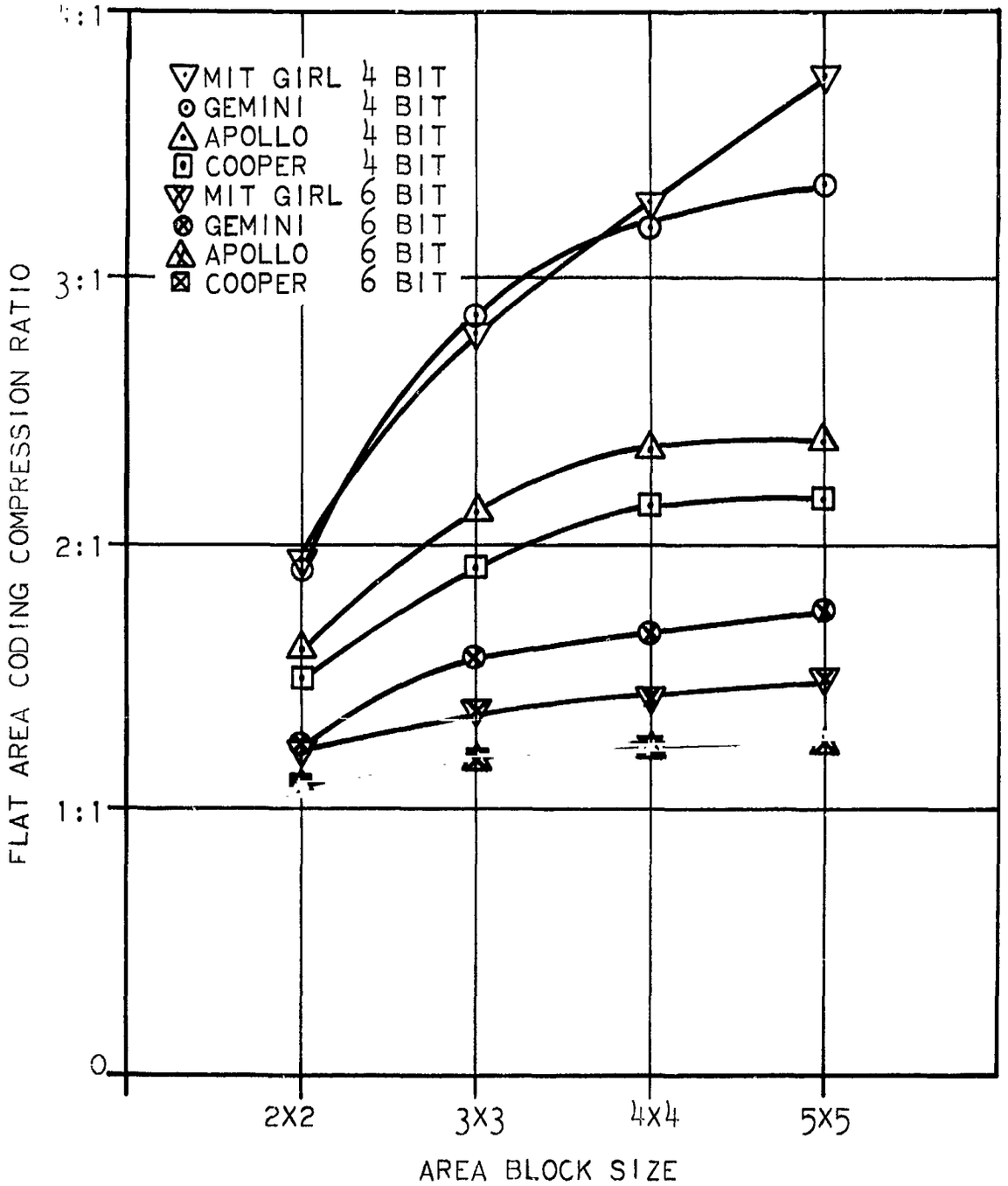

FIGURE B.3-11

COMPRESSION RATIOS VERSUS AREA BLOCK SIZE FOR FLAT-AREA CODING WITH 4-BIT QUANTIZATION RELATIVE TO 4 BITS

3.9 CONCLUSIONS

FAC compression offers the best compromise between compression and implementation problems for the various area-coding techniques studied. The gross average compression values for FAC exceed those of any of the previous techniques previously studied [a] such as delta modulation, Roberts encoding, previous-element encoding, and run-length coding. Although relative to these other methods area coding does not represent a substantial increase in compression, the technique is an information-preserving one that may have other applications. However, based on the desired goal of a 6:1 compression, area coding is eliminated in its present form as a satisfactory technique to achieve this compression goal.

[a] Final Report MSC Advanced Television Study, July 31, 1963.

SECTION 4

N-DIMENSIONAL PROCESSING

4.1 INTRODUCTION

In theory, it is possible to operate on the video signal at various points in a television system with the objective of increasing the efficiency of the system. Three areas of processing were investigated in this study. These areas were: (1) two-dimensional optical processing before the sensor; (2) one-dimensional analog processing after the sensor; and (3) one-dimensional digital processing after the analog-to-digital converter. An analysis of each of these areas is presented in the following sections.

4.2 TWO-DIMENSIONAL OPTICAL SPATIAL FILTERING

4.2.1 Introduction

In a generalized video system it is possible to operate on the signal at various portions of the system to increase system efficiency. This section will concern itself with the investigation of the possibility of operating on the optical signal in advance of the video sensor. In theory it will be shown that it is possible to perform exotic experiments with optical spatial filtering; however, the value and use of these experiments becomes debatable when practical constraints are considered. Two separate areas that could have application to a televised manned spacecraft application were considered. The first area considered the application of techniques of spatial filtering using coherent illumination while the second area was concerned with the application of techniques of spatial filtering using incoherent illumination.

In the coherent case, the results were obtained using collimated monochromatic light and for all practical purposes the results are similar to those which would be obtained with coherent illumination. Since coherent illumination imposes physical constraints of size and power for a typical space mission, the monochromatic case will be referred to as the coherent illumination case and will be assumed to be physically realizable.

The incoherent case can be considered analogous to the coherent case; but the types of filters are quite different. Before the experimental set-up is described, the discussion of program goals and the results of the analysis of optical techniques will be presented. A bibliography of references applicable to spatial filtering is given in paragraph 4.2.8. It was the goal of the spatial filtering analysis to determine if (1) the spatial filtering techniques could result in the desired compression of 6:1 and/or (2) the techniques could be used in conjunc-

tion with various compression techniques to achieve the desired compression goal.

4.2.2 Coherent Systems

A coherent optical system is one in which relative phases of the light waves in various parts of the system are invariant with time, and it is one which requires a point source of light for illumination. Point-source illumination then implies that phase fronts, or surfaces of constant phase, exist along the light path; therefore, the illumination striking a plane has a phase which is time invariant with respect to the phases at all other points on the plane. In particular, if the light is collimated and strikes the plane at normal incidence, all points on the plane have the same phase.

Consider now Figure B.4-1 which acts as a two dimensional Fourier analyzer.

S_1 = point source of monochromatic light
L_1 = collimating lens
P_1 = input function (transparency), f (x, y)
L_2 = spherical lens
P_2 = frequency plane, F(p, q)

If f(x, y) denotes the specular amplitude transmission of the transparency in plane P_1 and F(p, q) denotes the complex amplitude distribution of light in plane P_2, the illumination is a monochromatic plane wave when d = f. With the lens coherently illuminated the light-amplitude distributions at the front and back focal planes are related by a two-dimensional Fourier transform.

$$F(p, q) = \iint_{-\infty}^{\infty} f(x, y)\, e^{j(px + qy)}\, dx dy \qquad (1)$$

where p and q represent spatial frequency variables in radians per unit distance; however, the variables in P_2 are in units of distance related by the scale factors of

$$\xi = \frac{\lambda f p}{2\pi} \qquad (2)$$

$$\eta = \frac{\lambda f q}{2\pi} \qquad (3)$$

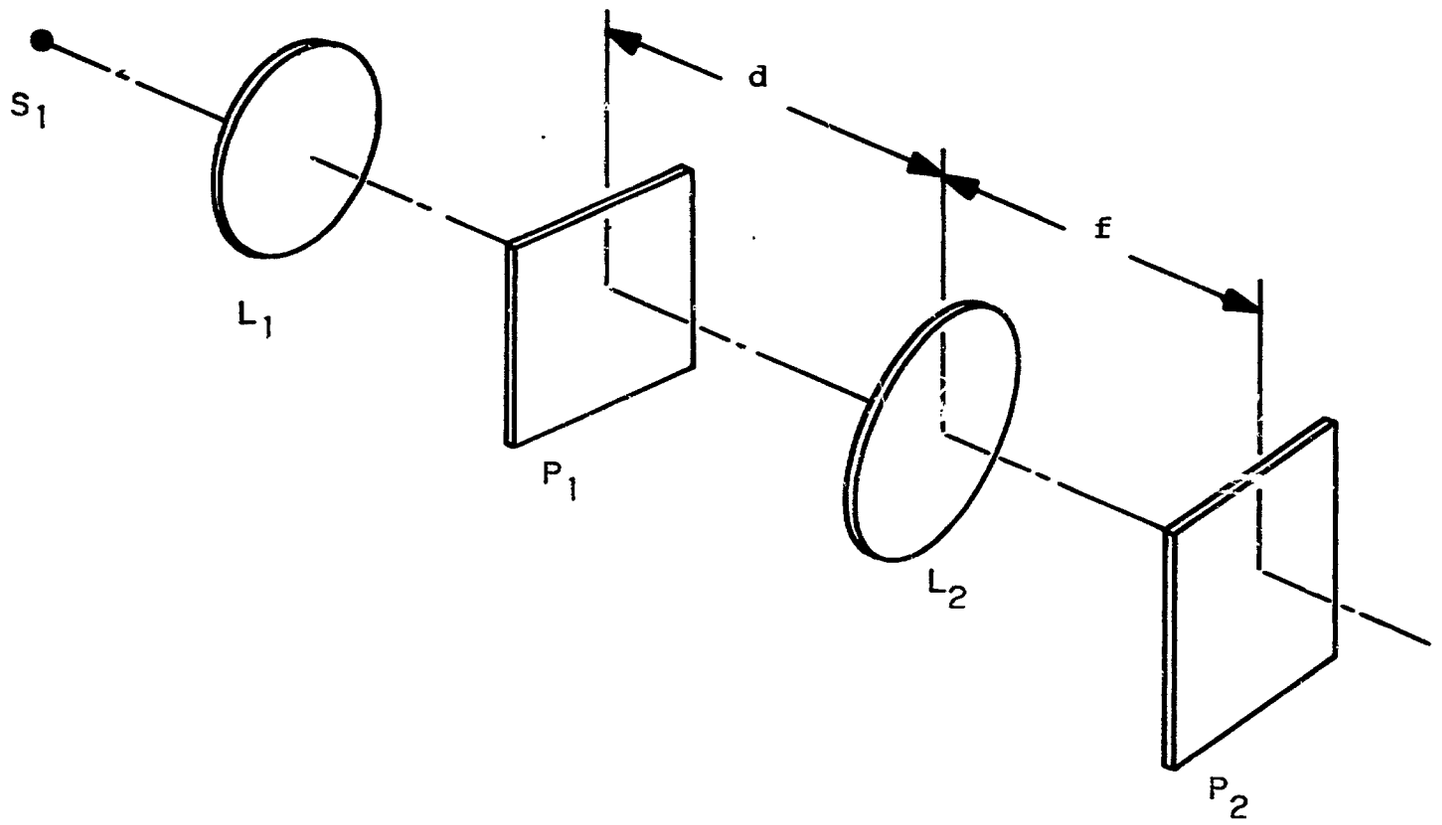

FIGURE B.4-1

OPTICAL FOURIER ANALYZER

where

ξ = the direction parallel to x,
η = the direction parallel to y,
λ = the wavelength of the illumination,
f = the focal length of the spherical lens, and
$p/2\pi$ = spatial frequency (lines/mm).

Utilizing the fact that a spherical lens can take the Fourier transform of a complex distribution of light, it is possible to construct an optical system by a sequence of lenses to take successive Fourier transforms. Figure B.4-2 shows a coherent optical processing system, where

S_1 = point source of monochromatic light,
L_1 = collimating lenses,
P_1 = input plane (transparency), f (x, y),
L_2 = objective lens,
P_2 = frequency plane, F (p, q),
L_3 = imaging lens, and
P_3 = output plane, r(x, y).

This can be readily shown by considering the following development. Assume that the detail in the transparency P_1 is sufficiently coarse that Huygen's principle can be applied. A monochromatic electromagnetic wave is described by its phase and magnitude as a function of the vector space. The space component of the electrical field vector in the x direction is given by

$$E_x = A(x, y, z) \cos [\omega t + \phi (x, y, z)] \quad (4)$$

where

A = amplitude factor,
ϕ = phase factor, and
ω = radian frequency of the wave.

Since the polorization effects are not of interest, any field vector can be represented by E. If the optical axis is taken in the z direction and only a few values of z are of concern, the field at any point z, can be denoted as E_1 where

$$E_1 = A(x, y) \cos [\omega t + \phi (x, y)] . \quad (5)$$

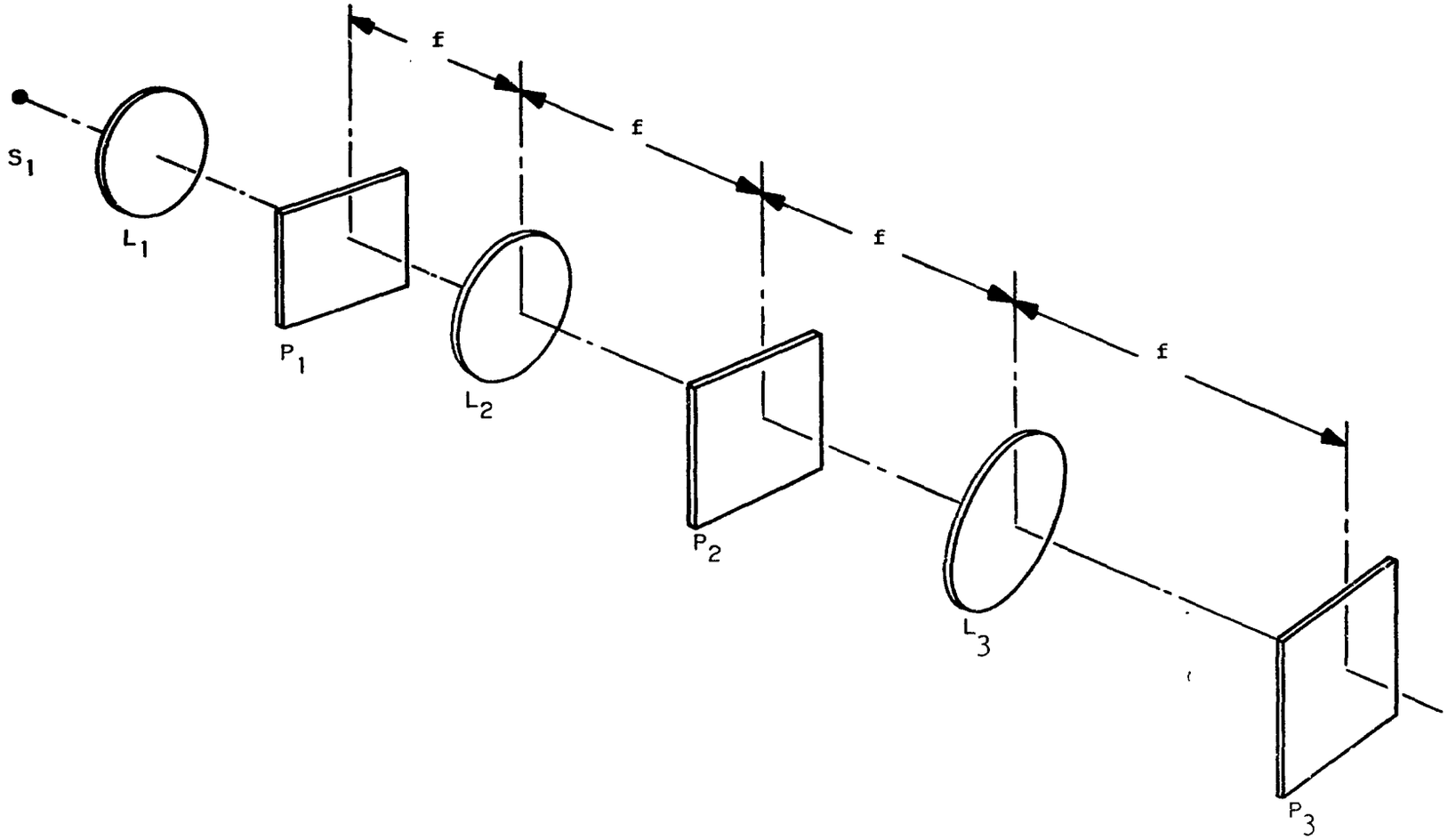

FIGURE B.4-2

COHERENT OPTICAL PROCESSING SYSTEM

but this can be written as

$$\hat{E}_1 = A(x, y)\, e^{j\phi\,(x, y)} \tag{6}$$

Consider now a transparency described by a transmission function $t^2\,(x, y)$ and a thickness function $\alpha\,(x, y)/2\,(n - 1)$ in wave lengths for $0 \leq t \leq 1$ and n the index of refraction of the transparency. The transparency can now be considered as a signal function

$$S\,(x, y) = t(x, y)\, e^{j\alpha\,(x, y)} \tag{7}$$

Light incident on this transparency yields an emergent wave

$$E_2 = A(x, y)\, t\,(x, y) \cos\left[\omega t + \phi\,(x, y) + \alpha\,(x, y)\right] \tag{8}$$

or

$$\hat{E}_2 = S\,\hat{E}_1. \tag{9}$$

The energy ξ of a light wave E is proportional to the time average E^2; therefore, for coherent optical systems

$$\xi = k\,\hat{E}\,\hat{E}^* \tag{10}$$

Consider now Figure B.4-3.

The light waves at planes P_1, P_2, and P_3 are denoted by

$$\hat{E}_1\,(x^1,\ y_1) \tag{11}$$

$$\hat{E}_2\,(x_2,\ y_2) \tag{12}$$

$$\hat{E}_3\,(x_3,\ y_3) \tag{13}$$

$\hat{E}_3$ and $\hat{E}_1$ form a Fourier pair with a phase factor $e^{j\beta\,(x_3,\ y_3)}$, that is

$$\hat{E}_3\,(x_3,\ y_3) = \mathcal{F}\left[(\hat{E}_1\ \ (x_1,\ y_1) \cdot e^{j\beta\,(x_3,\ y_3)}\right] \tag{14}$$

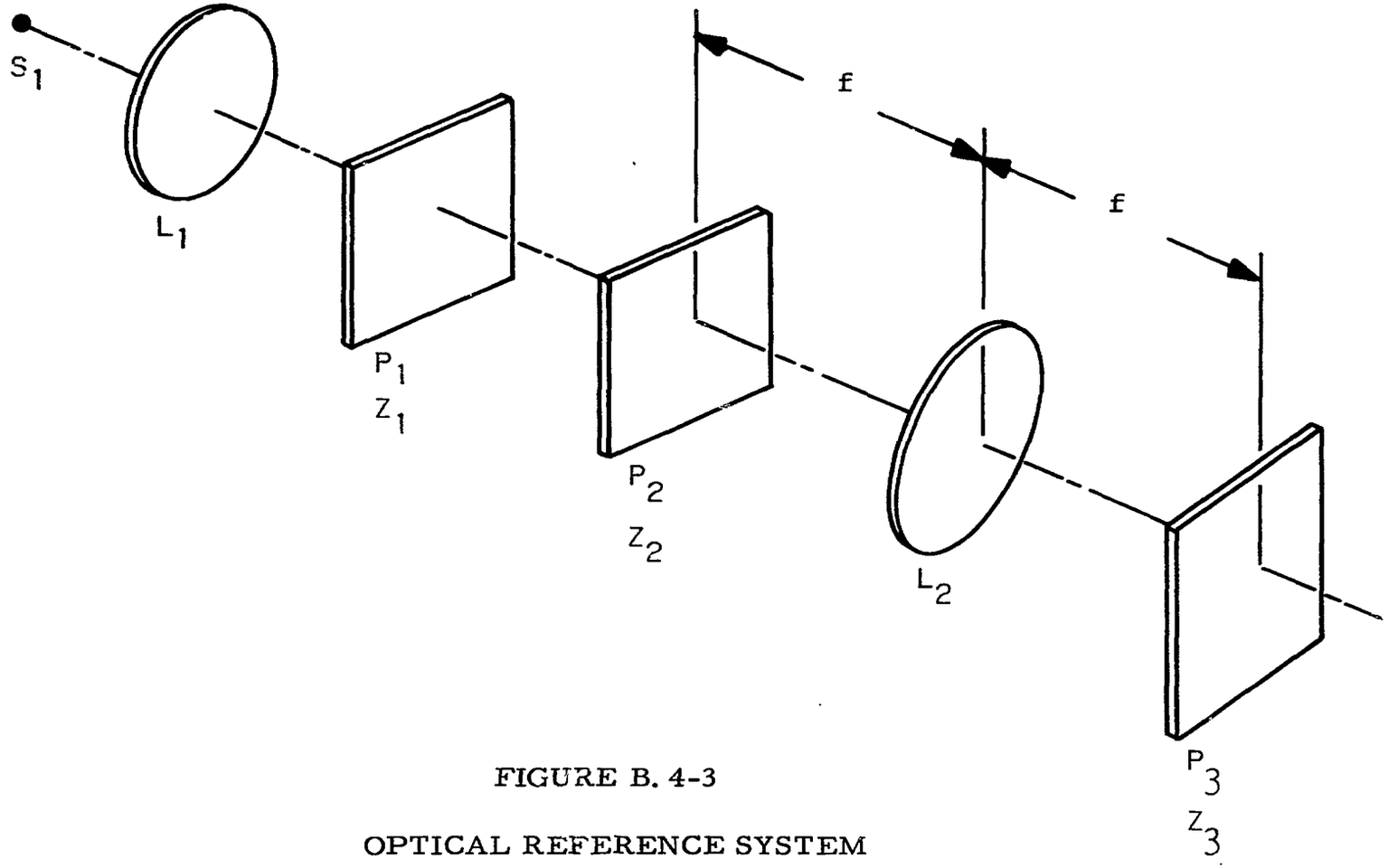

FIGURE B. 4-3

OPTICAL REFERENCE SYSTEM

where $\beta = f(Z_1)$. An exact Fourier transform exists between $\hat{E}_3$ and $\hat{E}_2$, that is, $\beta\ (x_3,\ y_3) = 0$ for $Z_1 = Z_2$. An exact transform does not exist anywhere else with respect to lens L_2, that is, $\beta\ (x_3,\ y_3) \neq 0$ for $Z_1 \neq Z_2$. The transformation from time domain (analog of the spatial domain) to the frequency domain requires the kernel function $e^{-j\omega t}$ whereas the transformation, from the frequency domain to the time domain employs the conjugate kernel $e^{+j\omega t}$.

A lens always introduces the kernel $\exp\left[j\ (2\pi/\lambda f)\ (x_n\ x_{n+1} + y_n\ y_{n+1})\right]$ in passing from plane P_n to plane P_{n+1}. If the scale factor of $\omega_x = \frac{-2\pi}{\lambda f}\ x_2$ and $\omega_y = \frac{-2\pi}{\lambda f}\ y_2$ is introduced, the kernel becomes $\exp\left[-j\ (\omega_x\ x + \omega_y y)\right]$. Therefore, since the $\mathcal{F}\ \{\mathcal{F}\ [f\ (x)]\} = f\ (-x)$, x_1 is mapped into $-x_3$ as the resultant of two successive transforms and the image at P_3 is reversed. If the coordinate system of P_3 is reversed, $\hat{E}\ (P_3) = \mathcal{F}^{-1}[E\ (P_2)]$.

If there is no transparency at P_2, lens L_3 takes the transform of the distribution at P_2 and at P_3 the distribution is

$$r\ (x,\ y) = \frac{1}{4\pi^2} \iint_{-\infty}^{\infty} F\ (p,\ q)\ e^{j\ (px\ +\ qy)}\ dp\ dq\ , \tag{15}$$

that is,

$$r\ (x,\ y) = f\ (-x,\ -y) \tag{16}$$

This is under the assumption that the system has unity magnification and sufficient bandwidth to pass the highest spatial frequency of the input function. Note that the output function is the inverted image of the input function.

If a transparency is now placed at P_1, and a transparency at P_2, whose transmission is given by $H\ (p, q)$, the modified light distribution at P_2 is

$$R\ (p, q) = F\ \ (p,\ q)\ \ H\ (p,\ q)\ . \tag{17}$$

The lens L_3 takes the Fourier transform of this distribution and displays it in plane P_3 as

$$r(x,\ y) = \frac{1}{4\pi^2} \iint_{-\infty}^{\infty} F\ (p,\ q)\ H\ (p,\ q)\ e^{j\ (px\ +\ qy)}\ dp\ dq \tag{18}$$

By use of the convolution theorem,

$$r(x, y) = \int_{-\infty}^{\infty}\int f(x-u, y-v)\, h(u, v)\, du\, dv \qquad (19)$$

From Equations 18 and 19 it is apparent that spatial filtering of some sort can take place by properly constructing a transmission filter H (p, q). The most obvious way to attempt to construct a filter is to use photographic film. Unfortunately film is sensitive to only intensity and not phase; therefore, other ways must be sought. In the past, the complex amplitude and phase distributions have been realized by synthesizing the two components separately and using the principle of superposition. This was accomplished by recording the amplitude $[H(p, q)]$ of the required complex function $[H(p, q)]$ on ordinary film and the phase function argument $[H(p, q)]$ by evaporating thin films on glass plates. Fortunately there exist optical techniques that allows the generation of light distributions proper phase and amplitude without the use of auxiliary phase plates. Figure B. 4-4 shows an optical technique construction of complex filters.

S_1 = point source
L_1 = collimator lens
L_2 = reference lens
P_1, P_2 = cross polarizers
P_3 = pin hole
LG= reference signal in liquid gate
L_3 = objective lens
P_4 = recording film plane

In plane P_4 the light distribution is given by

$$G(p, q) = R_o\, e^{j\, pb} + H(p, q). \qquad (20)$$

The liquid gate is necessary since variations in film thickness, refractive index, and surface quality affect the phase in a random fashion. This results in nonuniformities in the optical system since the wavefronts are disrupted and diffusion of the light at image point results. The diffusion results in displacement and/or defocussing effects. Interference patterns result in the form of parallel lines, concentric circles, and saddle points. The liquid gate overcomes these irregularities, but poses problems such as the difficulty in handling the liquid and the elimination of phasing. However, the advantages of the liquid gate in the form of reduction of light phase variation, ease of retaining film in a plane by the glass-plate cell, and the reduction of noise due to scratches and rough surfaces far outweigh the disadvantages.

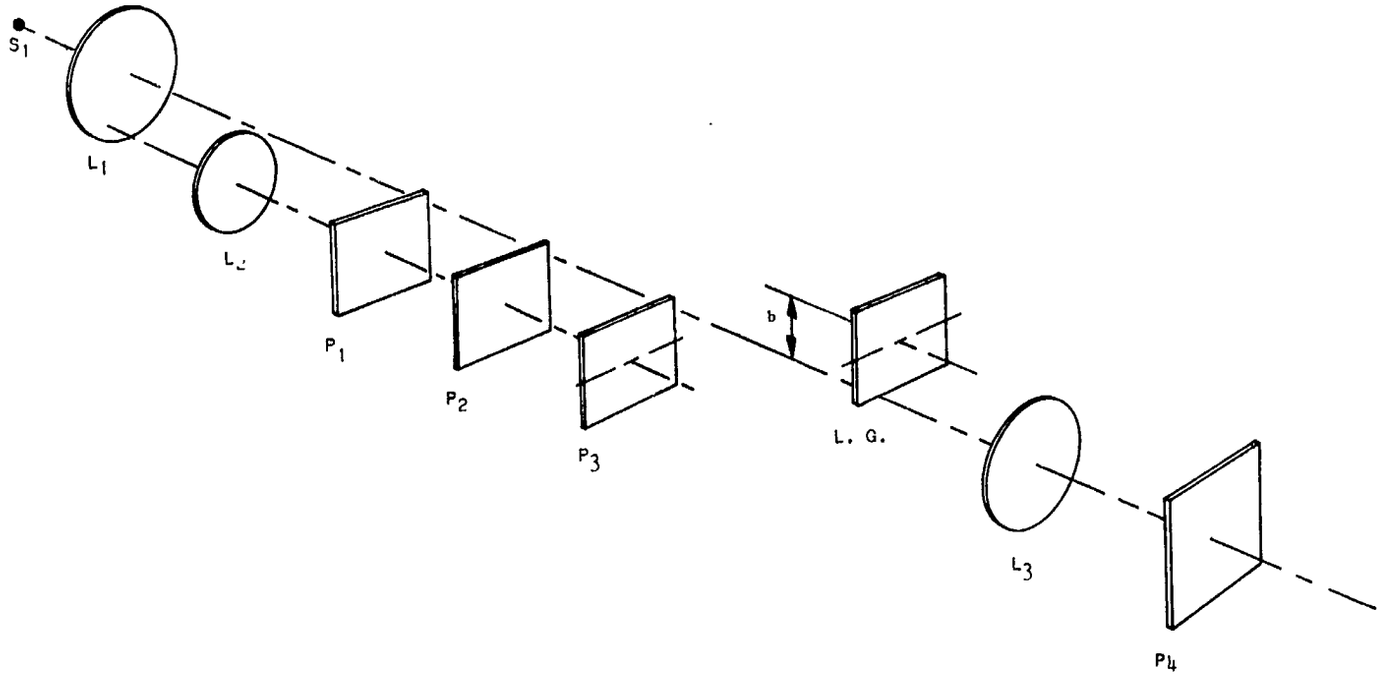

FIGURE B.4-4

TECHNIQUE FOR CONSTRUCTING COMPLEX FILTER

A near optimum filter that passes only a prespecified number of spatial frequencies and rejects all others may be constructed. This could be accomplished by selectively phasing the frequencies occupied by the signal so as to build up a large peak response to the desired signal while leaving the response to undesired frequencies essentially unchanged.

Consider now a mathematical model of the desired process. Let g (x, y) be the intensity function which is usually the reflectivity of the earth to radiation in some part of the electromagnetic spectrum. A sensor with the appropriate response takes a two-dimensional transform of the scene, a recording process another transformation, and finally a third transformation for the final processing of the information. Figure B. 4-5 represents the generalized process.

The original scene is subjected to a transformation T_1, and associated with the sensor is sensor noise and we have

$$N_1 = T_1 \left[g (x, y) \right] - s (x, y), \tag{21}$$

where s (x, y) is the sensor noise being a random process with a spectral density S (p, q) at N_2, the resultant is

$$N_2 = T_2 \left\{ T_1 \left[g (x, y) \right] - s (x, y) \right\} - n (x, y); \tag{22}$$

where n (x, y) is a random process of the film-grain noise with a spectral density N (p, q). Now let f (x, y) be equal to

$$f (x, y) = T_2 T_1 \left[g (x, y) \right] - T_2 s (x, y). \tag{23}$$

If b (x, y) is the desired signal out, we want to operate on

$$b (x, y) = f (x, y) - n (x, y) \tag{24}$$

to obtain the desired results. Hence it is necessary to determine whether a filter can be constructed that would maximize the ratio of the peak signal to the mean square noise energy.

Let
$$H (p, q) = \frac{k B^* (p, q)}{N (p, q) + T_2 S (p, q)} \tag{25}$$

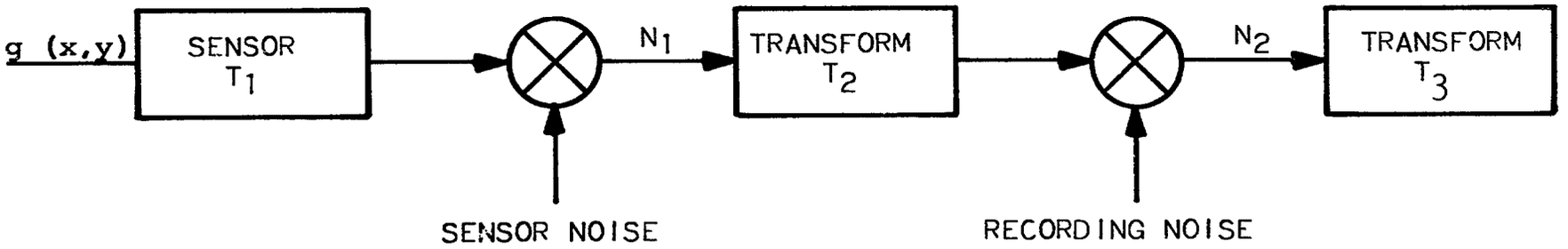

FIGURE B. 4-5

GENERALIZED SYSTEM MODEL

where

$$B(p, q) = \int_{-\infty}^{\infty}\int b(x, y)\, e^{j(px + qy)}\, dx\, dy \tag{26}$$

The signal to noise is therefore given by

$$S/N = \frac{1}{4\pi^2} \int_{-\infty}^{\infty}\int \frac{\left| B(p, q) \right|^2}{N(p, q) + T_2\, S(p, q)}\, dp\, dq \tag{27}$$

Figure B.4-6 represents one approach to this

where

$$r(x, y) = \frac{1}{4\pi^2} \int_{-\infty}^{\infty}\int B(p, q)\, H(p, q) e^{-j(px + qy)}\, dp\, dq \tag{28}$$

Since the noise is assumed to be uniform for all frequencies of interest

$$r(x, y) = k \int_{-\infty}^{\infty}\int f(x-u,\ y-v)\, b^{*}(u, v)\ du\, dv, \tag{29}$$

which is merely the crosscorrelation process.

4.2.3 Noncoherent System

The functional difference between coherent and noncoherent systems is that the former is linear in amplitude and the latter is linear in intensity. In general the noncoherent system does not act as a Fourier analyzer. For a noncoherent system, the optimum filter (reference function) must be realized in the space domain rather than the frequency domain. The problem is to find a reference function whose intensity transmission is

$$h(x, y) = \frac{1}{4\pi^2} \int_{-\infty}^{\infty}\int H(p, q)\, e^{j(px + qy)}\, dx\, dy. \tag{30}$$

If it can be assumed that the noise has a uniform spectral density for all (p, q) the solution to Equation 30 is

$$h(x, y) = s^{*}(-x, -y). \tag{31}$$

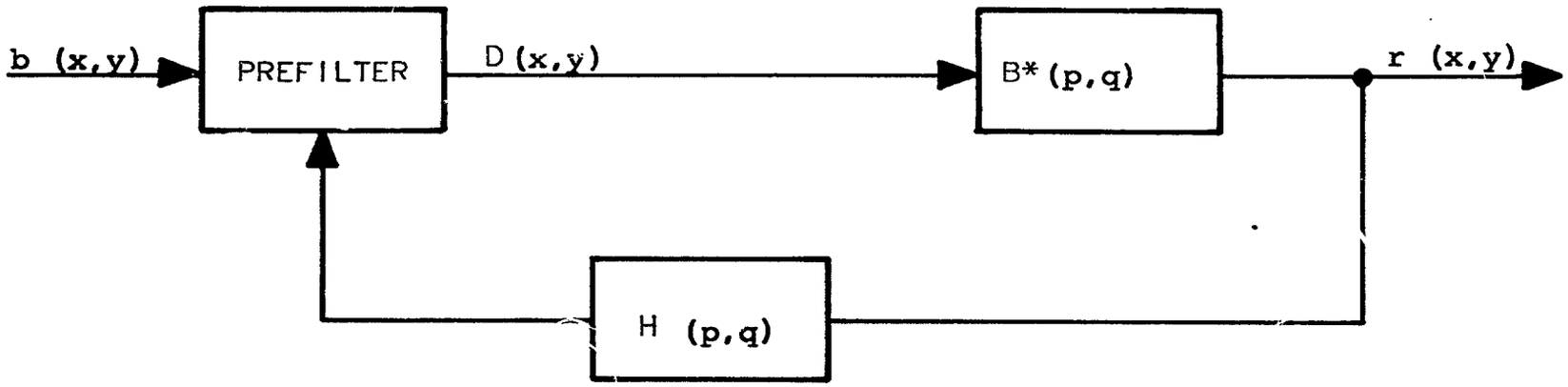

FIGURE B. 4-6

FILTER ANALYSIS REPPESENTATION

Unfortunately in the practical case, the noise spectral density is not uniform and in general h (x, y) is usually a complex function. To realize complex functions is quite a difficult problem. Consider now Figure B. 4-7. Where P_1 is an extended source of diffuse illumination not necessarily monochromatic, P_2 contains the transparency f (x, y), and P_3 contains the reference function.

The operation can be described as follows. Consider a ray of light from point (x, y) in P_1. This light passes through the point (x_2, y_2) in P_2 and is attenuated by a function f (x_2, y_2). The ray then passes through the reference function at a point (x_3, y_3) and is further attenuated by s $(-x_3, -y_3)$. From the geometry of Figure B. 4-7.

$$\frac{x_4}{\quad} = \frac{x_2 - x_3}{d} \tag{32}$$

and

$$\frac{y_4}{f} = \frac{y_2 - y_3}{d} \tag{33}$$

The intensity of the light in the image of the point (x_1, y_1) is the summation of all rays parallel to the ray described by

$$r\,(x_4, y_4) = \int_{-\infty}^{\infty}\int f\,(x_2, y_2)\; s\,(-x_3, -y_3)\; dx_3\; dy_3, \tag{34}$$

which can be rewritten as

$$r\,(x_4, y_4) = \int_{-\infty}^{\infty}\int f\,(x_2, y_2)\; s\left(\frac{x_4 d}{f} - x_2, \frac{y_4 d}{f} - y_2\right)\; dx_2\; dy_2. \tag{35}$$

By a change of variable

$$r\,(x, y) = k \int_{-\infty}^{\infty}\int f\,(x + u, y + v)\; s\,(u, v)\; du\; dv \tag{36}$$

Hence it has been shown that by acting on the distribution of the phases and amplitudes of the surface wave, the filtering curve can be modified. One approach that has been utilized is to change the phase distribution of the wave surface by placing a glass sheet with parallel faces covered with a series of randomly distributed transparent elements before a lens. Each element introduces a path difference equal to $\lambda/2$. A filter of this type will stop all

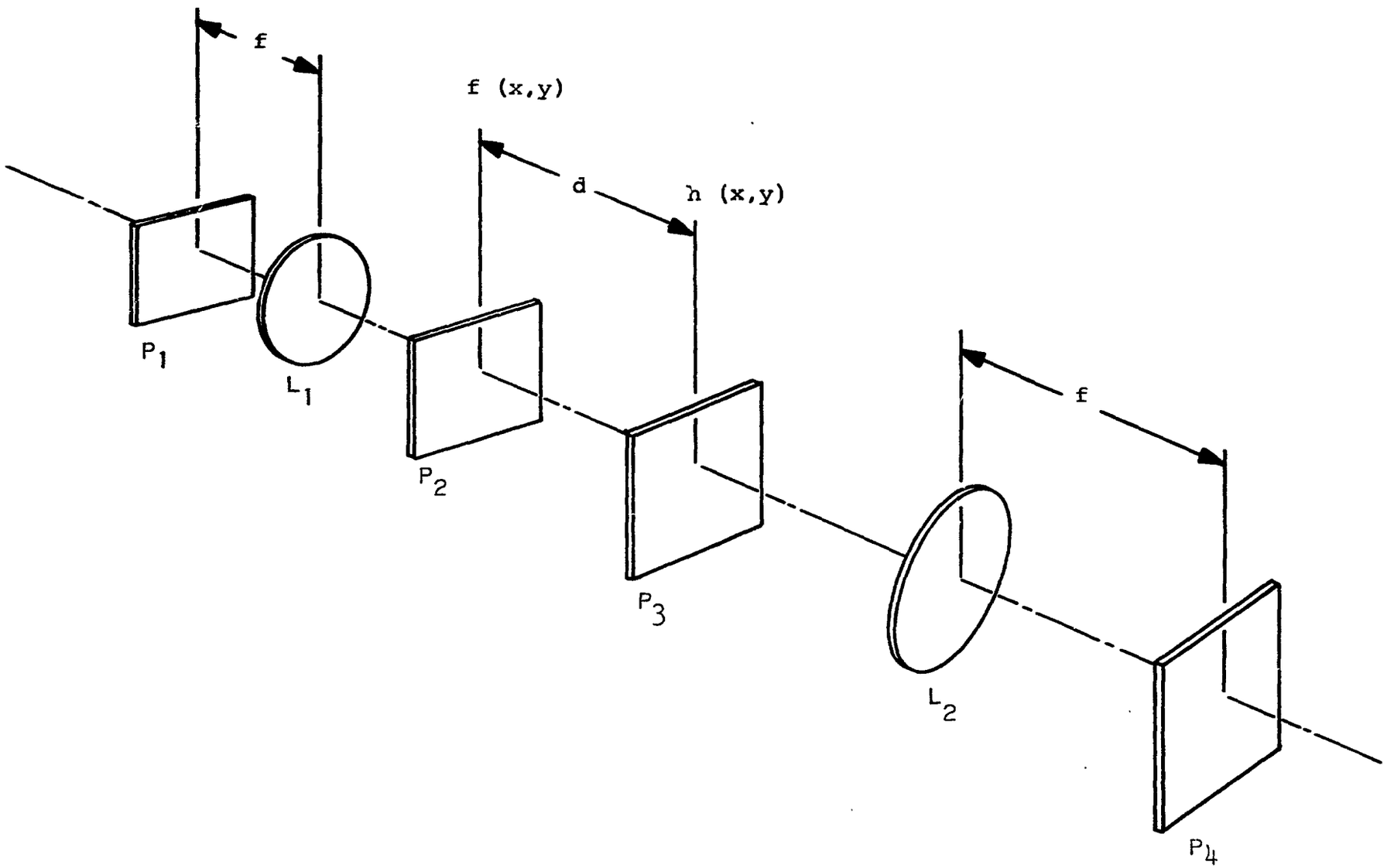

FIGURE B. 4-7

NONCOHERENT OPTICAL SYSTEM

frequencies above $1/P_o$. This generally has applications for smoothing out an image that is coarsely scanned. That is, the operation is an after-the-fact operation on the ground station. For example, if an image were scanned at 128 x 128 resolution and displayed on a crt without spot defocussing, the appearance of the image would be somewhat annoying. If a filter such as previously described were placed before the recording camera, the recorded image would be smoothed out. However, with digital television the same effect could be achieved by a slight amount of spot defocussing.

4.2.4 Compression Relationship

The purpose of the investigation of two-dimensional optical spatial filtering was to determine if a set of filters could be synthesized and used in conjunction with a compression technique such that the desired goal of a 6:1 or large compression could be achieved. In theory it is possible to operate on the spatial frequencies of the scanned image and increase redundancy by a technique similar to photographic image enhancement. This can be accomplished by suppressing the low frequencies. For this approach a mathematical model is quite impossible since the spatial filtering is merely a preprocessing technique that alters the statistical nature of the source. The hope here is that the alteration of the statistics is such as to increase the redundancy of the source.

Therefore, given a digital coding technique the gross average compression is

$$\overline{OPC} = \frac{H_o}{H_c} \tag{37}$$

Where H_o is the entropy of the uncoded signal and H_c is the entropy of the compressed source. When the spatial filter is inserted, in the system the source attains a new entropy H_n with the relationship of $H_n \leq H_c$. For this case the overall compression becomes

$$\overline{OPC}' = \frac{H_o}{H_n} \tag{38}$$

Therefore, it becomes necessary to determine the values of H_c and H_n for the various coding techniques under investigation. In this sense the spatial filter acts as the two-dimensional optical equivalent of the one-dimensional digital Previous Element Qualifier (PEQ) concept. It will be shown later that the PEQ technique does increase the compression. The PEQ statistical results will be discussed in paragraph 4.4.2. The optical approach is theoretical and it must be emphasized that practical constraints must be considered.

4.2.5 Optical Analysis

The purpose of this section is to determine the desired properties of an optical system. The following constraints will be considered for the analysis. Assume that the television system has a resolution of 600 line pairs and the test object will have a 15 x 21 mm format. Therefore, the lens must be capable of resolving 30 lines per mm at a minimum; therefore, the lens in the system will be required to have a resolution of 60 lines per mm. For a mercury arc source with an appropriate filter the wavelength that will be used will be 5460 angstroms. If the lens has a focal length of 305 mm, the usable spatial plane size in plane P_2 is given by

$$x_2 = \frac{f \omega_x \lambda}{2\pi} \tag{39}$$

where ω_x is the highest spatial frequency of interest, which will be 100 lines per mm. From Equation 39 the size of the spatial plane is 16.7 x 16.7 mm. This will ensure that operations at the lower frequencies can be performed; however, this imposes rather severe restrictions on the size of the point source of illumination. The larger the size of the source, the higher the lowest usable frequency that can be operated on.

For a focal length of 305 mm and aperture of 30 mm, the F number of the lens is given by

$$F = f/A, \tag{40}$$

where A is the aperture size which for the test object format size is 30 mm, the minimum F number is 10. However, if the resolution is 60 lines per mm, and an f/5 lens is used with a 305 mm focal length, the angular resolution is approximately 0.055 milliradian. The point image diameter is related to the angular resolution by

$$\theta = \delta/f \tag{41}$$

where δ is the point image diameter. With θ and the focal length specified, the minimum point image diameter is 0.017 mm. This value must be considered when calculating the point image diameter to ensure that the area of coherence is equal to or greater than the format size.

Consider now whether the relationship given by Equation 1 is a valid representation. Consider Figure B.4-8 where P_1 is a transparency and P_2 is a lens.

The disturbance at P_2 to the disturbance at a point in P_1 is given by

$$\sqrt{\frac{-j}{\lambda}}\, A \frac{f(x_o)}{\sqrt{r}} \quad e^{jkr} \quad \frac{(1 + \cos\theta)}{2} \Delta x_o \,, \tag{42}$$

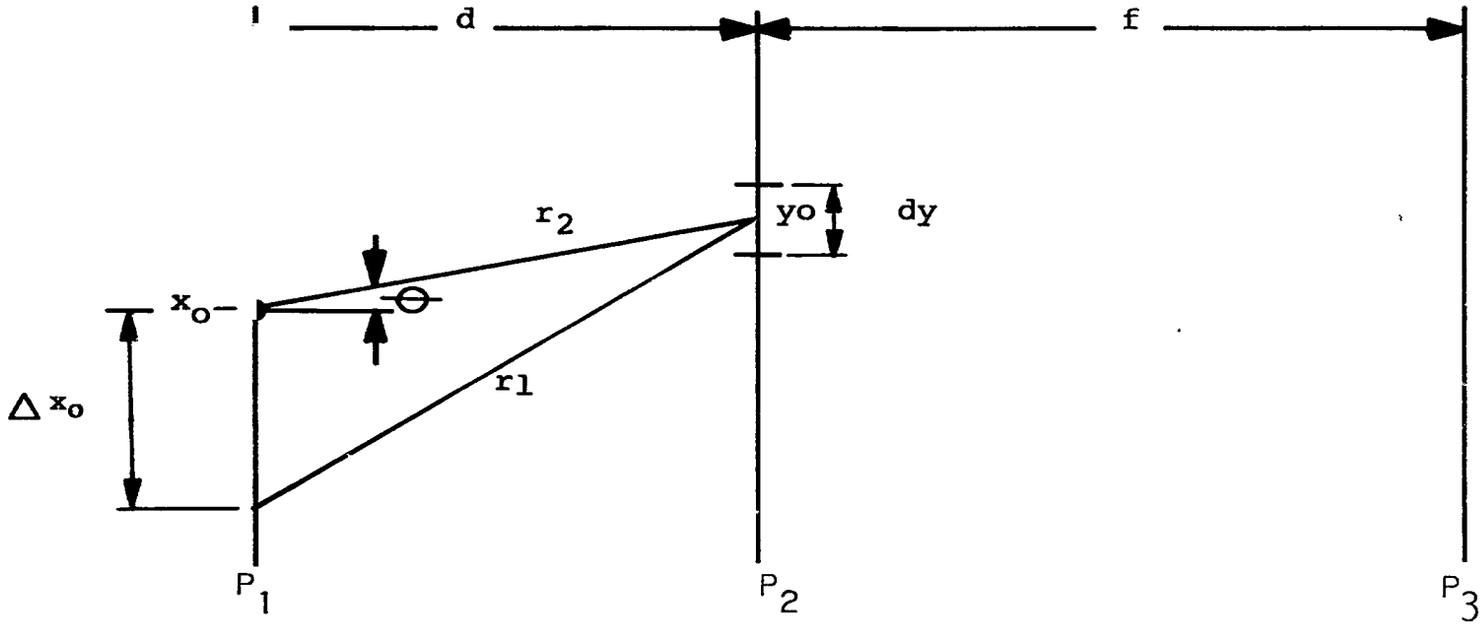

FIGURE B.4-8

SINGLE TRANSFORM PLANES

where

λ = wave length of light,

A = amplitude of illumination at x_o,

r = distance from X_o to Y_o,

θ = obliquity angle,

$f(x_o)$ = transmission of transparency at $x = x_o$, and

$k = 2\pi/\lambda$.

The incoming illumination E(x) is given by

$$E(x) = A(x)\, e^{j\theta(x)}, \tag{43}$$

where usually A(x) and $\theta(x)$ are constant. The total contribution y_o assuming $\theta(x)$ is the reference phase and set equal to zero is

$$g(y) = \sqrt{\frac{-d}{\lambda}}\; A \int_{P_1} \frac{f(x)\, e^{jkr}}{2\sqrt{r}}\, (1 + \cos\theta)dx \tag{44}$$

The obliquity factor is usually neglected by assuming θ remains small throughout the integration. This is true for $d \geq f$, but for $d \to \infty$, this is not true. Consider a small region in P_1 and its effect in P_2. For $|r_2 - r_1| >> \lambda$ the contribution at y_o averages to zero for $f(x_2) \doteq f(x_1)$. This allows the maximum value of θ as a function of d and the frequency content of f(x) to be calculated. For $|r_2 - r_1| >> \lambda$, this implies that

$$\left| \sqrt{d_1^2 + (x - y)^2} - \sqrt{d^2 + (x + \Delta x - y)^2} \right| >> \lambda \tag{45}$$

Equation 45 can be restated as

$$\left| 2x\,\Delta x + (\Delta x)^2 - 2y\,\Delta x \right| >> 2\,\lambda\, d \tag{46}$$

If the $(\Delta x)^2$ terms are neglected, Δx can be determined since

$$\Delta x >> \frac{\lambda\, d}{x - y} \tag{47}$$

It can be assumed that the obliquity factor can be neglected if

$$\frac{1 + \cos\theta}{2} \geq 0.99 . \tag{48}$$

Equation 48 implies that $\tan\theta \leq 0.2$. Substituting this into 47 results in

$$\theta = \tan^{-1}\left(\frac{x - y}{d}\right). \tag{49}$$

From 48 and 49, note that $\frac{x - y}{d} \leq 0.2$. Therefore, substituting this into 47 results in

$$\Delta x >> \frac{\lambda}{0.2} \tag{50}$$

Since Δx is the distance over which f(x) must not vary appreciably, the highest frequency in f(x) is given by

$$P_{max} = \frac{1}{\Delta x} << \frac{0.2}{\lambda} \tag{51}$$

Assuming that λ = 5460 angstroms, P_{max} = 368 lines per mm. In typical input signals the highest frequency encountered is approximately 30 to 60 lines per mm. Therefore, it is possible to neglect the obliquity factor. Hence, the analysis shows that the relationship for the Fourier transform is independent of the aperture and field of view. If the obliquity factor is ignored (which it can safely be), in one dimension the transform is

$$g(y) = \sqrt{\frac{-j}{\lambda}} \quad A \int_{P_1} \frac{f(x)}{\sqrt{r}} \quad e^{jkr} \quad dx . \tag{52}$$

A similar type development can be obtained in going from P_2 to P_3, with the resultant being expressed as Equation 1.

4.2.6 Experimental Setup

The experimental apparatus to perform the necessary experimentation is given in Figure B.4-9. The light source is a Spectroline Mercury Arc Lamp and the filter is a monochromatic Wratten filter to limit the wavelength to 5460 angstroms. The condenser lens is an ordinary off-the-shelf item whose characteristics are not critical. The pin hole necessary can be calculated from the area of coherence needed to illuminate the transparency. The area of coherence is given by

$$D = \frac{0.16\lambda R}{\rho} \tag{53}$$

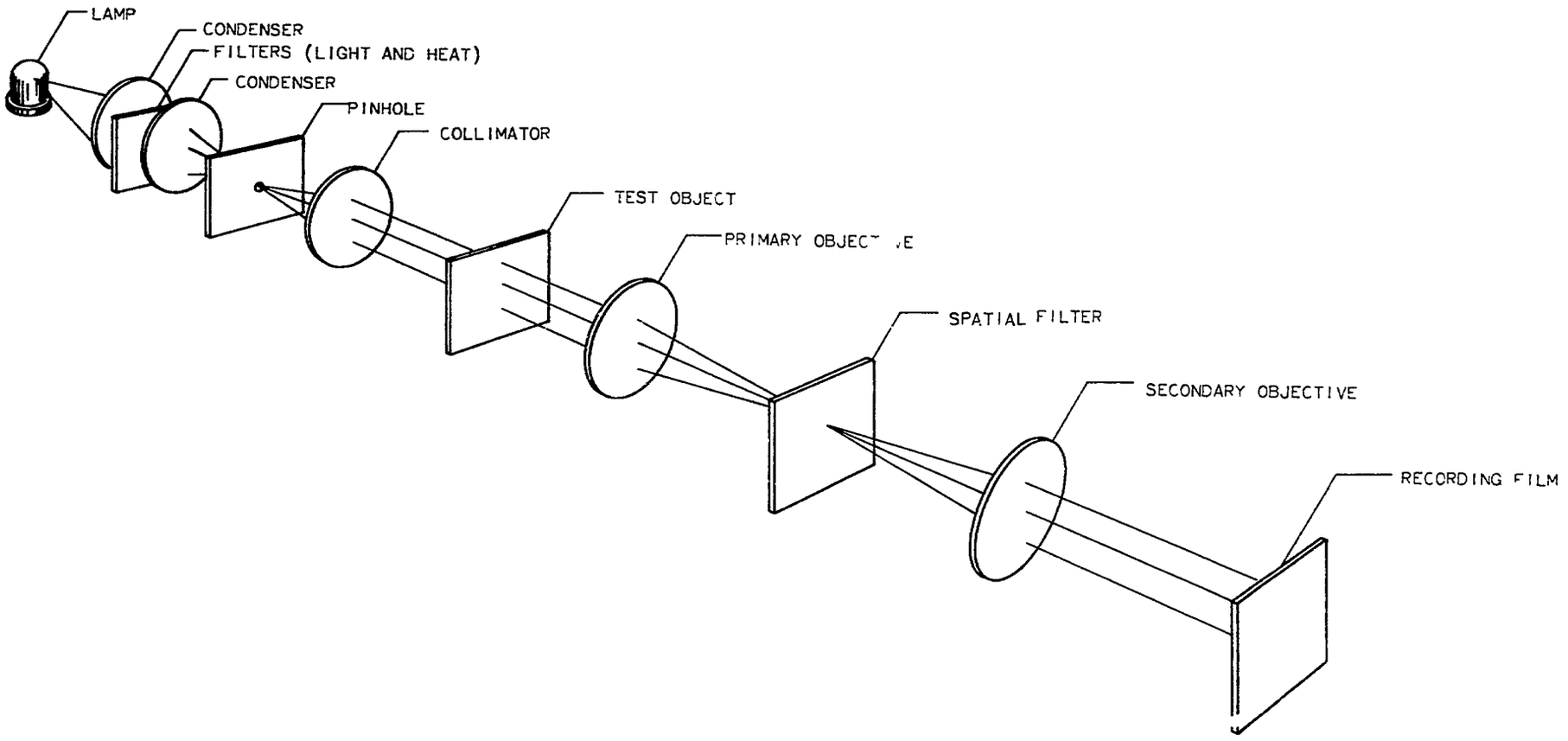

FIGURE B.4-9

TWO-DIMENSIONAL OPTICAL SPATIAL FILTERING
EXPERIMENTAL APPARATUS

where

λ = wavelength of light,

R = focal length of collimator, and

ρ = radius of point source.

Since D is specified by the test object photograph format and is equal to 30 mm, the pin-hole diameter necessary to achieve this is 0.005 mm. This imposes rather severe restrictions on the light source; however, implementation of the extremely small pin hole can be achieved by using a microscope objective as a reducing system. Before considering this, consider calculation of the displacement of the spatial frequencies. The displacement is given by

$$x = \frac{f \lambda \omega_x}{2\pi} \tag{54}$$

For a lens of 305 mm focal length and λ = 5460 angstroms, the displacement for the system is $x = 0.167 f_x$. For a spatial frequency 1 line per mm, the displacement is 0.167 mm. Hence, to ensure being able to operate on this frequency ρ should be < 0.080 mm. However, to have an area of coherence of 30 mm. requires ρ = 0.005 mm. Using a pin hole of 0.050 mm and a microscope objective of magnification of 10, a pin hole of 0.005 can be obtained at the focal plane of the collimator. Figure B.4-10 shows this for a microscope objective of 16-mm focal length.

The maximum frequency that can be passed is $f_{max} = \frac{A/2}{\lambda f}$ = 95 lines per mm. The collimator is a Gaertner L-360-N model with an 80-mm aperture and a focal length of 907 mm. The primary and secondary lenses are Eastman Kodak Aerostigmat lenses with a focal length of 305 mm at f/5. The test object is a 35-mm slide and the recording is made on type 3000 Polaroid film. Using the optical set-up as described, two-hour exposures were needed to obtain the diffraction pattern. This long time exposure limits the usefulness of the technique in a space mission.

4.2.7 Conclusions

The applications of spatial filtering have been in areas of data reduction, one- and two-dimensional data processing, statistical analysis, data storage and retrieval, image enhancement, and pattern recognition. Nowhere in the literature has there appeared an application of optical spatial filtering to video bandwidth compression.

The above applications of spatial filtering techniques can be classified as an after-the-fact operation; that is, no additional optical or electrical operation takes place after the filtering. Unfortunately in the field of television the operation is before-the-fact. It is possible to take a transparency and increase the

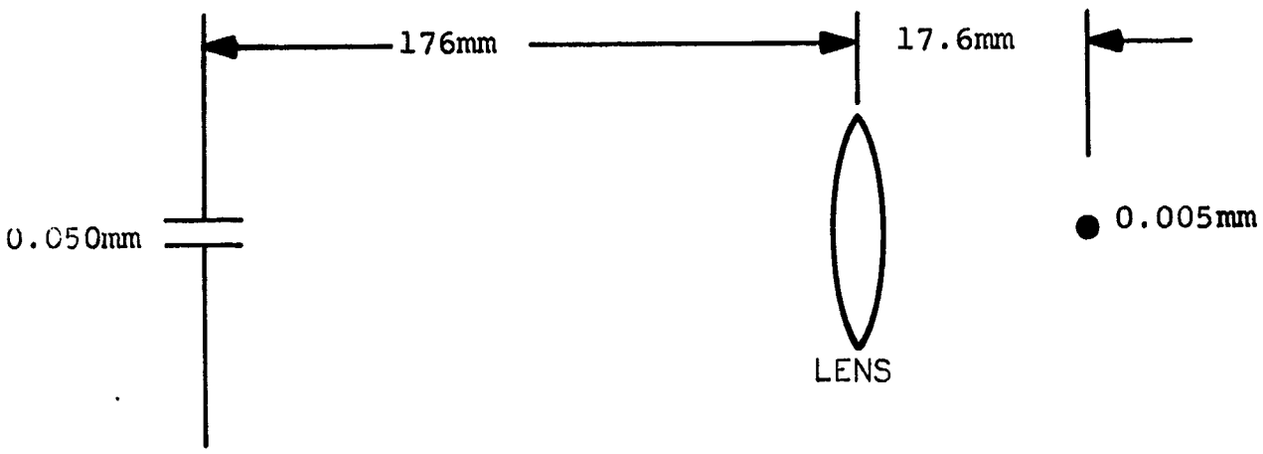

FIGURE B.4-10

PIN-HOLE REDUCTION SETUP

redundancy in the image by spatial filtering; however, the filtered image then is scanned with a sensor. In general, if it is assumed that the sensor is a vidicon or similar device with its inherent noise limitations, the gain in redundancy obtained by spatial filtering is virtually eliminated by the sensor. Therefore, it becomes apparent that with current sensors, spatial filtering will not obtain the desired compressions.

4.2.8 Bibliography

Graham, R. E. and Reynolds, F. W., "A Simple Method for the Synthesis and Evaluation of Television Images," Waves and Electrons, January, 1946.

Elias, P., Gray, D.S., and Robinson, D. A., "Fourier Treatment of Optical Processes," JOSA, Volume 42, 1952.

Epstein, L. I., "Design of Optical Filters," JOSA, Volume 42, No. 11, 1952.

Kovasznay, L. S. G. and Joseph, H. M., "Image Processing," Proceedings IRE, Voluem 43, May 1955.

Kovasznay, L. S. G., Joseph, H. M., and Newman, A., "Image Processing," National Bureau of Standards Report 4108, June 1955.

Toraldo, Di Francia, G., "Resolving Power and Information," JOSA, July 1955.

Linfoot, E. H., "Information Theory and Optics JOSA, Volume 45, No. 10, 1955.

Weinstein, W., "Images of Incoherent Illuminated Bright and Opaque Disks JOSA, Volume 45, No. 12, 1955.

O'Neil, E. L., "Transfer Function for An Annular Aperture," JOSA, Volume 46, 1956.

O'Neil, E., "Spatial Filtering in Optics," IRE Transactions on Information Theory, Volume IT-2, June 1956.

Mertz, L., "Optical Fourier Synthesizer," JOSA, Volume 46, No. 7, 1956.

Keim, R. E. and Kapang, N. S., "Image Synthesis and Lens Response Using Spot Diagrams," JOSA, Volume 48, No. 5, 1958.

Born, M. and Wolf, E., Principles of Optics, Pergamon Press, N. Y., 1959.

Aroyan, G. F., "The Technique of Spatial Filtering," Proceedings of the IRE, Volume 47, 1959.

Cutrona, L. J., Leith, E. N., and Porcello, L. J., "Data Processing By Optical Techniques," 3rd National Convention Conference Proceedings on Military Electronics, June 29, 1959.

Cutrona, L. J., Leith, E. N. and Porcello, L. J., "Coherent Optical Data Processing IRE WESCON Convention Record, Part 4, August 1959.

Cutrona, L. J., Leith, E. N. and Porcello, L. J., Filtering Operations Using Coherent Optics," Proceedings of National Electronics Conference, 1959.

Cutrona, L. J., Leith, E. N., Palermo, C. J. and Porcello, L. J., "Optical Data Processing and Filtering Systems," IRE Transactions on Information Theory, June 1960.

Van Blerkom, R.; et al; A Research Study of Improved Coding for Military Digital Television, IBM, Reports 1 and 2, Cont. No. DA 36-039 SC-87330 October 1960.

Kelly, D. H., "Image Processing Experiments," JOSA, Vol. 51, No. 10, October 1961.

Graham, D. N., "Two-Dimensional Filtering to Reduce the Effect of Quantizing Noise in Television," MS Thesis, MIT, January 1962.

Fruv, W. D., and Richmond, G. E., "Two Dimensional Spatial Filtering and Computers," Proceedings of National Electronics Conference, 1962.

Neiswander, R. S. and Harris, C. W., "Optical Techniques for Target Enhancement and Background Rejection," Proceedings of National Electronic Conference, 1962.

Montgomery, W. D., and Broome, P. W., "Spatial Filtering," JOSA, Vol. 52, No. 11, 1962.

Franconi, M., Modern Applications of Physical Optics, John Wiley and Sons, 1963.

Vander Lugt, A. B. and Rotz, F., "Optical Spatial Filtering Techniques," Radar Institute of Science and Technology, University of Michigan, January 1963.

van Heerden, P. J., "A New Optical Method of Storing and Retrieving Information," Applied Optics, Volume 2, No. 4, April 1963.

Smith, F. D., "Optical Image Evaluation and the Transfer Function," Applied Optics, Volume 2, No. 4, April 1963.

Vander Lugt, A. B., Signal Detection by Complex Spatial Filtering, Radar Laboratory Institute of Science and Technology, University of Michigan, July 1963.

Harris, J. L., "Image Restoration," Proceedings National Aerospace Electronics Conference, 1963.

Leith, E. N. and Upatnieks, J., "Wavefront Reconstruction with Continuous-Tone Objects," JOSA, Volume 53, No. 12, December 1963.

Revesz, G. and Shen, D. W. C., "The Application of Electro-Optical Filtering to Object Recognition," IEEE International Convention Record, Part 1, March 1964.

Vander Lugt, A. B., "Signal Detection By Complex Spatial Filtering," IEEE Transactions IT, Volume IT-10, No. 2, April 1964.

Harris, J. L, "Diffraction and Resolving Power," JOSA, Volume 54, No. 7, 1964.

Beall, W. H., "Statistical Analysis of Degradation in Scanned Image Systems," JOSA, Volume 54, No. 8, August 1964.

Hawkins, J. K. and Munsey, C. J., "Eulogismographic Nonlinear Optical Image Processing for Pattern Recognition," JOSA, Volume 54, No. 8, August 1964.

Cutrona, L. J., "Optical Computing Techniques," IEE Spectrum, Volume 1, No 10, October 1964.

4.3 ONE-DIMENSIONAL DIGITAL PROCESSING

4.3.1 Introduction

One-dimensional digital processing is the one-dimensional digital equivalent of the two-dimensional optical processor with one major difference. One approach to the digital processing is the PEQ (Previous Element Qualifier) concept. This type of processing takes place after the sensor and analog-to-digital converter; therefore, the change in statistics that results is not altered by other limitations in the system as with the optical process. This constitutes the major difference between optical processing and digital processing. The PEQ technique assumes that if element i and i + 2 have the same intensity, then it necessarily follows that element i + 1 should also have the same intensity. There exists a rather high probability that if i and i + 1 are not alike whereas i + 2 and i are alike, then i + 1 must have been altered by noise. This concept will be discussed in more detail in the next section.

4.3.2 PEQ Concept

The previous element qualifier concept is implemented in the following manner. The system compares the i and i + 2 elements and on the basis of this comparison decides whether the i + 1 element is a PE element or a 1-PE element. If the i and i + 2 elements are equal, the true value of the i + 1 element is assumed to be that of the i and i + 2 elements. The i + 1 element is then made equal to the i and i + 2; therefore, the i + 1 element becomes a PE element. Any difference which exists between the i + 1 element and the i element is assumed to be due to sensor noise. If the i and i + 2 elements are different, the value of the i + 1 element is unchanged.

Figure B.4-11 presents the sequence of events which result when employing the PEQ system on the given waveform f(t). E_1 is assumed to be a 1-PE value. E_1 and E_3 are compared and seen to be equal; therefore, E_2 is assigned the Y_3 quantizing level. E_2' and E_4 are compared and since they are different, E_3 is unchanged. Comparison of E_3 and E_5 results in E_4 being unchanged. Since E_4 and E_6 are different, E_5 keeps its normal value. Comparison of E_5 and E_7 results in E_6 being assigned the Y_2 quantizing level. The final value of E_7 would be determined by comparison of E_6' and E_8. To determine the effectiveness of the technique, the maximum PE and PEQ signals as a function of the sensor signal-to-noise ratio were mathematically derived. The computed results presented below determine in theory the maximum expected effectiveness of the PEQ concept at a specified signal-to-noise ratio.

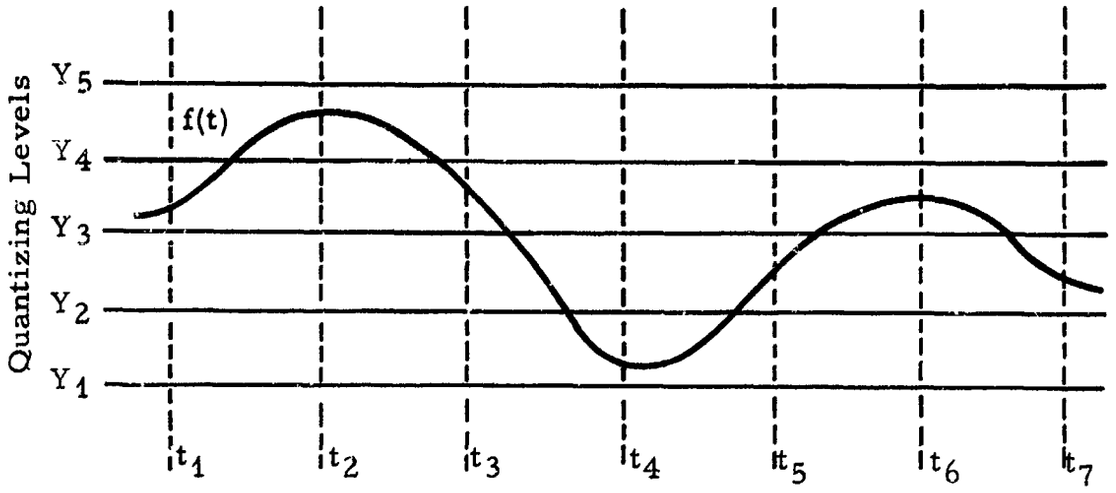

SIGNAL BEFORE PEQ

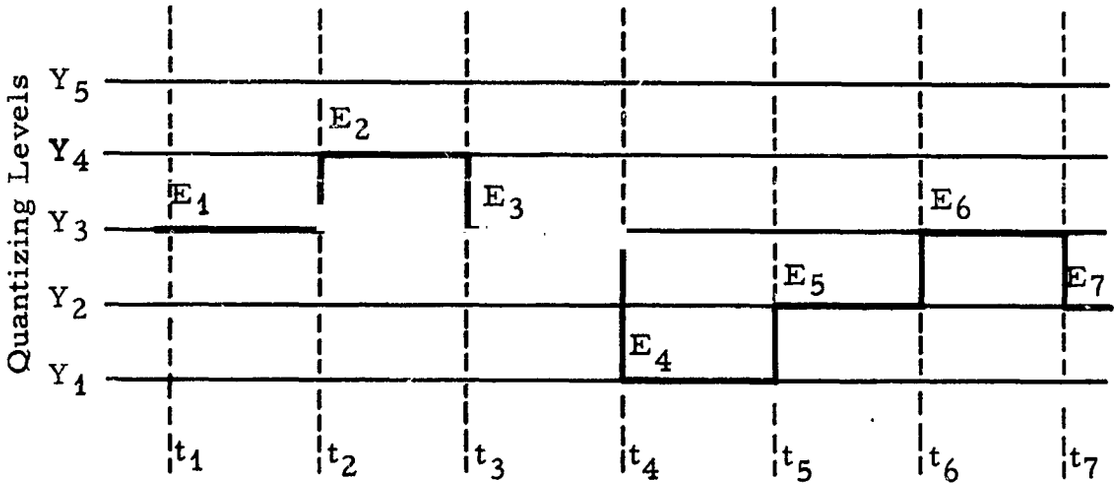

QUANTIZED SIGNAL BEFORE PEQ

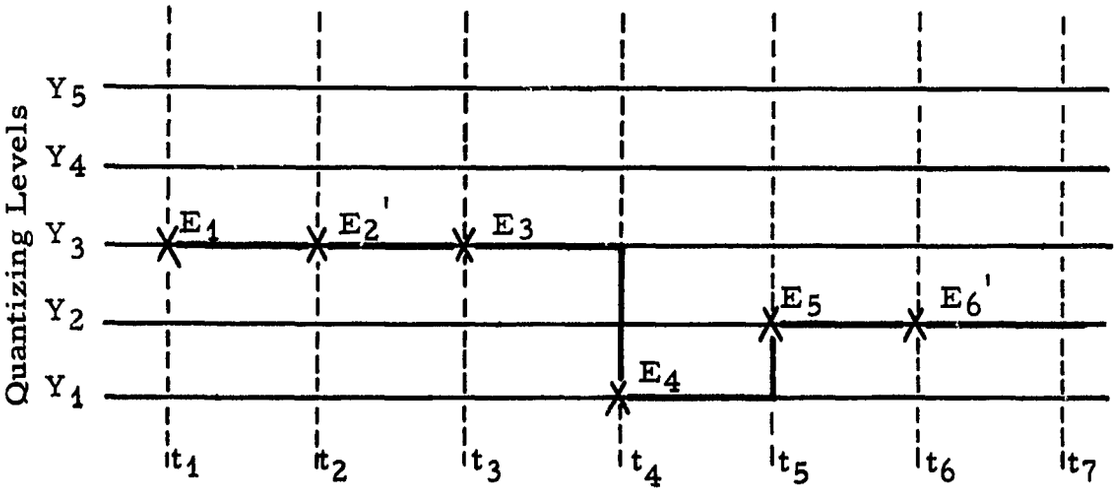

QUANTIZED SIGNAL AFTER PEQ

FIGURE B.4-11

PREVIOUS-ELEMENT QUALIFIER SEQUENCE DIAGRAM

4.3.3 Derivation of Signal-to-Noise Versus PE

If a nonvarying voltage is applied to an ideal analog-to-digital encoder, the resultant binary code will identify one particular level for each sample. Unfortunately, there is always some noise in the applied voltage and in the threshold levels. This paragraph derives the probability that an encoded level will be the same as the previous level. This is defined as the PE (previous element) probability and results in a curve of the maximum possible PE for a given system signal-to-noise ratio.

Figure B.4-12 shows an input signal level which falls a distance X above level 19. The curve is the gaussian probability density function for the noise which is riding on the input signal level. The noise has an rms value of σ, and Δ is the distance between quantizing levels.

The probability that the signal is correctly identified as level 19 is equal to the area under the gaussian curve labeled (2). The probability that the signal is identified as level 20 is equal to the area labeled (1). Similarly, P(21) = area (5), P(17) = area (4), and P(18) = area (3). This must be continued until the probabilities become insignificant.

The previous element probability is equal to the probability that the signal is encoded to the same level for the present sample as it was for the last sample. For the figure as shown this becomes

$$PE = \ldots + P(17)^2 + P(18)^2 + P(19)^2 + P(20)^2 + P(21)^2 + \ldots, \qquad (1)$$

which can be stated in general as

$$PE = \sum_{i=1}^{\infty} P(i)^2 \qquad (2)$$

This statement assumes the two samples are statistically independent. For a given ratio of δ/Δ, PE will vary as X/Δ varies from 0 to 1. Figure B.4-13 is a family of curves of PE versus the ratio X/Δ for various signal-to-noise ratios. For a 6-bit encoder with 64 levels, the peak-to-peak signal to rms noise ratio is $64/\delta$. For the curve of $\delta = \Delta$, Spp/Nrms = $64\Delta/\Delta$ = 64=36.1 db. The curves in Figure B.4-13 are separated by 6-db steps.

If a slowly varying waveform is applied to the analog-to-digital encoder, the average PE will be equal to the average value of the curve in Figure B.4-13 for the actual signal-to-noise ratio of the system. Therefore, it is assumed that a given signal-to-noise ratio will result in the average PE as X/Δ varies from 0 to 1.

Figure B.4-14 is a curve of PE averaged over X for each signal-to-noise ratio.

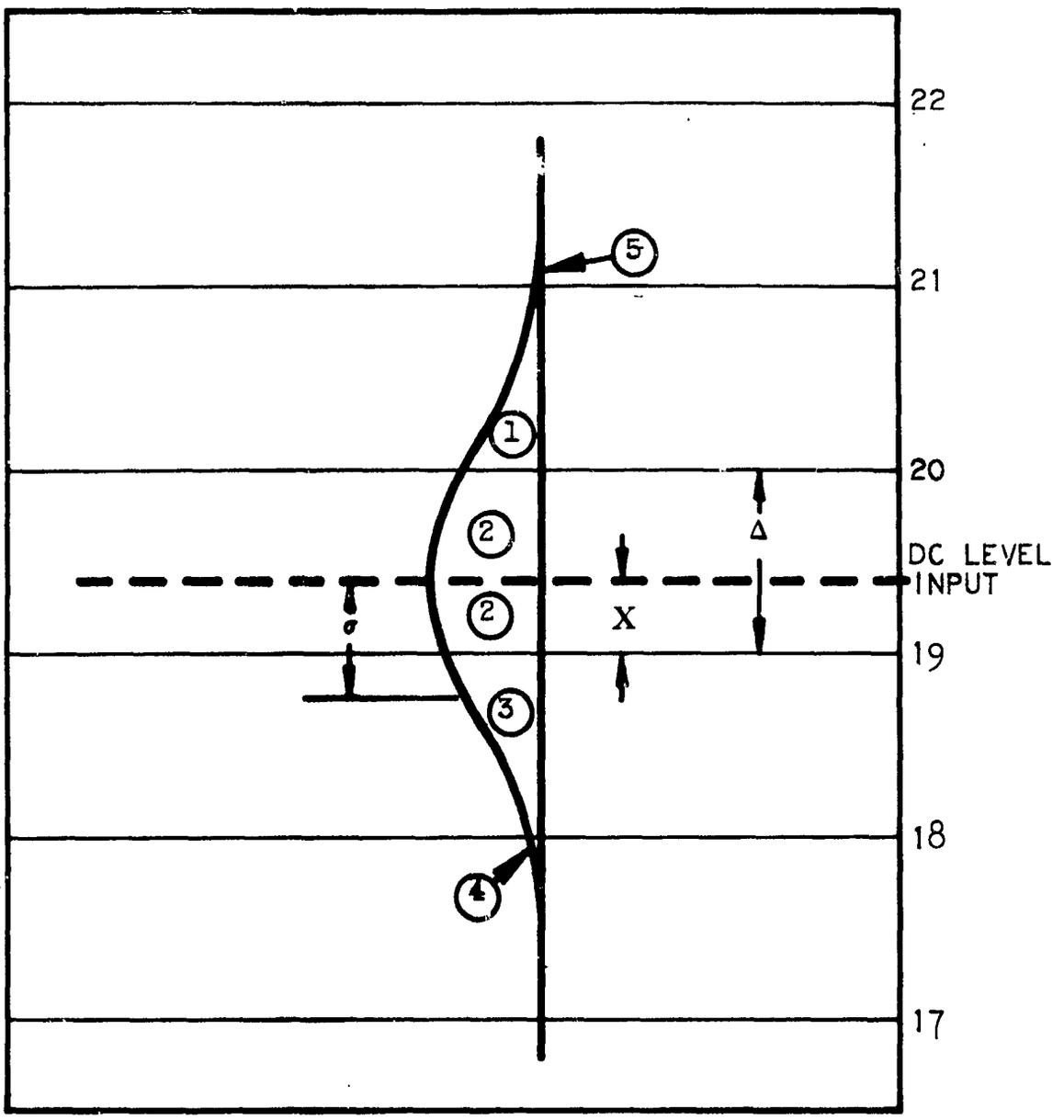

FIGURE B.4-12

DC INPUT LEVEL WITH GAUSSIAN NOISE

07314

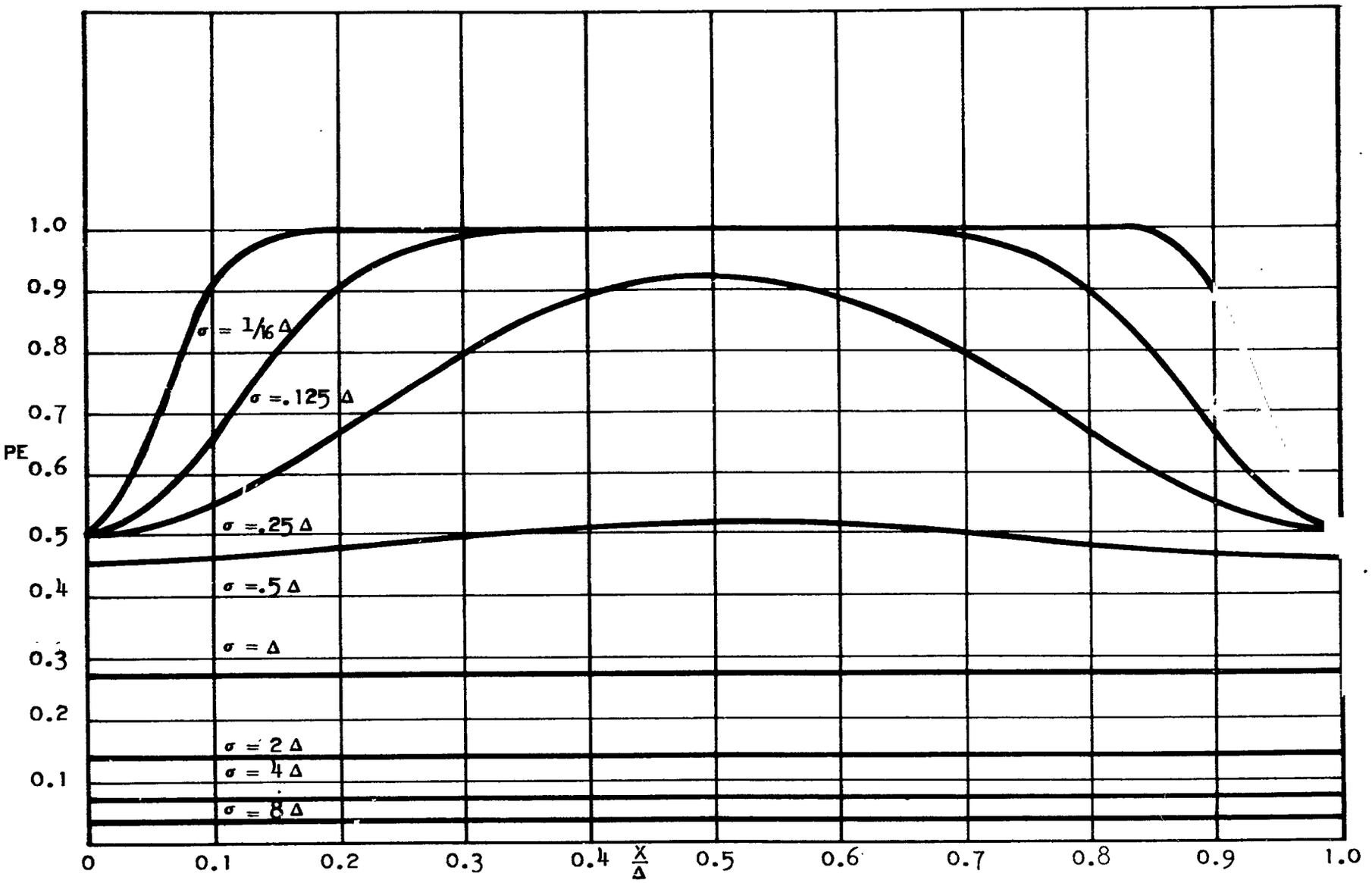

FIGURE B. 4-13

PE VERSUS DC POSITION BETWEEN QUANTIZING LEVELS

07314

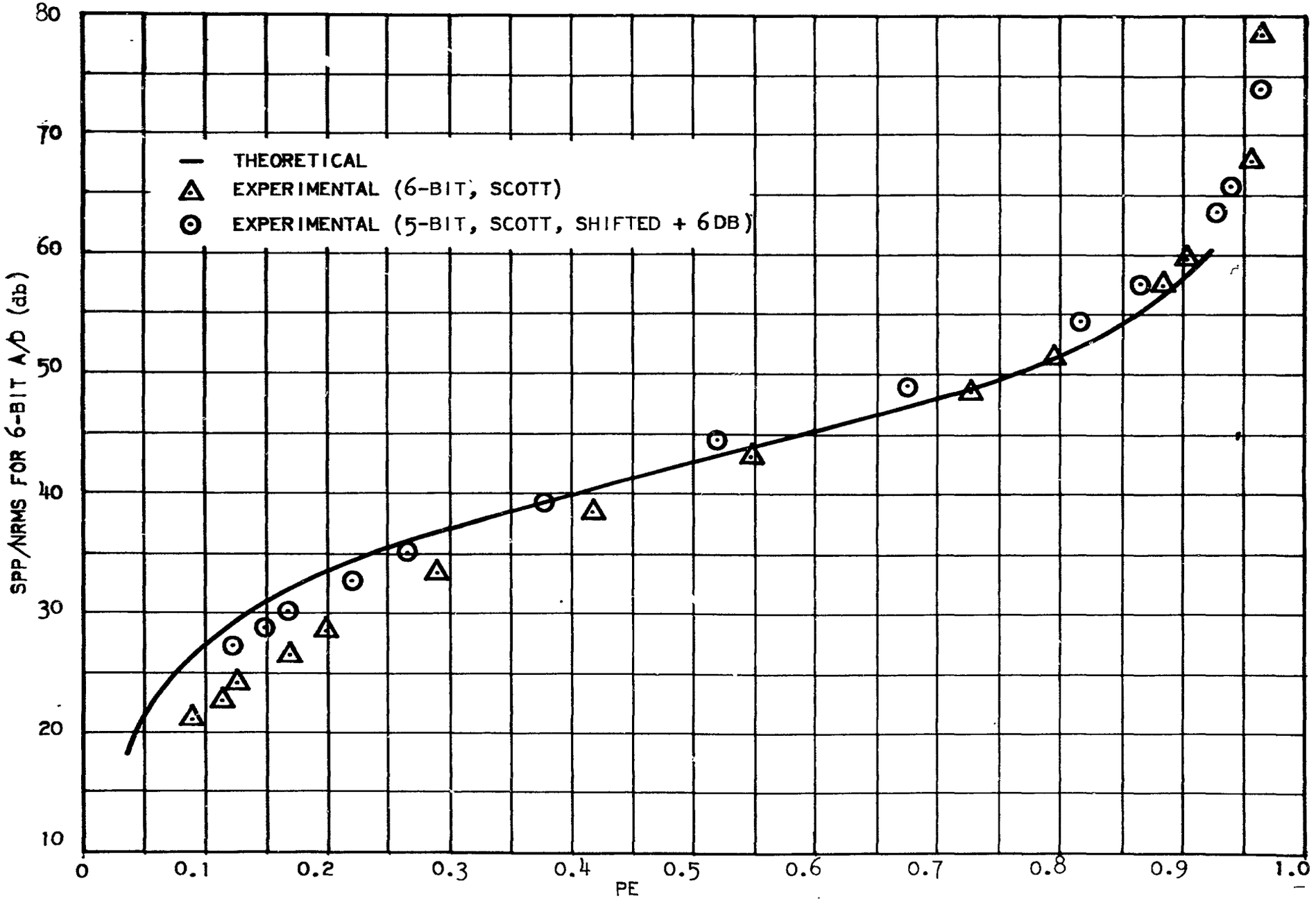

FIGURE B.4-14

PE VERSUS SPP/NRMS FOR A 6-BIT A/D ENCODER

07314

The signal-to-noise ratio scale is applicable to a 6-bit encoder only. If the encoder is reduced to five bits, the curve shifts downward by 6 db (i.e., 36.1 db on the scale becomes 30.1 db).

Experimental verification of this curve was attempted using the equipment setup shown in Figure B.4-15. Results are plotted in Figure B.4-14 directly for the 6-bit curve. The 5-bit curve is plotted, but is shifted upward by 6 db for comparison with the theoretical curve. The results show reasonable agreement, although for the lower values of signal-to-noise, PE is higher than predicted. This could be caused by the noise being nongaussian or by the assumption of independent samples being invalid.

4.3.4 Previous Element Probability Versus Sensor S/N for the PE and PEQ Systems

With a reasonable amount of additive gaussian noise in the signal from the sensor, some errors will be made by the analog-to-digital encoder. A dc level from the sensor thus has a finite probability of being encoded to the wrong level. With no noise this dc level would have a PE or a PEQ probability of 1. However, as the noise increases the PE and the PEQ probabilities both decrease. The PEQ system was designed to cancel some of this deterioration with a minimum of degradation to pictorial quality. The disorganization of the encoded video due to sensor noise sets an upper limit on the PE or PEQ values, and pictorial disorganization can only reduce it further. It is of interest therefore to predict this upper bound on PE for each system.

Assuming that the noise is additive gaussian and is of high enough frequency content to be statistically independent from sample to sample, the probability of a PE signal is given by Equation 1 and in a similar manner the PEQ probability can be derived, and is given by

$$P(PEQ) = \sum_{i=1}^{\infty} \left[P(i)^2\right]\left[2 - P(i)\right], \qquad (3)$$

Since $P(i) \leq 1$, PEQ is always greater than PE for any practical case where $P(i) \neq 1$.

At high signal-to-noise ratios it is possible for all of the noise to fit between two encoding thresholds when the original dc level is centered between these two thresholds. However, if the dc is centered on a threshold, then no matter how high the signal-to-noise ratio, P(i) cannot be 1 for any level. Therefore, at high signal-to-noise levels the curves shown in Figure B.4-16 separate into: (1) a maximum when the dc is centered between the thresholds, (2) a minimum when it is centered on a threshold, and (3) an average assuming that the video level is evenly distributed across the thresholds. The latter is generally the case when there is any actual video data. Therefore, for practical cases the average curves represent the upper limit on PE and PEQ probability and hence an upper

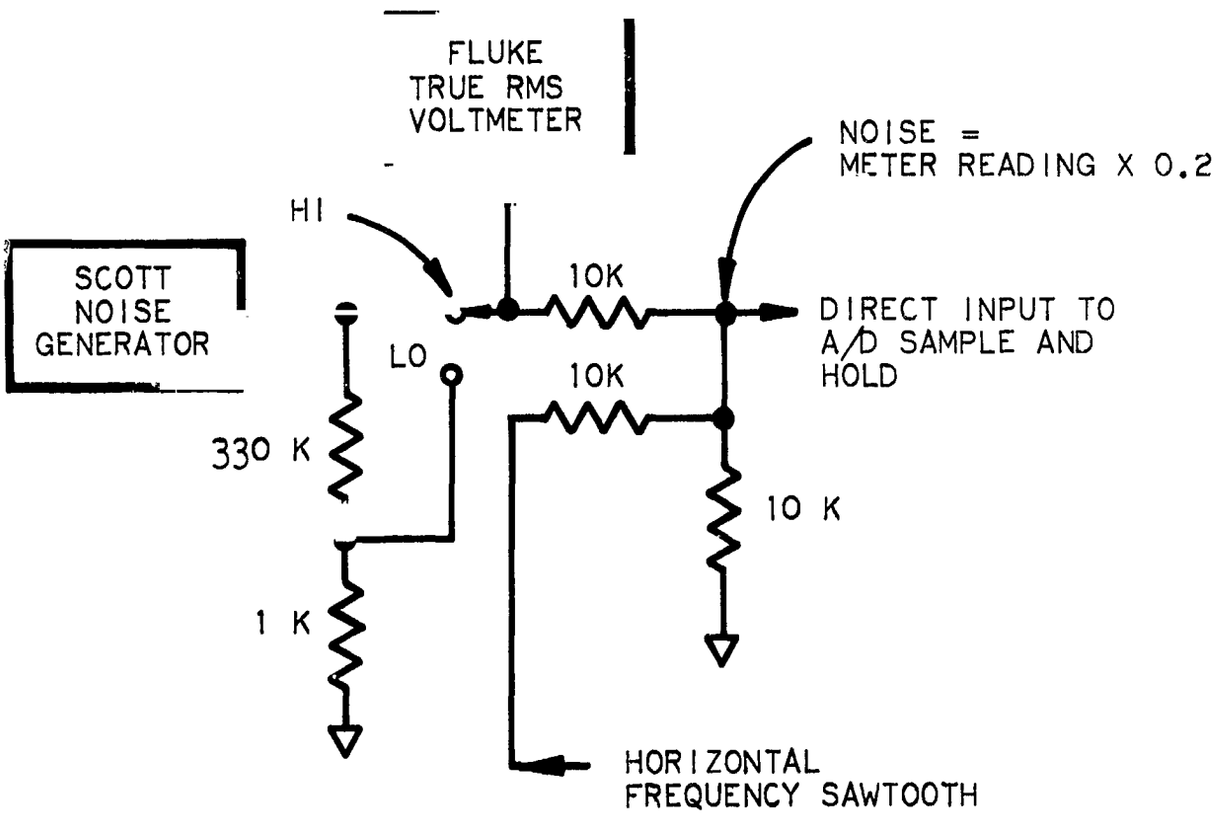

FIGURE B.4-15

EXPERIMENTAL PE VERSUS S/N SETUP

07314

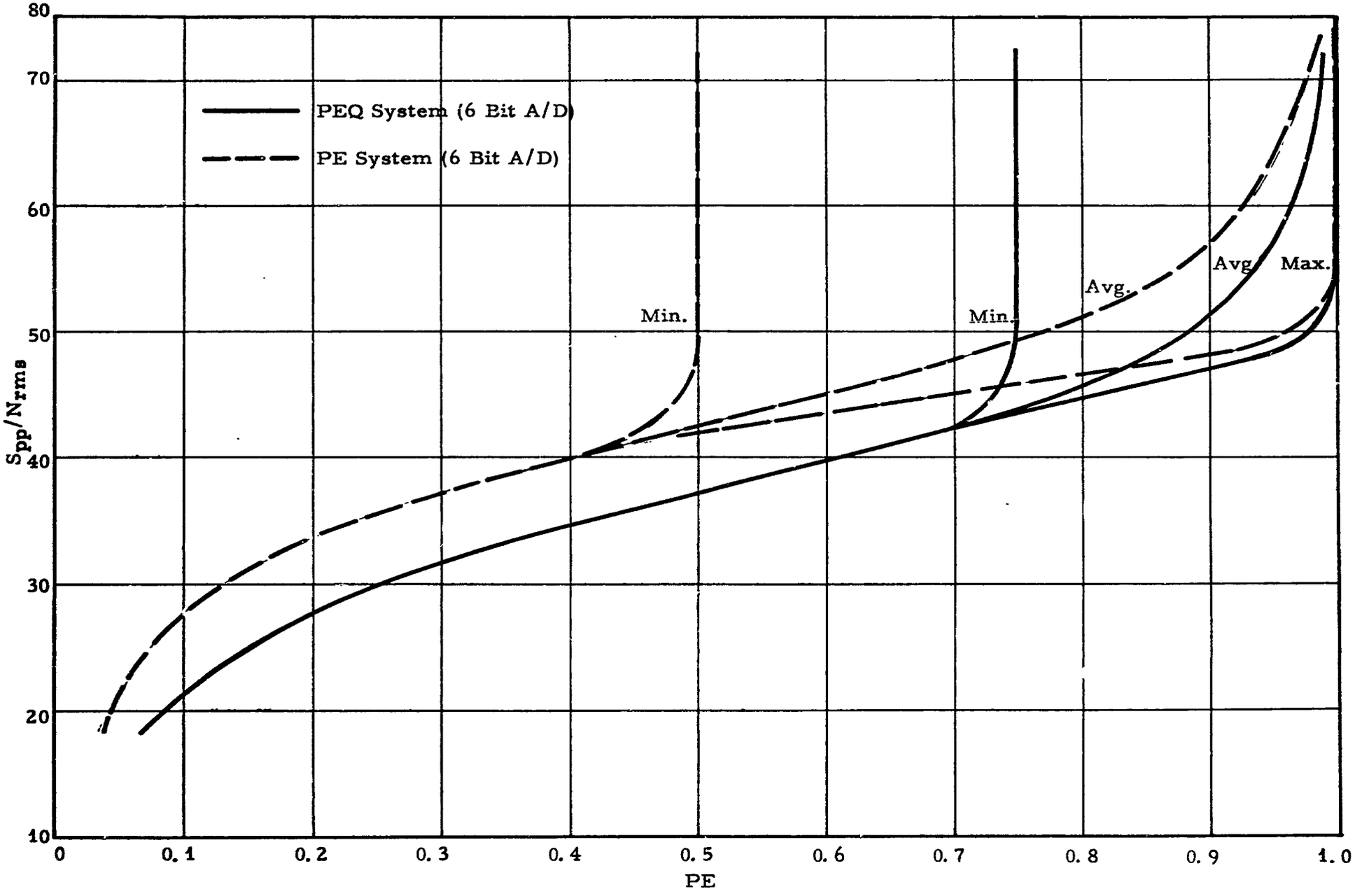

FIGURE B.4-16

PE VERSUS S/N FOR PEQ AND PE CODING SYSTEMS

limit on compression as established solely by the noise present in the sensor.

4.3.5 PEQ Hardware Implementation

For the following operational discussion, refer to the PEQ system block diagram, Figure B.4-17. The system, which has been constructed is built around four registers and two comparator circuits. The output of the i and i + 2 registers are compared, and if found equal the comparator output prevents the output of the i + 1 register from being transferred to the i register. Since the jam transfer gate between the i and the i + 1 registers is inactivated, the i register remains unchanged during the next time period; this results in the i + 1 element being made equal to the i and i + 2 elements. If the i and i + 2 registers are unequal, the comparator output level, when gated with the transfer pulse, activates the jam transfer network thus transferring the i + 1 element into the i register. In order to obtain the statistics of the qualified signal, the i and i - 1 registers are compared. The output of this comparator is then sent to the statistics taker where the PEQ statistics are determined.

4.3.6 Measurements

In order to determine the effect of the PEQ system on picture quality for various sensor noise levels, a series of photographs were taken on EDITS. Photographs were taken using the PEQ system at signal-to-noise ratios of 20, 30, and 40 db. For comparison purposes, pictures were also taken using PCM transmission. The previous-element statistics for both PEQ and PEC were also obtained as a function of the sensor signal-to-noise ratio. Photographs and statistics were obtained for 6, 4, and 3 encoding bits. The test pictures employed in this experiment were the following: RETMA test chart, lunar picture, Canadian Arctic, MIT Girl, Astronaut Cooper, and a white card. It was felt that the wide selection of test subjects would adequately show the effect of PEQ on high-contrast scenes and fine line resolution.

To show the meaning of a given change in PE, the average compression for PEC was calculated and plotted as a function of sensor signal-to-noise ratio. The average compression for a PEC system is given as

$$\overline{PEC} = \frac{N}{N + 1 - N(PE)}, \tag{4}$$

where N is the number of encoding bits. In the derivation of this formula, it is assumed that the (1 - PE) levels have a flat distribution. Although PEC is only one of many compression techniques, it tends to better display the significance of a change in the previous element count. A representative sample of the PEQ and the PEC photographs along with the supporting graphs is shown in Figures B.4P-1 through B.4P-9.

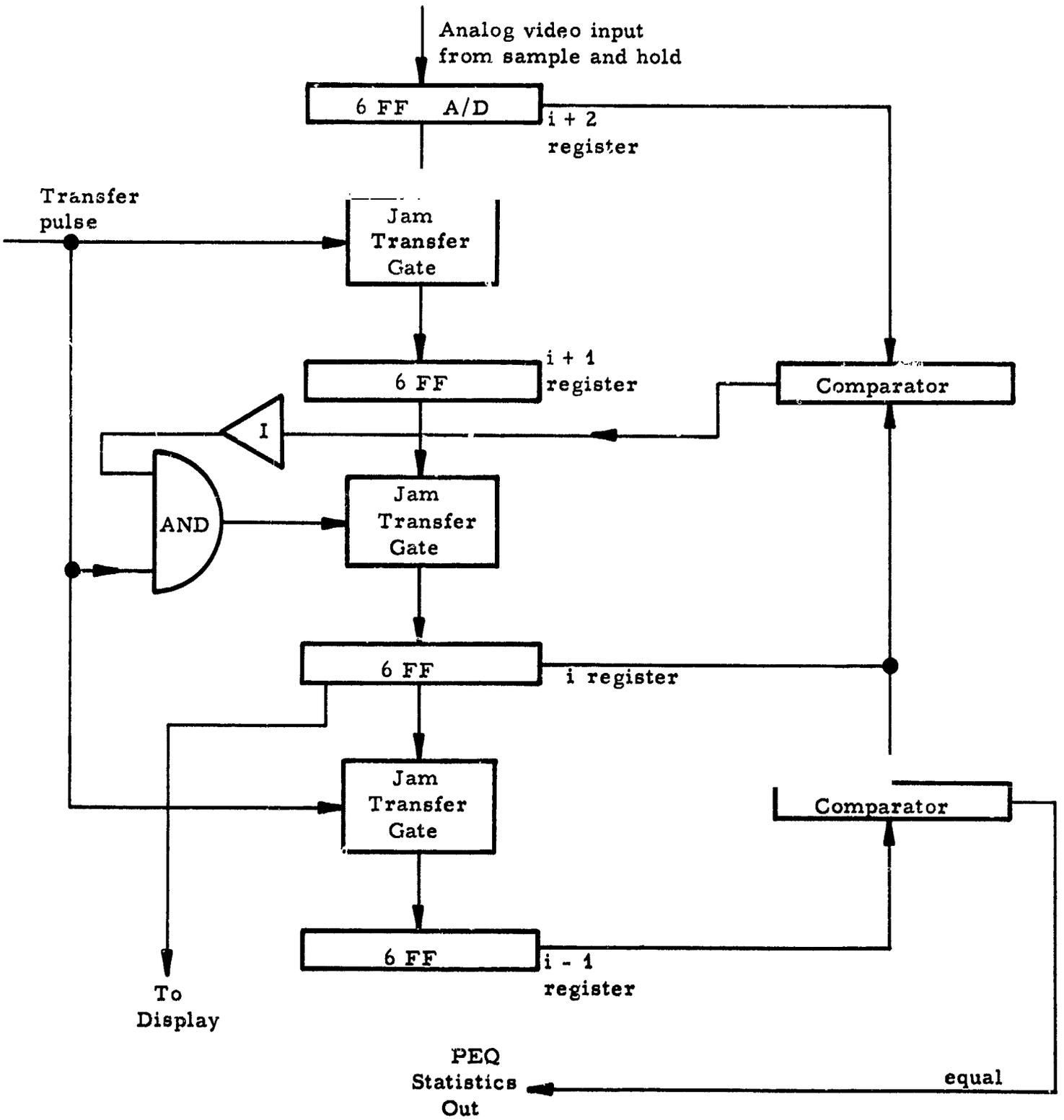

FIGURE B.4-17

PREVIOUS-ELEMENT QUALIFIER SYSTEM BLOCK DIAGRAM

To further subjectively display the noise-cleaning properties of PEQ, a photograph was taken in which all previous elements are displayed as dark areas and all nonprevious elements as light areas. For comparison, a PCM photograph of this type was also taken and is shown in Figure B.4P-10.

4.3.7 Conclusions

The major conclusion to be drawn from this investigation is that the PEQ system does not subjectively degrade the picture; the one exception to this is the RETMA test chart where fine-line resolution equivalent to or less than one scan element dimension is destroyed. In comparing the graphs of the various test subjects, it was noted that those relating to Astronaut Cooper, the Lunar picture, and the Canadian Arctic all behaved in a similar manner. For this set of test subjects the average compression was seen to increase with PEQ from 25-45% with the average increase being approximately 35 to 40%; this increase was for 4-bit encoding and signal-to-noise ratios of 30 to 40 db. At 3-bit encoding and low signal-to-noise ratios of 20 to 30 db, a change in the texture of the noise can be seen. With PCM the noise tends to give a "peppery" effect to the photograph, while with PEQ the noise takes on a more uniform appearance consisting largely of short line segments since the PEQ is merely a noise-stripping technique for either PCM or PEC. Although there is not a large increase in compression the technique could be used to increase the compression of a coding technique whose compression approaches the desired goal.

4.4 ONE-DIMENSIONAL ANALOG PROCESSING

4.4.1 Introduction

Due to the physical characteristics of the sensor used in an image-transmission system, the original redundancy in the optical signal is decreased by the addition of sensor noise. The efficiency of the system can be increased, thereby regaining some of the original redundancy, by operating on the signal at various points within the system. Optical processing has been previously discussed and it was shown that for the application of increasing redundancy, optical processing could not be employed. The PEQ concept was discussed in the previous section and it was found to be somewhat limited in the amount of redundancy that it could regain. This is due mainly because the data are quantized and, therefore, only a finite number of operations and decisions are possible. Therefore, the one-dimensional analog processing would appear to be the most logical choice for processing of the data. Previous approaches will be described along with a discussion of certain constraints which exist with this operating method when applied to a digital TV system such as EDITS.

One method used in some conventional systems is to pass the analog signal through a low-pass filter where the high frequencies are attenuated. This results in the analog-processed signal containing more redundancy and, therefore,

being capable of yielding a higher compression ratio. This is the simplest approach, but degrades the image drastically. Another technique which has been investigated by Bruce [a] of Bell Telephone Laboratories is the use of preemphasis and deemphasis networks. The preemphasis network is optimized to provide the maximum ratio of peak-to-peak signal-to-rms weighted noise. By placing the optimum preemphasis network before the PCM system and the corresponding deemphasis network after the PCM system, picture quality can be improved. "It is judged that a 4-digit picture with preemphasis and deemphasis is equivalent (subjectively) to a 5-digit picture without these networks."[b]

4.4.2 System Limitations

In a conventional PCM television system it is possible to reduce the bandwidth by analog processing and adjusting the sampling rate to properly match the processed bandwidth. In a pure digital TV system it is extremely difficult and impractical to perform normal analog processing. The preamplifier bandwidth is determined by the fact that video coming from the vidicon is in the form of pulses of the RZ type which are then sampled and held and converted to binary words. The video preamplifier bandwidth has been optimized for maximum peak signal-to-rms noise ratio. Therefore, it is not desirable in a digital system such as EDITS to place a filter before the sample-and-hold circuitry. The frequency spectrum of the video resulting from the digital scan consists of a carrier and its harmonics with each having sidebands; this carrier is 100-kc/s for EDITS. If a 50-kc/s low-pass filter is placed in this video chain, not only does the signal-to-noise ratio decrease, but much of the video information is removed. (The 50-kc/s cutoff frequency was chosen because it is one-half the 100-kc sample rate which exists in EDITS.)

Since it is not desirable to place a low-pass filter before the sample-and-hold, it was decided to place the filter between the sample-and-hold and the analog-to-digital converter and investigate the effect on PE probability and picture quality. These results were then compared with those obtained by the use of the PEQ technique. Although this is an unusual place for a filter, it is the only feasible location within EDITS.

4.4.3 Experimental Procedure

A switchable three-pole Bessel active filter was employed for this experiment. Amplitude and phase response curves for this unit are shown in Figures B.4-18 and B.4-19, respectively.

[a]Bruce, R. A., "Optimum Pre-Emphasis and De-Emphasis Networks for Transmission of Television PCM," IEEE Transactions on Communication Technology, September, 1964, pp. 91-96.

[b]Op. cit.

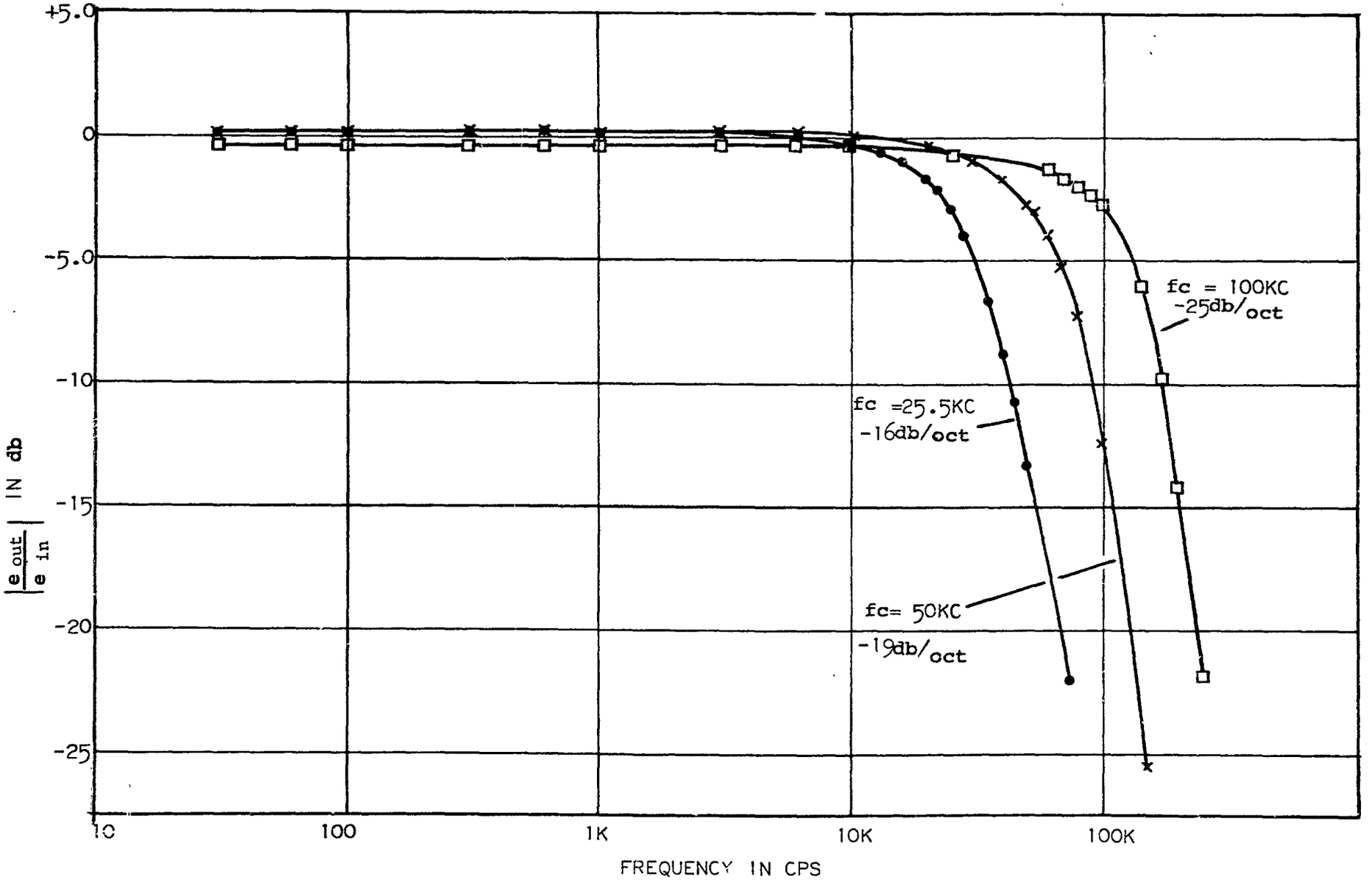

FIGURE B.4-18

AMPLITUDE RESPONSE CURVE FOR 3-POLE BESSEL ACTIVE FILTER

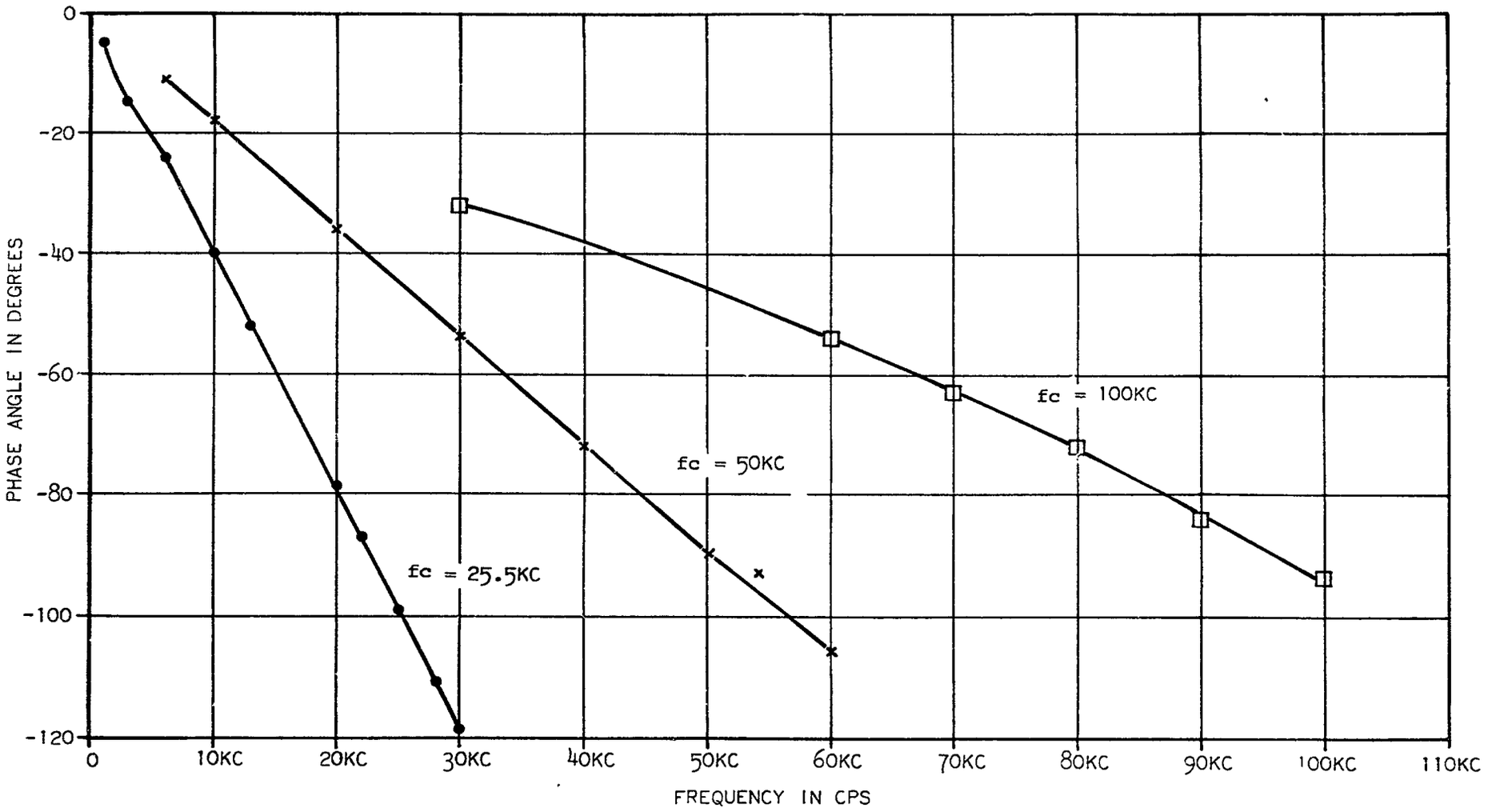

FIGURE B.4-19

PHASE RESPONSE CURVE FOR 3-POLE BESSEL ACTIVE FILTER

For this investigation the standard 256 x 256 raster and 100-kc sample rate was employed; the MIT-girl picture with 4-bit quantization was used as the test subject. After establishing the sensor signal-to-noise ratio, the filter cutoff frequency has varied downward from 50 kc and the PE count recorded for various cutoff frequencies. Photographs demonstrating the degradation of picture quality with decreasing bandwidth were taken at 50 kc, 25.5 kc, 12 kc, 6 kc, and the frequency at which the PE count was equal to that obtained by the use of the PEQ technique. This procedure was followed for sensor signal-to-noise ratios of 40 db, 30 db, and 20 db. These photographs are shown in Figures B.4P-11 through B.4P-13; graphs of PE probability and PEC compression as a function of filter cutoff frequency are shown in Figures B.4-20 and B.4-21, respectively.

Additional brief experiments comparing spot-wobble scanning (which consists of rapidly moving the display beam in an oscillatory motion about its nominal display position) and dot-interlace scanning (in which the elements interlace to form a diamond pattern), were conducted on a 128-x-256-element raster; the filter was not used in this study. The experiment consisted of taking a 6-bit picture using spot wobble and a 6-bit picture employing dot-interlace scanning and qualitatively comparing the results; the sensor signal-to-noise ratio was set at 40 db. These pictures are shown in Figure B.4P-14.

4.4.4 Conclusions

For sensor signal-to-noise ratios near 40 db, the PEQ technique is superior to one-dimensional analog processing. The cutoff frequency at which the PE probability of one-dimensional analog processing exceeds that of PEQ is at a value where the picture quality is inferior to the equivalent PEQ rendition. At sensor signal-to-noise ratios near 20 db, one-dimensional analog processing yields a higher quality picture than PEQ at the point where the PE probabilities of the two processes are equal; this is due to the filter softening the effects of the noise.

Dot-interlace scanning was shown to provide a more pleasing picture than spot wobble. This is due primarily to smooth curves being retained by dot-interlace scanning while spot-wobble yields a stairstep approximation to smooth curves. The detail rendered by the two techniques is nearly the same.

As a final statement, it should be noted that the investigation which has been conducted is not in the strict sense one-dimensional analog processing. An analog system is required to properly study this method of signal processing. Due to EDITS being strictly a digital system, it was not possible to perform one-dimensional analog processing in the usually conceived manner.

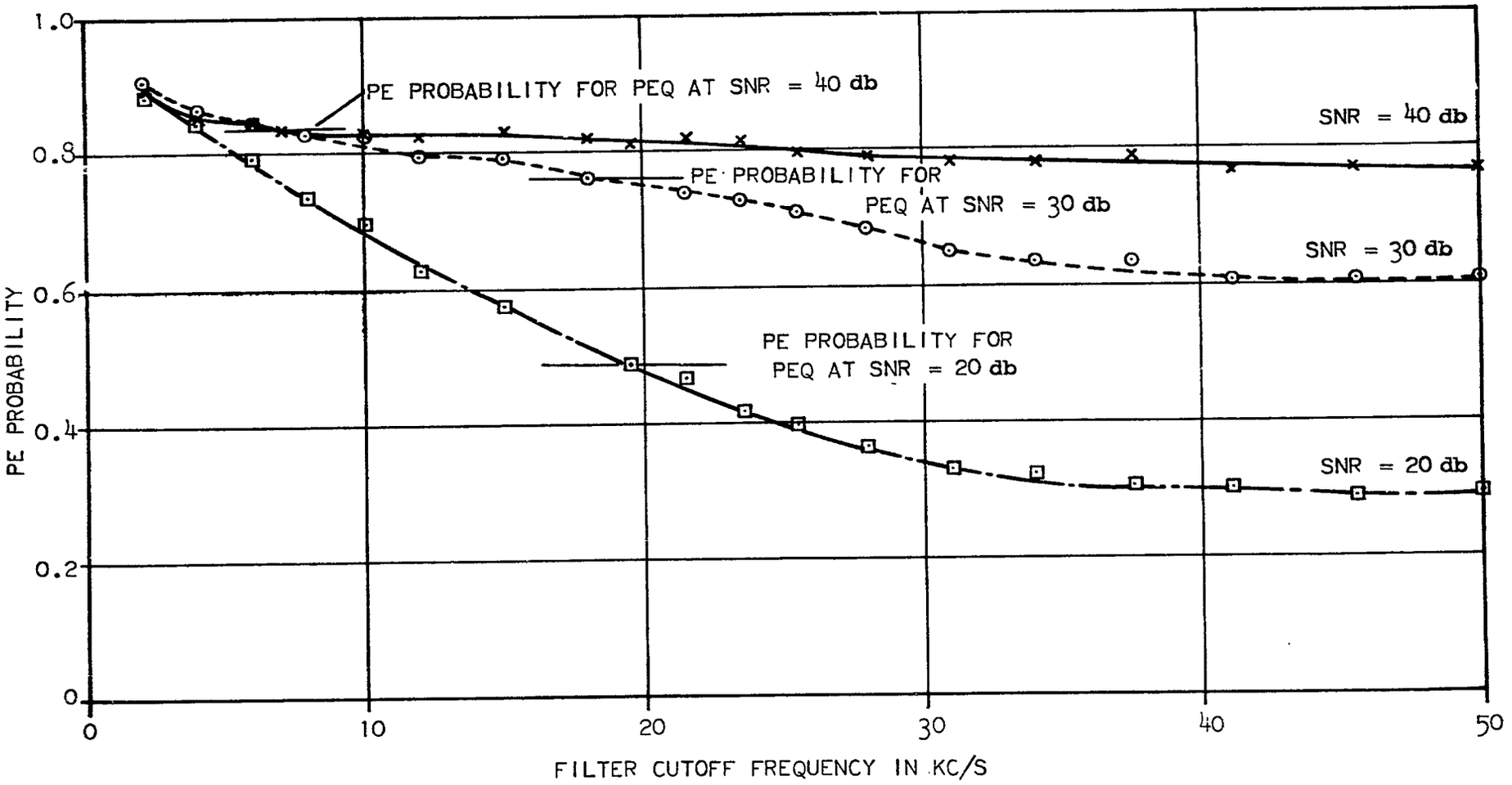

FIGURE B.4-20

PE PROBABILITY VERSUS ONE-DIMENSIONAL ANALOG PROCESSING FILTER CUTOFF FREQUENCY WITH VARYING SNR FOR 4-BIT MIT-GIRL PICTURE

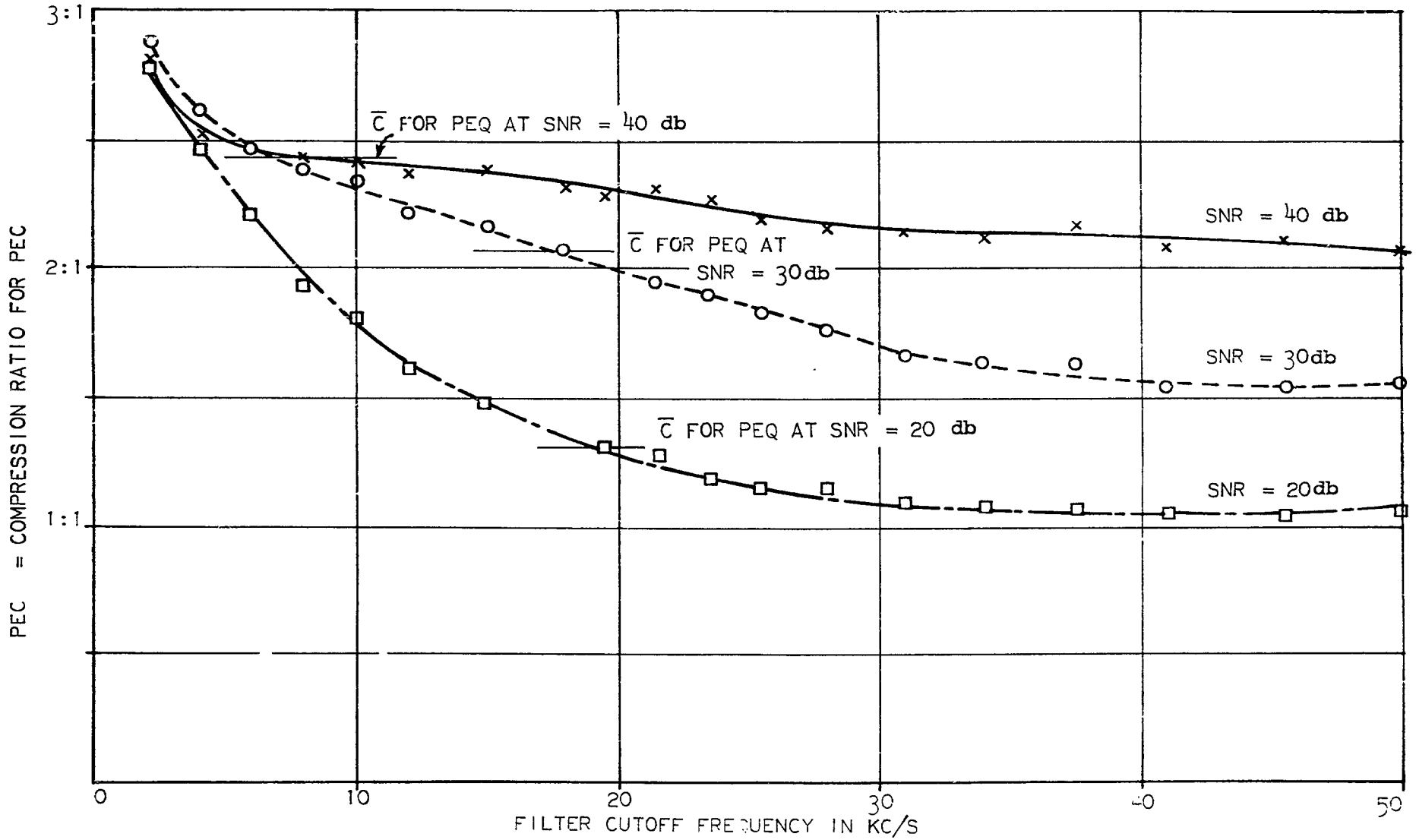

FIGURE B.4-21

COMPRESSION RATIO VERSUS ONE-DIMENSIONAL ANALOG PROCESSING FILTER CUTOFF FREQUENCY WITH VARYING SNR FOR 4-BIT MIT-GIRL PICTURE

SECTION 5

LINEAR APPROXIMATION

5.1 INTRODUCTION

The goal of the compression task was to find a coding technique that would result in a 6:1 compression. Frame-to-frame coding and area coding which are both information-preserving techniques did not meet the desired goal of a 6:1 compression. The next logical technique to investigate is run-length coding which also has the potential of achieving a 6:1 compression. Run-length coding can be considered as a zero-slope encoder. This technique is limited as to the maximum compression it can achieve. Modifications may be made on the run-length coding approach to obtain an increase in efficiency; one such modification being a zero-order predictor. Techniques of this nature remove redundancy by approximating the video signal. The allowable degree of the approximation is determined by the subjective fidelity requirements in the following manner. Assume that the data arequantized to N bits (or $n = 2^N$ levels) and place a tolerance band around each sample. Now consider any element j and store in the compressor memory the magnitude and location of j. Compare the magnitude of j and the j + 1 element. If the difference exceeds the tolerance band, transmit the magnitude and address of j to the buffer memory and place the magnitude and location of j + 1 in the compressor memory. If the difference between j and j + 1 is less than the tolerance band, discard the j + 1 element and continue the procedure by comparing the j + 2 element and the jth element. The gross average compression formula is given by:

$$\overline{LAC} = \frac{NEL}{(N + \log_2 E)(S + 1)} \tag{1}$$

where E = number of elements per line, L = number of lines per frame, and S = the number of samples sent to the buffer memory. Figure B.5-1 presents a waveform to illustrate the technique. Assume that the waveform given in Figure B.5-1 is quantized to 4 bits, and 5 bits are needed to specify location of the essential samples. The essential samples that must be transmitted with the zero-order predictor technique are designated as X. Therefore, the compression is given by

$$\overline{ZOC} = \frac{4(32)}{9(13)} = 1.09:1$$

Although, in general, this value will be higher for a typical frame of data, it follows that there should be other approaches available to increase the efficiency of such a technique. One approach is to add to the coding algorithm another algorithm that states an element will not be declared essential unless it and the

element that follows it is also outside the error-band. This is essentially implementing the PEQ concept with the zero-order predictor algorithm. In general, it will be assumed that if element j and j + 2 have the same intensity, element j + 1 must also have the same intensity. If the intensity of j + 1 is not like j and j + 2, then it will be assumed that j + 1 has been caused by noise and the coding algorithm strips or eliminates the noise from the frame. Consider now applying the modified zero-order predictor techniques to Figure B.5-1. It is apparent that elements 14 and 21 have been caused by noise and it will be shown that allowing a single consecutive error to exceed the error band will increase the efficiency. The compression for this approach is 4(32)/9(9) = 1.58:1. Thus, for the simple example chosen, the compression increases by 50% by allowing a single error to exceed the error band.

5.2 LINEAR-APPROXIMATION CONCEPT

A careful examination of Figure B.5-1 reveals that there could exist other coding techniques that could achieve a large compression by not only encoding zero-slopes as with the zero-order predictor, but encoding <u>all</u> slopes. The linear-approximation technique accomplishes this. Consider now a typical element j. The linear-approximation technique operates in the following manner. Elements j and j + 2 are connected by a straight line and the value of the straight line at sample j + 1 is interpolated. The actual element value at j + 1 is compared to the interpolated value. If the difference between these two values exceeds a pre-established error band, the value of the sample at j + 1 and $\Delta x = 1$ are transmitted to the buffer memory. If the difference does not exceed the error band, the element j and j + 3 are connected by a straight line and the interpolated values at elements j + 1 and j + 2 are calculated and compared to the actual element values. If these differences do not exceed the error band, the technique continues by connecting j and j + 4 with a straight line and calculating the differences. The gross average compression for transmitting the absolute magnitude and Δx is given by

$$\overline{LAC}_g = NEL/(N + \log_2 \Delta x)\ (S' + 1) \qquad (2)$$

Consider Figure B.5-1 to compare the efficiency of the zero-order predictor and the linear-approximation technique just described. For the given error band and consecutive errors outside the error band that were used for the zero-order predictor, the representation of the function is given by the O's which are the necessary points to represent the function with a series of slopes. The linear-approximation compression is given by 4(32)/9(4) = 3.56:1 which is an increase in compression by a factor of 2.25:1. It can be shown that the linear-approximation coding technique will always give a value of compression larger than that which can be achieved by the zero-order predictor for the same error criterion. Studies have been conducted previously which show that a compromise exists for the maximum Δx, compression, and implementation complexity. For the purposes of

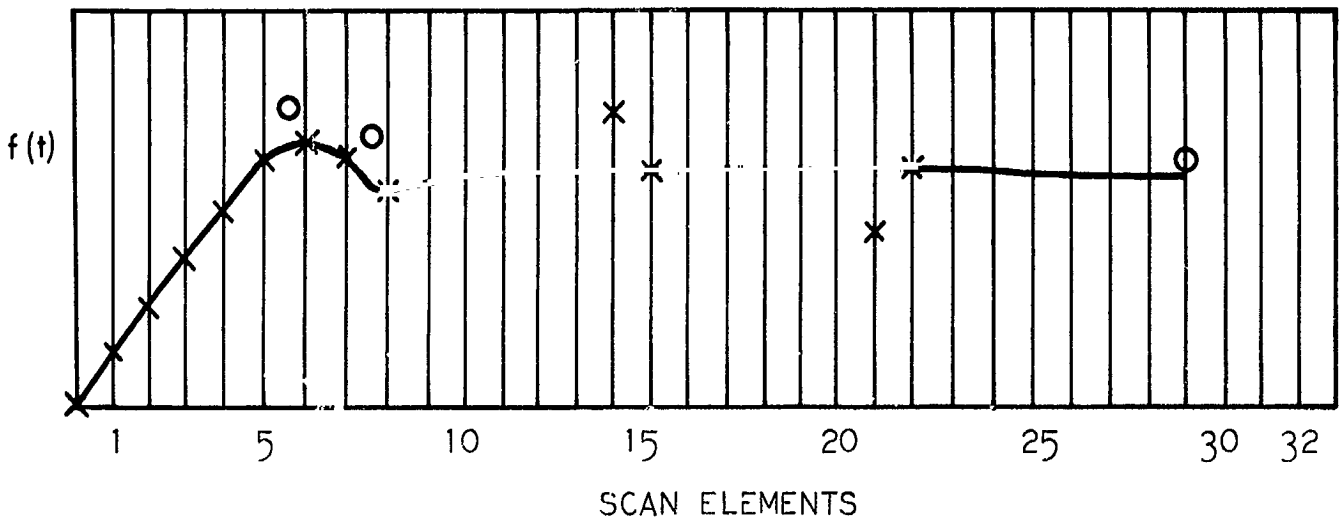

FIGURE B. 5-1

ANALYSIS WAVEFORM

this study Δx maximum was chosen to be 16. However, several calculations were made for $\Delta x = 32$ to illustrate the validity of the Δx choice. By increasing the error-band it becomes apparent that there is a limit to the amount of compression that can be achieved. Consider now adding the noise-stripping algorithm to the linear-approximation technique. Using Figure B.5-2 as a test line of video composed of 256 6-bit words, the compression and rms error can be calculated for a family of error-band sizes and allowable consecutive errors outside the error band. A computer program was written to calculate the compression for flat coding and the rms error relative to 6-bit quantization for an error band of ±1, ±2, and ±4 levels out of 64 levels, and for 0, 1, and 2 successive errors outside the error band. The gross average compression for flat coding (using formula 2) and optimum (Huffman) coding and the rms error are given in Table B-1. The percentage of full-scale rms error for 5-bit, 4-bit, and 3-bit quantization is 1.1, 2.97, and 5.97%, respectively. The results of this are given in Figure B.5-3. Several rather interesting points are raised by an examination of this curve. At an error band of ±2 with a single error allowed, the rms error for the PCM and linear approximation is nearly the same; however, the compression is 2.5 versus 1.5 for the equivalent PCM compression.

TABLE B-1

LINEAR-APPROXIMATION SIMULATION RESULTS

Item	No Errors			One Error			Two Errors		
Parameter error band	±1	±2	±4	±1	±2	±4	±1	±2	±4
Flat coding	0.93	1.64	3.12	1.88	2.72	4.12	2.56	3.20	5.56
Optimum coding	1.59	2.56	4.48	2.86	4.03	6.17	3.79	4.58	8.53
RMS error % full scale	0.9	1.77	3.40	2.35	2.76	4.53	3.34	4.05	5.39

For an error band of approximately ±3.3 and allowing two successive errors outside the error band, compression is 5.8 versus 2.8 for the equivalent PCM system. Or, for an error band of ±4 and 1 allowable error, the rms error is 1.5% less than the equivalent PCM system while the compression for linear approximation is double that of equivalent PCM. These results and others discussed in the JPL final report[a] led to a computer simulation of the encoding technique. An extension of the simulation, which allows a subjective evaluation of the coding technique, will be discussed in the following section.

[a] Final Report, Video Data Modulation Study, Electro-Mechanical Research, Inc., Sarasota, Florida, Prepared for Jet Propulsion Laboratory, California Institute of Technology, Pasadena, California, July 31, 1964.

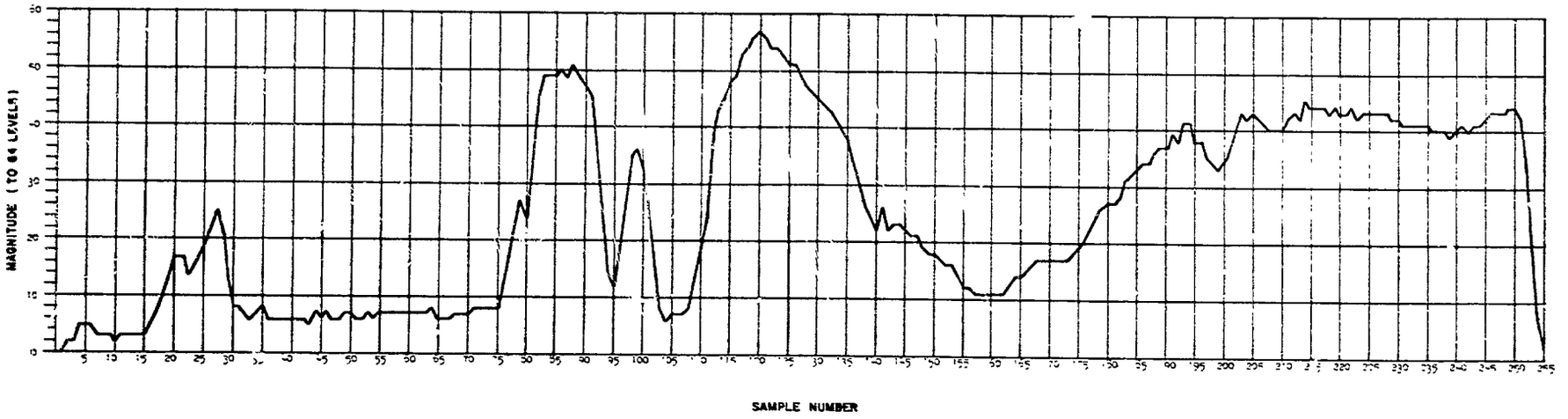

FIGURE B. 5-2

SINGLE LINE TRACE OF MIT GIRL

03186

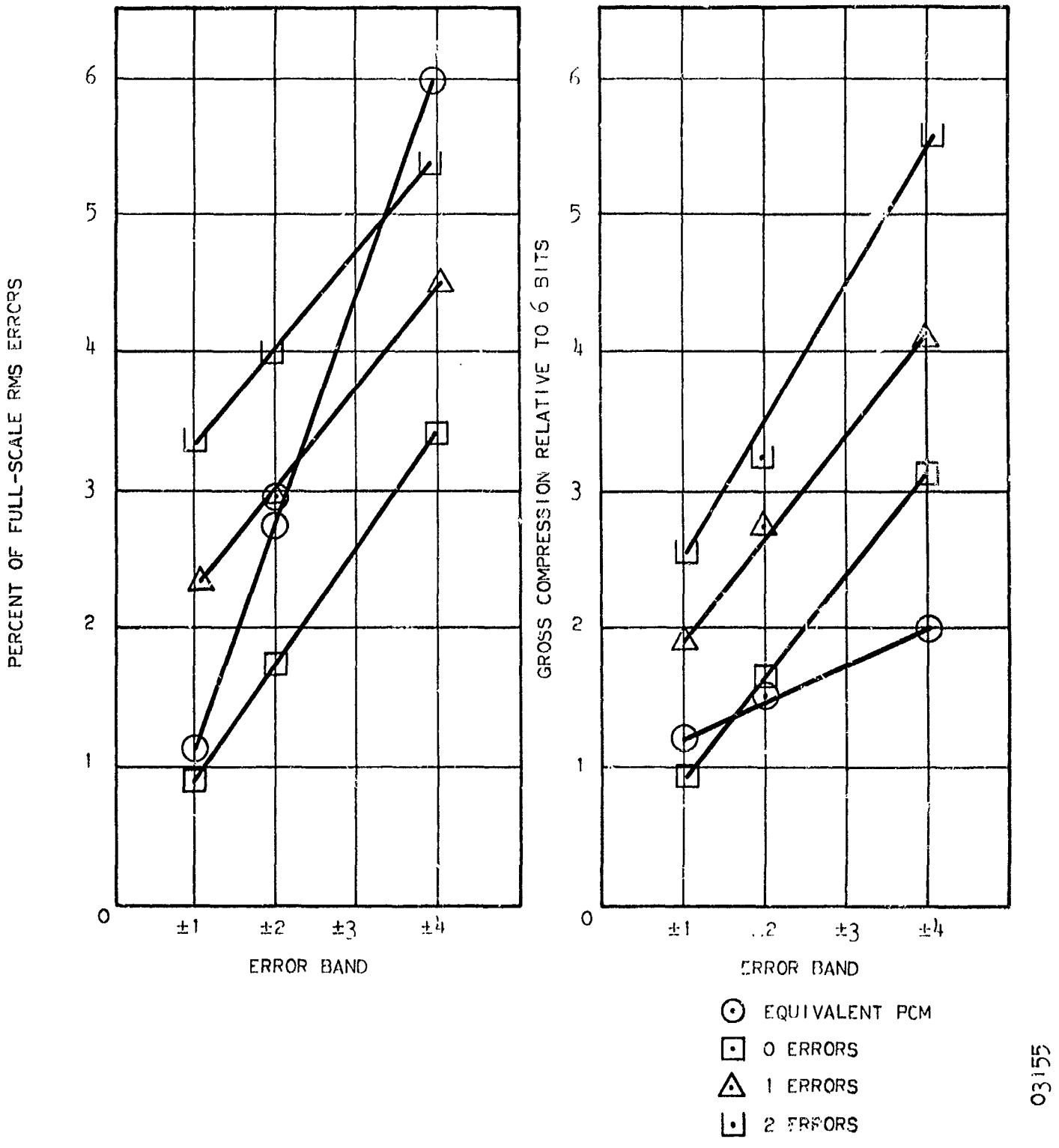

FIGURE B. 5-3

LINEAR APPROXIMATION COMPRESSION AND RMS ERROR RESULTS

5.3 COMPUTER SIMULATION

The linear-approximation coding technique with a variable error, variable number of allowable errors outside the error band, and a variable truncation represents a rather difficult problem in optimization. For example, allowing an error band set of ±1, ±2, ±3, ±4, ±5, and ±6 levels out of a possible 64 amplitude levels, allowing 0, 1, and 2 consecutive errors outside the error band, and truncations of Δx of 16 and 32, represents 36 parameter combinations per test object. Initially it was assumed that the system would be implemented using only a small number of error bands, no errors outside the error band, and a single truncation. It was believed that careful examination of the previous simulation of linear approximation would permit this; however, although it has been shown by subjective tests that the rms error can be related to subjective pictorial quality, the results are not absolute and a quantitative relationship has not been established. Therefore, it was decided that upon completion of the ASI/EDITS interface, the linear-approximation technique would be simulated, with the computer acting as an encoder-decoder, with the results displayed on EDITS. Figure B.5-4 shows the flow diagram of the linear-approximation program. To ensure proper operation of the technique a rather complicated line of video was manually simulated and processed on the computer for comparison purposes. Figure B.5-5 shows the original 252 elements in the line quantized to 6 bits and the decoded linear-approximation waveform for an error band of ±1 level, no allowable errors, and Δx truncated at 16 elements, which gave a compression of 1.26:1. Figure B.5-6 shows the original waveform and the linear-approximated version with an error band of ±2 levels. The compression for this case increases to 1.94:1 and the fidelity of this waveform is nearly the same as the ±1 error band. Figure B.5-7 shows the original waveform and the linear-approximated version with an error band of ±4 levels which results in a compression of 3.15:1. This is nearly a three-fold increase in compression over the ±1 error band, but with a decrease in fidelity. It might be mentioned that the PE probability for this line was 0.14 while the average PE for the entire frame was approximately 0.5. Therefore, this line, in a sense, represents a worst case and the average for the entire frame should be much higher than the particular line analyzed.

Based on the above encouraging results, and with the knowledge that a realistic evaluation of the coding technique can be achieved only by combining the compression ratio, complexity of implementation, and subjective quality factors, whole frames of data were processed and evaluated. Four test photographs were chosen for analysis. The choice included (1) an exterior shot of the Gemini capsule in simulated deep space; (2) the classical MIT girl photograph; (3) a view of three astronauts standing beside the Apollo capsule mock-up; and (4) a close-up view of astronaut Cooper in a space suit and helmet. Photographs (1), (3), and (4) appear to be representative of some possible scenes that may be encountered on a typical manned spacecraft mission. The MIT girl photograph was included for historical and comparative purposes due to its wide usage in previous studies. Due to the physical magnitude of the volume of photographs involved in a complete analysis, the technique was evaluated by first considering what parameter

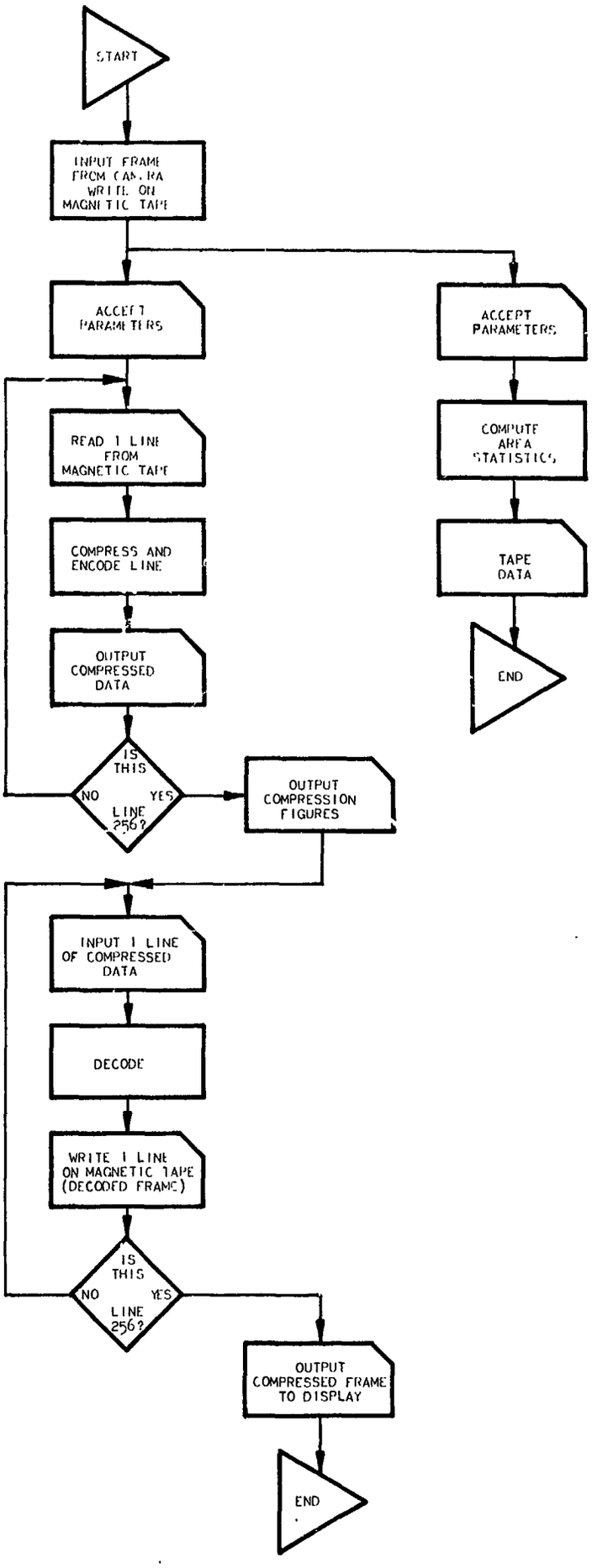

FIGURE B.5-4

LINEAR-APPROXIMATION AND AREA-CODING FLOW DIAGRAM

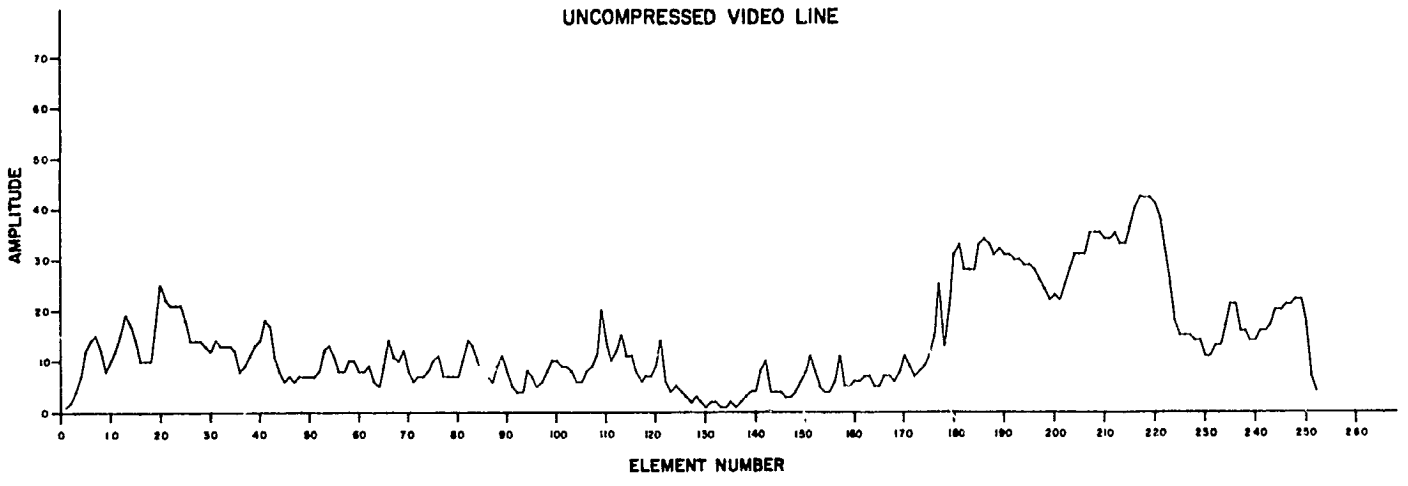

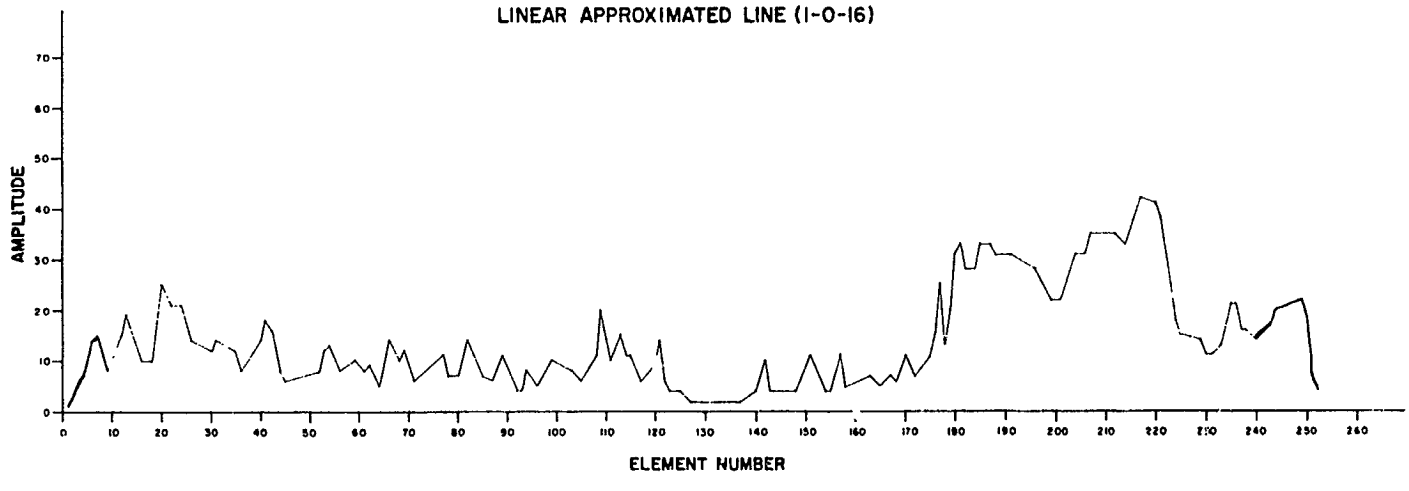

FIGURE B.5-5

COMPARISON OF NONCOMPRESSED VIDEO LINE
AND LINEAR APPROXIMATION VERSION FOR 1-0-16

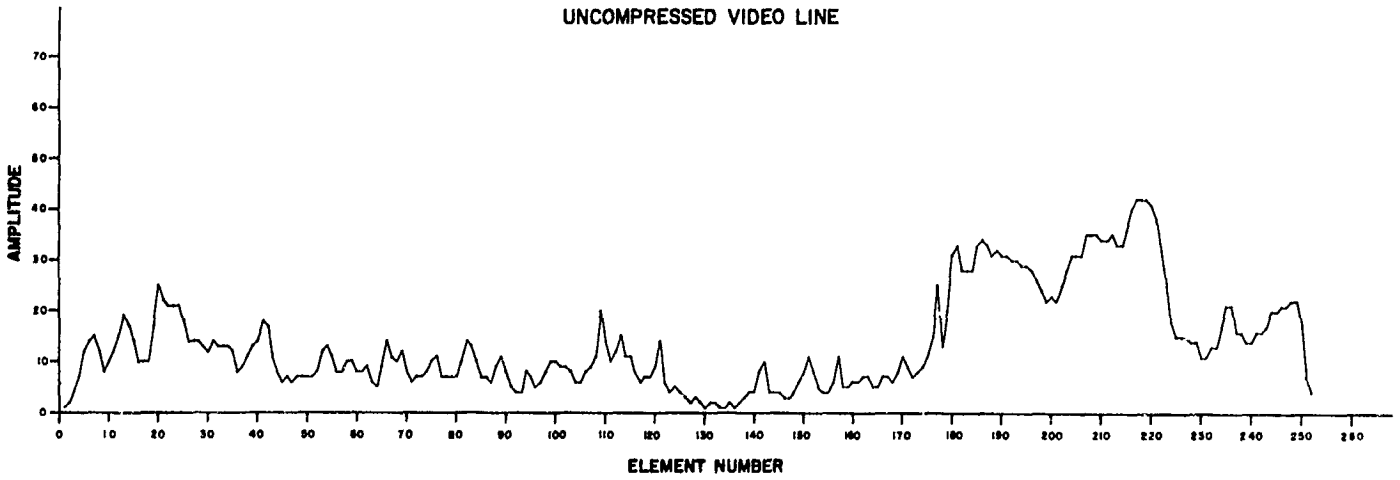

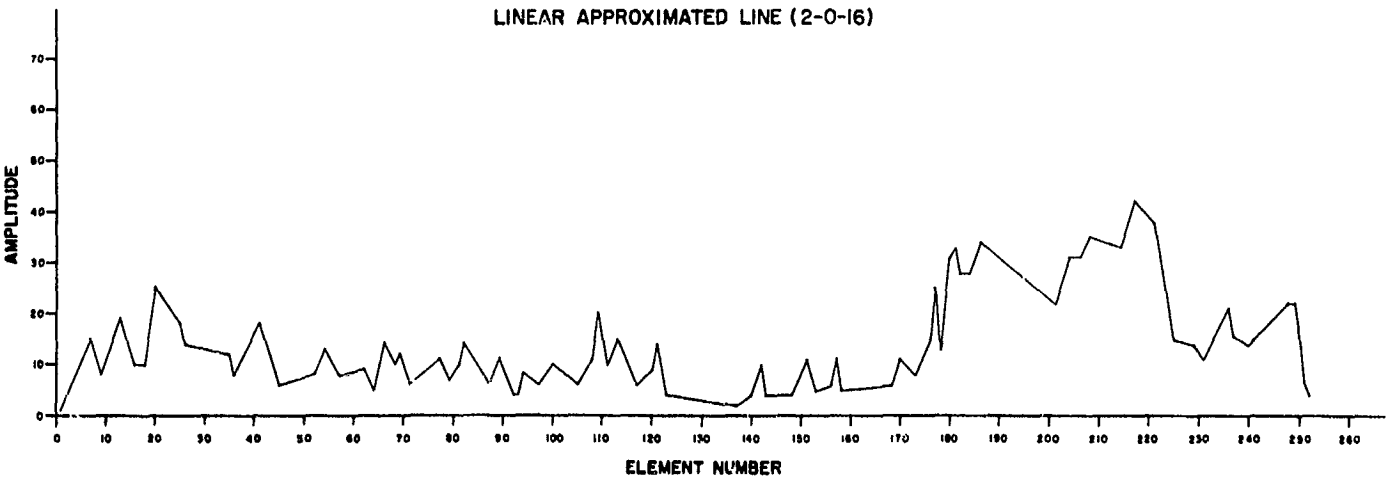

FIGURE B.5-6

COMPARISON OF NONCOMPRESSED VIDEO LINE
AND LINEAR APPROXIMATION VERSION FOR 2-0-16

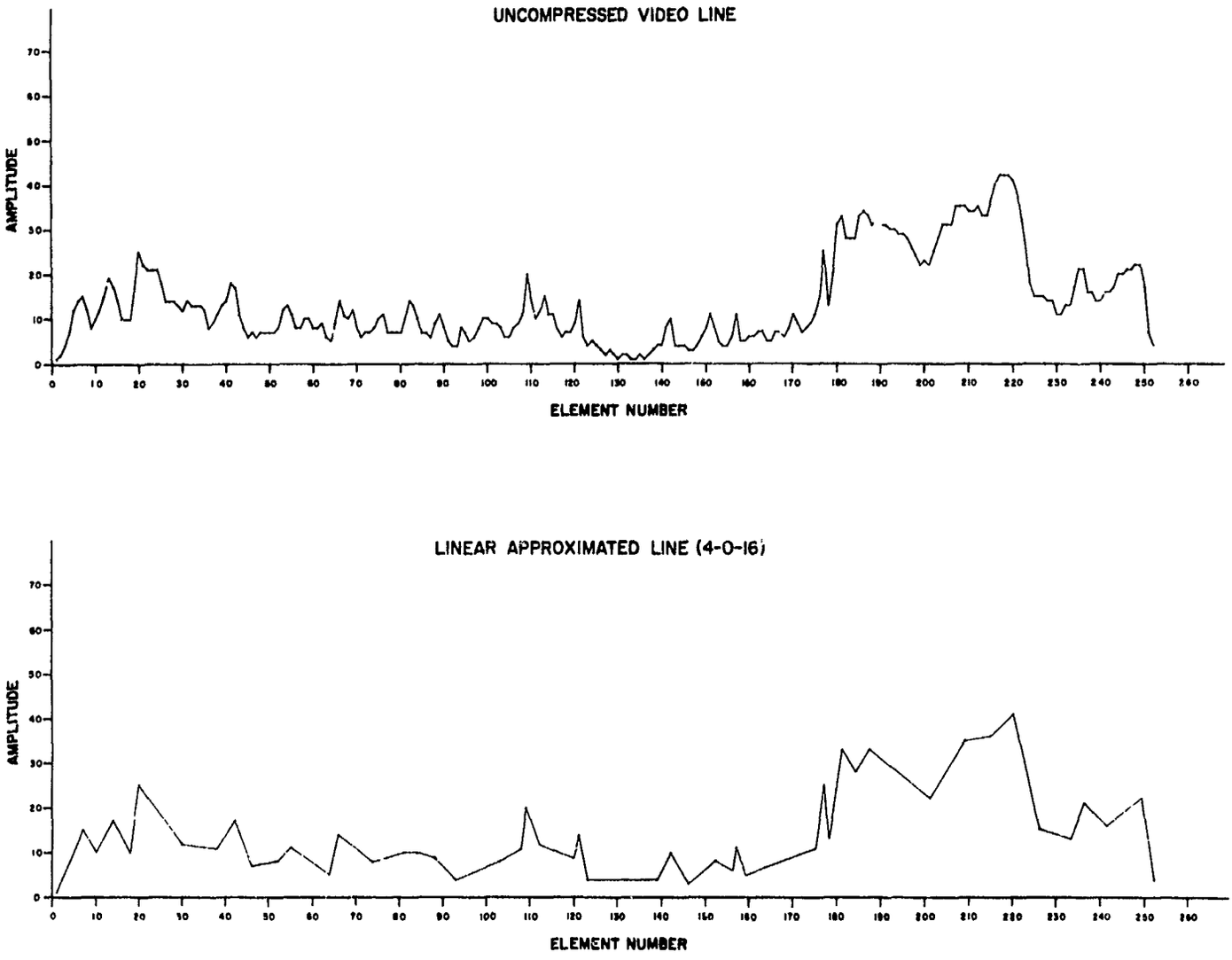

FIGURE B. 5-7

COMPARISON OF NONCOMPRESSED VIDEO LINE
AND LINEAR APPROXIMATION VERSION FOR 4-0-16

combinations resulted in the desired goal and selecting representative photographs satisfying these requirements. Therefore, the initial results of the simulation was a set of compression versus error band, allowable errors, and truncation values.

Figure B.5-8 plots compression as a function of error bands of ±1, ±2, ±3, ±4, ±5, and ±6 levels of 0, 1, and 2 allowable consecutive errors outside the error band, and a Δx truncation of 16. An examination of this curve reveals several interesting points. The Gemini and MIT-girl pictures represent a practical upper-bound on compression while the Cooper and Apollo pictures represent a practical lower-bound. Considering the Cooper photograph, it is apparent that the desired goal of 6:1 compression has not been achieved for pictorial material of this nature, but rather 4:1. The interesting aspect of this approach is that a 4:1 compression can be achieved with the following parameter combinations (1) ±6-0-16; (2) ±4-1-16; and (3) ±3-2-16. Note that by allowing a single consecutive error the physical size of the error band is decreased from ±6 levels to ±4 levels, not quite a 2:1 reduction, but sufficiently close to imply that the pictorial quality of the ±4-1-16 picture should be superior to the ±6-0-16 picture. This implication is supported by the PEQ analysis which showed that subjectively there was little difference between PEQ and PCM without PEQ. Since the single-allowable-error criteria is the PEQ concept applied to all slopes, it is anticipated that picture ±4-1-16 should be subjectively better or equivalent to the ±6-0-16 picture. Although the error-band can be decreased to ±3 if two consecutive errors are allowed, it remains to be seen whether the subjective quality is equivalent to the ±6-0-16 picture. Figure B.5P-1 shows these three photographs of the Cooper picture and a 4-bit and 6-bit original for comparison purposes. Unfortunately an examination of the ±6-0-16 and the ±4-1-16 photographs reveals that each approach has different artifacts and a clear-cut decision cannot be made; however, when the ±3-2-16 photograph is compared to the others there is definite degradation. Edge transitions are altered by the allowable errors while a large error-band alters the fine-line grain structure and gradual contours. Hence, depending upon the application, either approach could be employed. This set of photographs represents the lower-bound on compression for the technique.

Consider now the practical upper-bound on compression by considering the Gemini photographs. The Gemini and Cooper photographs were compressed for the parameter combinations of ±1, ±2, ±3, ±4, ±5 and ±6 levels; 0, 1, and 2 allowable errors and Δx truncations of 16 and 32. Figure B.5-9 plots the compression as a function of the error-band criteria, allowable-errors criteria, and a Δx truncation of 32. For the Gemini photograph, it is apparent that the desired goal of 6:1 compression has been achieved for pictorial material of this nature. A 6:1 compression can be achieved with parameter combinations of ±5-0-32, ±3-1-32, and ±2-2-32. Figure B.5P-2 shows the three Gemini photographs and the same comments which describe the Cooper photographs also apply here. It is apparent that except for the minor deficiencies, the linear-approximation technique is a subjectively suitable and useful digital television compression technique which will provide compressions from 4:1 to in excess of 6:1.

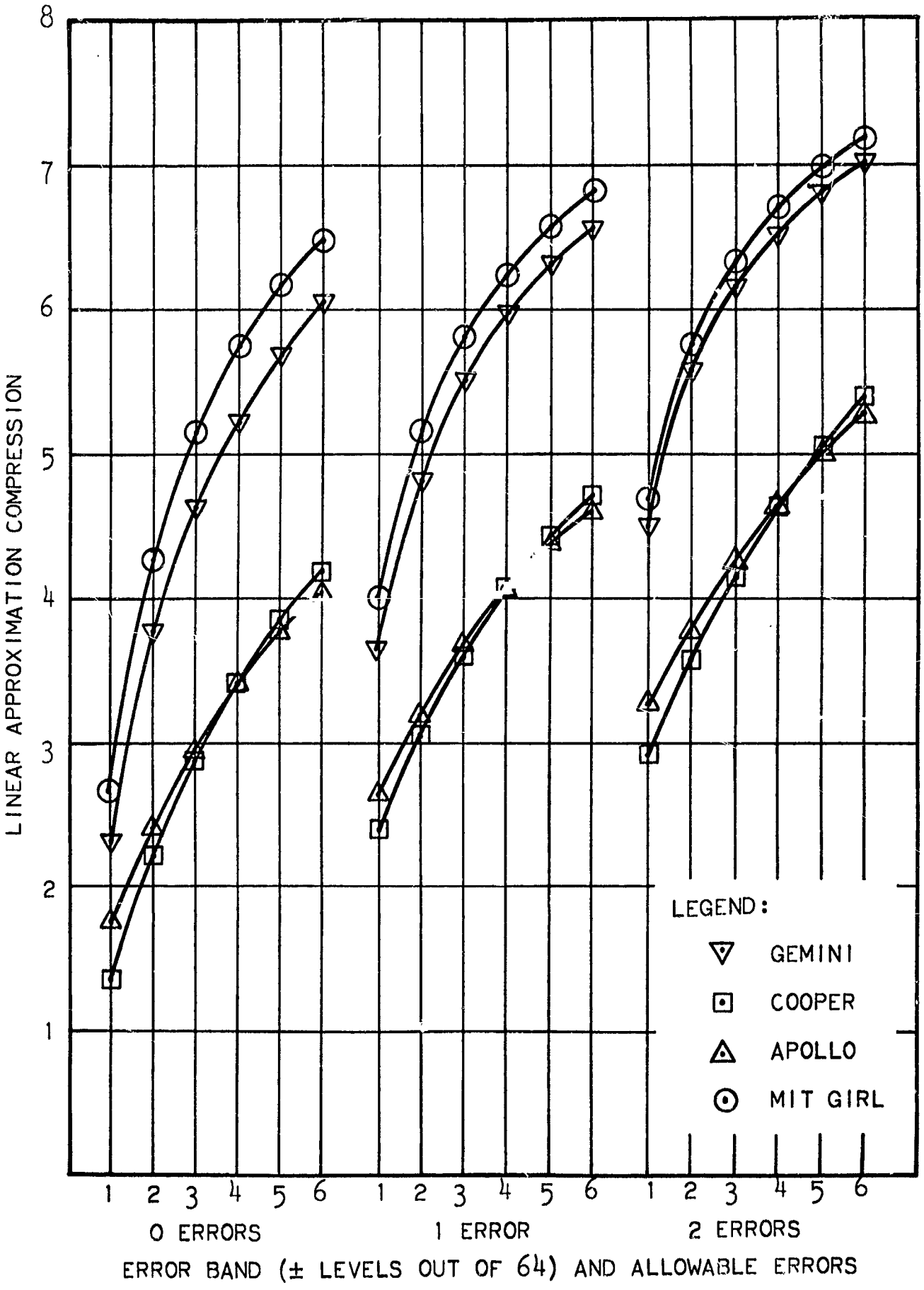

FIGURE B.5-8

LINEAR-APPROXIMATION COMPRESSION AS A FUNCTION OF ERROR BAND AND ALLOWABLE ERRORS FOR A TRUNCATION OF 16

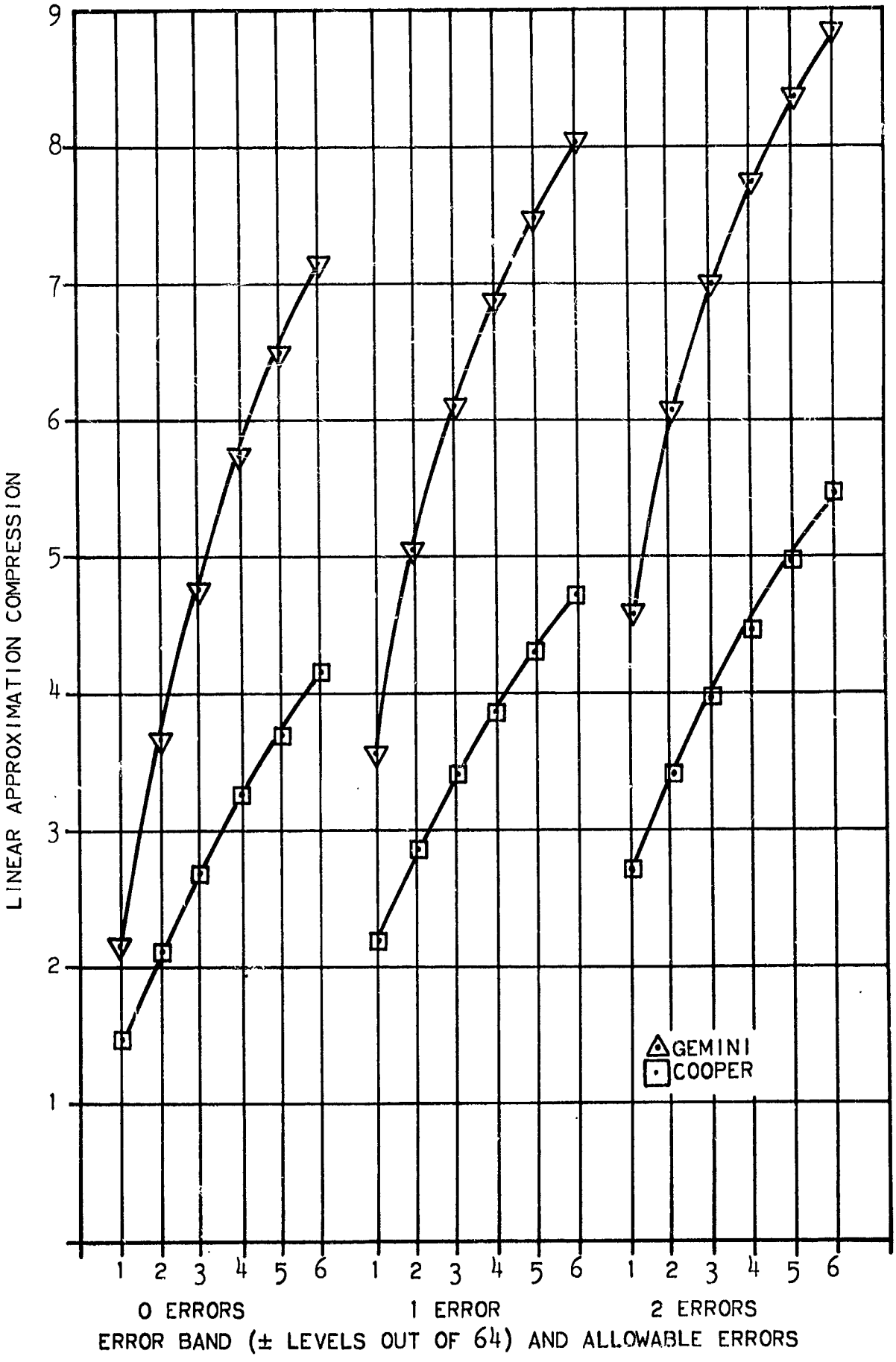

FIGURE B. 5-9

LINEAR-APPROXIMATION COMPRESSION AS A FUNCTION OF ERROR BAND AND ALLOWABLE ERRORS FOR A TRUNCATION OF 32

Figure B.5P-3 shows a ±4-1-16 compressed photograph of the Apollo picture with a compression of 4.05:1. For this particular picture the single-error criterion degrades the edge transitions appreciably; however, the photograph represents 1.5-bits per element which is a rather substantial compression in comparison to other techniques. At the other extreme, Figure B.5P-4 presents the MIT-girl photographs of ±2-0-16 and ±4-0-16 representing compressions of 4.15:1 and 5.7:1, respectively. There is essentially no difference between the original and the linear-approximated version of 2-0-16 representing a 4:1 compression. For compression approaching 6:1 the image quality is somewhat degraded yet the essential features remain and are readily identifiable. Figures B.5P-5 and B.5P-6 represent compressed photographs of various other combinations. Note that in Figure B.5P-5 the 6-2-32 condition represents nearly 9:1 compression, but at a cost in fidelity.

Although these photographs represent a comparison of the original and the various linear-approximation parameter combinations, they should also be compared with other coding techniques. Figure B.5P-7 compares the Cooper picture encoded with (1) 2-bit delta modulation; (2) 2/3 Roberts; (3) 3/4 Roberts; (4) the 6-bit original; (5) the 4-bit original; and (6) the ±5-0-16 linear-approximation photo giving 1.58 bits per element. Based on entropy rather than compression, the 6-bit-per-element PCM has the highest entropy; in descending order, the others are 4-bit-per-element PCM, 3-bit-per-element Roberts, 2-bit-per-element Roberts, 2-bit-per-element delta, and 1.58-bit-per-element linear approximation. The question posed by Figure B.5P-7 is what technique gives the best subjective picture for the minimum entropy. It becomes apparent that it is necessary to trade subjective quality for compression to determine the best operating system. Immediately the 2/3 Roberts system is eliminated on poor subjective quality. Although the 3/4 Roberts cannot be eliminated directly on this basis by comparing the entropy of the remaining two systems, it is eliminated on a compression basis. This merely leaves the 2-bit delta and the 1.58-bit linear-approximation systems. At this point, the "softness" quality of the delta outweighs its implementation ease and the linear-approximation technique is judged to be the best overall system. The softness and limited step response of the delta system is evidenced by the complete loss of the features of the teeth. Therefore, in general, the delta system loses the fine detail structure of the picture, and compared to the linear approximation picture, is judged inferior.

The implementation of the linear-approximation coding technique will be discussed in Appendix F. An encoder design at a 100-kc rate has been shown without the buffer store. The physical size of the buffer store can be determined by obtaining a histogram of the number of segments per frame. Figure B.5-10 plots a histogram for the ±5-0-16 Gemini picture which has a 5.7:1 compression. The distribution shows that the maximum buffer size required is of 500 bits. The mean value of the distribution is given by $\mu = \Sigma_k \; p_k \; x_k = 26.58$; that is, the mean number of segments per line is 27 which represents 270 bits (the maximum number of bits per line is 500 whereas the minimum number of bits is 170). Given a scene and its compression, it is possible to minimize the size, overflow, and underflow of the buffer.

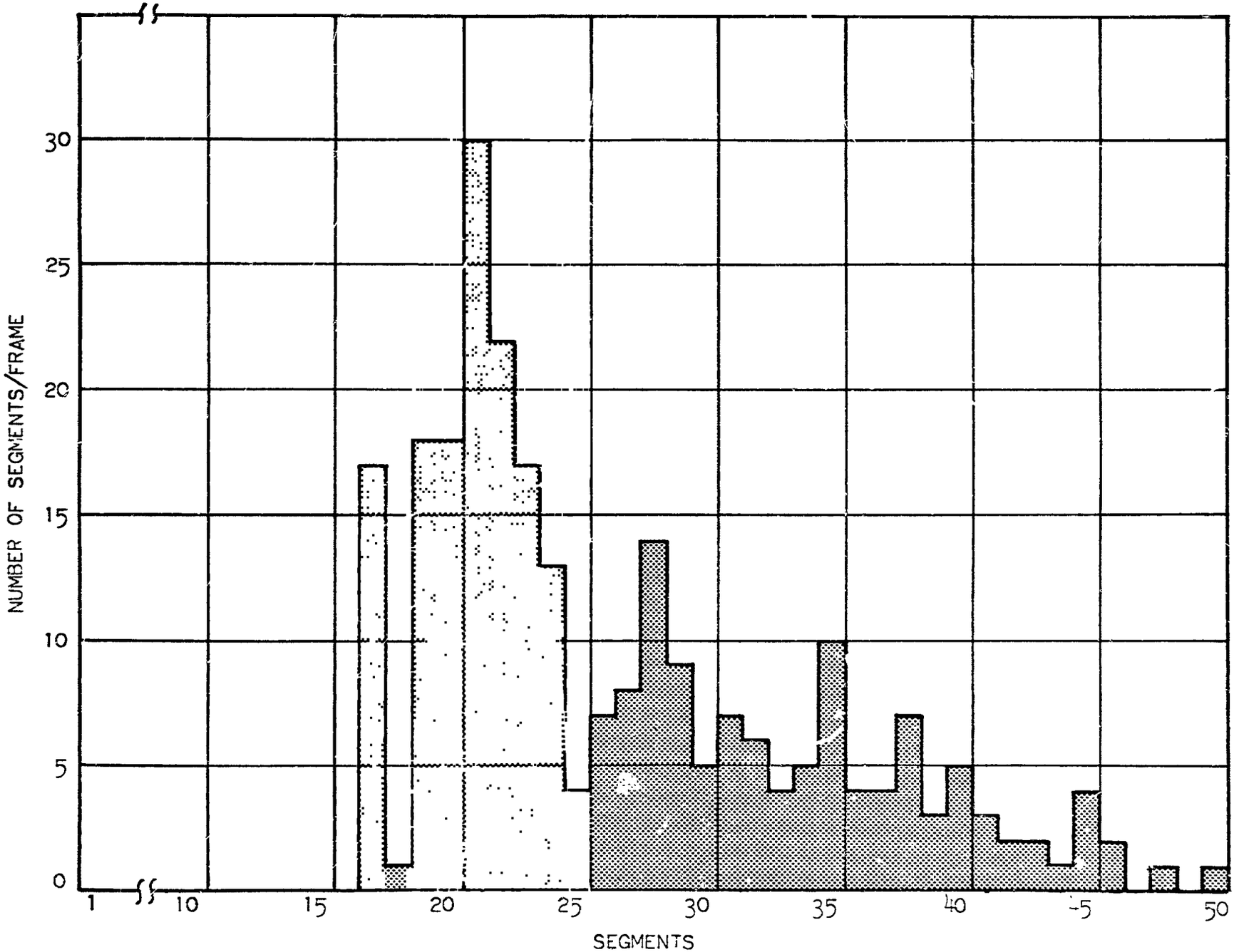

FIGURE B.5-10

HISTOGRAM OF NUMBER OF SEGMENTS PER LINE
FOR GEMINI 5-0-16

5.4 FORMAT DESIGN FOR THE LINEAR-APPROXIMATION DATA-COMPRESSION SYSTEM

5.4.1 Introduction

The linear-approximation system utilizes digital television techniques to approximate the video waveform of each horizontal line of the scanning raster by a curve made up of straight-line segments. The information required for picture reproduction consists of the amplitudes and raster coordinates of the intersections, or vertices, of the line segments. In the case of transmission over an ideal data link, the data compression achievable is determined by the characteristics of the data source together with the established fidelity requirements. To be specific, pictures of a stipulated quality can be represented by some average number of vertices per television line; the average number of transmitted bits per line is the product of the average number of vertices per line and the number of bits required to define a vertex. Since there are no errors in transmission, the vertex coordinates completely suffice for horizontal synchronization, and the only nondata bits which must be transmitted consist of a short pattern, once per frame, for vertical synchronization. These vertical synchronization bits are a mathematically negligible fraction of the total bits. The compression achieved under these conditions is termed gross average compression.

In any practical system application there are errors in the received data caused by noise in the communication channel, and the system design must provide for satisfactory operation in spite of these errors. The requirement for operation in the presence of errors inevitably leads to the addition of redundant bits to the data format. The task of the format designer is to choose the form of redundancy which leads to the highest net compression; included in this task is the design of an optimum data-processing technique for the receiving terminal.

In general, the system can be designed to operate at higher and higher error rates by increasing the number of redundant bits in the format, thus, increasing the bandwidth requirements of the data link. For example, if the system performs adequately at a bit-error rate of 10^{-3} and a bandwidth B_1, an error correcting scheme can be found for which the system has equal performance at a 10^{-2} bit-error rate, at a higher bandwidth B_2. Also, a communication link which has an error rate of 10^{-2} at a transmitter power P_1 can be improved to a 10^{-3} bit-error rate by increasing the transmitter power to P_2. The error-correcting scheme yields an increase in net compression only if $B_2/B_1 < P_2/P_1$. This is the type of tradeoff considered in designing the data format.

One of the major objectives of the format design is to achieve reliable synchronization. In a well-designed system, synchronization should be maintained even at bit-error rates which cause significant picture degradation to allow for the possibility of receiving useful information even under conditions of marginal performance. Methods of achieving stable synchronization, even at high bit-error rates, have been developed for conventional PCM systems and these

methods, with some necessary modifications, are the basis for the linear-approximation system synchronizing scheme. Paragraph 5.4.3 describes several important aspects of conventional PCM synchronization, and the problems involved in synchronizing linear-approximation data. Before designing the synchronization system, it is necessary to establish the form of the transmitted data words; this is the subject of the following section.

5.4.2 Data Coding

The linear-approximation evaluation program is being carried out on video data generated by a 256-line television raster with 256-elements per line; the intensity of each element is encoded to six bits. With the present system configuration, the maximum line-segment length is 16 elements.

There are two obvious ways of coding the transmitted data: the first method is to transmit 14-bit words where six bits give the vertex amplitude and eight bits represent the horizontal position of the vertex; the second method uses 10-bit words, six bits for amplitude and four bits representing the number of elements between vertices. For the case of errorless transmission, the second method is obviously superior since it requires a smaller bandwidth and, hence, yields the higher net compression. At significant error rates, however, the picture fidelity would be much worse with the second method because horizontal position errors are accumulative; thus, the choice of coder would depend on the bit-error probability of the system.

Another possibility is to use an error-correcting code to transmit the ten data bits representing the amplitudes and distance between vertices. One of the shortest available codes for this purpose is the Hamming (14, 10) code; the code words are 14 bits in length, having ten data bits and four check bits. This code corrects all single errors in transmission.

Figure B.5-11 shows a comparison of the three possible coding techniques. The average number of television lines having one or more errors (either vertex amplitude or position) was chosen as the criterion of picture fidelity. To compare the three coding schemes we calculate the net compression achieved for the case of one line per frame having an error; for this case, the fact that the 10-bit code method accumulates position errors has little significance. As discussed in the introduction, net compression is calculated in terms of equivalent saving in transmitter power; the power requirements for a typical system are given in Figure B.5-12.

Table B-2 gives a direct comparison of system performance with each of three data codes, expressed in terms of power saving relative to the 14-bit code without error correcting. The values in column two were read directly from Figure B.5-11 and the values in the third column were derived from Figure B.5-12 by reading the signal-to-noise values corresponding to the bit-error probabilities in column two. The bandwidth equivalent power saving for the 10-bit code was calculated by taking 10 log 14/10.

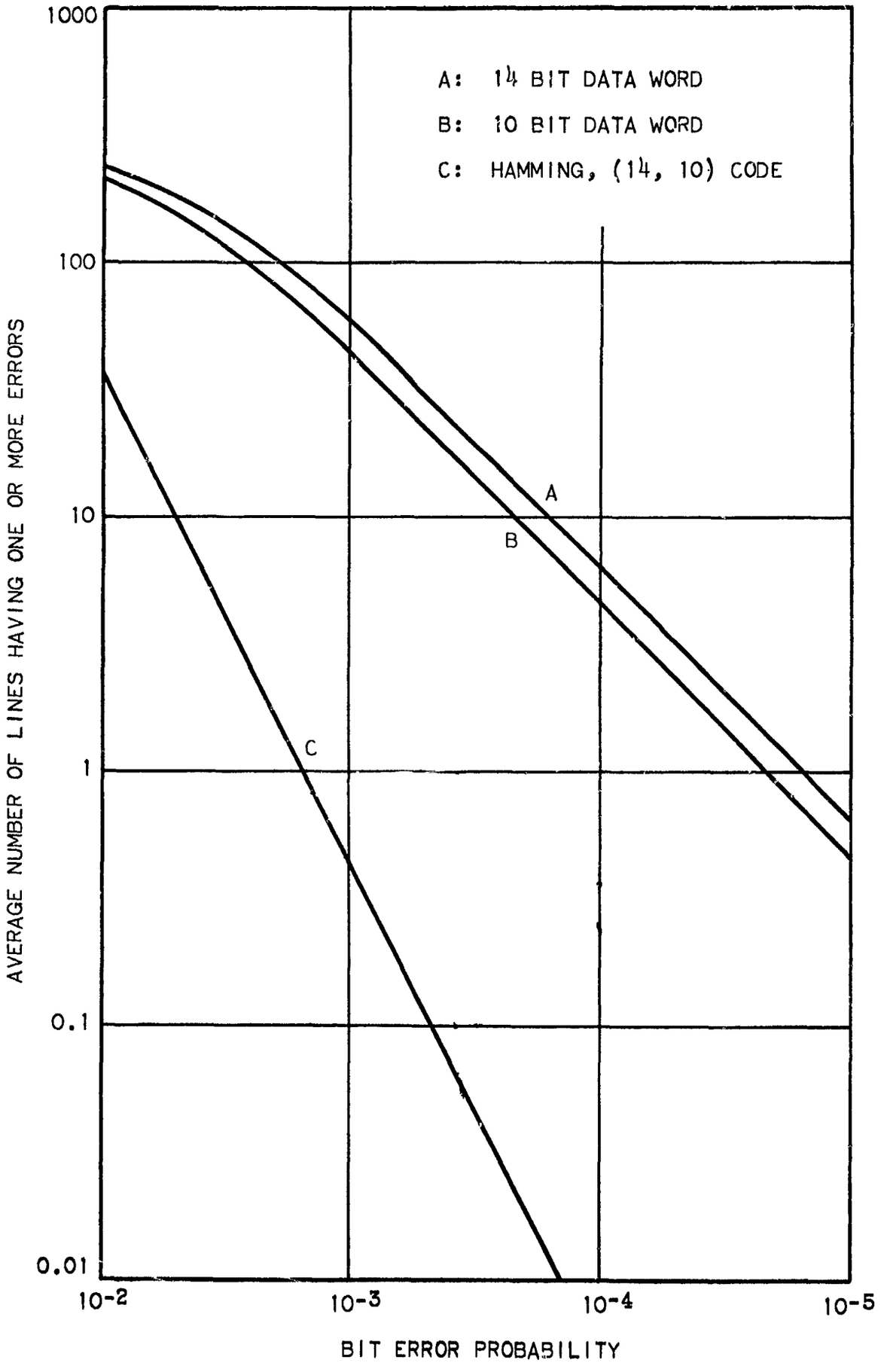

FIGURE B.5-11

SYSTEM PERFORMANCE VERSUS BIT-ERROR PROBABILITY

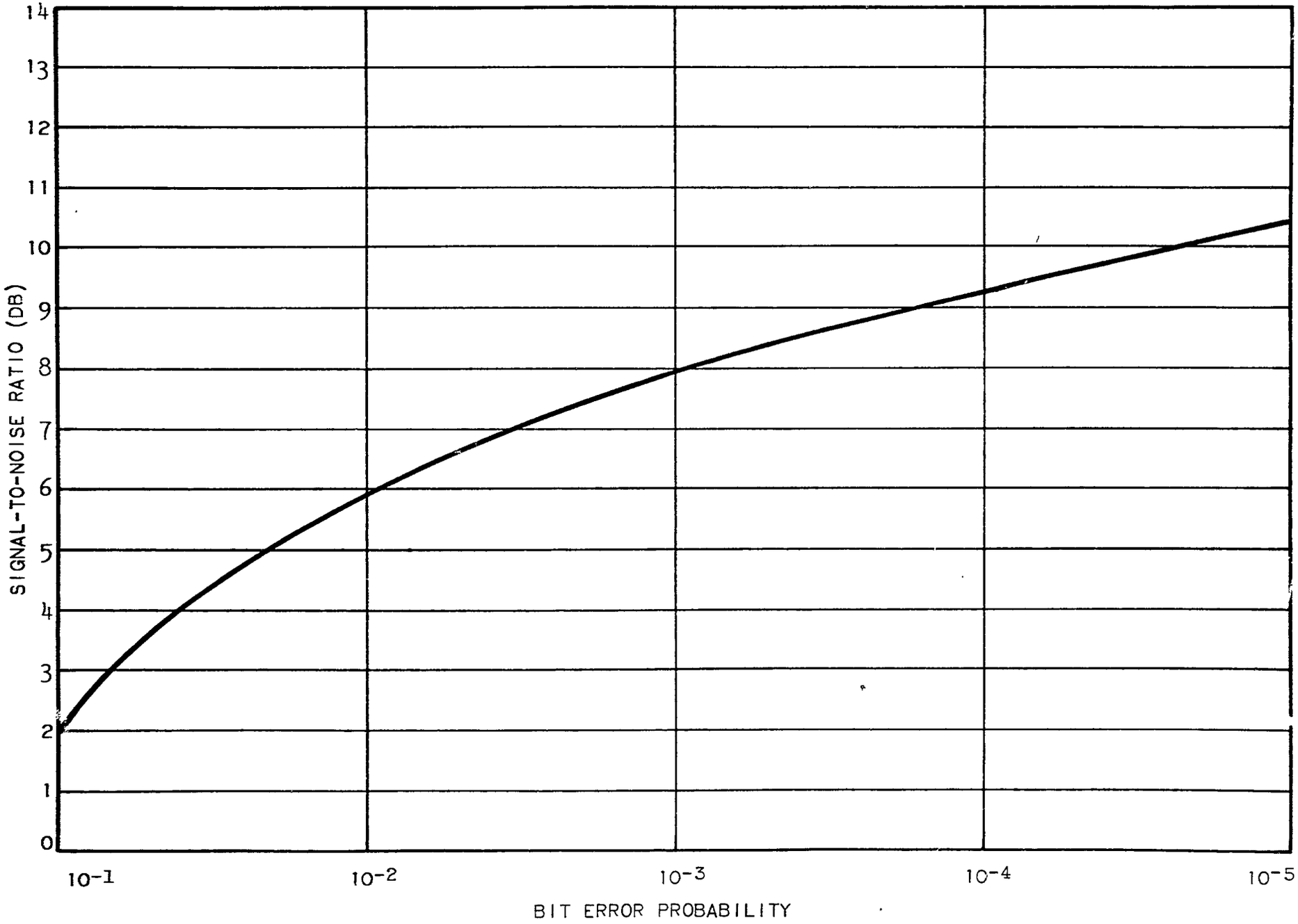

FIGURE B.5-12

REQUIRED SIGNAL-TO-NOISE RATIO VERSUS BIT ERROR PROBABILITY
FOR DIFFERENTIAL PHASE-SHIFT MODULATION

TABLE B-2

COMPARISON OF SYSTEM PERFORMANCE

Data Code	Bit Error Probability for only 1 line frame with an error	Power Saving Relative to 14-Bit Code (db)	Bandwidth Equivalent Power Savings Relative to 14-Bit Code (db)	Net Power Savings Relative to 14-Bit Code (db)
14 bit	1.6×10^{-5}	0.0	0.0	0.0
10 bit	2.3×10^{-5}	+0.2	+1.46	+1.66
Hamming (14, 10)	1.5×10^{-3}	+2.5	0.0	+2.5

TABLE B-3

SEARCH-MODE CALCULATIONS

e	$P_c(e)$	$P_d(e)$	$P_{fm}(e)$	$P_t(e)$
0	0.68	1.8×10^{-12}	5.4×10^{-10}	0.68
1	0.95	7.3×10^{-11}	2.2×10^{-8}	0.95
2	0.994	1.4×10^{-9}	4.2×10^{-7}	0.994
3	0.9995	1.8×10^{-8}	5.4×10^{-6}	0.9995
4	0.99996	1.7×10^{-7}	5.1×10^{-5}	0.99991
5	0.999997	1.2×10^{-6}	3.6×10^{-4}	0.9996

TABLE B-4

LOCK-MODE CALCULATIONS

e	$P_c(e)$	$P_d(e)$	$P_{fm}(e)$	$P_t(e)$
0	0.68	1.8×10^{-12}	3.6×10^{-11}	0.68
1	0.95	7.3×10^{-11}	1.5×10^{-9}	0.95
2	0.994	1.4×10^{-9}	2.8×10^{-8}	0.994
3	0.9995	1.8×10^{-8}	3.6×10^{-7}	0.995
4	0.99996	1.7×10^{-7}	3.4×10^{-6}	0.99994
5	0.999997	1.2×10^{-6}	2.4×10^{-5}	0.99997

As shown by the last column of the table, the highest net compression is achieved by using the Hamming, (14, 10) error-correcting code. This coding technique optimizes the system for applications where minimum transmitter power is the governing criterion. If, however, minimum bandwidth is the determining factor in the system design, then the 10-bit code should be selected.

5.4.3 PCM Synchronization Techniques

Conventional PCM Systems

Frame-Synchronization Technique. The basic synchronization technique is to insert, usually at the beginning of each commutation sequence (data frame), an n-bit binary word which identifies the location of the first bit of the data frame. Synchronization at the receiver is achieved by employing correlation techniques to recognize the frame synchronizer word; the usual implementation is a shift-register recognizer. Each group of n data bits is compared to the synchronization pattern and a synchronization signal is generated for each comparison which results in a correlation above a prescribed threshold.

The synchronization process usually involves three distinct modes of operation which can be described as follows:

> Search Mode. In this mode, the correlator is set to tolerate relatively few errors. Operation in this mode terminates with generation of the first frame-synchronization signal. Because of the high correlation threshold, there is a high probability that this initial synchronization signal is a true one. The probabilities of true synchronization and false synchronization are functions of synchronization pattern length only.
>
> Check Mode. The purpose of this mode is to increase the confidence that true synchronization has been detected. The procedure is to count bit-synchronization pulses and establish an aperture at the correlator exactly one frame length after the first frame synchronization signal. The correlation threshold is lowered in this mode to achieve a high probability of recognizing the true synchronization pattern. If the result of the check is negative, the system reverts to the search mode. After one or more positive checks, the exact number depending on the system requirements, the lock mode is initiated.
>
> Lock Mode. This mode utilizes the aperture at the correlator, as in the check mode, but the criteria for returning to the search or check mode vary from system to system, depending on requirements and design philosophy. In general, selection of the lock-mode parameters is aimed at minimizing the percentage of

data lost due to being out of synchronization. The system usually includes a means of measuring the bit-error rate; knowledge of the error rate is then used to optimize the criteria for returning to the search or check mode.

Subsystem Design Equations--Search Mode. The synchronization subsystem design is based entirely on various probabilities which must be optimized in accordance with the system requirements. A number of papers exist which give the derivations of equations for calculating the required probabilities. Most of the symbols and equations in the following analysis are taken from Magnin.[a]

The probability that the correlator recognizes the transmitted synchronization pattern when the received pattern is in the shift-register recognizer, is a function of the bit-error rate, the pattern length and the number of errors allowed in the correlation. Elementary combinatorial analysis leads to the following equation for the probability that the transmitted code arrives in the correlator with e or fewer errors:

$$P_c(e) = \sum_{i=0}^{e} (q)^i (1 - q)^{n-i} C_i^n ; \qquad (1)$$

where, q = independent bit-error rate,

n = number of bits in synchronization pattern,

e = number of errors allowed in the correlator, and

C_i^n = the binomial coefficient symbol.

The probability that the correlator recognizes a random group of n data bits as the synchronization pattern is

$$P_d(e) = (1/2)^n \sum_{i=0}^{e} C_i^n . \qquad (2)$$

If the analysis is made for the worst case, when the correlator begins its search just after a synchronization code pattern, the probability P_{fm} that a false synchronization be detected in one frame can easily be calculated.

$$P_{fm} = 1 - \left[1 - P_d(e)\right]^{m-1} ; \qquad (3)$$

[a]Magnin, J. P., Digital Synchronization of PCM Telemeters, Electro-Mechanical Research, Incorporated, Sarasota, Florida.

where m equals the number of bits in the frame, including the synchronization pattern.

This equation assumes a synchronization pattern having autocorrelation properties equal to, or better than, a random group of n data bits for all degrees of partial overlap in the correlator. In other words,

$$P_x(e) \leq P_d(e), \quad 0 < x < n ;$$

where, x equals degree of overlap in the correlator.

Willard[a] shows that patterns meeting this criterion exist for all $n \geq 2$ with $q \geq 0.1$. Thus, Equation 3 is valid at least over the range of parameters to be considered in this study.

The probability P_t that the true synchronization pattern is recognized in the first search frame is,

$$P_t = (1 - P_{fm})\, P_c\, (e) . \tag{4}$$

The probability P_n that no synchronization signal is generated in the first search frame is

$$P_n = (1 - P_{fm})\, (1 - P_c) . \tag{5}$$

The accumulated probabilities of false synchronization, P_{fk}, true synchronization P_{tk}, and no synchronization, P_{nk}, after K frames in the search mode are:

$$P_{fk} = \frac{P_{fm}\, (1 - P_n^{K})}{1 - P_n} , \tag{6}$$

$$P_{tk} = \frac{P_t\, (1 - P_n^{K})}{1 - P_n} , \text{ and} \tag{7}$$

$$P_{nk} = P_n^{K} . \tag{8}$$

Subsystem Design Equations--Check Mode. In the check mode, the apriori knowledge of the number of bits in the frame is used to determine whether the pattern detected in search was actually the transmitted synchronization word or a suitable arrangement of random data bits. The object of check-mode analysis is to determine the optimum number of checks and the number of errors to be tolerated in the correlator to meet the system requirements at a given bit-error rate. A

[a] Willard, Merwin W., Technical Report on Optimum Code Patterns for PCM Synchronization, Dynatronics, Inc., Orlando, Florida, 3 October 1960, rev. 15 July 1961.

the location of the synchronization word within the data frame cannot be established by counting bits or words at the receiving terminal. The synchronization scheme designed for use with the linear-approximation system uses a conventional search mode and a modified lock mode with no intermediate check mode. Extremely stable synchronization performance is maintained with a bit-error probability of 10^{-2}. Details of the synchronization system are presented in paragraph 5.4.4.

5.4.4 Linear-Approximation Data Synchronization

Horizontal Synchronization

Search Mode. Horizontal synchronization is achieved by inserting a 42-bit synchronization code pattern at the end of each television line. The operation of the search mode is exactly as described in paragraph 5.4.3. Table B-3 describes the search-mode performance of the synchronization system for a bit-error probability of 10^{-2}. This high error rate was chosen since it is desirable to have good synchronization even under conditions of marginal picture fidelity. The search mode calculations were made on the assumption of 294 bits per television line; this number of bits corresponds to 18 line segments using the Hamming, (14, 10) code plus 42 synchronization-code bits.

The last column of Table B-3 shows that the probability of achieving synchronization during the first received line is maximized at 0.99991 with the correlator set to allow four errors; this correlator setting is, therefore, optimum for search-mode operation.

Lock Mode. As soon as the first synchronization signal is generated in the search mode, the system switches to lock-mode operation. In the lock mode advantage is taken of the following two facts, which were not applicable in the search mode:

1. Having achieved horizontal synchronization in the search mode it is possible to separate the data into words and to calculate the horizontal position of each transmitted vertex.

2. Since the maximum segment length is 16 elements, there must be at least 17 data words per frame.

Because of the above facts, one need not look at every combination of 42 consecutive bits, as was necessary in the search mode, but only at those combinations which start at the beginning of a word; also, one can eliminate the first 17 words of each line from the search for a synchronization pattern. This mode of operation greatly lowers the probability of false synchronization and, therefore, raises the probability of true synchronization detection.

Table B-4 shows the lock-mode parameters, using the same symbols as for the search mode. Although the expected number of words per line is approximately 18, the probabilities in Table B-3 were calculated on a worst-case basis by assuming 36 words per line. For this case,

$$P_{fm} = 1 - \left[1 - P_d\,(e)\right]^{36-16}$$

$$= 1 - \left[1 - P_d\,(e)\right]^{20}$$

The last column of Table B-4 shows that optimum lock-mode performance is achieved with the correlator set to allow five errors. With this setting, the probability of true synchronization on each line is 0.99997, or synchronization will be missed approximately once in 130 frames.

Horizontal position is monitored to detect an out-of-synchronization condition. Since the position calculation can never exceed the number 256, unless decoding errors are made, the system reverts to the search mode if this number exceeds a preset limit.

Vertical Synchronization

The vertical synchronization scheme is similar to that used for horizontal synchronization; the pattern length is the same, namely 42 bits. The vertical search mode begins only after horizontal synchronization is achieved. All 42-bit combinations do not have to be examined but only those occurring at the end of each horizontal line. Since there are 256 lines and 294 bits per line, the vertical search-mode probabilities are almost exactly the same as the horizontal search-mode probabilities.

In the lock mode, the vertical synchronization performance can be made even better than the horizontal synchronization performance because an effective lock-mode aperture can be established by counting lines.

5.5 LINEAR-APPROXIMATION STUDY CONCLUSIONS

This study has demonstrated that linear approximation satisfies the requirements for a 6:1 gross average compression on Gemini-type pictorial material and a 4:1 compression on Cooper-type pictorial material. Several trade-offs must be considered when designing a linear-approximation system for a particular mission. It is possible to increase the compression on Gemini-type material by increasing Δx to 32; however, this increases the size, weight, and power of the system while simultaneously decreasing the compression for Cooper-type (fine-detail) material. Also, a trade-off exists between the error-band size and the number of allowable errors. Given a fixed desired compression of 6:1, it is possible to achieve this

with an error-band of ±K with no errors or with an error-band of ±(K-k) for k > 0 with a single consecutive error outside the error-band. The single error degrades some of the edge transitions while the larger error-band and no errors outside the error-band destroys fine detail. Therefore, depending upon the mission, each technique has its subjective advantages and disadvantages.

The data format has several interesting trade-offs. It is possible to minimize either the bandwidth or power depending upon the need. It is possible to specify (1) the amplitude and absolute location of the end points of the slopes; (2) the amplitude and Δx distance between end points; or (3) the amplitude, Δx distance, and redundant bits for error-correction of the amplitude and Δx bits. The analysis revealed that the amplitude and Δx method has an equivalent power for bandwidth savings of 1.46 db over either of the other techniques. However, the (14, 10) code has a net power saving of 2.5 db over the amplitude and actual location of x approach, and it has a 0.84 db saving over the amplitude and Δx approach. However, both the 14-bit and 10-bit per segment approaches require a bit error probability of approximately 10^{-5} for one line per frame in error, while the (14, 10) code requires a bit error probability of approximately 10^{-3} for the same condition. Therefore, the (14, 10) code is recommended. This results in a decrease in gross average compression of 1.4:1; that is, given a gross average compression of 8.4:1, the net average compression[a] is 6:1, or given a gross average compression of 6:1, the net average compression is 4.3:1.

The synchronization problem of the linear-approximation technique poses no serious difficulties and for the (14, 10) code and for one line per frame in error, the required bit error probability is 1.5×10^{-3}. Using a 42-bit synchronization word, the probability of obtaining synchronization on the first line is 0.99991.

[a] Net compression = $\dfrac{\text{uncompressed bits}}{\text{compressed bits + error-correcting bits}}$.

APPENDIX C

DIGITAL-COMMUNICATION-CHANNEL ANALYSIS

APPENDIX C

TABLE OF CONTENTS

SECTION 1

THE BITS-PER-CYCLE PROBLEM

1.1 BASEBAND WIDTH RELATED TO SIGNALING INTERVAL

The baseband (video) occupancy of a digital signaling system is determined primarily by the signaling interval T, illustrated in Figure C.1-1. To a secondary extent, occupancy is determined by the waveshape within T.

Let the signal sent be s(t). Let the energy E during T be defined by

$$E = \int_{-\frac{T}{2}}^{\frac{T}{2}} \left[s(t)\right]^2 \, dt. \tag{1}$$

If, during T, s(t) is allowed to have a maximum, A, then Equation 1 is clearly maximized by choosing a waveform,

$$s(t) = A \tag{2}$$

for the duration T. This makes

$$E = A^2 T. \tag{3}$$

A conceivable signal would be the sequence...0, 0, 0, A, 0, 0, 0..., where the elements of the sequence each exist for time T. Since there is only one pulse of A amplitude and T width, a Fourier integral transform defined by the pair

$$F(f) = \int_{-\infty}^{\infty} f(t)\, e^{-j\omega t} \, dt, \text{ and} \tag{4}$$

$$f(t) = \int_{-\infty}^{\infty} F(f)\, e^{j\omega t} \, df \tag{5}$$

(where $\omega = 2\pi f$), may be used to study the spectrum occupancy.

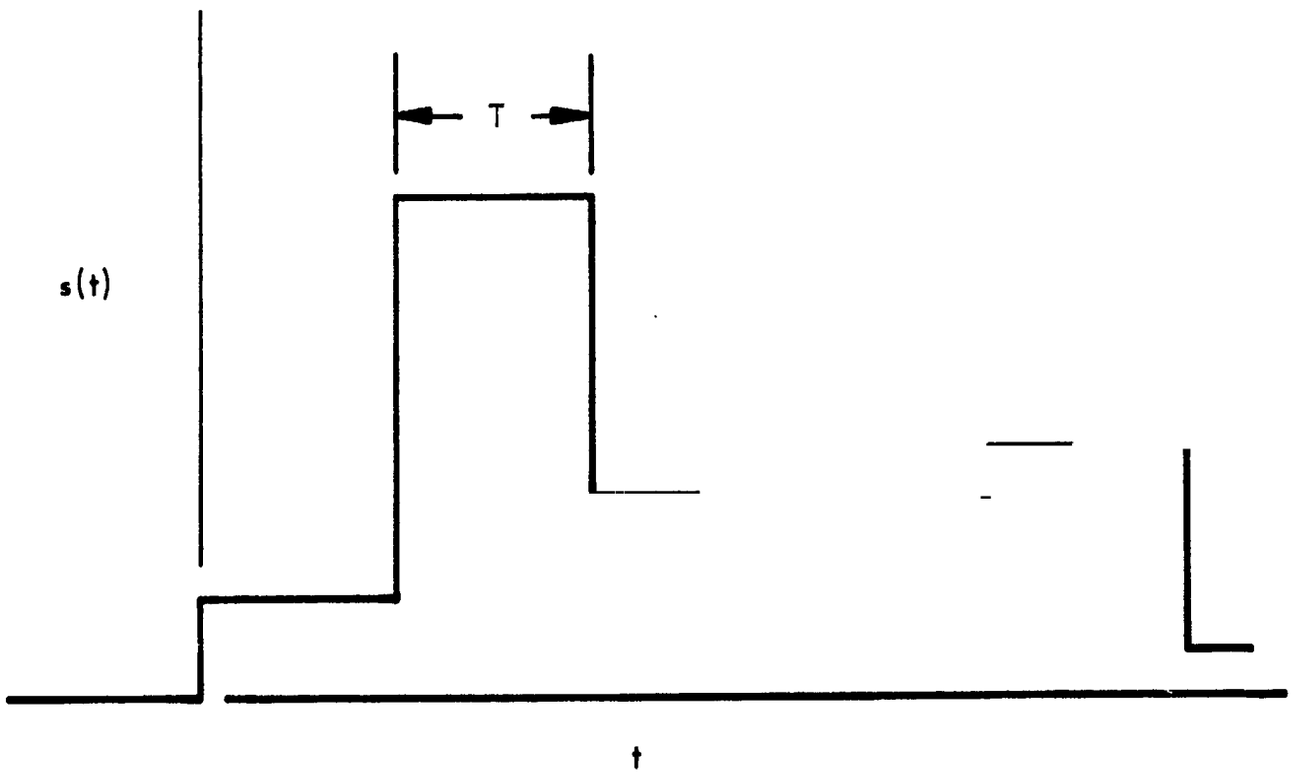

FIGURE C.1-1

SIGNALING INTERVAL T

The well known result for a single, origin-centered, rectangular pulse of area AT and width T is

$$F(f) = \int_{-\frac{T}{2}}^{\frac{T}{2}} Ae^{-j\omega t}\,dt = AT\,\frac{\mathrm{Sin}\left(\frac{\omega T}{2}\right)}{\left(\frac{\omega T}{2}\right)}, \tag{6}$$

which has zeros at n/T, n = 1, 2, 3...∞ as illustrated in Figure C.1-2.

From Figure C.1-2, it can be seen that the half-power points are at about ±0.45/T. This could be taken to be the "bandwidth occupancy" definition. However, another bandwidth occupancy definition leads to an easily remembered and reasonable result. Equation 7 converts the amplitude spectrum of Equation 6 to the energy density spectrum given by Equation 8.

$$E(f) = \left|F(f)\right|^2 . \tag{7}$$

$$E(f) = A^2T^2\left[\frac{\mathrm{Sin}\left(\frac{\omega T}{2}\right)}{\left(\frac{\omega T}{2}\right)}\right]^2 . \tag{8}$$

Integration of Equation 8 from -∞ to + ∞ gives the total E in the pulse.

$$E = \int_{-\infty}^{\infty} A^2T^2\left[\frac{\mathrm{Sin}\left(\frac{\omega T}{2}\right)}{\left(\frac{\omega T}{2}\right)}\right]^2 df = A^2T, \tag{9}$$

where $\omega = 2\pi f$.

If E were generated by a uniform-energy-spectral-density source with an energy spectral density A^2T^2 equal to the peak energy spectral density of Equation 8, then that source would necessarily occupy a total bandwidth of 1/T with energy uniformly distributed from f = -1/2T to f =+1/2T. Thus, the energy rectangular equivalent (ERE) bandwidth of pulse AT is 1/T independent of A.

Consider the baseband with frequencies from 0 to ∞; then, the lower-sideband (negative frequencies) amplitude spectral components add coherently to double

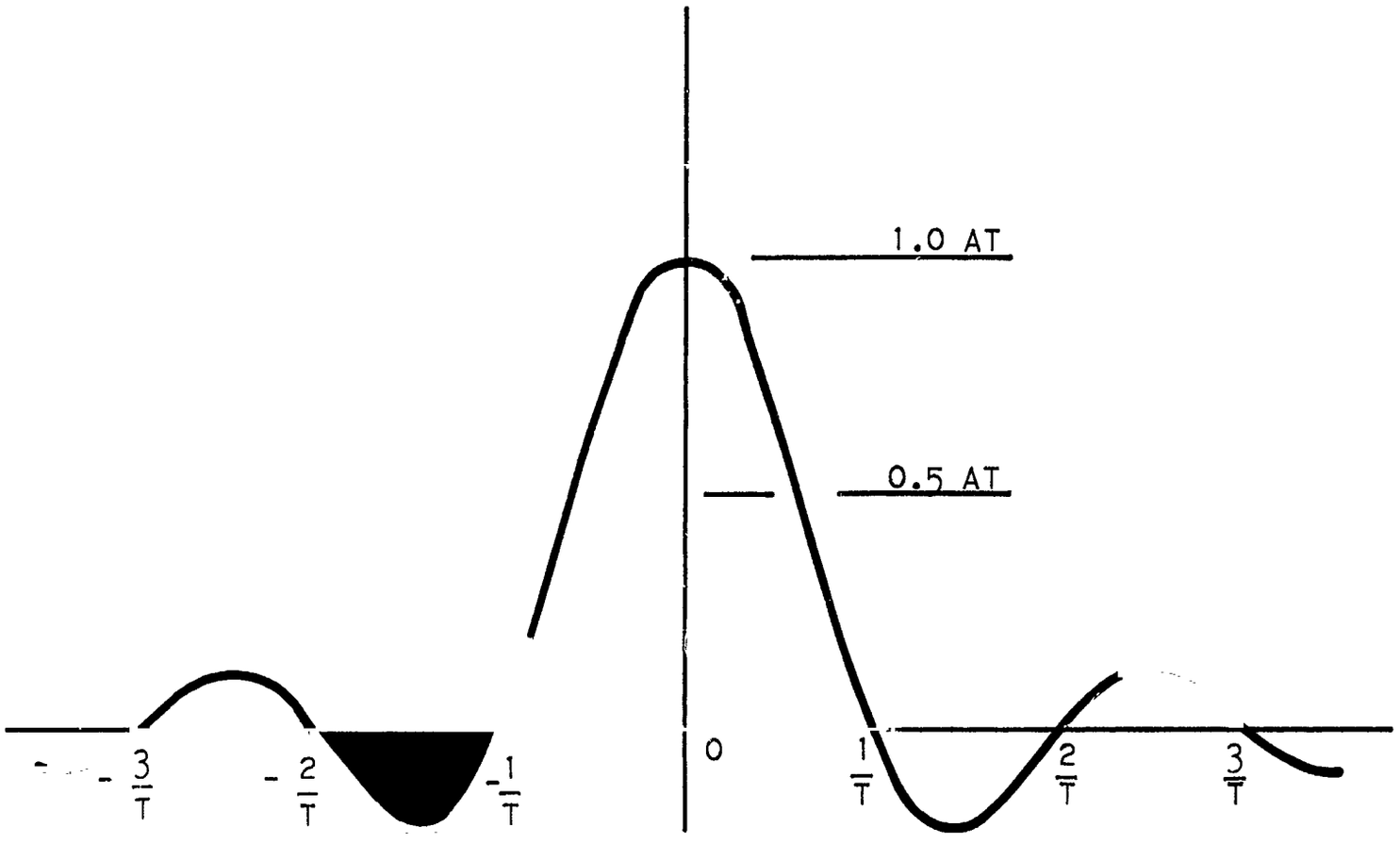

FIGURE C.1-2

GRAPH OF AT $\dfrac{\sin\left(\frac{\omega T}{2}\right)}{\left(\frac{\omega T}{2}\right)}$

the upper-sideband energy spectral components. The single-sided energy spectral density has an ERE bandwidth of one-half that of the double-sided energy spectral density. Thus, baseband occupancy in cycles per second is one-half the signaling rate for rectangular pulses. That is, the ERE baseband width is 1/2T, where 1/T is the signaling rate.

1.2 RF BANDWIDTH RELATED TO BASEBAND WIDTH

1.2.1 Double Sideband

Let pulse AT of Equation 2 be applied to a unit cosinusoidal carrier $\cos 2\pi f_c t$ of carrier frequency f_c. This yields a transmitted signal

$$v(t) = s(t) \cos 2\pi f_c t, \tag{10}$$

which may be further expressed as

$$v(t) = \frac{s(t)\, e^{j2\pi f_c t}}{2} + \frac{s(t)\, e^{-j2\pi f_c t}}{2} . \tag{11}$$

In the Fourier integral transform, $e^{\pm j2\pi f_c t}$ is a shifting operator with respect to the frequency domain. That is, if F(f) is the Fourier transform of f(t), then the Fourier transform of $f(t)e^{\pm j2\pi f_c t}$ is $F(f \mp f_c)$.

From Equation 6, one has the Fourier transform of the pulse AT. Converting Equation 6 by

$$\omega = 2\pi f \tag{12}$$

yields

$$F(f) = \frac{AT \sin(\pi f T)}{(\pi f T)} . \tag{13}$$

Combining this result for the spectrum of s(t) with Equation 11 for v(t) yields the spectrum

$$V(f) = \frac{AT}{2} \frac{\operatorname{Sin} \pi (f - f_c) T}{\pi (f - f_c) T} + \frac{AT}{2} \frac{\operatorname{Sin} \pi (f + f_c) t}{\pi (f + f_c) t} \tag{14}$$

sketched (not to scale) in Figure C. 1-3.

From paragraph 1. 1, it can be seen that the ERE bandwidth of F(f) is 1/T, the signaling rate. Since V(f) is clearly made up of F(f) shifted by f_c, it can likewise be concluded that the ERE bandwidth of V(f) for those $0 < f < \infty$ also equals the signaling rate.

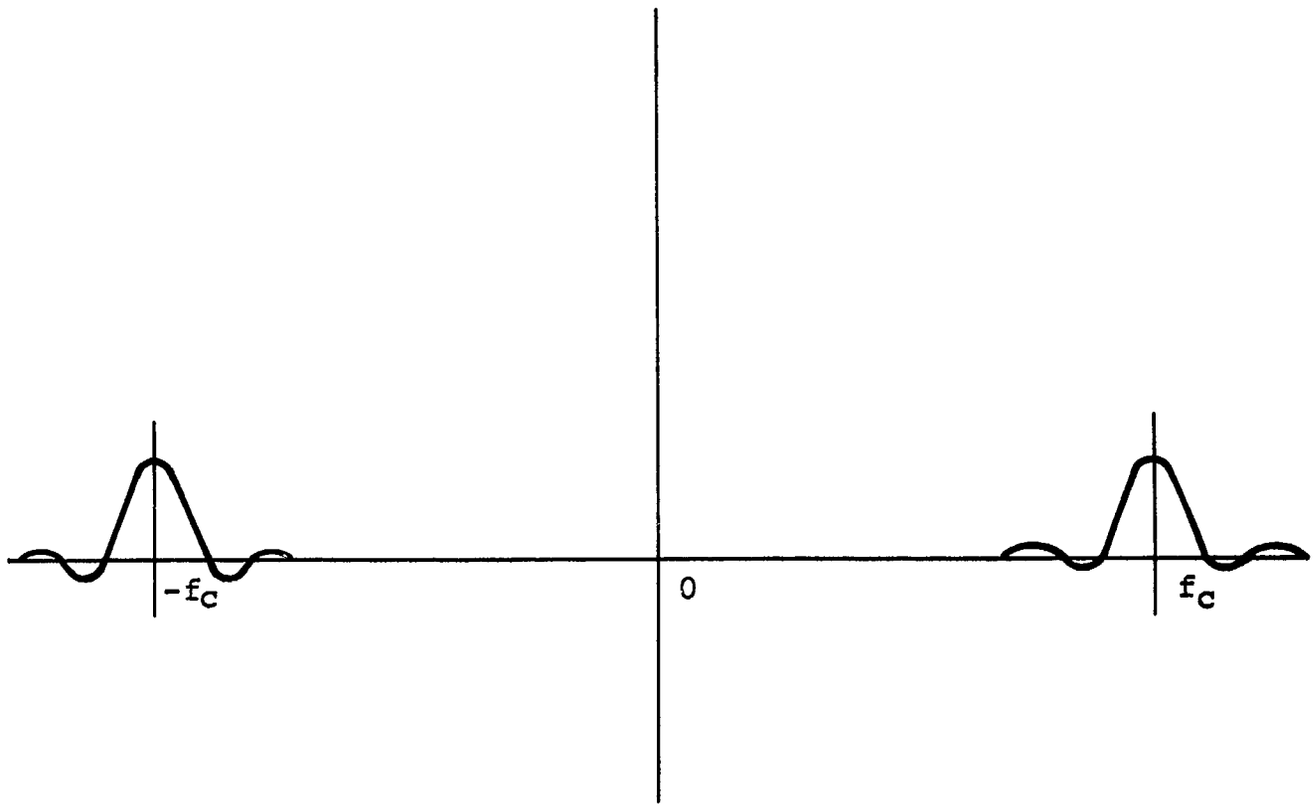

FIGURE C. 1-3

TRANSLATION OF BASEBAND SPECTRUM TO CARRIER BAND

1.2.2 Single Sideband

The conclusion of paragraph 1.1 showed that the baseband ($0<f<\infty$) ERE bandwidth of the signal pulse AT is one-half the signaling rate. At the conclusion of paragraph 1.2.1, it was seen that the ERE bandwidth of the double-sideband transmitted signal is equal to the signaling rate. Thus, there is an unavoidable 2X bandwidth expansion between baseband and carrier band. Transmitting both sidebands does offer the advantage of allowing, in principal, distortion-free recovery of s(t) by means of a simple, noncoherent-detector receiver.

A possible way of recovering the 2X bandwidth expansion factor would be to transmit single sideband, i.e., filter out the (redundant) sideband of frequencies less than f_c. However, in this case noncoherent (envelope) detection introduces unwanted signal distortions, particularly for signals made up of pulse and step functions. The area of single-sideband pulse distortion is complex and, in detail, beyond the scope of this part of the study. Nevertheless, a short qualitative discussion with liberal reference to the literature is appropriate because single-sideband transmission is not the recommended way to recover the the 2X bandwidth expansion factor within the context of this study; although it is the way actually used in commercial television to "almost" recover the 2X bandwidth expansion.

Around the late 1930's and early 1940's, leading electrical engineers such as Goldman [a], Nyquist [b], and Kell [c] considered the problem of television picture detail distortion when the video signal was transmitted by double, vestigial, and single sideband. Nyquist and Pfleger's paper is the most readable and a brief illustration of their findings by means of quoted text and drawings follow.

> "Distortion to be considered in single-sideband transmission as compared with double-sideband transmission arises in three ways.
>
> 1. A slowly varying in-phase component may be present due principally to the inaccurate location of the carrier frequency with respect to the edge of the filter characteristic.

---

[a] Goldman, S., "Television Detail and Selective-Sideband Transmission," PROC. IRE, November 1939, p. 725.

[b] H. Nyquist and K. W. Pfleger; "Effect of the Quadrature Component in Single Sideband Transmission," Bell System Technical Journal, January 1940, p. 63.

[c] Kell, R. D. and Fredandel, G. L.,"Selective Sideband Transmission in Television" RCA Review, April 1940, p. 425.

2. The edge of the filter characteristic where the carrier is located may be so designed that there is a net distortion due to failure of the vestigial sideband to be accurately complementary to the principal sideband.

3. A quadrature component is present which results in considerable distortion of the envelope of the received wave under ordinary conditions.

"In-phase component" means a component whose carrier is in phase with the steady-state carrier; "quadrature component" means a component whose carrier is in quadrature with the steady-state carrier."

Nyquist's paper is principally concerned with the third of these effects, namely, the quadrature component.

> "Figure C. 1-4 [a] indicates the magnitude of the transfer admittance characteristic which will be assumed. The characteristic is made up of two half-cycles of a sine wave separated by a horizontal portion. The phase shift versus frequency characteristic is a straight line. In order to simplify subsequent sketches this constant delay has been put equal to zero. To take account of any constant delay it is sufficient to displace the computed curve by an amount equal to the delay. The characteristic of Figure C. 1-4 may be separated into two components as indicated in Figure C. 1-5 where the top one gives rise to the in-phase component and the bottom one to the quadrature component. F_c is the carrier frequency for single-sideband computations, and it is assumed that F_c is great in comparison with the bandwidth.... Figure C. 1-6 shows the equivalent low-pass characteristics. Curve g_0 gives rise to the in-phase component and curve b_0 to the quadrature component. Figure C. 1-7 shows the low-pass characteristic which is equivalent to the original characteristic for double-sideband computations with the carrier located in the middle.
>
> "Figure C. 1-8 gives the computed envelope for a single transition when this transducer is used on a single-sideband basis. The figure shows the rectangular sent wave, the envelope of the in-phase component, the envelope of the quadrature component, and the envelope of the resultant wave.... Figures C. 1-9 and C. 1-10 show the single sideband envelopes for a unit dot and a unit space, respectively. C. 1-11 shows two dots in succession."

---

[a] Figure numbers in the quote are changed for sequence consistency in this report.

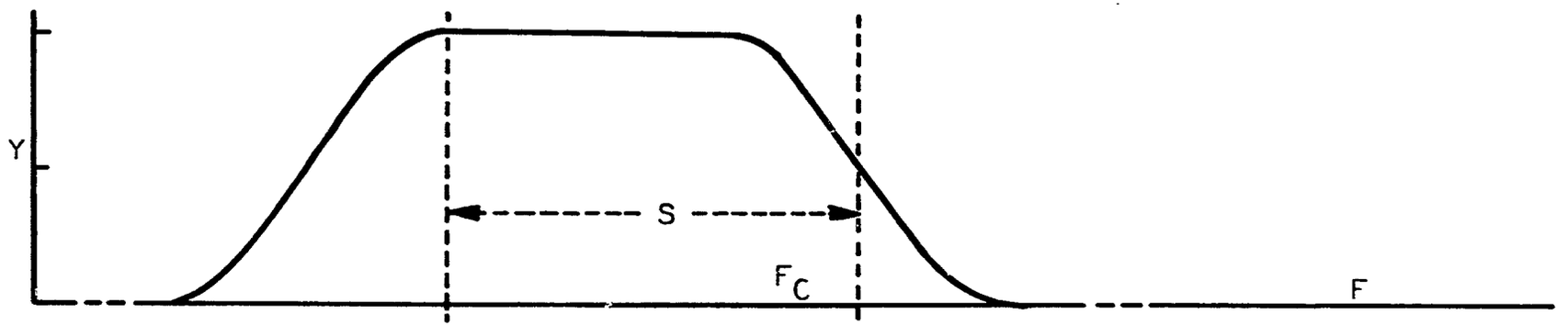

FIGURE C.1-4

IDEALIZED TRANSFER ADMITTANCE CHARACTERISTIC.
(BANDPASS SYSTEM WITH NO DELAY DISTORTION;
F_c IS THE CARRIER AND S THE FUNDAMENTAL DOTTING FREQUENCY.)

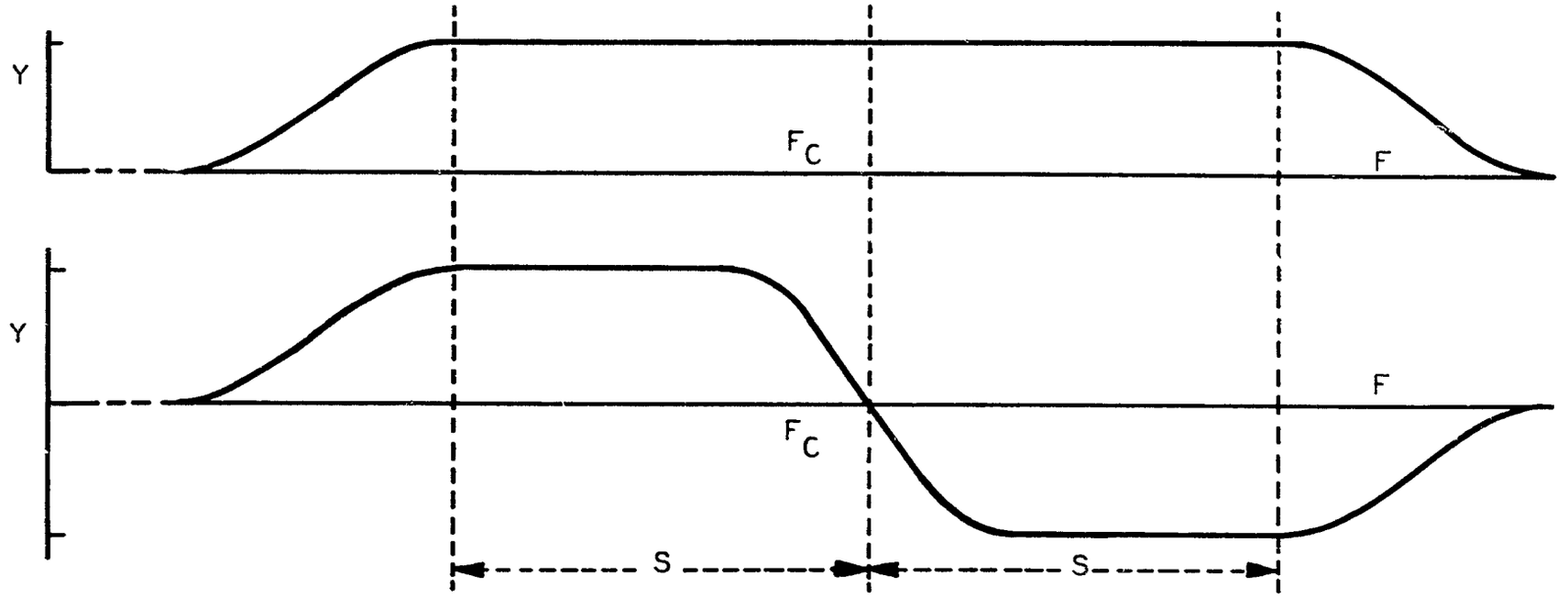

FIGURE C. 1-5

GRAPHICAL ANALYSIS OF TRANSMISSION CHARACTERISTIC.
(THE SUM OF THESE CHARACTERISTICS EQUALS THAT IN FIGURE C. 1-4.
THE UPPER GIVES RECEIVED SIGNALS WITH CARRIER IN PHASE,
AND THE LOWER, IN QUADRATURE WITH THE SENT WAVE.)

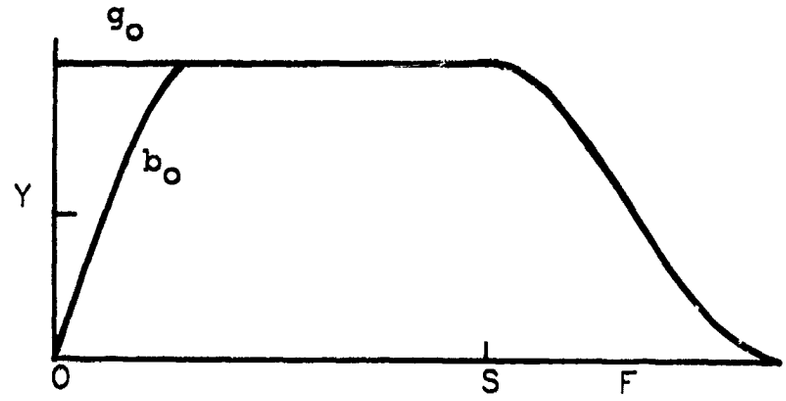

FIGURE C. 1-6

EQUIVALENT LOW-PASS FILTER CHARACTERISTIC.
(USED IN COMPUTING ENVELOPES OF RECEIVED SIGNALS
FOR SINGLE SIDEBAND TRANSMISSION.)

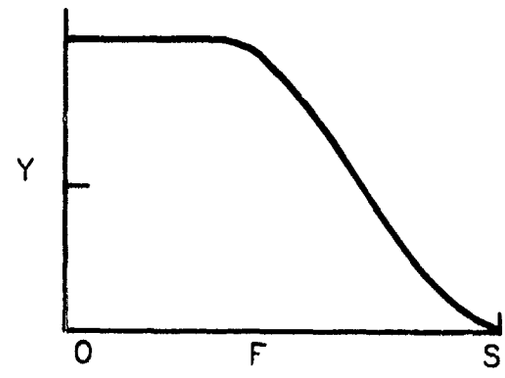

FIGURE C. 1-7

EQUIVALENT LOW-PASS FILTER CHARACTERISTIC.
(USED IN COMPUTING ENVELOPES OF RECEIVED SIGNALS
WITH MID-BAND CARRIER.)

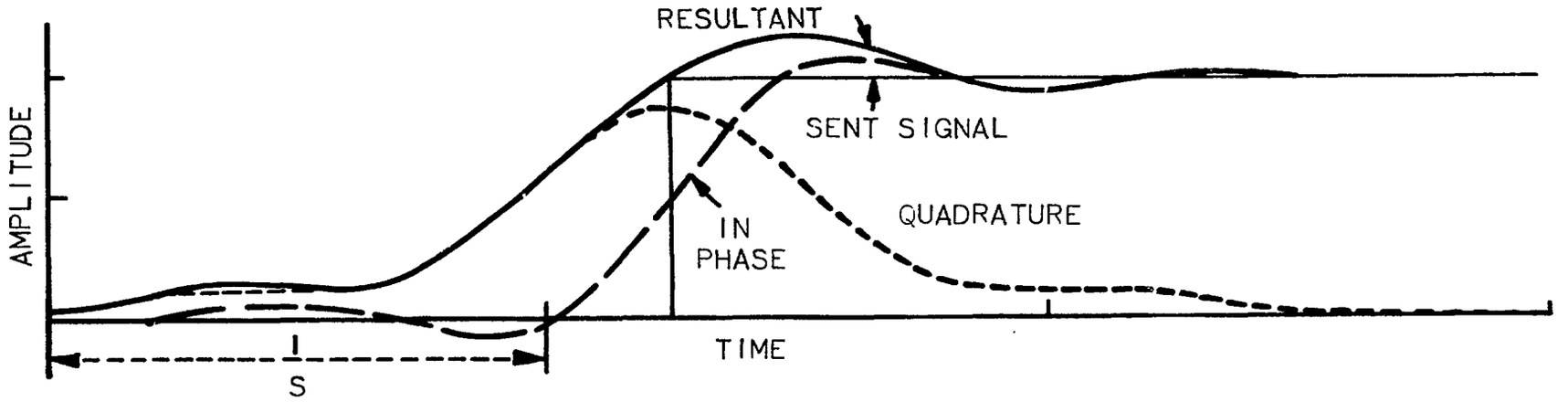

FIGURE C. 1-8

ENVELOPE OF RECEIVED WAVE COMPONENTS FOR
SINGLE TRANSITION, CHARACTERISTIC AS SHOWN IN FIGURE 1-4

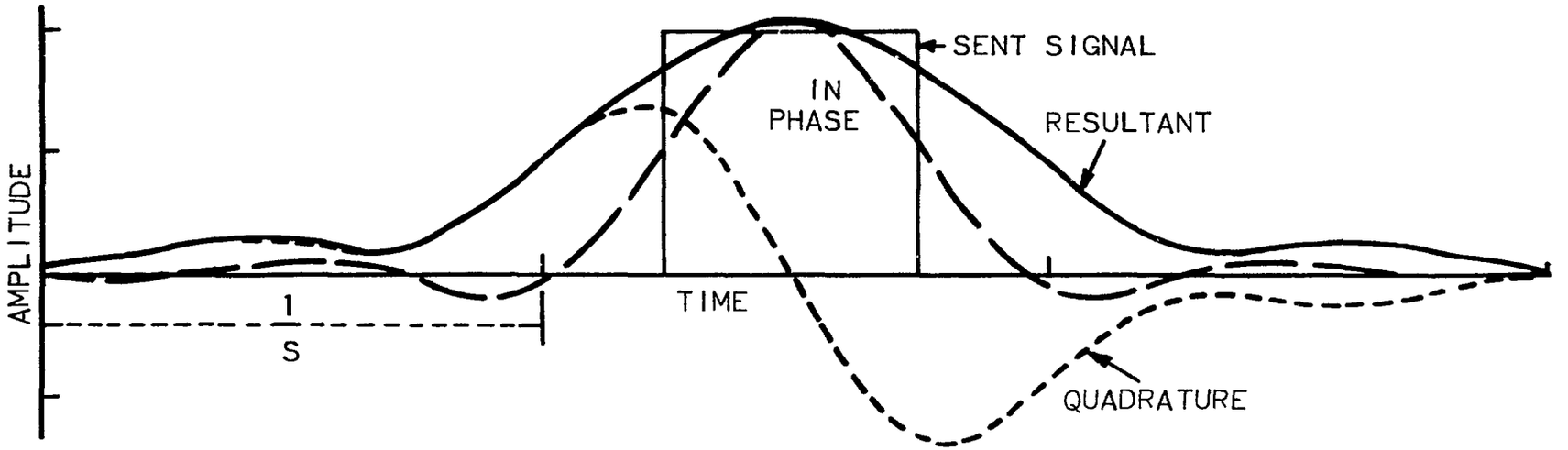

FIGURE C. 1-9

RECEIVED SIGNAL FOR SINGLE DOT,
CHARACTERISTIC AS IN FIGURE C. 1-4

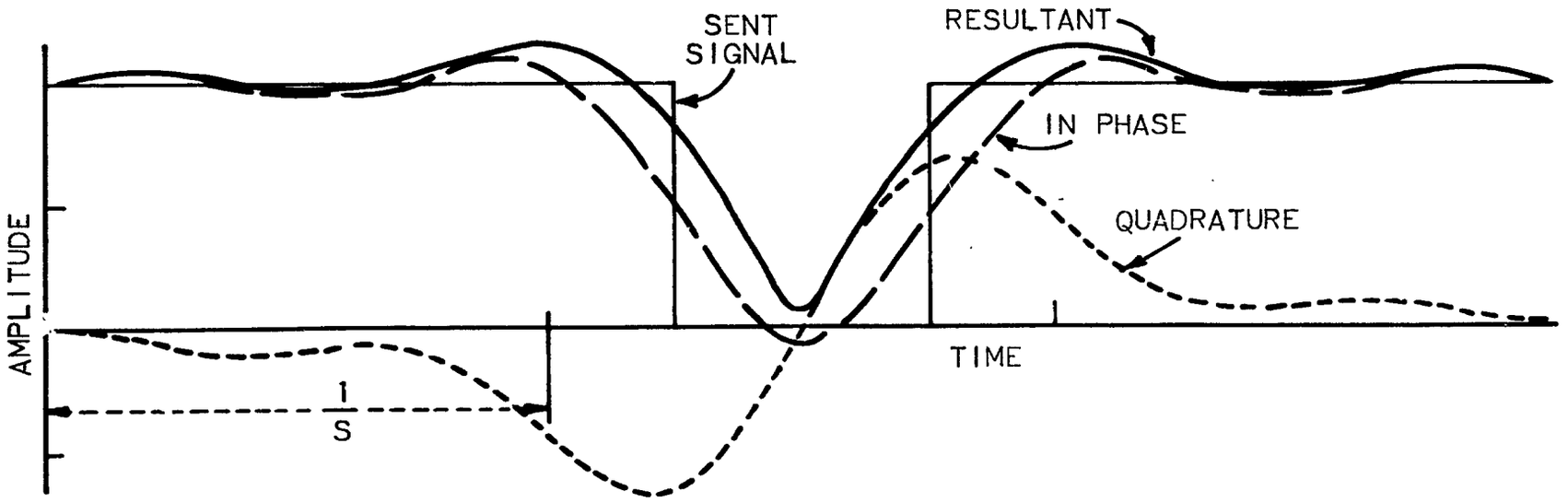

FIGURE C. 1-10

RECEIVED SIGNAL FOR SINGLE SPACE, CHARACTERISTIC AS IN FIGURE C. 1-4

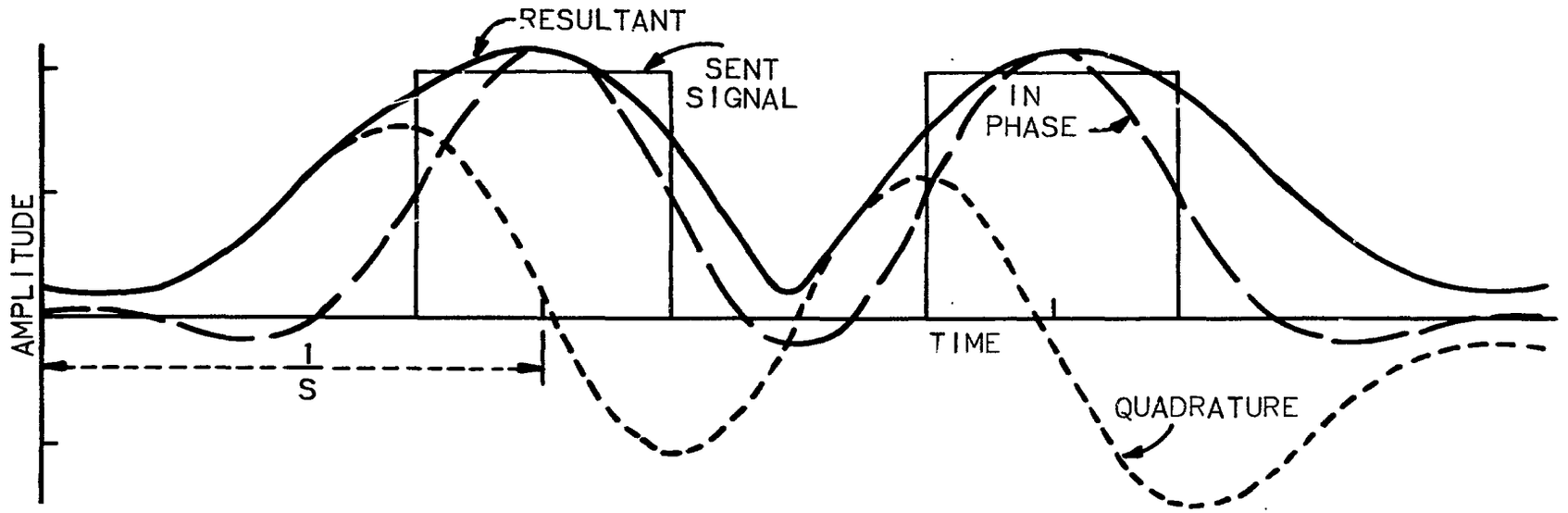

FIGURE C.1-11

RECEIVED SIGNAL FOR TWO DOTS IN SUCCESSION, CHARACTERISTIC AS IN FIGURE C.1-4

It is evident from the numerous examples that if a threshold in the receiver were placed at a level 1/2 of the maximum pulse height, the threshold transition of the in-phase component would, within a constant delay, accurately locate the leading edge of an isolated pulse. For the double pulse case.... 0, 0, 0, 1, 0, 1, 0, 0, 0.... the leading edge of both pulses is accurately located by the in-phase component. But when the quadrature component is added to the in-phase component, the leading edges of the pulses are shifted, or biased, in the time domain, the amount of bias being dependent on past signal history. It appears that bit synchronization would be hard to achieve--the apparent bit location being an averaged function of signal history.

If the signal f(t) is translated to the carrier band by f(t) cos $2\pi f_c t$ and then passed through a selective sideband filter of the form in Figure C. 1-4, it can still be recovered in a distortionless form if (1) it is retranslated to baseband by coherent detection (i. e., multiplications by cos $2\pi f_c t$), (2) the carrier is centered on the slope of the characteristic, and (3) if the characteristic is complementary (i. e., if the lower vestigial sideband components are one minus their equivalent upper sideband components in magnitude). The characteristic of Figure C. 1-4, when translated to zero frequency, folds about that point with the lower sideband portion filling in the low frequency depression in the upper sideband.

However, coherent distortionless reception is not without such practical difficulties as carrier recovery, carrier and selective-sideband relative stability, generation of the selective-sideband relative stability, generation of the selective-sideband signal in the spacecraft, and the assurance of complementarism in the vestigial sideband. A vestigial sideband is needed to recover the carrier, and this in itself prevents attainment of the full 2X bandwidth recovery theoretically associated with time-single-sideband operation. If coherent detection is required for distortionless selective sideband transmission, one may as well use another method (also using coherent detection) which enables a true 2X bandwidth recovery over double-sideband transmission. This method is called double-sideband orthogonal carrier transmission.

1. 2. 3 Double-Sideband Orthogonal Carriers

Consider two message signals, f(t) and g(t). Place f(t) on a cosine carrier, f(t) cos $2\pi f_c t$ and g(t) on a sine carrier, g(t) sin $2\pi f_c t$. Now, add the two signals to form a transmitted signal

$$m(t) = f(t) \cos 2\pi f_c t + g(t) \sin 2\pi f_c t. \qquad (15)$$

Now recover f(t) and g(t) by passing m(t) through two product demodulators, one utilizing cos $2\pi f_c t$ as a local oscillator signal and the other utilizing sin $2\pi f_c t$.

The demodulator output for the cosine channel will be

$$m_c(t) = f(t)\ (\cos\ 2\pi f_c t)\ (\cos\ 2\pi f_c t) + g(t)\ (\sin\ 2\pi f_c t)\ (\cos\ 2\pi f_c t)\ . \qquad (16)$$

which reduces to

$$m_c(t) = \frac{f(t)}{2}\ \left[\cos\ 4\pi f_c t + \cos\ (0)\right] + \frac{g(t)}{2}\ \left[\sin\ 4\pi f_c t + \sin\ (0)\right]. \qquad (17)$$

Passing $m_c(t)$ through a filter which takes out the $2f_c$ component leaves a cosine-channel-detected signal given by

$$M_{cd}(t) = \frac{f(t)}{2}\ . \qquad (18)$$

In a like manner, the sine-channel-detected signal is given by

$$M_{sd}(t) = \frac{g(t)}{2}\ . \qquad (19)$$

If the signals f(t) and g(t) each have a signaling rate R/2 and a baseband ERE bandwidth R/4, the total signaling rate is R and the total baseband width is R/2. Now, each signal f(t) and g(t) has a double-sideband ERE bandwidth equal to R/2 and both f(t) and g(t) can be fitted into the same ERE bandwidth occupancy R/2. Thus, by using both phase-orthogonal carriers, one can fit a signaling rate of R into an ERE double-sideband bandwidth of R/2. This means a bandwidth occupancy at carrier band (rf) of 1/2 cps per signaling interval per second. The cost for this performance is the relative complexity of having a data splitter, two parallel channels in the transmitter, and two parallel coherent detector channels in the receiver followed by logic and a data combiner.

1.3 INFORMATION RATE RELATED TO SIGNALING INTERVAL

1.3.1 Bits per Signaling Interval

If the signal is allowed to take on N states during a signaling interval T, then the bits per signaling interval B is given by

$$B = \log_2 N\ . \qquad (20)$$

Since the transmitted signal is given by Equation 15, the system states during the signaling interval T can be specified by the allowable states of f(t) and g(t). Further assume that f(t) and g(t) remain constant at f and g, respectively, during a signaling interval. If f can take on N_f states and g can take on N_g states, then (since f and g are noninterfering) there are $N_f N_g$ possible

signaling states during a signaling interval T. Under these conditions, the number of bits per signaling interval is given by

$$B = \log_2 (N_f N_g) = \log_2 N_f + \log_2 N_g, \tag{21}$$

indicating the presence of two separate information channels. For the special case of

$$N_g = N_f, \tag{22}$$

Equation 21 becomes

$$B = 2 \log_2 (N_f). \tag{23}$$

For N_f equal to 4 states, a plot of combined signal states is given in Figure C.1-12.

1.3.2 Bit Error Probability Versus Signal-to-Noise Ratio

The receiver in a multistate communication system must have thresholds placed between the signal states in order to estimate which signal state was transmitted. In the system of Figure C.1-12, decision levels are placed equidistant from the system states in each channel. This makes the decision level distance D equal to 1/3 the peak received-signal-state level in each channel. Ideally, the received level in a system with proper AGC would fall on, and only on, a valid system state. However, receiver noise will add to the received signal and perturb its apparent location away from the desired signal state. Since $\frac{\sigma}{\sqrt{2}}$ is the standard deviation of the received noise in a coherent channel, in order to assure an adequately small probability of error,

$$D = k \frac{\sigma}{\sqrt{2}} ; \tag{24}$$

where k must be chosen large enough (order of 3 or 4 or so) to ensure a sufficiently small probability that one signal state will be perturbed over the threshold into the neighboring signal-state territory.

The peak received signal state in each channel, A_c, is given by

$$A_c = 3D. \tag{25}$$

Combining Equations 24 and 25 gives

$$A_c = 3k \frac{\sigma}{\sqrt{2}} . \tag{26}$$

Finally, the peak transmitted signal A occurs when both channels are simultaneously transmitting, so that

$$A = A_c\sqrt{2} \tag{27}$$

as seen from Figure C.1-12. Finally, this yields

$$A = 3k\sigma\ , \tag{28}$$

which can be rewritten as

$$\frac{A}{\sigma} = 3k. \tag{29}$$

Note that A^2 is the peak envelope signal power received and σ^2 is the noise power received so that the receiver signal-to-noise ratio is given by

$$(S/N)_{pern} = A^2/\sigma^2, \tag{30}$$

where pern means peak envelope to rms noise.

Equation 30 is simply Equation 29 squared so that

$$(S/N)_{pern} = 9k^2 \tag{31}$$

Since k is, by definition, the number of standard deviations that the threshold lies from the nearest signal state, one can write the probability of error, P_e, given as

$$P_e = 2\int_k^\infty p(x)\,dx, \tag{32}$$

where p(x) is the normalized (i.e., $\sigma = 1$) probability density function of the noise involved. For large S/N the probability density function p(x) is gaussian and Equation 32 can be derived from a function tabulated in Burington[a] as the function $1/2\,(1+\alpha)$ versus X. P_e is then given as

$$P_e = 2\left[1 - 1/2\,(1+\alpha)\right] \tag{33}$$

for the independent variable X in Burington being k in this derivation. Typical values of P_e versus k and $(S/N)_{pern}$ are as follows:

---

[a] R. S. Burington; Handbook of Mathematical Tables and Formulas, Handbook Publishers, Inc., Sandusky, Ohio, 1954, pp 273 through 276.

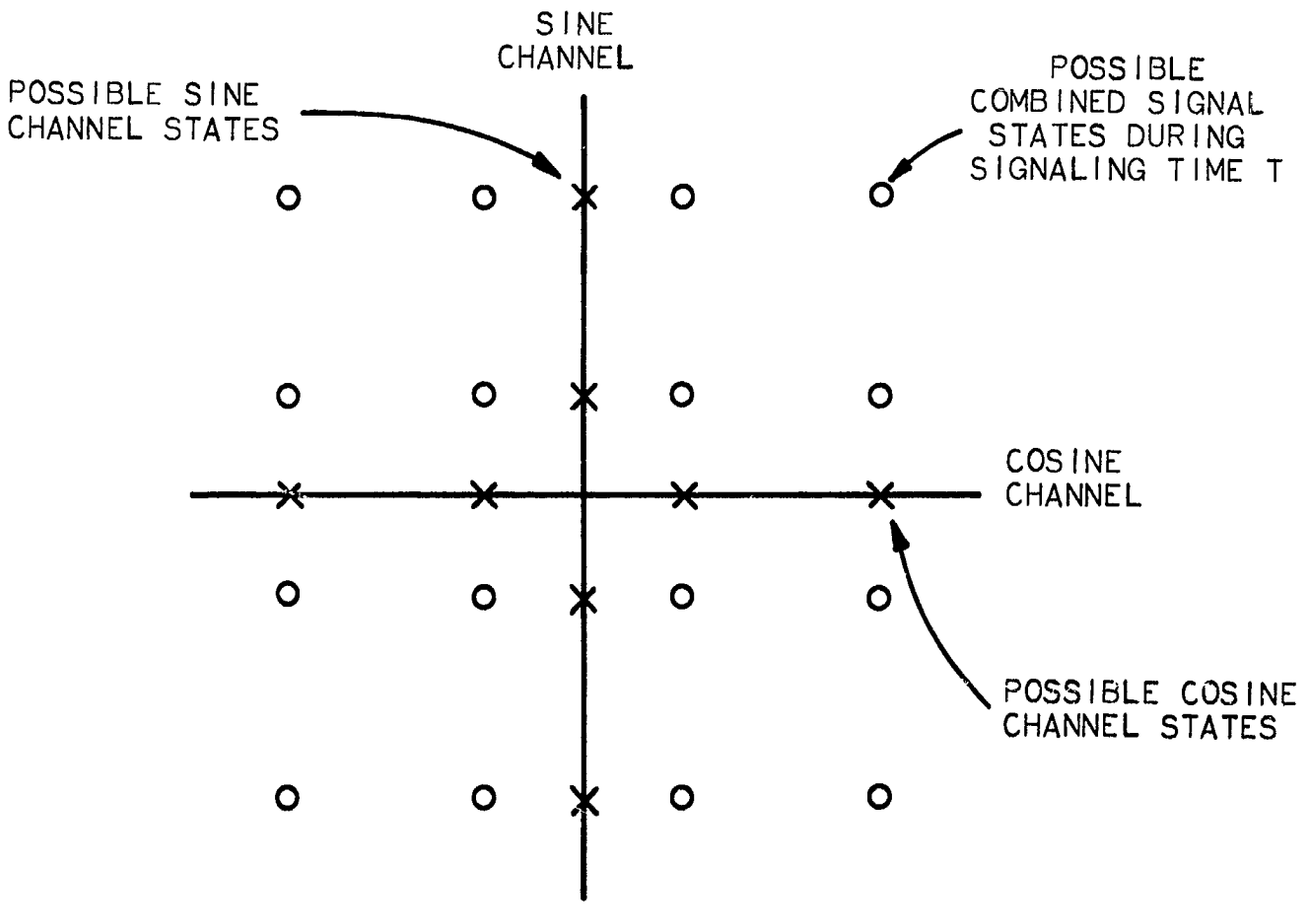

FIGURE C. 1-12

DOUBLE SIDEBAND ORTHOGONAL CARRIER SYSTEM SIGNALING STATES

k	$(S/N)_{pern}$	P_e
2	15.6 db	4.56×10^{-2}
3	19.1 db	2.6×10^{-3}
4	21.6 db	0.66×10^{-4}

Approximately 20 db is required for successful operation of two-bit-per-picture-element compression systems. This is to be compared with 30-db-peak-envelope signal to rms noise required for average good viewing of analog TV signals.

1.4 INFORMATION RATE RELATED TO RF BANDWIDTH

It has been noted that the baseband bandwidth occupancy is one-half the signaling rate; also, for double-sideband transmission, carrier bandwidth occupancy equals the signaling rate. The number of bits per signaling interval B depends upon the number of signaling states available. With 16 states (4 bits) available per signaling interval, and transmitting double sideband at one cycle per signaling internal, EMR has demonstrated a method of transmitting 4 bits per cycle of carrier band (rf) occupancy. The signal states are sufficiently close to one another in signal space to require a peak-envelope signal-to-noise ratio on the order of 20 db for successful operation at usably low error probabilities.

SECTION 2

SURVEY OF EXISTING SYSTEMS

While the development given in Section 1 leads naturally to an orthogonal carrier, multisignal-state system, it is also necessary to supplement such deductive reasoning with an inductive feeling for the existing state-of-the-art To this end Table C-1 has been prepared with comments on some of the reviewed papers. A bibliography of the papers is included at the end of this appendix. To assist in obtaining an overall view, these papers have been reviewed with the intent of plotting the bits-per-cycle performance versus signal-to-noise ratio for the systems discussed. These plotted points may then be compared with the basic Shannon relation

$$C/W = \log_2 (1 + S/N) \tag{34}$$

also plotted in Figure C. 2-1. Here, C = channel capacity in bits per second and W = the bandwidth in cycles per second.

Figure C. 2-1 does not in itself constitute a "handy guide" to modulation system selection because many factors such as terminal complexity, cost, maintainability, variable-speed asynchronous operation capability, tolerance to both parabolic and linear delay distortion, tolerance to amplitude and phase changes, phase jumps and frequency offset must be evaluated in addition to the C/W versus signal-to-noise performance. Nevertheless, a system engineer will get some feel from the figure for not only what is possible (the theoretical systems) but also what is typical (existing or experimentally measured systems). Figure C. 2. 1 is plotted for the most part at a nominally acceptable probability of error of 10^{-4}.

In most experimental cases, the best that can be achieved is only within 1 db of theoretical. In many cases, particularly telephone-line modems, within 5 to 10 db of theoretical is an achievement because of such nongaussian disturbances as impulse noise, improper bit or sample time synchronization, pulse distortion, and intersymbol interference due to less than optimum line equalization. Many of these nongaussian disturbances prevalent in commercial and military common-carrier type links can be designed out of space-ground-space communication links, so it is not the province of this study to consider them further. However, some systems with particularly low C/W for their operating signal-to-noise ratio are plotted in Figure C. 2-1. These systems are those subjected to extensive nongaussian disturbance.

To consider further both the question of operational disturbances and the C/W versus S/N aspects of modulation the reader is recommended to consider a book by Bennett and Davey [a] which became available late in this study program.

---

[a] W. R. Bennett and J. R. Davey; Data Transmission, McGraw Hill, 1965.

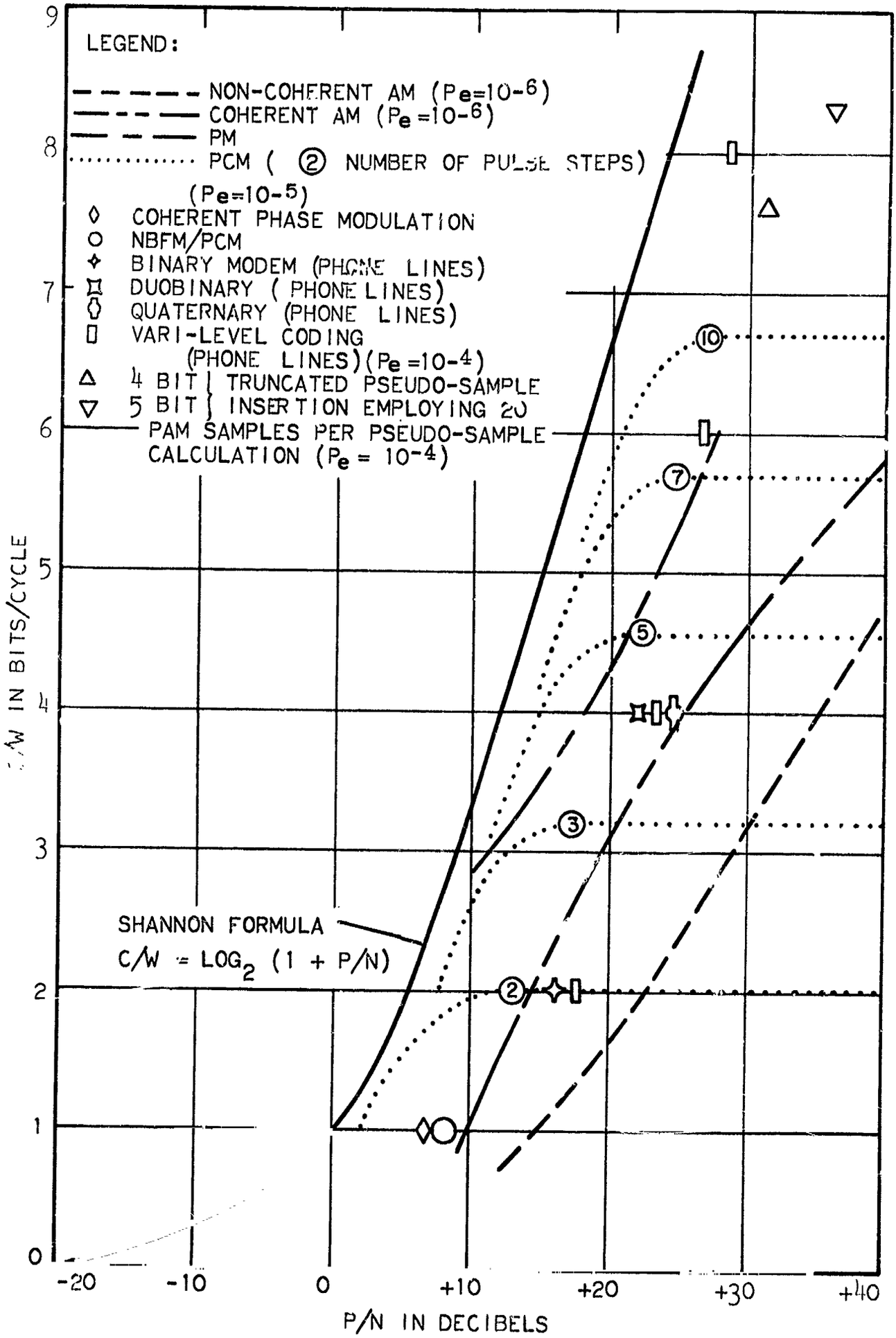

FIGURE C.2-1

PER-CYCLE CHANNEL CAPACITY VERSUS SIGNAL-TO-NOISE RATIO

TABLE C-1

SELECTED PAPERS DISCUSSING MODULATION SYSTEMS

Author	Year	Country	Theoretical, Experimental, Discussion	AM*						FM*				Pulse and Digital*												Remarks
				AM	AM-DSB	AM-DSB/SC	AM-SSB	CSSB	VSB	FM	WBFM	NBFM	FBFM	PM	AM-PM	PAM	PPM	PCM	PDM	PSK	DPSK	FSK	PAM/FM	PCM/FM	PCM/PM	PCM/FSK	ASK	
Oliver, B. M., Pierce, J. R. and Shannon, C. E. The Philosophy of PCM.	1948	U. S. A.	Theoretical							X								X									Presents the basic theory of PCM and its advantages. Compares PCM with other broadband systems by use of large-index FM. Gives the equation for channel capacity versus SNR for PCM.
Jackson, W. Communication Theory, Chapter 3; paper by Z. Jelonk	1953	England	Theoretical	X						X						X	X	X	X									Seems to be a very good reference. Gives equations and curves for the systems.
Becker, H. D., and Lawton, J. G. Theoretical Comparison of Binary Data Transmission Systems.	1958	U. S. A.	Theoretical, Experimental			X	X	X												X		X						Coherent PSK system is theoretically the optimum binary data transmission system. Includes curves of P_e versus $E(1-\rho)(2N_o)$ where $\rho = -1$ for coherent PSK and P_e versus B for PSK and FSK systems. CSSB should not be employed when spectrum economy is of prime importance.
Hancock, J. C. An Introduction to the Principles of Communication Theory.	1961	U. S. A.	Theoretical	X	X	X	X			X	X	X		X		X	X	X	X									Chapter 2 compares systems on the basis of input and output S/N ratios and the required bandwidth. A curve of transmission rate versus S/N for $P_e = 10^{-5}$ for PCM systems is given on page 181, curves of $(S/N)_o$ versus $(S/N)_i$ are given for AM-SSB/SC, AM-DSB, FM, and PCM on page 232.
Wiler, J. M. Digital Data Communication Techniques.	1961	U. S. A.	Discussion						X	X				X														The paper presents a general discussion on each of the various elements of a typical communication channel.
Arthurs, E., and Dym, H. 1962 On The Optimum Detection of Digital Signals in the Presence of White Gaussian Noise- A Geometric Interpretation and a Study of Three Basic Transmission Systems.		U. S. A.	Theoretical																	X		X					X	Gives derivation and curves for P_e versus S/N with the number of levels as a parameter. Includes graph of BW efficiency versus number of levels.

TABLE C-1

SELECTED PAPERS DISCUSSING MODULATION SYSTEMS

Author	Year	Country	Theoretical, Experimental, Discussion	AM*						FM**				Pulse and Digital†													Remarks
				AM	AM-DSB	AM-DSB/SC	AM-SSB	CSSB	VSB	FM	WBFM	NBFM	FBFM	PM	AM-PM	PAM	PPM	PCM	PDM	PSK	DPSK	FSK	PAM/FM	PCM/FM	PCM/PM	PCM/FSK	ASK	
Campopiano, C. N. A Coherent Digital Amplitude and Phase Modulation Scheme.	1962	U. S. A.	Theoretical												X												Discusses the AM-PM systems of Cahn, Hancock and Lucky, and the author. The systems are compared on the basis of detection reliability. The author's system is said to yield a slightly better performance with a much simpler mechanization. He has equations for P_e.
Hancock, J. C. On Comparing the Modulation Systems.	1962	U. S. A.	Theoretical		X	X	X				X	X				X				X	X	X						Gives graph of P_e versus ratio of signal energy to noise spectral density. Also has graph of β (signal power required on a per bit per second basis under the influence of a given noise spectral density) as a function of P_e.
Keenan, R. K., and Mannex, H. R. Spacecraft Communications Systems.	1962	U. S. A.	Theoretical, Discussion							X			X	X														Gives table of communication path losses, calculation of transmitter carrier power, graphs of Input S/N versus BW/Bit rate and frequency versus power for various systems, and a graph of effective noise temp. versus frequency. Has information to get bits/cycle versus S/N.
Lucky, R. W., and Hancock, J. C. On the Optimum Performance of N-ary Systems Having Two Degrees of Freedom.	1962	U. S. A.	Theoretical											X	X												X	Gives P_e versus S/N and channel capacity versus S/N. Channel capacity in bits/symbol.
Martin, D. L. Data Communications.	1962	U. S. A.	Discussion																	X		X						Shows spectral distribution for FSK and FSK multiplexing.
Weaver, C. S. A Comparison of Several Types of Modulation.	1962	U. S. A.	Theoretical	X						X						X						X		X	X			The probability of making an error is derived for the systems along with a discussion of transmitter and receiver bandwidth. Graphs are given for P_e versus S/N and Mean Square Error versus S/N.

TABLE C-1

SELECTED PAPERS DISCUSSING MODULATION SYSTEMS

Author	Year	Country	Theoretical, Experimental, Discussion	AM*						FM*				Pulse and Digital*												Remarks
				AM	AM-DSB	AM-DSB/SC	AM-SSB	CSSB	VSB	FM	WBFM	NBFM	FBFM	PM	AM-PM	PAM	PPM	PCM	PDM	PSK	DPSK	FSK	PAM/FM	PCM/FM	PCM/PM	PCM/FSK	ASK	
Wolf, J. K. On Comparing N-ary Systems.	1962	U. S. A.	Theoretical																	X								Gives a technique for obtaining equivalent error probabilities for N-ary system.
Balakrishnan, A. V. Space Communications, Chapter 7, "Sampled Data Modulation Systems" by R. Saunders.	1963	U. S. A.	Discussion													X	X	X					X			X		Good subjective comparison of PCM systems. Graphs include average error rate per information bit versus S/N for various PCM systems and error-correcting systems. Includes a short discussion on orthogonal systems.
Glenn, A. B. and Lieberman, G. Performance of Digital Communications Systems in an Arbitrary Fading Rate and Jamming Environments.	1963	U. S. A.	Theoretical																		X	X						The effects of fading rate on the performance of the systems is studied. Curves for P_e versus S/N are provided.
Lender, A. Duobinary Technique for High-Speed Data Transmission.	1963	U. S. A.	Theoretical, Experimental							X												X						Duobinary technique has speed capability equal to that of quaternary systems (2 bits per cycle when both sidebands of carrier are considered). A Duobinary FM system is analyzed and a curve of P_e versus normalized SNR for Binary FSK and Duobinary FSK is given.
Lord, John B. and Lytle, D. W. High-Speed Communication in Synchronous Band-limited Channels.	1964	U. S. A.	Theoretical													X												Discusses two methods, Pseudo Sample Insertion (PSI) Technique and Vestigial Interpolation Filter (VIF) Technique, for eliminating errors due to alias spectra. Gives equations for calculating S/N for both PSI and VIF and curve necessary to get bits per cycle for PSI.
Melas, C. M. and Gorog, E. A Digital Data Transmission System with Optimum Bandwidth Utilization.	1964	France	Theoretical, Experimental				X																					A data-transmission system is described which replaces conventional modulation by binary coding and filtering. With a quaternary input, 2.4 bits per cycle of bandwidth can be obtained. The technique is used for transmission over lines.

TABLE C-1

SELECTED PAPERS DISCUSSING MODULATION SYSTEMS

Author	Year	Country	Theoretical, Experimental Discussion	AM*						FM*				Pulse and Digital*													Remarks
				AM	AM-DSB	AM-DSB/SC	AM-SSB	CSSB	VSB	FM	WBFM	NBFM	FBFM	PM	AM-PM	PAM	PPM	PCM	PDM	PSK	DPSK	FSK	PAM/FM	PCM/FM	PCM/PM	PCM/FSK	ASK	
Rumble, D. H. The Use of Conventional Microwave Channels for the Transmission of Data at Megaband Signaling Rates.	1964	U. S. A.	Theoretical																	X							Discusses differentiated NRZ and biphase modulation techniques. The paper states that differentiated NRZ can usually be used for as high as 1.5 bits per cycle of BW where BW is defined by the -5 to -6 db region. Biphase can be used up to 0.5 bits per cycle.
Shagena, J. L. and Kvarda, J. C. A New Multi-Level Coding Technique for Digital Communications.	1964	U. S. A.	Theoretical, Experimental	X																							Discusses varilevel coding technique in connection with telephone lines. A system employing a combination of amplitude and biphase modulation is used to demonstrate the coding technique. Gives a table for bits per cycle to be expected and a curve of P_e versus S/N.

*Glossary

AM	Amplitude Modulation	AM-PM	Amplitude Modulation - Phase Modulation
AM-DSB	Amplitude Modulation - Double Sideband	PAM	Pulse Amplitude Modulation
AM-DSB/SC	Amplitude Modulation - Double Sideband/Suppressed Carrier	PPM	Pulse Position Modulation
AM-SSB	Amplitude Modulation - Single Sideband	PCM	Pulse Code Modulation
CSSB	Coherent Single Sideband	PDM	Pulse Duration Modulation
VSB	Vestigial Sideband	PSM	Phase Shift Keying
FM	Frequency Modulation	DPSK	Differential Phase Shift Keying
WBFM	Wideband Frequency Modulation	FSK	Frequency Shift Keying
NBFM	Narrowband Frequency Modulation	PAM/FM	Pulse Amplitude Modulation/Frequency Modulation
FBFM	Feedback Frequency Modulation	PCM/FM	Pulse Code Modulation/Frequency Modulation
PM	Phase Modulation	PCM/PM	Pulse Code Modulation/Phase Modulation
ASK	Amplitude Shift Keying	PCM/FSK	Pulse Code Modulation/Frequency Shift Keying

Chapter 11, "Comparisons of Modulation Methods," is especially recommended reading. It is interesting to find that for a 4 bit-per-cycle modulation method, the orthogonal carrier system developed above (and called quadrature AM, suppressed carrier, coherent detection in Bennett and Davey) is among the highest performers, equaling polar baseband (not a carrier system) and vestigial sideband, suppressed carrier in terms of C/W versus S/N performance. Bennett and Davey's figure for maximum steady-state signal power S/N is 20.8 db for a P_e of 10^{-4}. This is to be compared with a figure of 21.6 db for a P_e of 0.66×10^{-4} which, based on a k = 4, was computed from the simple derivation in paragraph 1.3.2 of this appendix.

SECTION 3

FOUR-BITS-PER-CYCLE MODEM BLOCK DIAGRAM AND PERFORMANCE

3.1 SYSTEM

3.1.1 Transmitter

The transmitter in the system is, in effect, two parallel, bipolar, coherent, four-level-amplitude-shift-keying, suppressed-carrier modulating systems operating at "half rate" and having their outputs linearly added and amplified for transmission. For instance, in Figure C. 3-1, top half, the serial data at a 20-megabit rate enters the data splitter and emerges as two 10-megabit data streams. Each data stream is encoded on a 2-bit basis to a 4-level-amplitude signal which enters a channel whose carrier is in phase quadrature with the other channel. The modulated outputs are added together at low level and sent through a linear amplifier to the transmitter. There is a very strong requirement for adder and final amplifier linearity if channel crosstalk is to be avoided.

The resulting signal is transmitted at a signaling rate of 5×10^6 signaling intervals per second and produces a double-sideband spectrum with first zeros at $f_c \pm 5$ Mc. The spectrum has an ERE bandwidth occupancy of 5 Mc. Two channels of 2 bits per signaling interval each are occupying this spectrum for an overall effect of a 20-megabit data stream occupying a 5-Mc bandwidth. This 5-Mc bandwidth occupancy can be further assured by placing a 2.5-Mc, low-pass premodulation filter between the output of the data splitter and the product modulators.

3.1.2 Receiver

The receiver is, like the transmitter, a parallel device with separate coherent-detection channels for the sine and cosine channels. It is illustrated in the lower part of Figure C. 3-1. This demodulator is a complex receiver because all possible information is being extracted from the incoming carrier and data stream in order to achieve maximum demodulation efficiency. Carrier phase must obviously be retrieved to operate each of the phase-quadrature channels. Bit timing, or PCM signal conditioning, must be accomplished to establish sampling and dump times for the reset integrators. In this case however the signaling interval periods T must be recovered from a multilevel carrier signal instead of a binary one.

The threshold units contain three thresholds at -2/3, 0, and +2/3 of peak quadrature channel carrier amplitude. The center threshold placement is unaffected by transmission-link amplitude changes but the other two thresholds must be located with respect to the current estimate of maximum channel carrier amplitude. An alternative to tying the nonzero thresholds to the channel carrier amplitude is to have excellent AGC in the receiver ahead of the data-detection

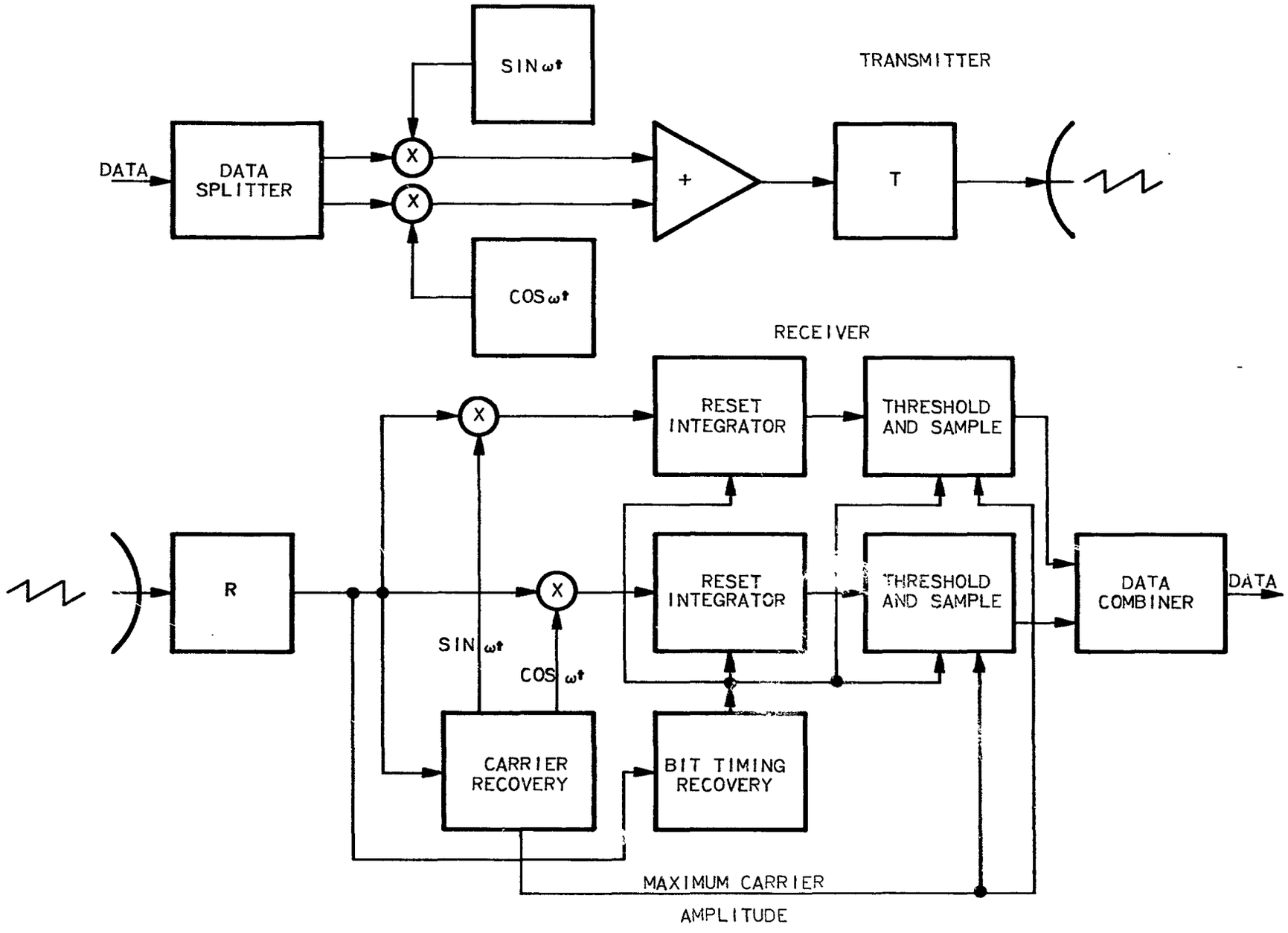

FIGURE C.3-1

TWO-CHANNEL COHERENT PHASE QUADRATURE SYSTEM

circuits. Each threshold unit makes a "2-bit" decision as to which of 4 amplitude levels was transmitted. The decisions at a 5-Mc rate on each of the two channels are combined with logic circuitry in the data combiner to reconstitute the original 20-megabit data stream in 4-bit increments.

3.2 PERFORMANCE

3.2.1 Ideal Case

The ideal (i.e., no premodulation filter) performance of the system was covered in paragraph 1.3.2 in which a bit error probability was derived as a function of k directly related to signal-to-noise ratio. Although termed a "bit error" probability, the derived figure P_e is in reality a word-error probability for a 2-bit (4 level) word on each channel. To estimate correctly the transmitted system signal state, each of the two channels must independently make a correct decision. Thus the probability P_{csd} of a correct state decision is given as

$$P_{csd} = (1 - P_e)^2 \tag{35}$$
$$= (1 - 2P_e + P_e^2),$$

which for $P_e \geq 10^{-2}$ reduces to the approximate expression

$$P_{csd} \doteq 1 - 2P_e. \tag{36}$$

Thus, the 4-bit word error probability, P_{e4}, is given by

$$P_{e4} = 1 - P_{csd} = 2P_e. \tag{37}$$

For a 4-bit word in error, the expected number of bits in error is 2.5. The probability of getting 2.5 bits in error (on an expected value basis) is $2P_e$, which reduces to a quasi bit-error probability of $0.8\,P_e$. By this reasoning, P_e (calculated in paragraph 1.3.2) is very close, on a conservative basis, to the bit error probability and was so referenced.

3.2.2 Filter-Factor Case

If a premodulation filter is employed in the transmitter to limit rf sideband splatter, the output of the modulating channel modulators will not, in some data sequences, attain full-rated amplitude at the sampling times. That is, at the sampling times the received amplitude will not be as far away from the decision thresholds as it would have been had there been no premodulating

filtering. The less distance there is, the greater is the possibility of a noise perturbation into the next signal state territory. To compensate for this reduced noise immunity the signal-to-noise ratio must be increased.

The worst case is the transmission of a string of −1's followed by a +1. In one signaling interval T the output signal will, for a one-pole RC filter with low-pass cutoff at $f_\ell = 1/2T$, rise to within $1 - e^{-\pi} = 0.9565$ of the total step height of 2. Therefore, at the proper sample time the waveform will be at −1 + 2 times (0.9565) = +0.9130. This point is 0.9130 −0.667 = 0.2463 away from the nearest threshold at +2/3. Now instead of fitting $k\sigma$ worth of noise into 1/3 the peak channel carrier level, the same $k\sigma$ worth of noise must now be fitted into 0.2463 of the carrier level. The channel peak carrier level must now be 4.06 $k\sigma$ instead of 3 $k\sigma$, an increase of 1.35 in amplitude or 2.6 db. Adding the 2.6-db filter factor to the 21.6-db ideal signal-to-noise ratio of paragraph 1.3.2 yields a final figure of 24.2-db signal-to-noise ratio for a quasi bit error probability of 0.528×10^{-4} occupying 5-Mc at carrier band while transmitting a 20-megabit serial data stream.

SECTION 4

BIBLIOGRAPHY

1. Arthurs, E. and H. Dym, "On the Optimum Detection of Digital Signals in the Presence of White Gaussian Noise - A Geometric Interpretation and a Study of Three Basic Data Transmission Systems, "IRE Trans on Communications Systems, December 1962, pp 336-372.

2. Balakrishnan, A. V., editor, Space Communications, New York, McGraw-Hill, 1963, papers by E. Rechtin and others. Chapter 2, "Sampled Data Modulation Systems" by R. Saunders.

3. Becker, H. D. and Lawton, J. G., Theoretical Comparison of Binary Data Transmission Systems, Cornell Aeronautical Lab Report No. CA-1172-S-1, May 1958.

4. Campopiano, C. N., "A Coherent Digital Amplitude and Phase Modulation Scheme," IRE Transactions on Communications Systems, March, 1962, pp 90-95.

5. Glenn, A. B., and Lieberman, G., "Performance of Digital Communications Systems in an Arbitrary Fading Rate and Jamming Environments," IRE Trans. on Communication Systems, March, 1963, pp 57-67.

6. Hancock, J. C., An Introduction to the Principle of Communication Theory, McGraw-Hill, New York, N. Y., 1961.

7. Hancock, C., "On Comparing the Modulation Systems," Proceedings of the National Electronics Conference, pp 45-50, Vol. 18, 1962.

8. Jackson, Communication Theory, Academic Press, Inc., New York, 1953, pp 77-81.

9. Keenan, K. K. and Mannex, "Spacecraft Communications Systems," Aerospace Electronics, November 1962, pp 19-25.

10. Lender, A., "Duobinary Technique for High Speed Data Transmission," IEEE Transactions, May, 1963, pp 214-218.

11. Lord, J. B. and Lytle, D. W., "High Speed Communications in Synchronous Bandlimited Channels," 10th National Communication Symposium, Utica, New York, 5-7 October 1964, pp 319-329.

12. Lucky, R. W., Hancock, J. C. "On the Optimum Performance of N-ary System Having Two Degrees of Freedom," IRE Trans on Communications Systems, June 1962, pp 185-192.

13. Martin, D. L., "Data Communications," Space Aeronautics, Part 2, November 1962, pp 30-33.

14. Melas, C. M., and Gorog, E., "A Digital Data Transmission System with Optimum Bandwidth Utilization," 10th National Communication Symposium, Utica, New York, 5-7 October 1964, pp 330-341.

15. Oliver, B. M., Pierce, J. R., and Shannon, C. E., "The Philosophy of PCM," Proc. of IRE, 1948, pp 1324-1333.

16. Rumble, D. H. "The Use of Conventional Microwave Channels for the Transmission of Data at Megaband Signaling Rate", 1964 International Convention of Military Electronics Conference Proceedings, pp 311-313.

17. Shagena, J. L., and Kvarda, J. C., "A New Multi-Level Coding Technique for Digital Communications," 1964 Interntl. Conv. on Mil. Elect. Conf. Proc., pp 326-331.

18. Weaver, C. S., "A Comparison of Several Types of Modulation," IRE Transactions on Communication Systems, March, 1963, pp 96-101.

19. Wier, J. M., "Digital Data Communication Techniques," Proc. of IRE January 1961, pp 196-209.

20. Wolf, J. K., "On Comparing N-ary Systems," IRE Transactions on Communication Systems, June 1962, pp 216-217.

APPENDIX D

DIGITAL COLOR TV INVESTIGATION

APPENDIX D

TABLE OF CONTENTS

SECTION 1

INTRODUCTION

Color television transmission is a direct extension of monochrome television transmission techniques, wherein three independent, colorimetric properties of an image must be conveyed for proper reproduction of the image in full color.

Monochrome TV systems used for normal visual image reproduction purposes are designed to match approximately the spectral response (luminosity function) of the human eye. Thus, a high quality monochrome system is capable of conveying approximately the same brightness (luminance) sensation to the TV viewer as he would perceive by directly viewing the object (within the dynamic range limits of the system).

For color-TV transmission, the hue of the colored image (the prominent spectral characteristic--red, yellow, green, etc.) and the saturation of the image (determined by the amount of white or neutral light in relation to the light energy of the predominant hue) must be transmitted in addition to the luminance information. Collectively, hue and saturation properties are termed chrominance.

Thus, the majority of color-TV effort throughout this country and abroad has been centered around the development and evaluation of methods for efficient transmission of high fidelity color signals (composed of luminance and chrominance information) within the transmission channel allocations established for monochrome TV.

The color-TV study effort on this contract has proceeded in parallel with the supporting experimental color-TV work (described in Section 3 of this appendix) to arrive at recommendations for color-TV system approaches which will satisfy future MSC requirements. The study effort included:

1. The study of basic colorimetry as related to color TV.

2. The review of past and present color-TV techniques.

3. The determination of probable MSC color-TV functions and typical operating parameters.

4. The determination of ground rules for the application of color TV to MSC missions.

5. The selection of the most promising system approaches for satisfying MSC requirements.

SECTION 2

STUDY EFFORT

2.1 BASIC COLORIMETRY RELATED TO COLOR TV (A Summary)

Colorimetry is defined as the science of measurement and specification of color.

Color-TV employs the additive principle, in which a wide range of colors can be reproduced by the proper additive mixtures of primary light sources. The selected primaries are not unique. Any three can be used so long as no two can be combined to match the third. Red, green, and blue primaries (qualitatively speaking) are generally used, since they provide the greatest range of reproduced colors using positive mixtures of primaries.

The measurements and specification of colors based on this three-primary principle are called tristimulus colorimetry. Tristimulus colorimetry is based on two premises.

1. Color is a three-dimensional property of light (hue, saturation, and luminance)

2. The amounts of primary light needed to match an unknown color can be used to specify this color numerically

The International Commission on Illumination (ICI) has published standardized primary-color mixture data on a selected set of R, G, and B primaries. These data were obtained from an average of a large number of colorimetric measurements. These measurements employ unit amounts of R, G, and B primary light (not equal in absolute energy terms, however, due to the eyes' response characteristic) to produce a reference white or neutral at a specified luminance level. Then, the number of R, G, and B primary units are determined to match all narrowband spectral colors (generally obtained from a monochromator) of equal energy across the visible spectrum. Standard R, G, B color mixture curves are plotted from these data.

The hue and saturation of a particular color are determined by the ratio of R, G, B primary units, while the luminance is proportional to the absolute energy levels of the primaries multiplied by the luminosity function of the eye. For neutral light, $L_R = 0.3$, $L_G = 0.59$, $L_B = 0.11$, based on the primaries used in U.S. commercial color-television.

The ICI also has established a standardized method of specifying the chromaticities of all realizable colors. The standard data are derived from the R, G, B color

mixture curves; however the primary R, G, B units have been linearily transformed [a] into a fictitious set of primaries termed X, Y, and Z so that only positive chromaticity coordinates need be used to specify all colors. (In the R, G, B system, negative values of the primaries are needed to match certain highly saturated colors.)

These x, y chromaticity coordinates (or trichromatic coefficients) are equal to the ratios of the primary units, independent of absolute energy levels. By plotting these coordinates on normal axes, the chromaticities of all realizable colors can be shown in graphical form. This graph is known as the ICI chromaticity diagram, and is given in Figure D.2-1. This diagram may be thought of as a color map which locates each particular color in terms of its chromaticity value.

Full specification of a color requires definition of its absolute luminance value as well as its chromaticity. Where luminance is a function of all three primary levels in the R, G, B system, only the Y primary carries luminance information in the ICI X, Y, Z system. Thus, complete identification of a color is achieved by specifying the values of x, y, and Y.

By plotting the location of a particular set of three primaries, the gamut of reproducible colors is formed by the triangular area obtained by connecting these three primaries with straight lines. Figure D.2-1 shows the triangular gamut of colors which may be reproduced by U.S. commercial color-TV systems. Also, the gamut of theoretically reproducible colors obtained by mixtures of any two primaries is seen to fall along a line. The position on the line is determined by the relative luminosity levels (intensities) of the primaries.

The general hues associated with the various areas of this diagram are shown in Figure D.2-2. The central area is made up of colors of low saturation and zero saturation (neutral or white). Maximum-saturation colors appear at the edges of the diagram.

2.2 REVIEW OF PAST AND PRESENT COLOR-TV TECHNIQUES

2.2.1 Introduction

The great majority of published color-TV literature deals with the development of various analog-color-TV techniques. From the colorimetric standpoint, these various techniques may be grouped into two major categories, namely: two-color systems and three-color systems. Since the ground rules of this study (to be given later) specify that the color fidelity of the selected system(s) must be generally equivalent to commercial color-TV quality, the two-color system

[a] Based on Grassman's Law which effectively states that if equivalent lights are added to or subtracted from equivalent lights, the resultant lights are equivalent.

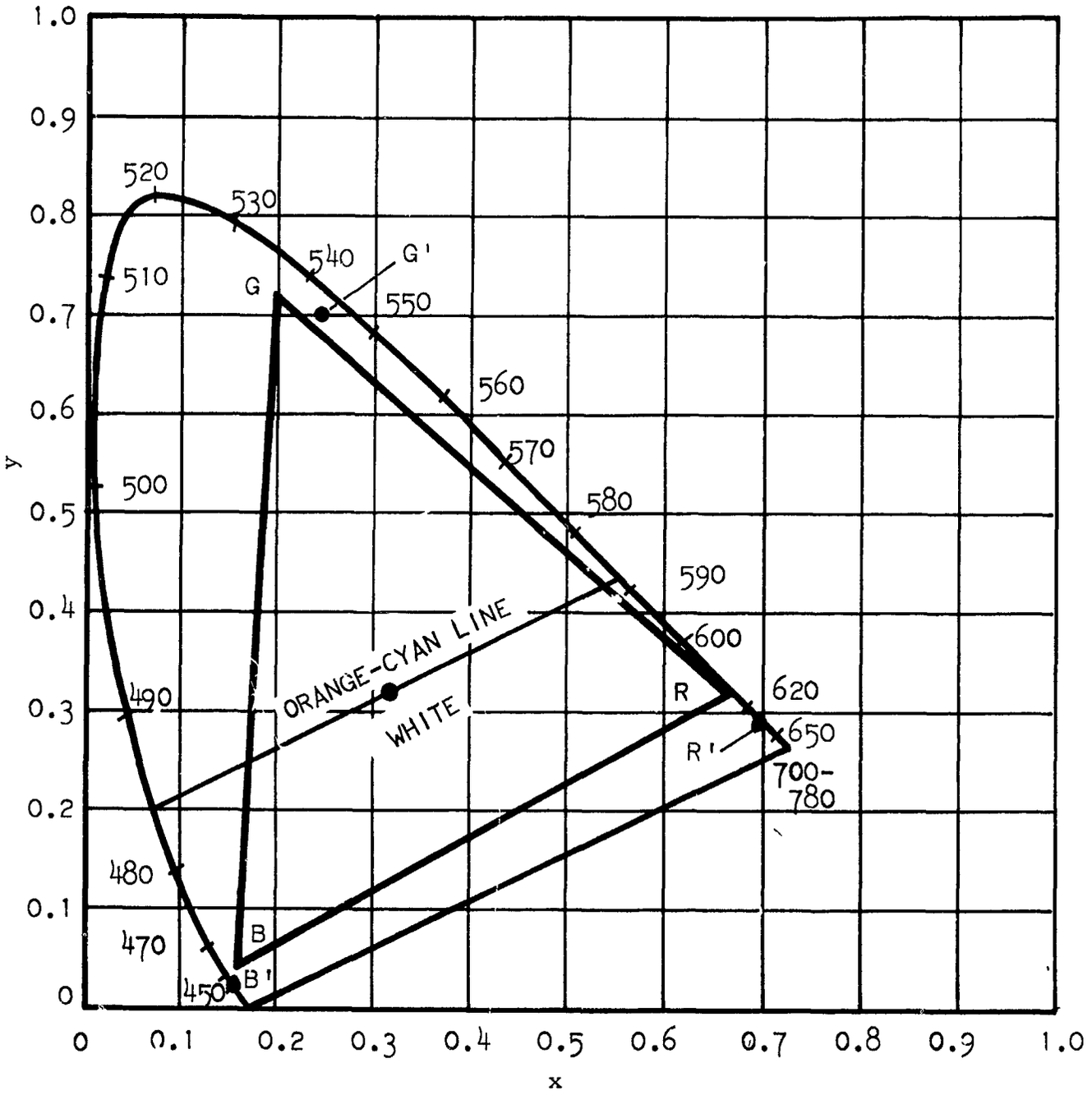

FIGURE D.2-1

CHROMATICITY DIAGRAM SHOWING R, G, B PRIMARY TRIANGLE AND ORANGE-CYAN LOCUS LINE

12074

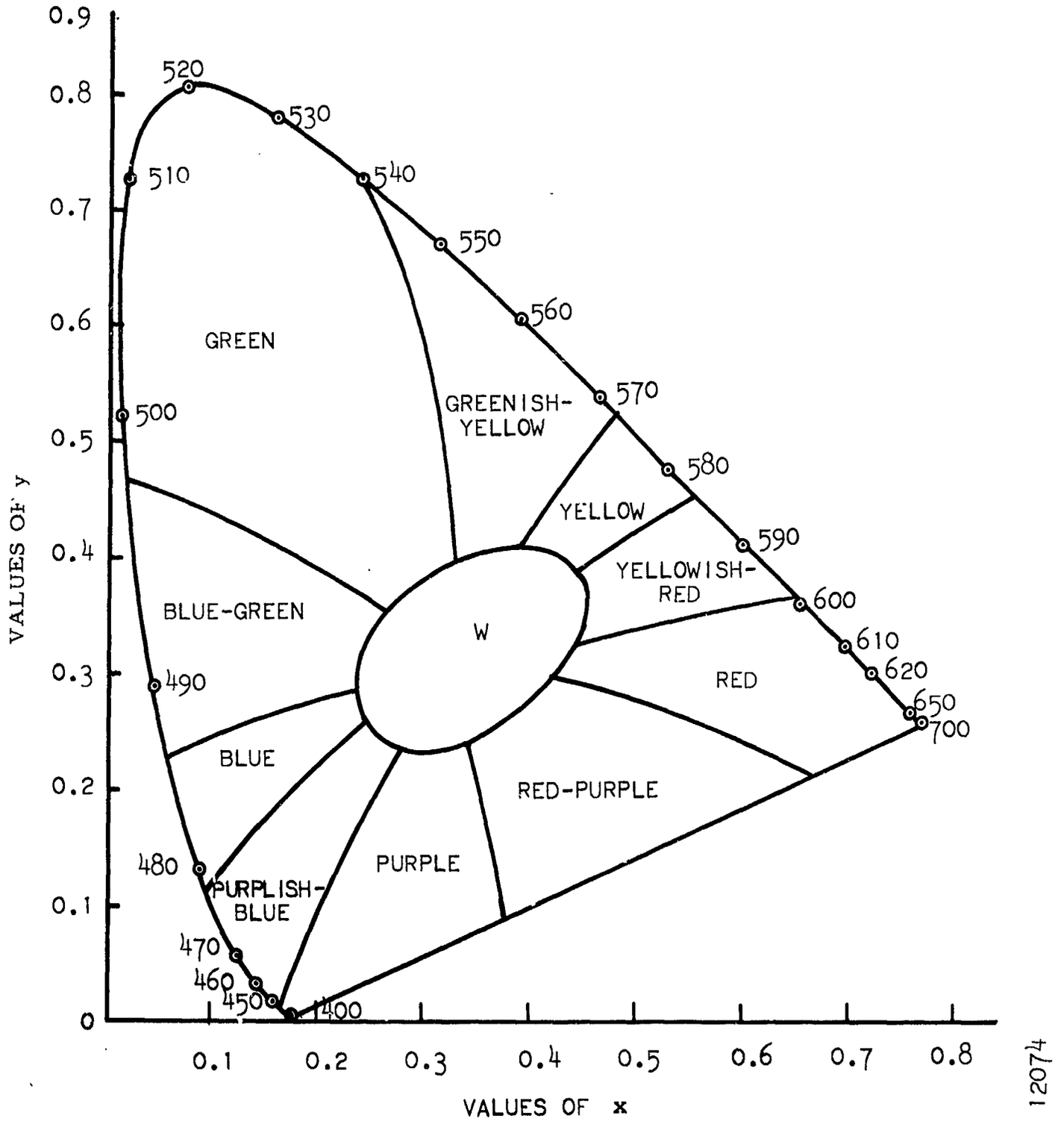

FIGURE D.2-2

ICI x, y CHROMATICITY DIAGRAM

category was eliminated from serious consideration due to its restricted gamut of reproduced color hues and saturations (see the orange-cyan line on Figure D.2-1 for an example). Thus, the study is principally concerned with three-color systems, which employ additive mixtures of red, green, and blue primaries (qualitatively speaking) or linear transformations of R, G, B (into luminance, M, and "color difference" signals, R-M, B-M, and G-M for example) to reproduce a suitably wide range of chromaticity values.

From the data processing (and transmission) standpoint, the major system categories are: simultaneous, sequential, and simultaneous/sequential (or hybrid) types.

2.2.2 Simultaneous Systems

The simultaneous systems effectively employ three (or four, in the case of the latest color cameras which use a separate luminance camera) individual sensors to generate the luminance and chrominance data. Simultaneous transmission of the separate signals may be most readily accomplished by: (1) space-separation, as might be employed in a closed circuit color system in which an individual video coaxial line is used for each signal; and (2) by a frequency-separation process. The most basic frequency-separation method as shown in Figure D.2-3 would involve the use of separate carrier frequencies properly positioned to provide transmission spectrum space for the sidebands of each modulating video signal. Of course, this arrangement is very wasteful of transmission bandwidth and has no practical potential.

Present commercial (NTSC) color TV employs a far more efficient form of frequency separation of the luminance and chrominance signals (see Figure D.2-4). The chrominance data designated as in-phase, I, and quadrature-phase, Q, signals of reduced but still adequate bandwidth[a] modulate subcarriers which are positioned near the upper end of the wide-band luminance signal spectrum (as shown in Figure D.2-5). Through careful choice of subcarrier frequency, the chrominance signal components are frequency-interlaced with respect to the luminance signal components, which minimizes the crosstalk between these sources. The instantaneous phase of the resultant of the subcarriers (resultant of the quadrature modulation process) represents the hue of the color being transmitted, and its amplitude represents the saturation of the color. Figure D.2-6 shows the location of the I and Q axes on the chromaticity diagram. After decoding of the received data (depicted in Figure D.2-7) the common luminance and separate chrominance signals are displayed on a tricolor kinescope.

A modified version of the NTSC color system has been under intensive development in West Germany during recent years. Known as PAL (Phase Alternation Line), the system employs a method of alternating the phase of the I chrominance

---

[a] Fink, D. G. (Editor), Television Engineering Handbook, McGraw-Hill, N. Y., N. Y., 1957, pp. 9-6 through 9-10.

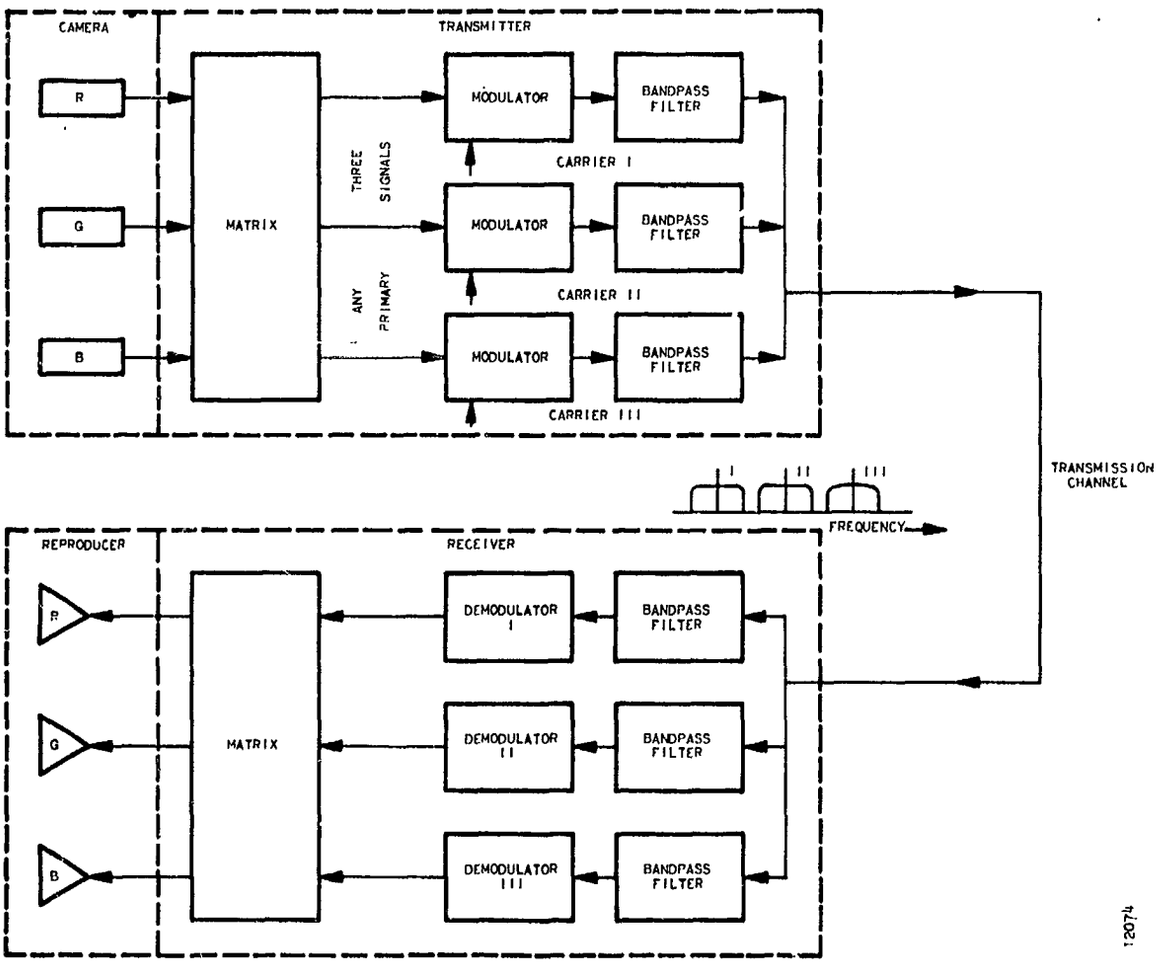

FIGURE D.2-3

FREQUENCY-MULTIPLEXED (SIMULTANEOUS) SYSTEM

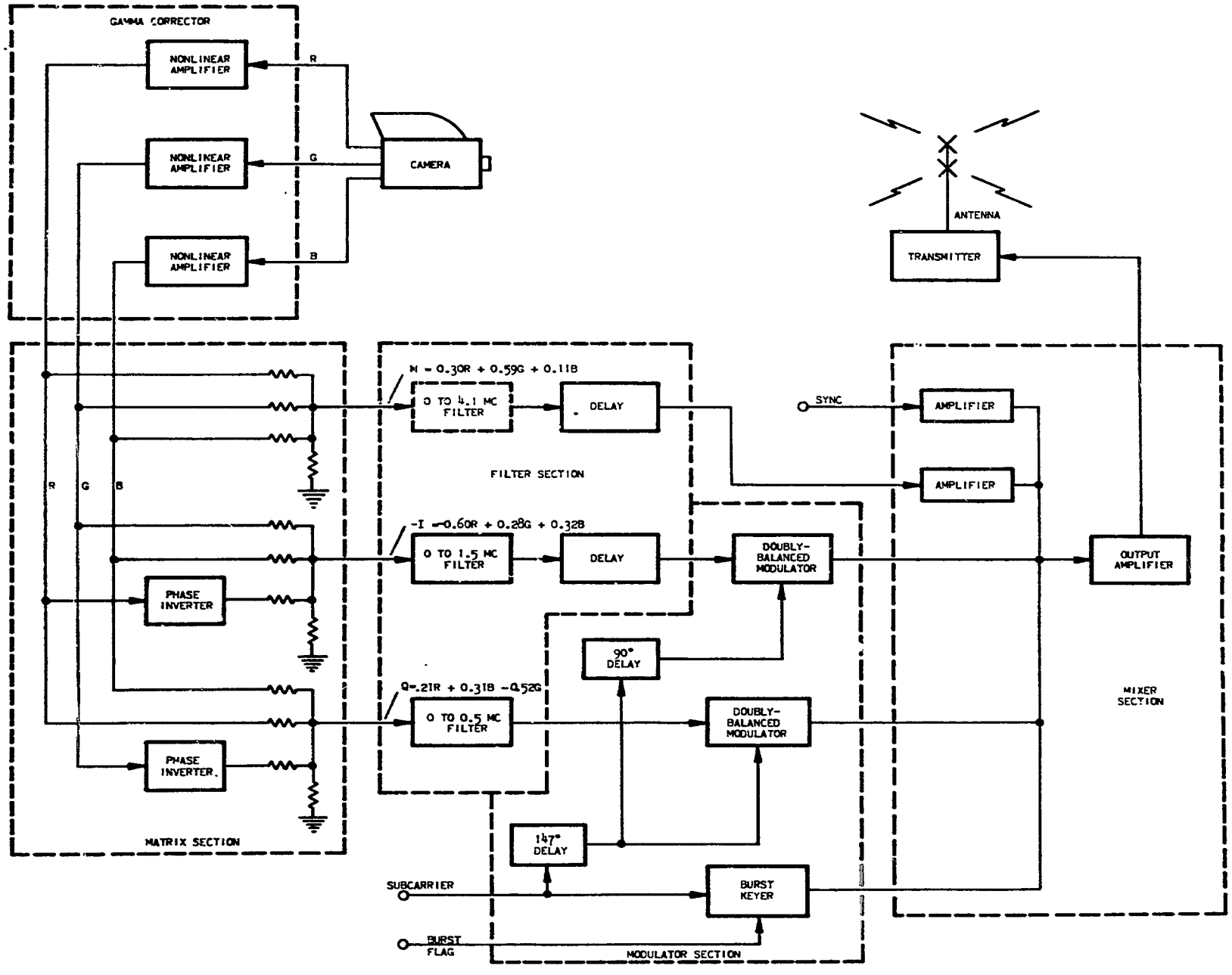

FIGURE D-2-4

NTSC TRANSMITTING SYSTEM

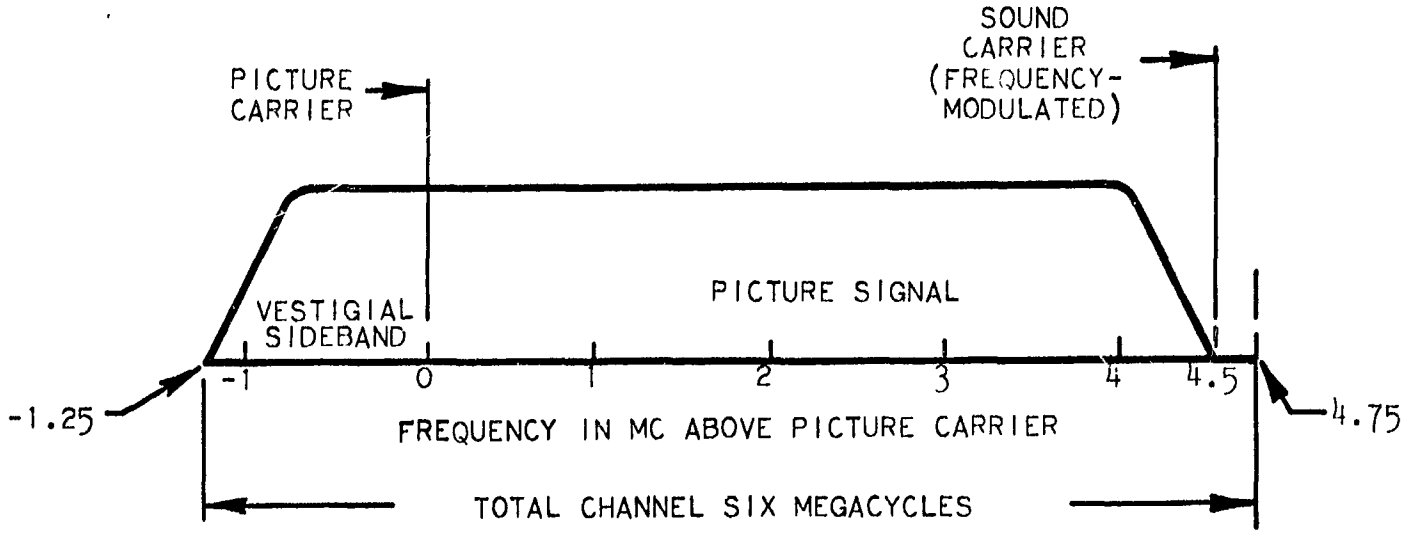

(a) MONOCHROME

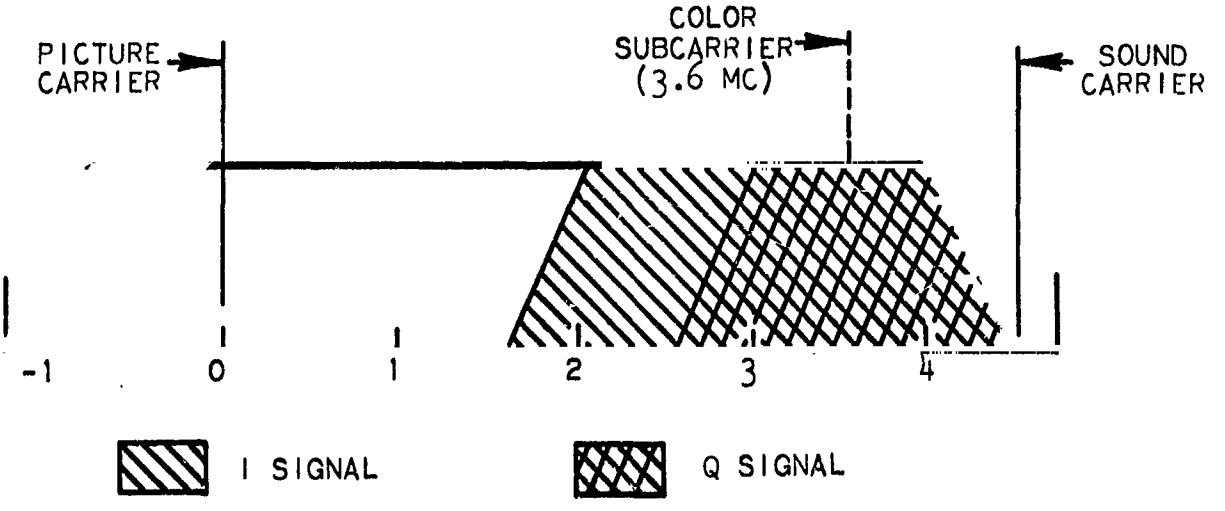

12074

(b) COLOR

FIGURE D.2-5

MONOCHROME AND COLOR TV CHANNELS

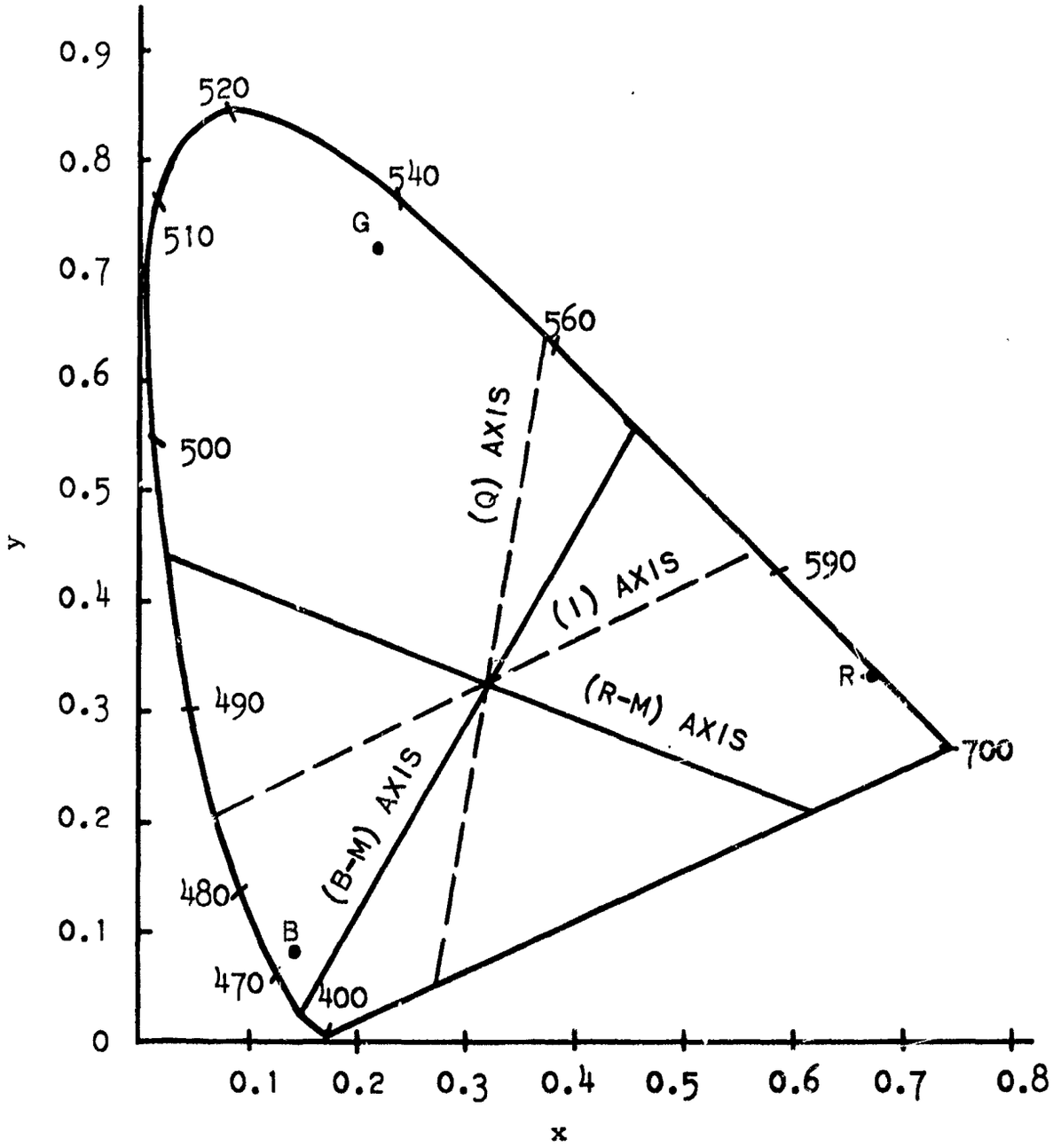

FIGURE D.2-6

NTSC TRANSMISSION PRIMARIES IN CHROMATICITY DIAGRAM

12074

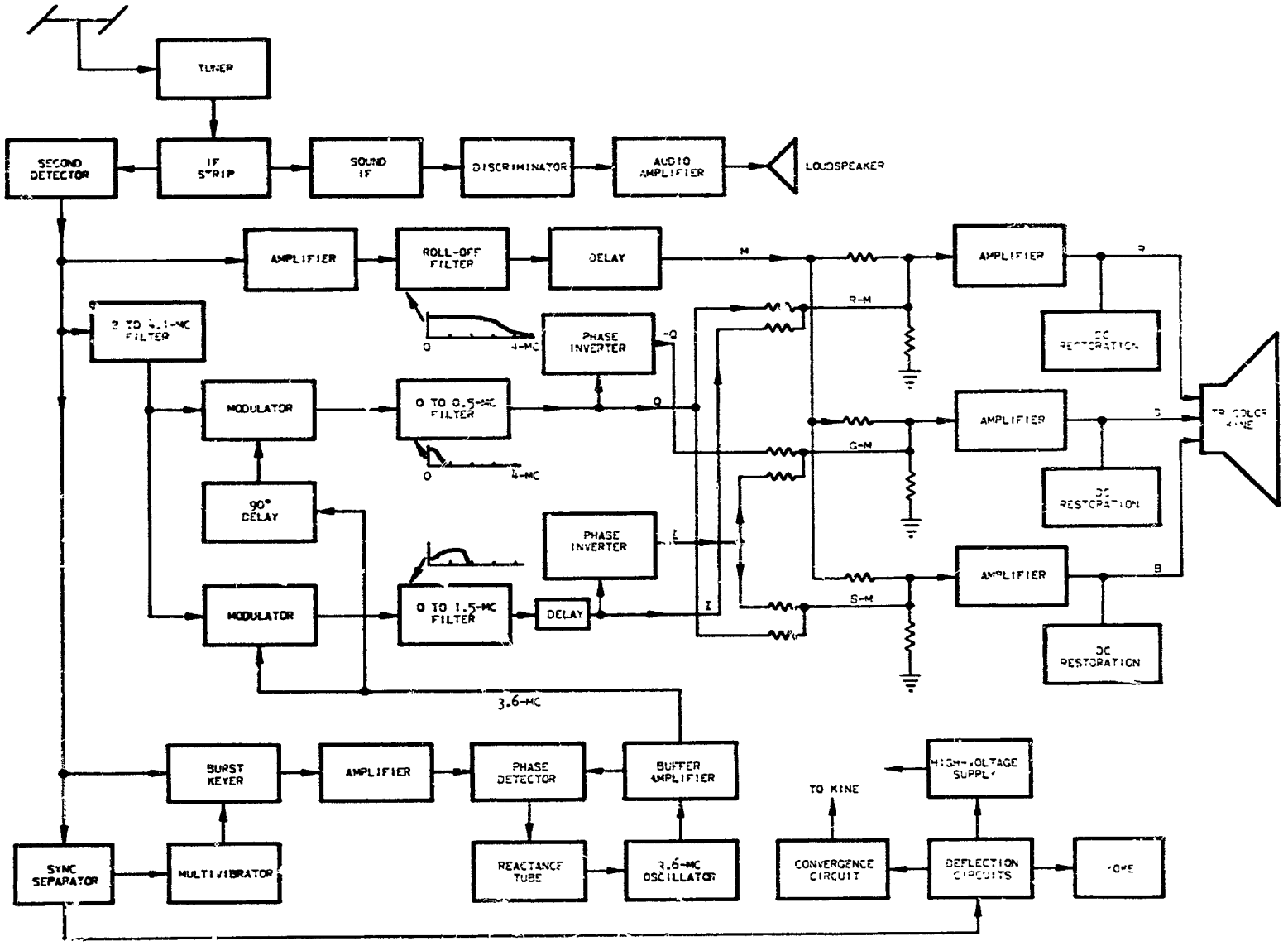

FIGURE D. 2-7

NTSC RECEIVING SYSTEM

subcarrier data on a line-by-line basis to average out phase errors (to which the basic NTSC system is susceptible) and thereby minimize degradation in chrominance fidelity under certain adverse signal-transmission conditions. The system currently is under evaluation in Europe.[a]

2.2.3 Sequential Systems

The sequential systems may be divided into field (or frame) sequential, line-sequential, and dot (or element) sequential types. These systems share the common functional characteristic of achieving separation of the R, G, B, color signals by time-separation (time-multiplexing) of the data. Figure D.2-8 depicts the very basic time-multiplexed system block diagram.

In the case of the field-sequential system, the color-sampling process is sufficiently slow to permit use of a rotating R, G, B filter wheel in front of a single TV sensor. At the receiving end, a similar filter wheel, synchronized with the filter at the transmitter, is used in front of a single TV display tube to provide sequential R, G, B image fields which the eye (under proper conditions) then combines into a full color image. The CBS field sequential system developed in the 1940's and early 1950's is representative of this method. The principal advantage of the system is its relative simplicity, resulting from the use of a single TV camera and a single TV display. Its principal disadvantages from the commercial broadcast standpoint are its noncompatibility with existing monochrome TV receivers, its susceptibility to "color fringing" resulting from excessive motion of the object during the color-sampling period, and its poor utilization of transmission bandwidth (thus, requiring a reduction in resolution to stay within the FCC-allocated monochrome bandwidth).

Only brief mention will be made here of the other two sequential methods, line and dot. The initial line-sequential system was developed by Color Television, Inc. in the late 1940's in competition with the CBS field sequential and RCA dot-sequential systems. The system proved functionally unsatisfactory because of line "jitter" and line "crawl" effects which seriously degraded image quality. Also, it offered no significant advantage from the standpoint of simplicity, since the line-switching speeds precluded the use of a rotating-filter wheel, single camera, and single display approach; instead, required camera and display methods are at least equal in complexity to the simultaneous color TV method. The dot sequential system was intensively developed by RCA (and others) during the same time period, and from this evolved the improved simultaneous (NTSC) method employed today in commercial practice.

2.2.4 Simultaneous/Sequential System

The most promising simultaneous/sequential or hybrid-type system is a recent French development known as SECAM (translated as "sequence and memory") and is shown in simplified form in Figure D.2-9. This approach combines the simultaneous R, G, B signal generation/transformation and luminance data-transmission

---

[a] Electronics, 22 March 1965, pp. 97-108.

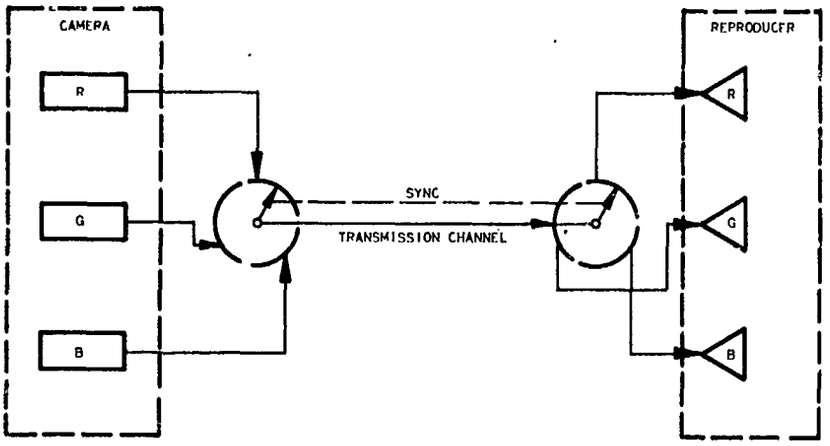

FIGURE D.2-8

TIME-MULTIPLEXED (SEQUENTIAL) SYSTEM

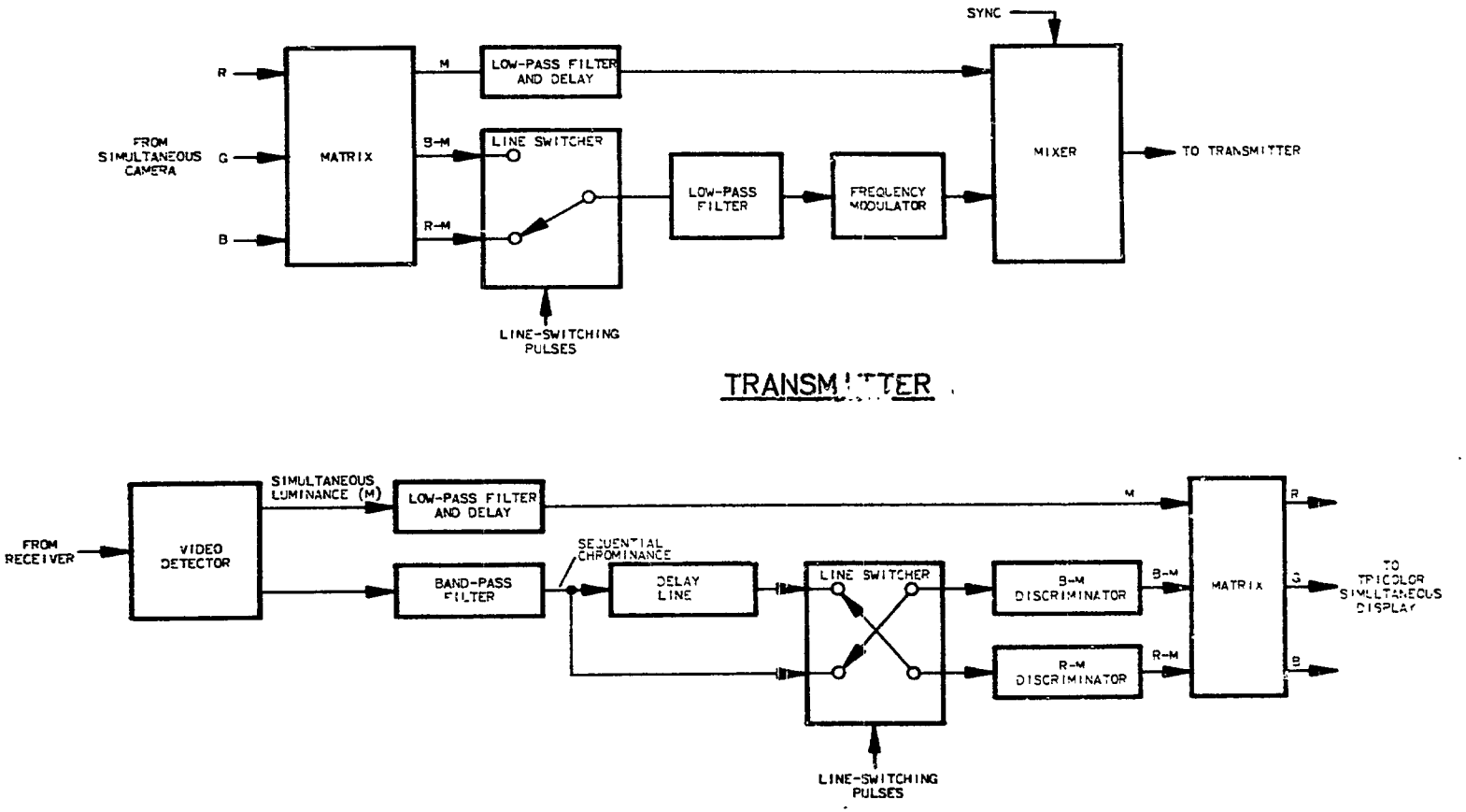

FIGURE D.2-9

STANDARD SECAM SYSTEM (SIMPLIFIED)

features of the NTSC system with a form of line-sequential chrominance signal transmission. The principal objective of this design is to achieve many of the desirable operational features of the NTSC system while eliminating the undesirable chrominance signal phase-sensitivity characteristic. SECAM endeavors to accomplish this by transmitting the essential chrominance data (color-difference signals R-M and B-M)[a] in a line-sequential manner. Since only one chrominance subcarrier signal is present at a given time, there is no necessity to employ the NTSC two-phase subcarrier modulation technique. Instead, the chrominance signal is caused to frequency-modulate a single subcarrier, thus providing good immunity against signal phase-shift effects due to the nature of the FM process.

Since SECAM actually transmits less chrominance information than the NTSC method, it might be expected that the chrominance fidelity of the reproduced image would suffer. However, previously referenced subjective tests have shown that the eye's chrominance acuity is appreciably below its luminance acuity. Where the NTSC system makes very effective use of this property along the direction of scan (by band-limiting the chrominance data), the SECAM system also takes advantage of the same property in the direction normal to the scan lines. This is accomplished by alternating on a line-to-line basis between the transmission of the R-M and B-M signals. A one-line delay device is used at the receiver, and--by synchronous line switching--a particular chrominance signal is read out and then repeated on the next line before being updated with new information. This effectively halves the chrominance resolution in this normal direction; however, based on SECAM field-test results, the subjective fidelity of the reproduced color image is essentially equivalent to NTSC image fidelity.

2.2.5 NTSC System Characteristics

Advantages

The NTSC system has two advantages:

1. The system has more than 10 years of operational experience behind it.

2. The NTSC simultaneous color signals can be handled in the TV studies in a manner similar to high quality monochrome TV practice (switching, fades, etc.).

Disadvantages

The disadvantages of the NTSC system are as follows:

---

[a] Since M is composed of R, G, B, the green signal component is also recoverable at the receiver.

1. Color distortion due to phase sensitivity of the quadrature-modulation process.

   a. "Static" phase shift--long-term shifts due to transmission-path anomalies.

   b. Differential phase shift--Generally caused by nonlinearities in transmission equipment.

   Color subcarrier phase error should be held to $\pm 5^{\circ}$. A 10° error can produce a noticeable hue shift.

2. Color errors due to single-sideband distortion. This causes colors to smear out from an edge in the direction of scan.

3. Operating complexity--Four interdependent operating controls are required, namely, brightness, contrast, hue, and saturation.

4. The phase sensitivity of the system causes magnetic tape recording to be very critical. A complex, costly recorder is required to achieve the required time base accuracy necessary for maintenance of subcarrier phase precision. The constancy of tape speed must be about an order of magnitude better for recording of NTSC color signals than is required for quality recording of monochrome TV signals. Color recording requires a speed that is constant within ±0.015%.[a]

   Both RCA and Ampex have suitable video recorders: however, they cost approximately $10,000 more than high quality monochrome TV recorders.

2.2.6 PAL System Characteristics

Advantages

Simple PAL. This system minimizes the effects of color subcarrier phase shifts by using the eye to integrate between color errors of opposite sign which are produced on successive scan lines. The PAL receiver in this simple version is similar to the NTSC receiver, except for the addition of the electronic switching circuitry to reverse the phase of the "I" demodulator on a line-by-line basis.

---

[a] Wireless World, Vol. 69, No. 9, September 1963, pp. 421-425.

This "eye averaging" process works well up to about 25^{o} phase errors, at which point the eye can perceive the difference in color between the two successive lines. This causes a condition known as the "venetian blind" effect, which can be minimized by readjusting the phase of the local subcarrier (this control corresponds to the hue control on the NTSC receiver).

Deluxe PAL. In this system, line-to-line phase errors are averaged electronically at the receiver. This is done by using aone-line delay device (similar to the SECAM delay unit) to permit the delayed and "live" signals in successive lines to be present simultaneously for purposes of averaging.

Here, the subjective effects which caused the eye to perceive the "venetian blind" effect are eliminated; thus, the color errors associated with subcarrier phase shifts are minimized without the need for readjustment of local subcarrier phase. Thus, there is no need for a phasing (hue) control in the deluxe PAL system.

Common Advantages. The advantages of PAL that are common to the simple and deluxe versions are:

1. Magnetic tape recording requirements relative to tape speed control are less stringent than NTSC, but are believed to be well in excess of monochrome requirements.

2. The PAL signal, which is simultaneous in nature, can be handled in the TV studies in a similar fashion to that employed with high quality monochrome TV.

Disadvantages

By averaging the chrominance signals associated with two successive lines, the outputs (E_I and E_Q) of the I and Q demodulators actually are $E_I \cos \epsilon$ and $E_Q \cos \epsilon$, where ϵ is the subcarrier phase error. Thus, for a 30^{o} phase error, the demodulator outputs are only 87% of the correct output. This represents an error in color-saturation values, since the subcarrier amplitude determines saturation levels. Therefore, a saturation control is required on PAL receivers to compensate for this effect.

The PAL approach doesn't eliminate the primary source of the phase sensitivity problem, namely quadrature modulation of the chrominance signals, but instead acts to minimize the chrominance errors which would otherwise result. Perhaps this cannot be considered a real disadvantage of the system; however, it

is believed that a more optimum approach would be one directed at removing the original source of the error rather than attempting to minimize its effect once it occurs.

The subcarrier frequency must be shifted slightly relative to the NTSC standard to minimize an otherwise objectionable dot-crawl effect occurring on monochrome receivers. This indicates that the 180° phase reversal of the I subcarrier has a detrimental effect on subcarrier signal cancellation on the TV display. The shifted subcarrier frequency (equal to an odd multiple of one-quarter the line-scan frequency plus 25 cps) is believed to represent a necessary but undesired compromise operating condition for the system.

2.2.7 SECAM System Characteristics

Advantages

As previously stated, this system is designed to eliminate the phase-sensitivity problems experienced with the NTSC method. This is accomplished by transmitting the chrominance information in a sequential manner on a line-to-line basis. Frequency modulation of a single subcarrier then is permissible, rather than quadrature modulation of two subcarriers. This results in improved fidelity of the chrominance data under transmission conditions which provide moderate-to-high receiver input signals. As a result of this operation, neither hue nor saturation controls are required on the SECAM receiver. This is indicative of its operational simplicity compared with the NTSC system.

The SECAM signal can be satisfactorily recorded on standard quality monochrome video tape recorders. The requirement on tape-speed constancy is in the range of ±0.4%.[a]

Disadvantages

Since the chrominance data are frequency-modulated, the chrominance subcarrier amplitude does not vary with changes in color saturation. Whereas the subcarrier level goes to zero for a white (neutral) image with the NTSC system, the full subcarrier amplitude would be transmitted in the SECAM system (producing an undesired dot pattern on monochrome receivers) if special provisions were not made to attenuate it. SECAM employs two methods of reducing the effects of subcarrier interference. First, the chrominance signal is transmitted at only 16% of the peak amplitude of the luminance signal. Second, the frequency-modulated chrominance signal is passed through a transmitter filter with an inverted bell-shaped characteristic, the greatest attenuation being located at the center frequency of the subcarrier (neutral color condition). This filter produces a corresponding reduction in the amplitude of the

[a] Wireless World, Vol. 69, No. 9, September 1963, pp. 421-425.

transmitted subcarrier signal. At the SECAM color receiver, a complementary filter is employed in the chrominance channel to boost the subcarrier amplitude back to the required level.

The above techniques, although effective in reducing the subcarrier interface level to an acceptable point for monochrome receiver operation, produce the undesired result of lowering the signal-to-noise ratio in the chrominance channel. In moderate-to-high signal strength conditions, acceptable color fidelity is achieved; however with fringe area reception, color fidelity can be seriously degraded--thus making this characteristic a major weakness in the system.

Since chrominance information is only updated on an every-other-line basis, color detail in the vertical direction is approximately one-half that obtained in the NTSC system. However, as indicated previously, SECAM proponents claim (and have demonstrated in a number of field tests) that the resolution of the composite SECAM image (luminance plus chrominance signals) is subjectively equivalent to NTSC image resolution.

For signal handling within TV studios, there are indications that best performance is achieved by operating with the basic R, G, B camera signals in parallel rather than with the composite color signal. This presumably is due to the sequential nature of the chrominance data, which could produce some transient error effects depending upon signal switching times.

2.3 COLOR TELEVISION SYSTEM FUNCTIONS AND TYPICAL OPERATING PARAMETERS FOR MSC MISSIONS

2.3.1 Discussion of System Functions

Based on a review of the literature sources available during this study, it is EMR's understanding that specific, detailed requirements for the use of color-TV in MSC missions have not been established to date. However, by considering those applications for which there is presently a requirement for monochrome video transmission, EMR has selected certain of these functions as the basis for defining probable future functional requirements of color-TV systems. The principal criterion used in this selection process was whether the addition of the color capability would significantly enhance the value and/or effectiveness of the function being performed. Two general, functional, color-TV categories evolved from this process; namely, (1) real-time dynamic monitoring and (2) non-real-time, static monitoring.

Category 1 encompasses the important biomedical monitoring functions in which facial and other body movements of the crewmen are remotely monitored by medical specialists. The color-TV system used for this purpose should have reasonable motion-rendition capability. Also, in order to maintain color-image fidelity, the system should not be subject to serious color "fringing" and color "breakup" effects in the presence of object motion.

The category 2 function encompasses the transmission to earth of static pictorial data in which the accurate rendering of color detail is of primary importance. Input pictorial material may include color photographs, color sketches, and live subjects in a nondynamic condition.

2.3.2 Typical System Operating Parameters

Category 1 functions can be performed with a medium-resolution system operating at moderate frame rates. Typical parameters would be:

Resolution--300 TV lines

Frame rate--10 to 15 per second

Category 2 functional requirements can be satisfied by employing single-frame[a] recordings of higher resolution. Typical parameters would be:

Resolution--500 lines

Frame period--As dictated by transmission-bandwidth considerations

2.4 GROUND RULES FOR THE APPLICATION OF COLOR TELEVISION TO MSC MISSIONS

1. The color system shall be capable of reproducing a wide color gamut (generally equivalent to NTSC).

2. There is no requirement for compatibility with monochrome broadcast TV transmission standards.

3. The system shall exhibit a high degree of operational stability (maintenance of color fidelity) under expected signal-transmission conditions.

4. The system shall employ nonexotic TV sensors of the general type in use with or under development for monochrome space TV applications.

5. The system shall produce color-TV signals suitable for magnetic-tape recording in the spacecraft (for delayed readout) and for similar recording at the ground stations.

---

[a] As used herein, a frame refers to a complete color frame.

6. Performance must be evaluated relative to system complexity, reliability, weight, size and power requirements.

7. Any proposed digital color-TV system must offer a significant potential advantage over possible analog methods.

2.5 SELECTION OF PROMISING COLOR-TV APPROACHES FOR MSC APPLICATIONS

2.5.1 Real-Time Monitoring Function

Most-Promising Analog Systems

The real-time monitoring function associated with the previously defined Category 1 system could be achieved with any of the three basic analog color methods. However, since the functional requirements are not unlike those for commercial color reproduction, there should be some benefit from the results of that development work in selecting the best method. With the requirement for minimum color "fringing" and color "breakup" and in the interest of efficient utilization of transmission bandwidth, the NTSC and PAL simultaneous systems and the SECAM hybrid system have been shown to have definite advantages over the field-sequential method (for a given frame rate and given image resolution). Also, based on the known phase-sensitivity of the NTSC chrominance signal, the SECAM method might prove generally superior to the NTSC method for transmission conditions which may exist in the MSC mission. However, note that the basic SECAM technique also suffers from certain previously discussed problems. Also, the PAL approach would warrant consideration.

Most-Promising Digital System

By employing digital techniques in conjunction with essential analog color-TV processes, a color system concept evolves which overcomes the major operational limitations of the basic analog system. Of the several feasible system combinations, the digital version of the SECAM method looks most promising. Figure D.2-10 is a block diagram of the proposed approach. The system is essentially analog SECAM up to the output of the luminance and chrominance low-pass filters. At this point, the wide-band luminance signal is digitally encoded (probably with 3/4 Roberts) at an appropriate rate and the narrow-band chrominance data are similarly encoded at a correspondingly lower rate. These signals are then combined by time-multiplexing them prior to transmission. At the receiver output, the demodulated composite color signal is fed to a demultiplexer, which provides separate luminance and line-sequential chrominance outputs. These digital signals then feed individual (Roberts) decoders whose analog outputs are coupled through

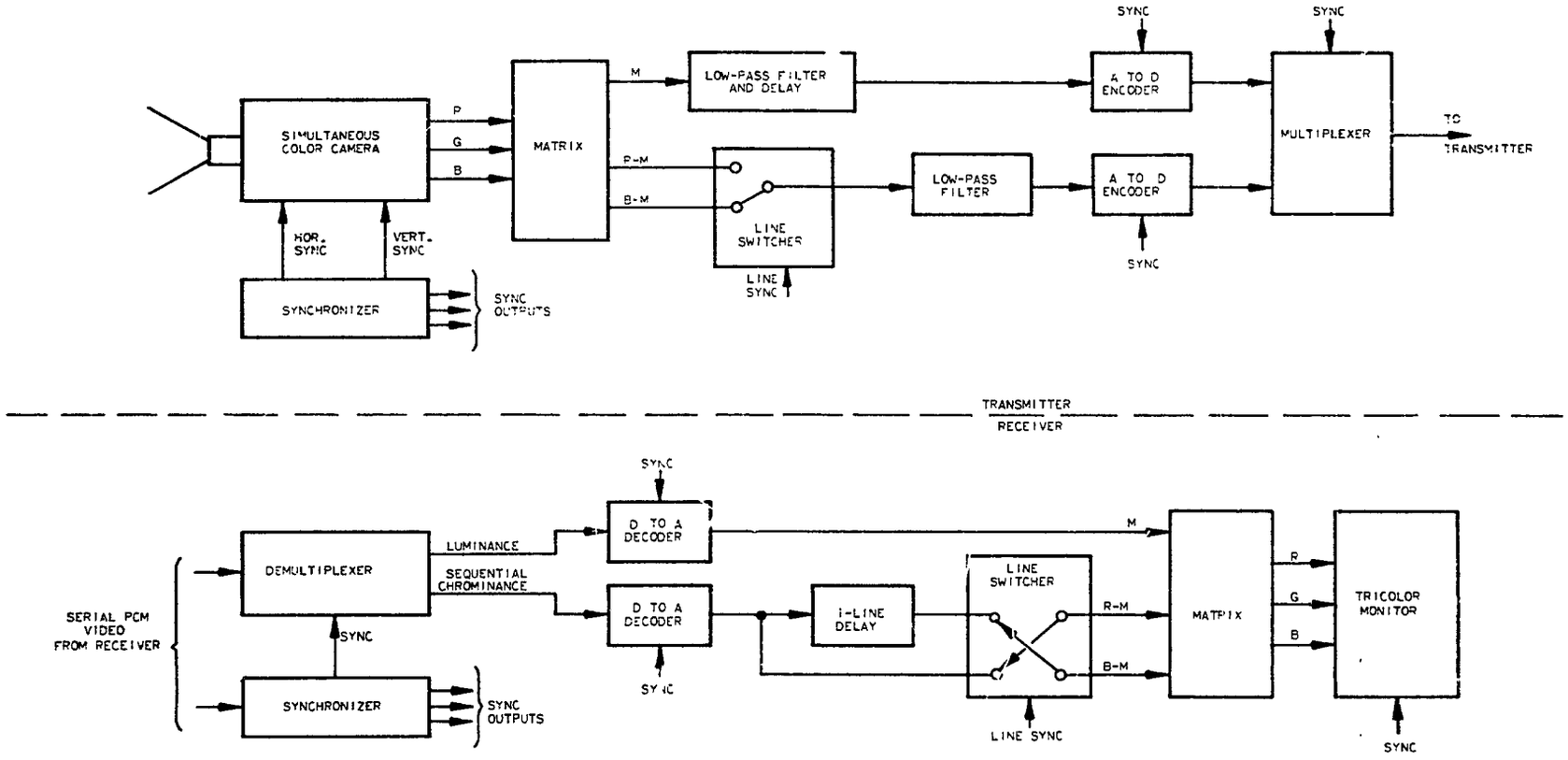

FIGURE D.2-10

DIGITAL SECAM COLOR SYSTEM

SECAM-type switching and matrixing elements to the tricolor display.

Comparison of Best Digital and Analog Approaches

Digital SECAM. The principal advantages of the digital SECAM system over the conventional SECAM and other analog color techniques are: (1) the chrominance data are transmitted with the same stability and accuracy as the luminance data, and (2) the composite transmitted-color-signal stability and accuracy are enhanced by virtue of the digital nature of the video data.

Bit-rate requirements are rather high, however. Assuming a nominal 2 Mc luminance bandwidth and a chrominance bandwidth of 0.5 Mc (for 15-frame-per-second TV with approximately 400-line resolution), the required bit rate for three-bit Roberts coding of luminance and chrominance signals is:

Luminance--2 Mc x 2 samples per cycle x 3 bits per sample	=12 megabits per second
Chrominance--0.5 Mc x 2 samples per cycle x 3 bits per sample	= 3 megabits per second
Total	15 megabits per second

Modified Analog SECAM. If the "compatibility with monochrome TV standards" is not a requirement (and the ground rules have indicated that it is not for expected MSC missions), the door is wide open for a very significant improvement in SECAM system operation.

The principal modification to the system would involve relocation of the center frequency of the FM subcarrier. The major known weakness of the present SECAM system (namely, unsatisfactory color fidelity on marginal receiver input signal levels) can be eliminated by raising the subcarrier frequency to a location above the high end of the luminance channel. This improvement results from transmitting the frequency-modulated chrominance information at full amplitude. Since there is no monochrome TV compatibility requirement, no subcarrier attenuation is necessary. There is a requirement to keep the chrominance signal from interfering with the luminance signal. This can be achieved by spacing the subcarrier center frequency a sufficient distance above the luminance signal spectrum to accommodate the maximum frequency deviation of the subcarrier without objectionable interaction with the luminance-signal components. Use of a low-pass filter that rolls off at the top of the luminance band in the color receiver luminance channel will assure that this interaction is held to an acceptably low level.

Figure D.2-11 shows that the center frequency of the subcarrier might be raised

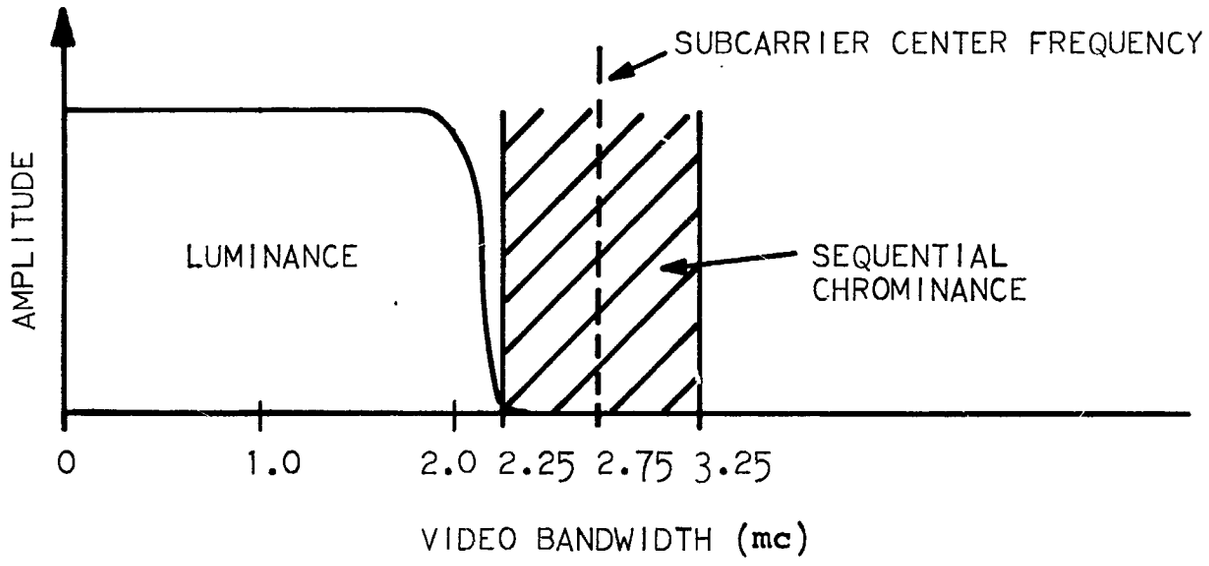

FIGURE D. 2-11

MODIFIED ANALOG SECAM

to 2.75 Mc with the bandwidth parameters assumed for the digital SECAM system, permitting a frequency deviation of ±0.5 Mc to convey the chrominance information. Thus, the total video-bandwidth requirements would be increased approximately 60% to 3.25 Mc in order to contain the 2.0-Mc luminance signal plus the 0.5-Mc FM chrominance subcarrier signal.

As previously stated, the above modifications would be expected to eliminate the major known weakness of the SECAM system. In addition, any requirement for additional vertical resolution could be achieved by using additional scan lines per TV frame (at the expense of increased bandwidth and/or reduced frame rate).

Modified PAL System. The subcarrier frequency used in PAL could be raised above the luminance pass band to minimize crosstalk between luminance and chrominance signals. However, the PAL approach still operates within the constraints imposed by the basic chrominance subcarrier quadrature modulation process. Also, magnetic-tape-recording requirements would not be lessened by this modification, and color desaturation effects would be encountered in the line-to-line chrominance error averaging process.

It is concluded therefore that the modified PAL system offers fewer advantages than does the modified analog SECAM system for MSC applications.

Selection of the Most Promising Real-Time-Monitoring, Color-TV System

It is concluded that both the digital version and the modified analog version of SECAM can satisfy the expected MSC real-time mission requirements. Each of these techniques is believed to be superior to other color-TV coding methods considered in this study.

Although the digital SECAM system offers certain operational advantages in the area of signal stability and accuracy, it is believed that the performance of the modified analog SECAM system will be satisfactory for the great majority of near-future MSC real-time color TV monitoring applications involving earth-orbital and lunar reconnaissance missions. Since implementation of the analog system is simpler than the digital version, the modified analog SECAM system is considered to be the best overall choice for this function.

2.5.2 Non-Real-Time Monitoring Function

Basic System Selection

The modified analog SECAM approach could be employed for this function as well as for real-time monitoring. However, the field-sequential [a] approach is

[a] Also known as frame-sequential where noninterlaced scanning is employed.

considered to be the best choice for very low-frame-rate or single-frame transmission because it offers several outstanding advantages. Since it employs only a single camera plus a filter disc assembly (as contrasted with the three or four cameras used in the simultaneous SECAM system), it is significantly simpler and cheaper, requires less input power, and is smaller and lighter in weight.

Comparison of Digital and Analog Approaches

The choice of the optimum approach (from the above standpoint) is between the pure analog field-sequential system and the digital version of this same system. Figure D. 2-12 depicts this digital system, the relative simplicity of which is evident from the block diagram.

As to the choice between the analog and the digital versions, one particular operational feature of the digital system is believed to be of sufficient importance in sequential color-TV transmission to warrant its selection as the best system choice. This feature relates to the high degree of time-base stability and precision obtainable in a digital-TV system. For accurate registration of the three time-sequential, primary-color-image fields which constitute the complete color frame, time-base stability and precision is essential. The digital frame-sequential system can provide the required data accuracy on an element-by-element, line-by-line, and field-by-field basis. The feasibility of achieving comparable time-sequential data accuracy with a pure analog system is in considerable doubt, particularly where magnetic recording of the data is employed for delayed readout purposes.

Selection of Most Promising Non-Real-Time Monitoring System

It is concluded that the digital frame-sequential color system, can best satisfy this application. It is a relatively simple system and yet offers good performance capability in terms of precision and stability of color data transmission.

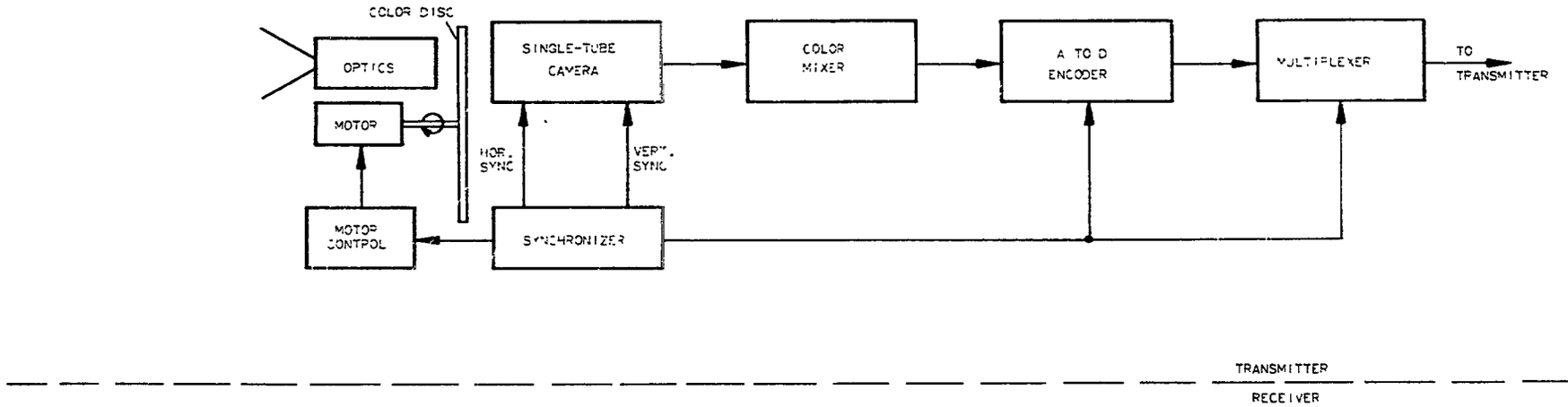

FIGURE D. 2-12

DIGITAL FRAME-SEQUENTIAL COLOR SYSTEM

SECTION 3

DIGITAL COLOR-TV EXPERIMENTAL EFFORT

3.1 INTRODUCTION

The experimental color-TV work performed during this study can be divided into five phases:

1. Modification of the EDITS system for color reproduction
2. Preliminary full-color frame-sequential recording
3. Gamma measurement and adjustment
4. Final color reproduction and fidelity assessment
5. Measurement of primary color signal statistics and compression potential

3.2 MODIFICATION OF THE EDITS SYSTEM FOR COLOR REPRODUCTION

3.2.1 Investigation of the Properties of Polacolor Film

It was decided at the outset of this study to use Polacolor film as the medium for recording displayed color images. With a print-development time of approximately 60 seconds, this was seen to be by far the best method available for rapid assessment of TV image quality as equipment operating parameters were varied. Initially, however, EMR was doubtful that acceptable results could be achieved by sequentially recording three separate primary color images on a single piece of color film. Therefore, the minimum initial objective of the experimental phase was to obtain single primary-color reproductions of TV display images by using matched sets of color filters in front of the TV camera and the film camera. Through examination of the separate primary color images produced by various digital coding methods, it was hoped that a subjective assessment could be made of the relative fidelities of the resulting TV images.

Based on initial single-color exposures of the Polacolor film, it became clear early in the program that this method of image assessment was not desirable. The major problem results from the basic nature of the subtractive color processes used in photography (a general color-film characteristic, not limited to Polacolor). The maximum transmission densities of three typical photographic dyes are shown in Figure D.3-1. Rather than having ideal, independent spectral "passbands," where exposure to blue light (for example) would decrease the density of the yellow dye and thus correspondingly increase blue light transmission, there is a

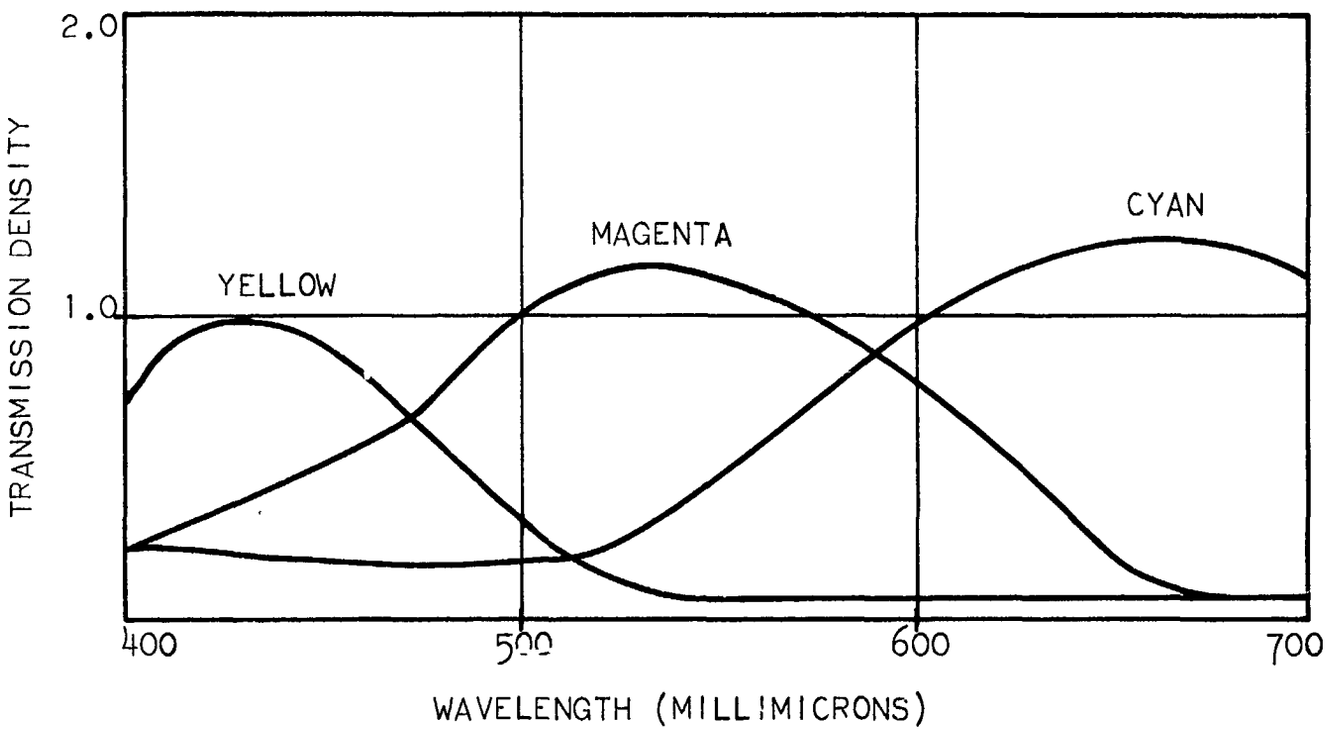

FIGURE D. 3-1

TRANSMISSION DENSITY CURVES
FOR A TYPICAL SET OF PHOTOGRAPHIC DYES

substantial amount of "crosstalk" or overlap between the dye characteristics. Therefore, when the developed photographic print is exposed only to blue light, the absorption characteristics of the magenta and cyan dyes affect the blue image. They distort the photometric values of this image, making it very difficult to obtain any meaningful results from such an assessment. Similar effects exist to varying degrees with exposure to other colored light. It was therefore determined that this was not a desirable image-assessment method, and emphasis was then shifted to the investigation of the sequential exposure of Polacolor film to three primary colors to produce full-color reproductions.

3.2.2 Sequential R, G, B Exposure Experiments

Kodak filters of the Wratten Type No. 29 (Red), No. 61 (Green) and No. 47B (Blue)[a] were employed as the color-separation filters in these tests. Through a series of outdoor measurements conducted on a trial-and-error basis, it was determined that Polacolor film could be sequentially exposed to red-, green-, and blue-filtered light from the selected object to produce (with the proper R, G, B exposure ratio) a well-balanced full-color print. The exposure ratios determined from these outdoor tests were:

$$\text{R to G to B} = 1 \text{ to } 5 \text{ to } 7$$

3.2.3 TV-Display Color-Balance Tests

The feasibility of sequential R, G, B exposure of Polacolor having been determined from outdoor tests, color photographs were made with the EDITS TV raster (P-4 phosphor) as the self-luminous test object. The initial objective of these measurements was to determine the proper relative R, G, B exposures to cause the normally bluish raster to appear as a neutral (gray) source when recorded on Polacolor film. Figure D.3-2(A) shows the spectral characteristics of the color filters and the TV display. Due to the much lower speed of Polacolor compared with the black-and-white Polaroid film normally employed (ASA 75 compared with ASA 3000), the maximum film camera aperture size was used for recording red, green, and blue images; the display brightness remained fixed (at a point suitably below excessive phosphor saturation and beam defocussing). Exposures were varied by repeating the TV frame scan sequence a selected number of times for each primary color.[b] The exposure ratios resulting from these tests were:

$$\text{R to G to B} = \underbrace{63 \text{ to } 37 \text{ to } 21}_{\text{TV Frames}} = 5 \text{ to } 2.9 \text{ to } 1.7$$

[a] The chromaticity coordinates of these filters are shown in Fugure D.2-1 as points R', G' and B'.

[b] A multiple-frame counter unit was designed and incorporated into EDITS to facilitate selection of multiple-frame exposures.

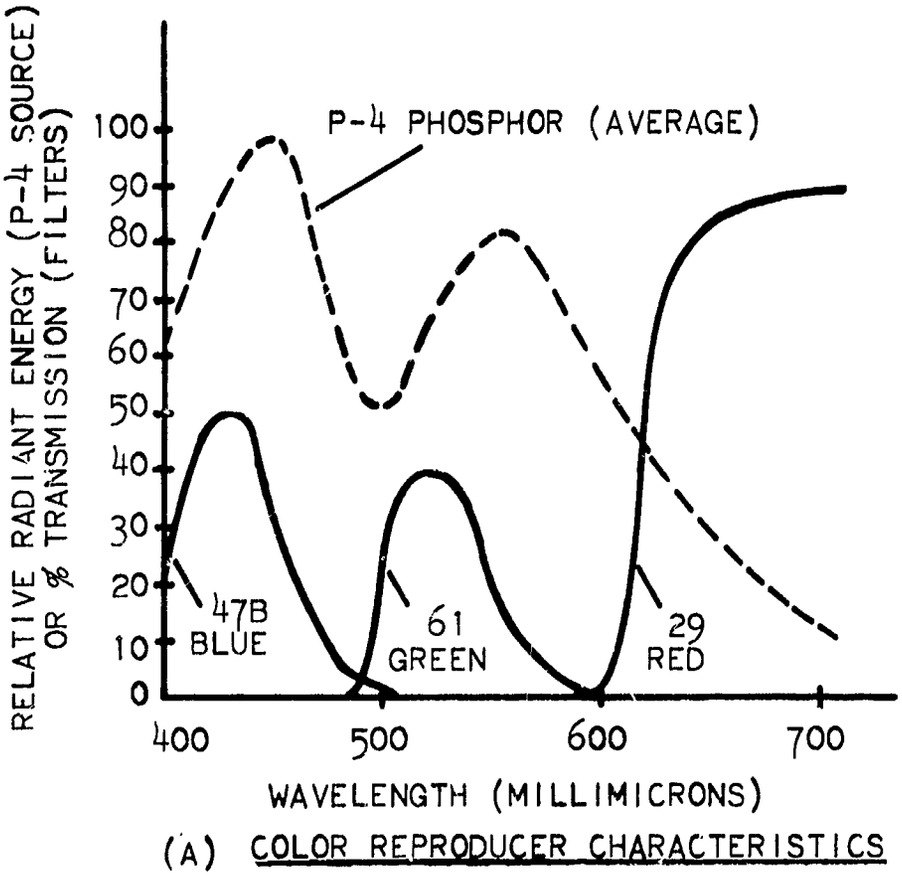

(A) COLOR REPRODUCER CHARACTERISTICS

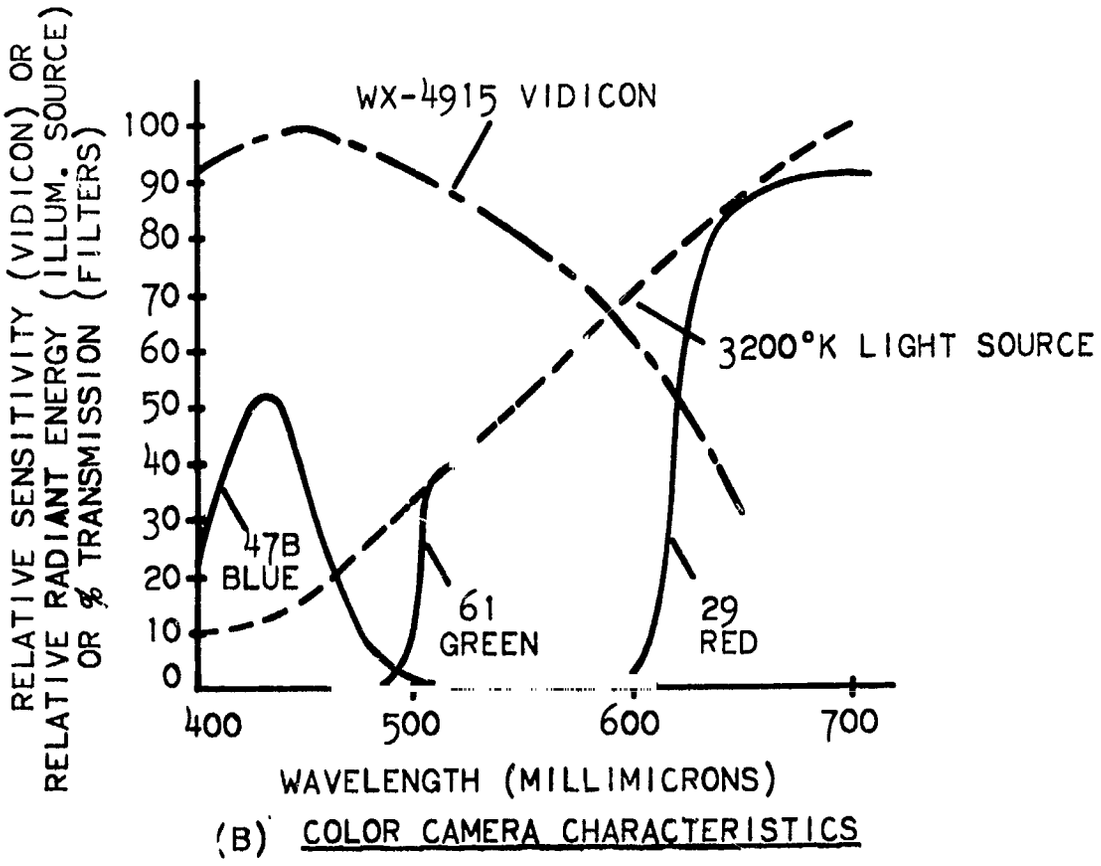

(B) COLOR CAMERA CHARACTERISTICS

FIGURE D. 3-2

SPECTRAL CHARACTERISTICS OF COLOR FILTERS, DISPLAY, VIDICON, AND ILLUMINATION SOURCES

Following the above "static" display color balance measurements, tests were performed to select the proper combination of display drive voltage (peak to peak) and dc bias voltage (brightness setting) to dynamically record over the full contrast range of the Polacolor film.

3.2.4 TV Camera Color Balance Tests

The choice of vidicon tube type for the color experiments actually was made prior to the start of this contract. Since the basic monochrome EDITS system is designed to use a slow-scan, all-electrostatic vidicon sensor, the choice was restricted to a tube of this general type possessing adequate spectral response throughout the visible spectrum (400 to 700 millimicrons) and having proper slow-scan characteristics. Through discussions with Westinghouse, it was determined that their type WX-4915 tube should prove suitable for this purpose. Accordingly, two vidicons of this type were purchased (on company funds) and were employed throughout the experimental color program.[a] Figure D.3-2(B) shows the spectral characteristics of the WX-4915 and the Kodak color filters, which are identical to those used at the display. Also shown is the spectral characteristic of the 3200° Kelvin incandescent lamp source used to illuminate the colored test objects.

Camera color balance measurements were made with the camera viewing a neutral (white) test object. Color balance was obtained by selecting the proper values of neutral-density filters for use in series with the two "higher gain" color channels (which are red and green, due to the relatively small amount of blue energy available from the 3200° Kelvin source) to produce camera signal output levels equal to the lower gain (blue) channel.

The approximate camera channel "sensitivities" were found to be:

R to G to B = 3 to 3 to 1

3.3 PRELIMINARY FULL-COLOR FRAME-SEQUENTIAL RECORDING

Following the above color balance tests, a series of preliminary full-color digital pictures were made in the frame-sequential manner by means of the color-adapted EDITS system. PCM, Roberts, and Delta coding methods were employed in this series.

Assessment of the reproductions pointed out several problem areas in the system. Prominent among these were (1) an appreciable increase in image contrast, compared with the original test object, combined with a restricted photographic contrast range, (2) noticeable hue errors in reproduced colors of low saturation

[a] One WX-4915 failed during the course of the study; however, the second tube performed satisfactorily for the remainder of the program.

(pastels), and (3) a mechanical problem of accurate registration of the three primary images sequentially recorded on Polacolor film. In the interest of simplicity, the changing of film camera filters was done by physically detaching the film-chamber section of the Polaroid camera from the lens iris and shutter section and then placing the appropriate filter (3- by 3-inch size) between the film plane and the lens assembly. This is not a problem in an operational-type field or frame-sequential color system, since color-filter switching can be achieved with a rotating, segmented filter wheel. In the present case, the problem was minimized by repositioning the film chamber section with extreme care after each filter change.

Problems (1) and (2) were known to be the result of either the operating characteristics of EDITS, of the Polacolor recording characteristic associated with the sequential, multiple-frame-exposure method employed; or both sources. The following paragraph summarizes the tests performed in resolving these problems.

3.4 GAMMA MEASUREMENT AND ADJUSTMENT

3.4.1 General

Both the observed high image contrast and hue errors were indicative of gamma distortion in the system. This was confirmed when measurements indicated a midrange system gamma in excess of 3.0 and severe compression in the low-light region.

In order to locate the principal sources of these distortions, a series of tests were conducted as described below.

3.4.2 Polacolor Outdoor Tests

Color photos were made of a standard gray scale using: (1) single, unfiltered (normal) exposures; (2) single, sequential R, G, B exposures; and (3) multiple, sequential R, B, G exposures. A densitometer then was used to measure the reflection densities of the gray scale steps on the reproduced Polacolor prints, and these step density values were plotted against corresponding step densities of the standard gray scale chart. From this plot, it was determined that Polacolor in the normal exposure mode and in the single, sequential R, G, B exposure mode has approximately a unity gamma characteristic over the major portion of its dynamic range. However, midrange gamma was found to increase to 1.2 when 10 repetitive exposures of each primary color were used. Also, there was an increased tendancy toward white saturation under this condition. It was therefore concluded that multiple-frame exposure of Polacolor was partially responsible for the high system gamma, but the major effect appeared to be related to EDITS operating characteristics.

3.4.3 EDITS-Equipment Transfer-Characteristic Measurements

First, photometric measurements were made on the TV display to determine its transfer characteristic. These tests showed that at relatively low drive levels (three volts into the display) an approximate square-law characteristic prevailed. At higher drive levels (eight-volts input), the transfer characteristic more nearly approximated a linear function because of display saturation effects.

Next, the vidicon camera transfer function was measured using several illumination levels. It was found that the vidicon exhibited a low-light level "cutoff" effect when operating under reduced illumination conditions. This condition was essentially eliminated by raising the illumination to a value just below the level which caused camera highlight saturation.

With these variables known, a series of system gamma measurements were made with the equipment operating over the range of conditions previously considered. Figure D.3-3 summarizes the test results obtained. Curve No. 1, resulting from the use of low camera illumination and low display drive, essentially duplicates the operating conditions under which the initial EDITS color photos were made. Curve No. 2 shows a significant reduction in low-light-level saturation resulting from the use of optimum TV camera illumination. Curve No. 3 represents the most linear transfer characteristic obtained in the tests. It was achieved by combining a high display drive condition with an optimum camera-illumination condition. It was subsequently found that this display drive condition caused excessive display beam defocussing. Curve No. 4 then represents the final compromise condition arrived at for Polacolor recording. This was achieved with multiframe, sequential R, G, B exposure, using optimum camera illumination and a medium level of display drive input (approximately five volts). The residual effects of highlight saturation limited the maximum contrast range (approximately 15 to 1), and the moderately high midrange gamma (approximately 2.0) is the result of the nonoptimum characteristics of the Polacolor film and the EDITS electronics as employed in the TV color-recording mode. Finally, Curve No. 5 represents the similar compromise operating conditions employed for EDITS monochrome recording using Polaroid type 3000 film.

3.5 FINAL COLOR REPRODUCTIONS AND FIDELITY ASSESSMENT

3.5.1 Test Objects

Two full-color magazine covers [a] were selected as test objects for the final color reproduction series. These photographs include a reasonably wide range of pictorial characteristics in terms of the image detail and the chrominance values represented.

---

[a] Apollo Mockup, Aviation Week, May 7, 1962.
Mercury Periscope, Product Engineering, August 1, 1960.

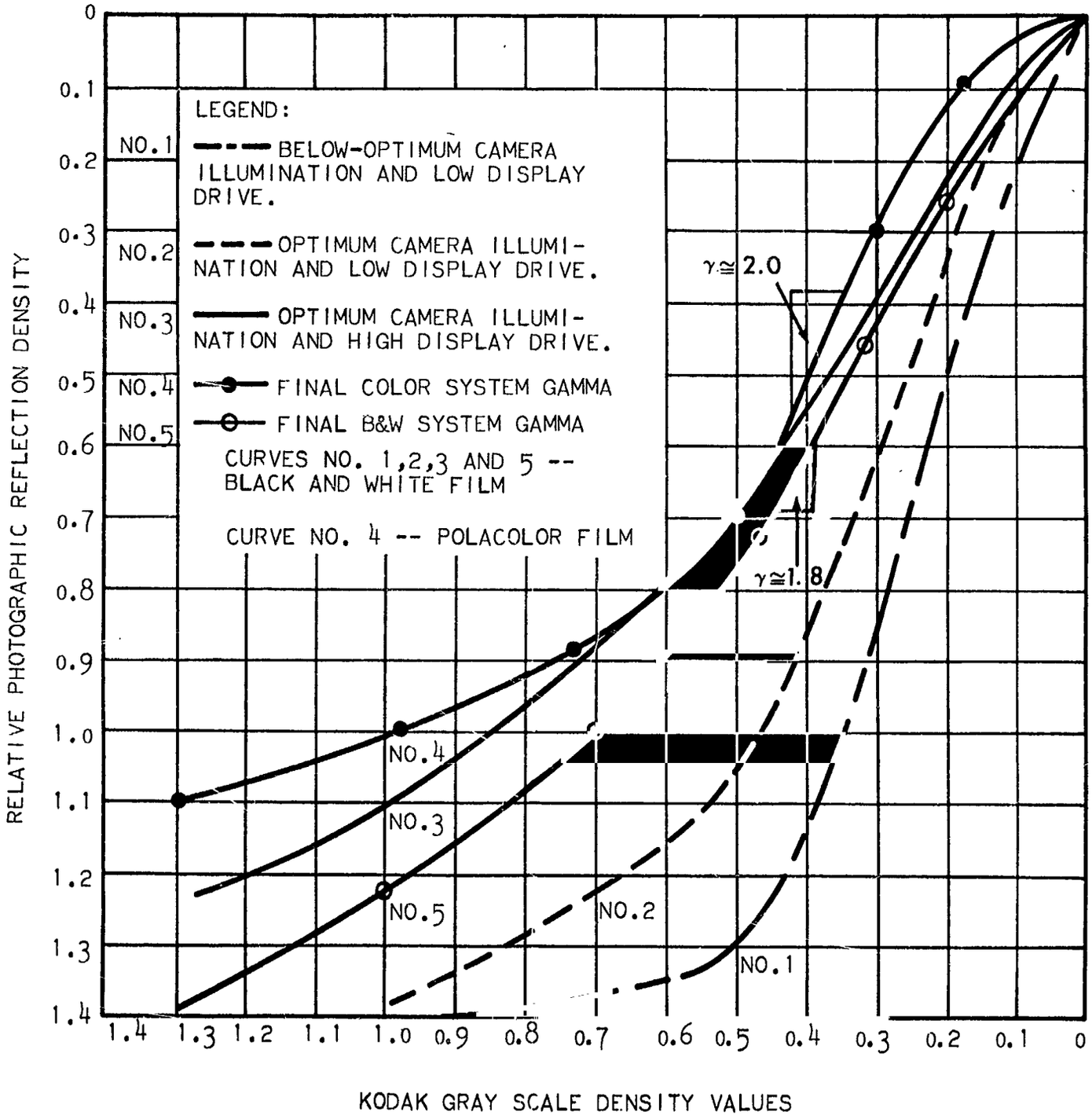

FIGURE D.3-3

GAMMA CHARACTERISTICS OF EDITS SYSTEM RECORDED ON BLACK AND WHITE FILM AND POLACOLOR FILM

3.5.2 Assessment of Series No. 1--Apollo Mock-Up

Coding Conditions

Polacolor reproductions of the sequential-frame digital color TV images produced on EDITS are shown in Figure D.3P-1.[a] Four digital coding conditions are represented, namely, six-bit PCM, three-bit PCM, 3/4 Roberts coding[b] and two-bit delta modulation.

Fidelity Assessment

Six-Bit PCM. Although the primary objective of this photographic series is to obtain a relative assessment of image fidelities of the several digital coding conditions, it is interesting to compare the six-bit PCM image fidelity with the original test object.

The most noticeable difference observed is image resolution. The optical scale factor employed here (in order to include all object dimensions of interest) results in 240 active scan elements (and lines) covering a 7- by 7-inch test object area. Thus, relative to the test-object dimensions, there are approximately 34 scan elements (or lines) per inch. Since this resolution is appreciably below normal newspaper resolution, the resolution degradation is to be expected.

Relative to overall fidelity, the reproduced chrominance values in the central area of the six-bit photo are surprisingly close to the original, considering the fact that the system has a gamma of approximately 2.0. However, the limited dynamic recording range does introduce certain luminance and color saturation errors. Also, edge and corner shading effects in the camera and the display degrade image fidelity in these areas.

Random noise from the vidicon preamplifier is not seen in the six-bit or other EDITS color photos due to the noise-averaging effects produced in the multiframe exposure method employed.

Three-Bit PCM. Errors are noticeable both in chrominance values and luminance values as a result of the coarseness of signal quantization. However, note that the three-bit sequential-frame color system exhibits considerably less "contouring" than does a three-bit monochrome TV system. The explanation for this is that the full-color TV image is actually the composite of three individual three-

---

[a] Figure numbers containing P refer to photographs in Volume II of this report.

[b] The 3/4 Roberts signal is made up of a small-amplitude, 16-level, pseudo-random noise signal which is added to the analog video signal (and subsequently subtracted from the video at the receiver) prior to encoding as a three-bit PCM signal.

bit primary color images. Since the eight possible levels of each color signal are combined in various proportions with the other signals to reproduce all possible hues and saturations, appreciably more than eight levels will be displayed and recorded. Thus, contouring effects are minimized on normal, colored scenes. However, in the case of a neutral-colored image reproduction, which is made up of equal proportions of R, G, B signals, luminance gradations in the neutral scene would exhibit contouring effects equivalent to those produced by a digital monochrome TV system.

The 3/4 Roberts Coding. The Roberts method essentially eliminates all visual evidence of three-bit contouring effects at the expense of a slight increase in fine-grain noise. Except for this noise effect, the overall picture fidelity is judged to be essentially equivalent to six-bit PCM.

Two-Bit Delta Modulation. Two principal deficiencies are noted in the delta photograph. First, the image is noticeably "softer," resulting from the limited step function response of the system. Second, pronounced chrominance errors are observed along the direction of scan (bottom to top in this photograph) on dark-to-light transitions of high contrast. This again appears to result from limited step-function response, but the additional effect of a variable delta response to the three primary-color signal transitions (generally of different amplitudes) produces the hue errors which show up as smearing following such transitions.

3.5.3 Assessment of Series No. 2(a)--Mercury Periscope

Coding Conditions

Figure D.3P-2 shows the group of photographs reproduced by the same digital coding techniques used with the Series No. 1 Apollo pictures.

Fidelity Assessment

Six Bit PCM. The resolution on the test object in this series is equal to approximately 42 scan elements (or lines) per inch. Although this represents a 25% increase in linear resolution over the Apollo pictures, the reproduced image would be expected to appear rather "soft" compared with the original test object.

Other comments made with respect to the six-bit Apollo picture fidelity generally apply here also.

Three-Bit PCM. The fidelity assessment made on the three-bit PCM Apollo reproduction also applies here.

The 3/4 Roberts Coding. The fidelity assessment made on the 3/4 Roberts Apollo reproduction also applies here.

Two-Bit Delta Modulation. The fidelity assessment made on the two-bit delta Apollo reproduction also applies here.

3.5.4 Assessment of Series No. 2(b)--Mercury Periscope

Coding Conditions and Equalization of Bit Densities

Two coding conditions are shown in Figure D.3P-3, namely, four-bit PCM and two-bit delta. Note that the two-bit delta picture is taken with increased magnification relative to the four-bit picture.

This magnification difference was produced to provide a direct comparison of PCM and delta image fidelities when an equal number of digital data bits are employed to encode equal-size areas of the test object. To make the two-bit delta "bit density" equivalent of that of the four-bit PCM, it was necessary to reduce the viewed area of the delta-coded area by 50%. This was accomplished by viewing and coding only 70% of the linear dimension of the test object coded with four-bit PCM.

Fidelity Assessment

With equal bit densities, the four-bit PCM photograph is noticeably sharper than the two-bit delta picture. This difference is not due to the difference in reproduced image sizes, but is the result of the limited step-function response of the delta system. In addition, the four-bit PCM picture does not exhibit the objectionable streaking effects following dark-to-light transitions which are seen on the delta reproduction (scanning is still from bottom to top in this series).

Comparing the 3/4 Roberts picture from Series 2(a) with the enlarged delta picture, it is concluded that 3/4 Roberts fidelity is subjectively superior to delta. In this case, the bit density of the Roberts picture is 25% lower than the bit density of the enlarged delta picture.

3.6 MEASUREMENT OF PRIMARY COLOR SIGNAL STATISTICS AND COMPRESSION POTENTIAL

3.6.1 Measurement Conditions

The EDITS statistics-taking capability was utilized to obtain previous-element (PE) statistics on frames of red, green, and blue video data derived from the two test objects used in the previous photographic series.

The statistics measurements were performed on video signals produced by four digital coding system variations; namely, six-bit PCM, four-bit PCM, three-bit PCM, and 3/4 Roberts. Data were taken at video signal-to-noise ratios of 40 db, 30 db, and 20 db.

3.6.2 Summary of Statistical Measurements

Tables D-1 and D-2 show the measured PE counts per frame and the computed PE ratios (PE measured count/Number of elements per frame) for the various conditions described above.

Examination of these data reveals that in the majority of cases, the PE statistics are approximately equal for all primary color signals at a given video S/N ratio and with a given coding condition. The only real departure from this occurs with six-bit and four-bit coding of the Mercury Periscope test object at S/N's of 40 db and 30 db. Here, the low levels of green and blue energy in the predominantly red background area cause the G and B video signals corresponding to this scanned area to fall at or near the zero level at the analog-to-digital encoder input. This results in increased PE readings on these particular frames.

In general, however, sensor noise is the principal factor controlling PE statistics for a given coding condition.

3.6.3 Compression Potential of Sequential-Frame, Color-TV Signals

The basic six-bit PCM sequential-frame color pictures require a total of 18 data bits to specify the brightness, hue, and saturation values of each picture element. If efficient, previous-element coding (PEC/Huffman type) is employed to effect data compression, the average gross compression, $\bar{C}_{PEC}$, relative to the six-bit reference picture is calculated from the formula:

$$\bar{C}_{PEC} = \frac{6}{1 + N(1 - PE)} , \qquad (1)$$

where N is the number of assigned bits per element with the selected coding method.

TABLE D-1

PRIMARY COLOR SIGNAL PE STATISTICS
USING APOLLO CAPSULE TEST OBJECT

Coding Condition	Video S/N (db)	PE (Frame)					
		Red		Green		Blue	
		PE Count	Ratio	PE Count	Ratic	PE Count	Ratio
Six-Bit PCM	40	14,600	0.265	15,000	0.27	15,700	0.28
	30	6,800	0.12	7,400	0.13	7,800	0.14
	20	2,700	0.049	3,000	0.054	3,200	0.058
Four-Bit PCM	40	34,300	0.62	35,200	0.64	36,100	0.65
	30	23,300	0.42	24,100	0.44	25,100	0.45
	20	10,300	0.19	10,700	0.19	11,200	0.20
Three-Bit PCM	40	41,400	0.75	41,900	0.76	42,500	0.77
	30	35,000	0.63	35,100	0.63	36,100	0.65
	20	18,600	0.34	19,200	0.35	19,800	0.36
Three-Quarter Roberts	40	34,900	0.63	35,000	0.63	35,800	0.65
	30	31,900	0.58	32,100	0.58	32,500	0.59
	20	19,200	0.35	19,600	0.35	19,900	0.36

TABLE D-2

PRIMARY COLOR SIGNAL PE STATISTICS
USING MERCURY PERISCOPE TEST OBJECT

Coding Condition	Video S/N (db)	PE (Frame)					
		Red		Green		Blue	
		PE Count	Ratio	PE Count	Ratio	PE Count	Ratio
Six-Bit PCM	40	14,400	0.27	24,200	0.44	28,300	0.51
	30	7,200	0.13	10,400	0.19	11,200	0.20
	20	3,200	0.058	3,600	0.065	3,700	0.067
Four-Bit PCM	40	35,700	0.65	42,900	0.78	45,000	0.82
	30	24,700	0.45	32,200	0.58	33,700	0.61
	20	11,300	0.20	13,000	0.24	13,700	0.25
Three-Bit PCM	40	43,900	0.79	47,800	0.86	49,300	0.89
	30	37,000	0.67	40,700	0.73	40,800	0.73
	20	20,000	0.36	22,900	0.41	23,300	0.42
Three-Quarter Roberts	40	37,500	0.68	38,900	0.70	41,200	0.74
	30	33,900	0.61	35,700	0.65	37,800	0.68
	20	20,500	0.37	22,200	0.40	22,800	0.41

By employing the PEQ (previous element qualifier) operation (see Appendix B, Section 4, paragraph 4.2) prior to the PEC function, the realizable compressions can be increased due to increased signal redundancy. The calculated percent increase in PE ratios using 3/4 Roberts coding are 4.5%, 25% and 70% for 40-db, 30-db, and 20-db video S/N ratios respectively.

Based on the average of 3/4 Roberts R, G, and B signal PE values for the two test objects, average compression, $\overline{C}_{PEC}$, was computed for the three S/N conditions, using Equation 1. In addition, similar calculations were made for the PEQ'd color signals. The results of these calculations are given in Table D-3.

TABLE D-3

AVERAGE 3/4 ROBERTS COLOR SIGNAL COMPRESSION USING PEC/HUFFMAN CODING

No.	Coding condition	Average Gross Compression $\overline{C}_{PEC}$*		
		S/N = 40 db	S/N = 30 db	S/N = 20 db
1.	3/4 Roberts + PEC/Huffman	3.1	2.7	2.1
2.	Same as No. 1 + PEQ	3.2	3.2	2.8

*Relative to six-bit PCM

This table shows that the average gross compression for 3/4 Roberts + PEC/-Huffman coding varies from 3.1 to 2.1 when the video S/N is varied from 40 to 20 db. When the PEQ operation is performed in addition to the above coding processes, the average gross compression figures remain more nearly constant with varying video S/N ratios (ranging from 3.2 to 2.8).

The number of bits per full-color picture element for a nominal compression of 3.0 equals:

$$\frac{18 \text{ bits (for 6-bit PCM)}}{3} = 6 \text{ bits per element}$$

3.6.4 Conclusions Relative to Compression of Sequential Color Signals

The basic 3/4 Roberts sequential-frame color system provides a compression of two to one relative to six-bit PCM (or nine bits per full-color picture element) independent of video S/N. Therefore, unless there is an urgent requirement to pack the maximum possible amount of data in a given transmission bandwidth, the use of PEC/Huffman compression coding of the signals probably is not warranted, due to the considerable resulting increase in equipment complexity.

SECTION 4

BIBLIOGRAPHY

1. Land, E. H., "Color Vision and the Natural Image, "Part I, Proc. National Acad. Sci. U.S., Vol. 45, pg. 115-129, January 1959; Part II, ibid, Vol. 45, pg. 636-44, April 1959.

2. Wilson, M. and Brocklebank, R. W., "Land Colour - A Discussion," Jour. British IRE, June 1961.

3. Fink, D. G. (Editor), Color Television Standards - NTSC, McGraw-Hill, N. Y., 1955.

4. Hunt, R. W. G., The Reproduction of Colour, Fountain Press-London, 1957.

5. Brown, G. H. and Lucky, D. G., "Principles and Development of Color Television Systems," RCA Review, Vol. XIV, June 1953, No. 2, pg. 144-204.

6. Cox, M. "Receiving SECAM," Wireless World, September 1965, pg. 432-436.

7. Fink, D. G. (Editor), Television Engineering Handbook, McGraw Hill, N. Y., 1957.

8. Proc. of the IRE, Vol. 42, No. 1, January 1954.

9. Carnt, P. S. and Townsend, G. B., Colour Television-NTSC System Principles and Practice, ILIFFE Books, Ltd., London 1961.

10. RCA Seminar on Color TV Transmission, Reprint from Broadcast News, Vols. 118-119, 1964.

11. Teacher, C. F., "Digital Color Television Techniques," 10th National Communications Symp., Utica, N.Y., October 5-7, 1964, pg. 472-481.

12. Wentworth, J. H., "RCA Color Television System," Broadcast News, No. 77, 1954.

13. Wentworth, J. H., Color Television Engineering, McGraw Hill, N. Y., 1955.

14. Rozier, J. and Lipkin, R., "Goals for an All-European TV System," Electronics, March 22, 1965.

APPENDIX E

DIGITAL TV EQUIPMENT AND SYSTEM CAPABILITY IMPROVEMENT STUDIES

APPENDIX E

TABLE OF CONTENTS

SECTION 1

OPERATIONAL ASPECTS OF MONOCHROME DIGITAL TV FOR MANNED SPACECRAFT APPLICATIONS

1.1 INTRODUCTION

A preliminary review has been made of literature dealing with anticipated near-future operational and equipment requirements for manned spacecraft applications, with particular emphasis on monochrome television applications. Relative to the NASA orbiting research laboratory (ORL) programs presently being defined, certain desired and/or required spacecraft television functions and operating characteristics are emerging.

Spacecraft television for initial ORL missions may be divided into two functional categories, namely:

1. Transmission-Type Television--The primary function of this equipment is to enable specialists at the ground station to monitor the crewmen in real-time for purposes of biomedical and behavioral assessments.

2. Closed-Circuit Television--This equipment will be employed for various spacecraft monitoring functions, such as viewing inaccessible areas and remote monitoring of operations which could create excessive hazards to the crewmen if direct observations were attempted.

1.2 TRANSMISSION-TYPE TELEVISION CHARACTERISTICS

Relative to the transmission-type TV equipment requirements, one significant characteristic is noted in addition to the normal requirements for reliable, space-qualified hardware of minimum size, weight, and power. This characteristic relates to the wide variation in minimum video data rates which may be acceptable for the various remote monitoring functions. It appears that the highest data rate requirements will be associated with real-time biomedical monitoring. Typical TV parameters are expected to be:

1. Frame rate--10 to 15/sec.

2. Resolution--500 TV lines

Certain other remote monitoring functions related to behavioral experiments (such as gross observation of crewmen performing specified operations) may require only one-third of the above horizontal and vertical resolution at the same

frame rates. A nine-to-one variation in required video basebands exists between these two conditions, and this very probably does not represent the extremes which are possible for this application.

In the interest of video transmission efficiency, it would be very desirable to employ a television system which incorporates the flexibility to operate effectively over wide parametric extremes. From the standpoint of spacecraft video-camera equipment design, digital TV hardware based on the EMR-EDITS operating principles is believed to be uniquely suited for this application. This type equipment incorporates a large degree of operational flexibility while maintaining basic data accuracy and operating stability.

In order to make most effective use of the variable-parameter digital video data, the TV transmission link also must incorporate operational flexibility. The ground-based video receiver should be designed to provide selectable bandwidths which are compatible with the transmitted video data rates. Thus, for fixed transmitter power, the video signal-to-noise ratio in the receiver will be improved as the data rate is lowered. Or, if a constant receiver signal-to-noise is desired over the entire range of data rates, the video transmitter power may be correspondingly reduced as the data rate is lowered. This mode of operation could effect a significant reduction in the total energy requirement of the spacecraft prime power source on ORL missions of long duration.

1.3 CLOSED-CIRCUIT TELEVISION CHARACTERISTICS

There is no compelling reason known to restrict the closed-circuit television data rates since transmission economy is not a factor. Pictorial quality (and data rates) approximating normal broadcast TV operation should prove generally satisfactory for presently envisioned monitoring functions.

In the interest of TV equipment interchangeability, it seems desirable to utilize similar TV camera equipment designs for both the transmission and closed-circuit functions. This will provide a good back-up for either system.

1.4 PRIMARY APPLICATIONS FOR MONOCHROME DIGITAL TELEVISION

Primary advantages of monochrome digital TV systems for MSC functions center around the following operational factors:

1. Ease of adjusting equipment for operation over a wide range of parameters. (Resolution, frame rate, quantizations)

2. Accuracy of the video data generation and processing functions.

3. Short-term and long-term operational stability of the D-TV equipment.

With this performance capability, a D-TV system can efficiently fulfill a variety of important image reproduction and transmission functions on MSC missions.

SECTION 2

DIGITAL TELEVISION SENSOR INVESTIGATION

At the outset of this study program EMR was of the opinion that a high resolution capability would be one of the principal requirements of a television sensor employed in future manned spacecraft applications. In addition, there were questions regarding the suitability of certain TV sensors, notably magnetic-deflection types, for digital TV operation because of possible limitations in response time in the deflection circuits.

Based on information obtained during this study program, neither of these considerations now appear to be a valid basis for selection or rejection of a particular sensor type. From the study of future NASA orbiting research laboratory operational and equipment requirements it is not apparent that TV sensor resolution requirements will be in excess of the capabilities of present vidicon and image-orthicon-type devices. Also, based on recent studies, no fundamental limitation to the application of magnetic deflection sensors to digital TV systems are foreseen. (See Section 3, paragraph 3.2.)

On this basis, it is concluded that digital television camera equipment designs impose no unique set of requirements on TV sensors. Therefore, sensor selection for digital TV will be based on the same operational and physical requirements and constraints that would apply to analog TV equipment.

Since there was no intent within the scope of this program to undertake a generalized study of sensor types suitable for future MSC television system applications, determination of the "non-uniqueness" of digital TV sensor requirements constituted completion of this study subtask.

SECTION 3

DIGITAL TELEVISION SENSOR SCANNING INVESTIGATION

3.1 IMPROVED DIGITAL SCAN OPERATION WITH ELECTROSTATIC VIDICONS

3.1.1 Problem

At the outset of this study program, EMR experienced difficulty in arriving at an optimum set of operating conditions when using the Westinghouse Electrostatic Vidicon [type WX-4384 (WL8079) slow-scan type]. EMR had not been successful in simultaneously achieving satisfactory levels of performance in several important areas listed below:

1. Satisfactory center resolution (400-500 TV lines nominal)
2. Satisfactory corner resolution (300 TV lines nominal)
3. Approximate equal corner resolutions
4. Satisfactory shading characteristic

3.1.2 Solution

It has now been determined that the major problem was not directly associated with the digital scanning operation but was associated with the basic vidicon tube operation itself. Two major changes were instituted in the course of the investigations leading to the solution of the problem:

1. The WX-4384 vidicon was replaced with a WX-4915 type in order to obtain the panchromatic response characteristic required for the color TV reproduction work.
2. A thorough adjustment procedure was carried out in which all reasonable combinations of vidicon control-element voltages were evaluated in terms of the above desired performance factors. Figure E.3-1 is a pictorial view of the electrostatic vidicon. The most critical elements in terms of the above factors are--
    a. G-3 focus

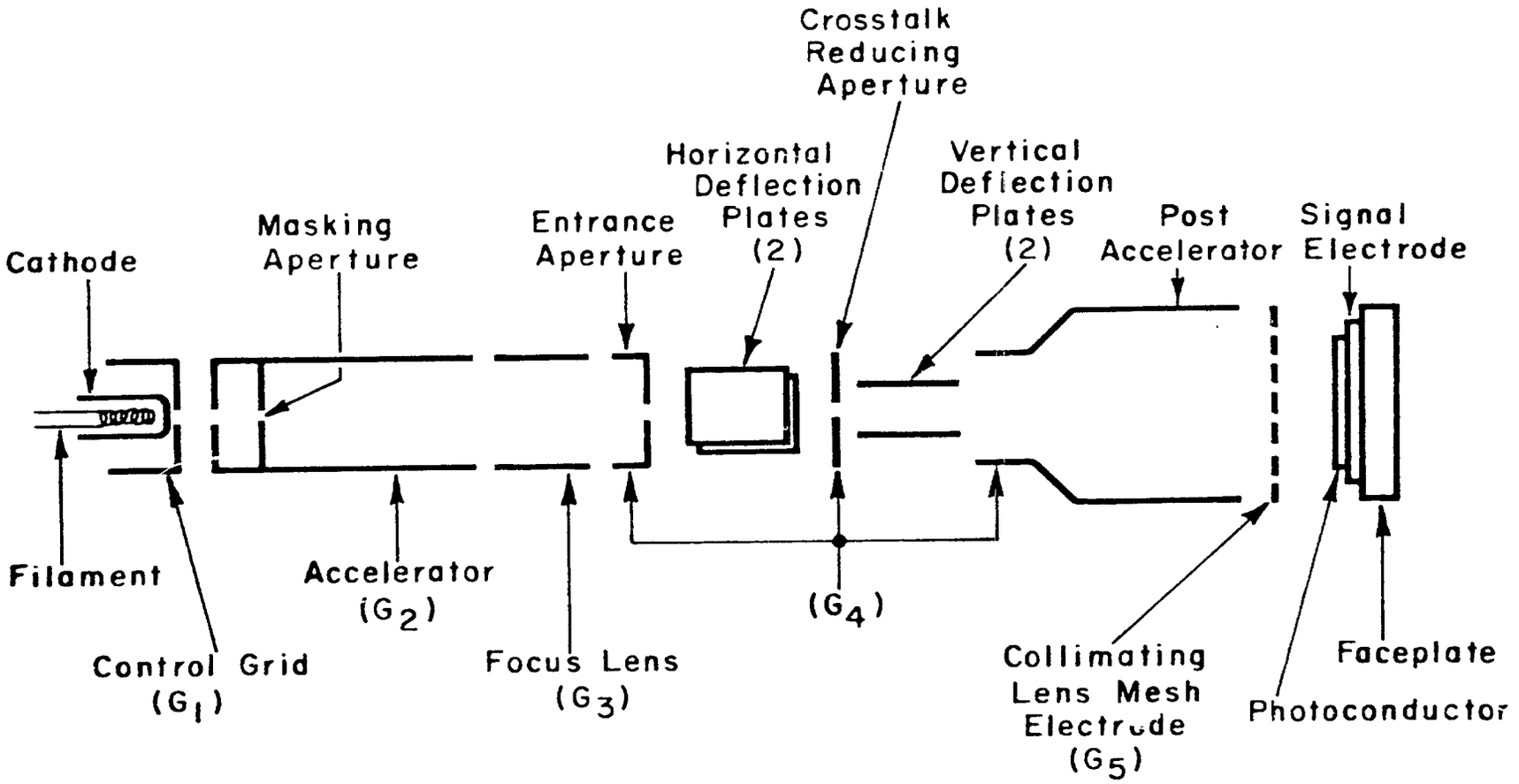

FIGURE E.3-1

PICTORIAL VIEW OF WESTINGHOUSE ELECTROSTATIC VIDICON

b. Horizontal Astigmatism[a]

c. Vertical Astigmatism[a]

The optimum astigmatism voltages determined for the particular WX-4915 in present use are as follows:

1. Horizontal Deflection dc voltages[b] = +4.8 v. and +7.4 v.
   2.6 v. differential

2. Vertical Deflection dc voltages[b] = +10.5 v. and +12 v.
   1.5 v. differential

3.1.3 Conclusions

A detailed alignment procedure has not been attempted on any other vidicons, since the WX-4915 was required for the color study. Therefore, the solution applied to other vidicons may require the combination of precise electrical alignment plus the proper vidicon design to alleviate these problems.

3.2 DIGITAL SCANNING CONSIDERATIONS RELATED TO MAGNETIC-DEFLECTION SENSORS

The use of digital scanning techniques for an image sensor requires a wider-bandwidth deflection system than is required by analog systems. The analog bandwidth requirement is generally determined by the maximum horizontal retrace time available. Commercial scanning rates which allow 8 microseconds for horizontal retrace need a horizontal deflection bandwidth of approximately 500 kc. This provides 10 risetimes (of 0.8 microsecond) for the retrace. Therefore, the beam will be repositioned with reasonable accuracy by the time the next horizontal line-scan begins.

---

[a]The deflection plate dc voltage normally is set equal to G-4 voltage except for a small differential voltage between the Hor. plates and between the Vert. plates for astigmatism correction.

[b]With reference to G-4 voltage (nominally 250 volts)

Digital scanning techniques require a wider bandwidth since the beam is deflected at the element rate. A reasonably good reproduction of the incremental-scan requires approximately five harmonics of the element rate. For EDITS, with a normal 100 kc element rate, a 500 kc bandwidth is satisfactory. Of course for any system slower than this, 500 kc is better (although the operation will not be noticeably different)

Since the yoke is the limiting factor in deflection bandwidth, EMR discussed yoke characteristics with manufacturers of these components. For an uncompensated yoke the first limiting factor is the self-resonant frequency (f_r) of the yoke inductance and the stray capacity. The resonant frequencies for two high-speed yokes with the following parameters are:

1. 240 microhenry push-pull yoke $f_r = 1.4$ Mc

2. 270 microhenry single-ended yoke $f_r = 2.1$ Mc

For element rates in the region of 400 kc, this straightforward approach of using standard yokes is satisfactory. The self-resonant frequency limit can be extended somewhat beyond the self-resonant frequency by experimentally compensating the yoke and/or the driving waveform.

For higher frequencies where the previous techniques are not applicable, an alternate technique is recommended. This is the addition of a small, very high frequency "tickler" coil. This coil would have few turns since it only has to deflect the beam an incremental distance (compared to a full-line retrace) and consequently it would have a very high self-resonant frequency. The main deflection still would be furnished by conventional deflection coils. This technique has been used for writing characters on conventional CRT displays where the deflection coils are not capable of sufficiently high frequency response.

SECTION 4

HIGH-SPEED ROBERTS SIMULATOR

4.1 INTRODUCTION

A review was made of various possible high-speed digital circuit techniques which could be investigated during this study program. It was concluded that the most meaningful results would be obtained by design and construction of a representative digital coding method which could be applied to commercial analog television signals for demonstration of high operating speeds and for ease of relative assessment of the quality of coded versus uncoded pictures. Also, it was decided that the selected design would employ microcircuit components where availability, cost, and performance considerations permitted.

The Roberts coding method was selected for this purpose. Based on previous study results, 3-bit PCM plus 4 bits Roberts pseudorandom noise were chosen as the desired coding parameters.

4.2 DESIGN APPROACH

A transistorized, portable television set was purchased to provide the standard analog video signals and for the purpose of image display. The Roberts coding simulator design permits rapid switching from the standard analog signal mode to the display of straight 3-bit PCM video or the display of 3-bit PCM video with the 4-bits of Roberts noise.

Figure E. 4-1 is a block diagram of the simulator. System timing is provided by a 10-Mc crystal oscillator. The digital section of the device is implemented by Motorola MECL integrated circuits. It consists of a pseudonoise generator running at the 10-Mc clock rate and certain sections of the quantizing circuits.

The analog signal is added to the pseudonoise signal by a resistance adder (in the initial breadboard model, a Fairchild microcircuit operational amplifier was tried, but it was found to be only conditionally stable at best and produced large amounts of ringing on the video steps). This video signal, with or without noise (switch-selectable), is then applied to seven parallel threshold circuits which quantize the video to eight levels. The circuit diagram for the Schmitt triggers, gates, and storage flip-flops is shown in Figure E. 4-2.

The binary levels out of the Schmitt triggers are adjusted to dc level and signal amplitude to be compatible with Motorola MECL logic. An AND gate is used to generate both the quantized level and its complement which are then shifted into the flip-flop by the clock pulse. This effectively quantizes the signal in time. The signal is quantized in amplitude by the threshold circuits. The

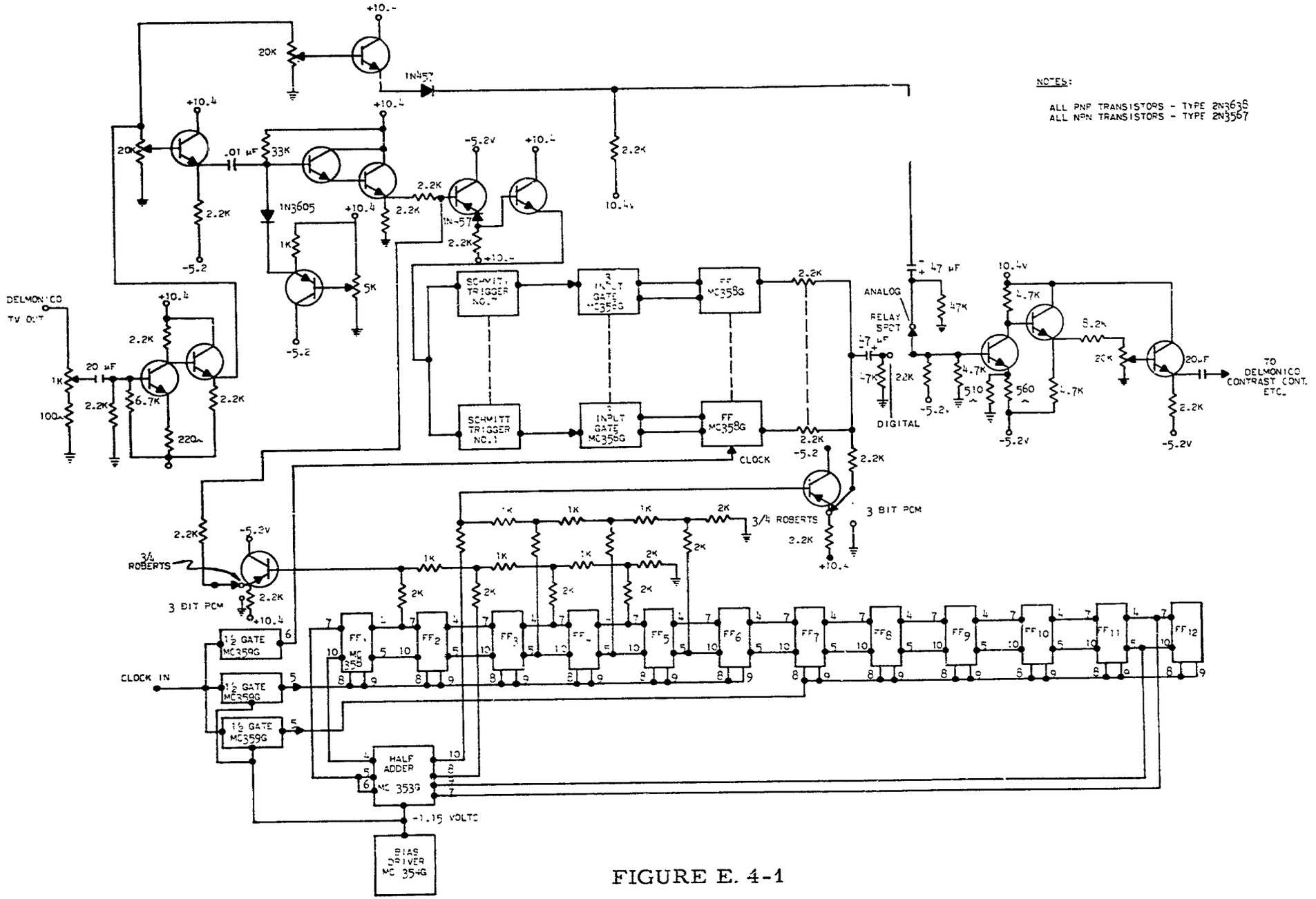

FIGURE E. 4-1

SIMULATOR BLOCK DIAGRAM

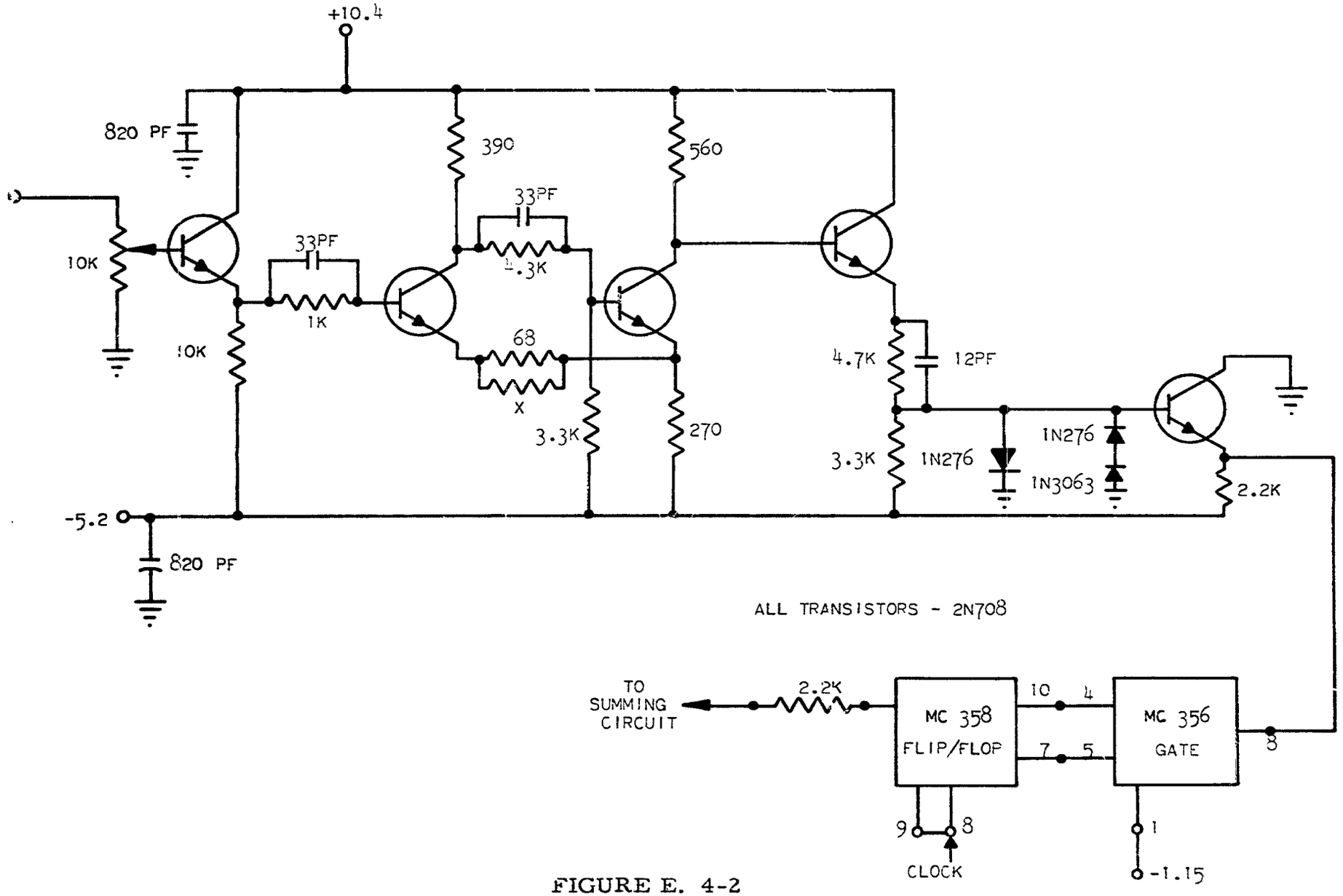

FIGURE E. 4-2

SCHMITT-TRIGGER CIRCUIT DIAGRAM

outputs of the flip-flops are summed by a resistive adder which can also add the complement of the pseudonoise signal previously added. This complemented noise is delayed one element-time (100 ns) because it is generated by the 2nd through the 5th stages of the shift register. The added noise at the input is generated by the 1st through 4th stages. The result is that the same noise that was added at the input is subtracted at the output.

The reconstructed video then is amplified and fed back into the television set for display on the CRT screen. The quantized video (with or without noise) then can be compared with the analog picture by switching between the two. This switching is done by relays to minimize the video path length.

4.3 RESULTS

On low signal-to-noise ratio pictures (less than 20-25 db) it is very difficult to tell which system is being used. At high signal-to-noise ratios the analog signal is definitely more pleasing than the 3/4 Roberts (due primarily to the residual Robert's noise), but it does not contain more information. The 3-bit PCM signal causes some detail to be lost between the quantizing levels but it still retains the coarse features of the image and would be adequate for some applications. In the mid-range of about 30-db signal-to-noise ratio, the analog signal appears approximately as noisy as the 3/4 Roberts. The 3-bit PCM picture is still slightly inferior due to the coarse quantizing effects.

APPENDIX F

LINEAR-APPROXIMATION-CODER DESIGN

APPENDIX F

TABLE OF CONTENTS

SECTION 1

INTRODUCTION

During the early months of this MSC study program, a company-sponsored linear-approximation-coder design effort was pursued in parallel with the direct study tasks. The initial objective of this effort was to develop operating linear-approximation hardware to support (by means of pictorial results) the theoretical work performed on this compression technique.

As the program progressed, it became clear that the physical hardware could not be designed and built with the desired parametric flexibility in time to obtain experimental results for the MSC study. At this point, the decision was made to defer further linear-approximation-coder design effort and to place heavy emphasis on (1) developing and checking out EDITS/ASI-210 digital-computer interface hardware and (2) preparing a flexible linear-approximation computer program.

The above combined efforts (1) and (2) provided the experimental pictorial results needed to complete the linear-approximation coding study for MSC. However, in the interest of completeness, a description of the actual coder design effort accomplished to date is included in the following section.

SECTION 2

HARDWARE DESIGN DESCRIPTION

A logical block diagram of the linear-approx nation encoder is shown in Figure F. 2-1, the timing generator is shown in Figure F. 2-2, and a timing diagram is shown in Figure F. 2-3. Initially all switches (C1 through C16) are closed. The sampling-pulse Sample 1 causes sample-and-hold circuit 1 to sample the video. Since switch C1 is closed, the first junction of the resistive divider is driven to the held value of sample 1. Sample-pulse 2 samples the video and holds this value as element 2. Sample-pulse 2 also opens switch C1. The last good element is held in sample-and-hold 16. Therefore, junction 16 and junction 2 of the resistor ladder are driven to the values held as element 16 and element 2, respectively.

At this point, only switch C1 has been opened. Therefore, if the held value of element 1 is not sufficiently close to the interpolated value of element 1 which is present at junction 1 of the divider, the amplitude of element 1 is transmitted and a code word describing the run-length is generated and transmitted. If the two compared values agree within the allowable tolerance, the encoding process continues. Sample-and-hold pulse 3 samples element 3 and opens switch C2. This generates a new interpolated value for element 1 and an interpolated value for element 2. These are compared with the actual values held in the respective sample-and-hold circuits. The process continues in this manner until one or more (depending upon the criterion employed) interpolated elements are in error. The amplitude of the last good element then is transmitted along with the run-length code.

Either a horizontal blank, a transmit gate, or a length-16 count will reset the timing registers and the process will begin again. A length-16 pulse is generated whenever 16 elements have been coded without an element having been transmitted.

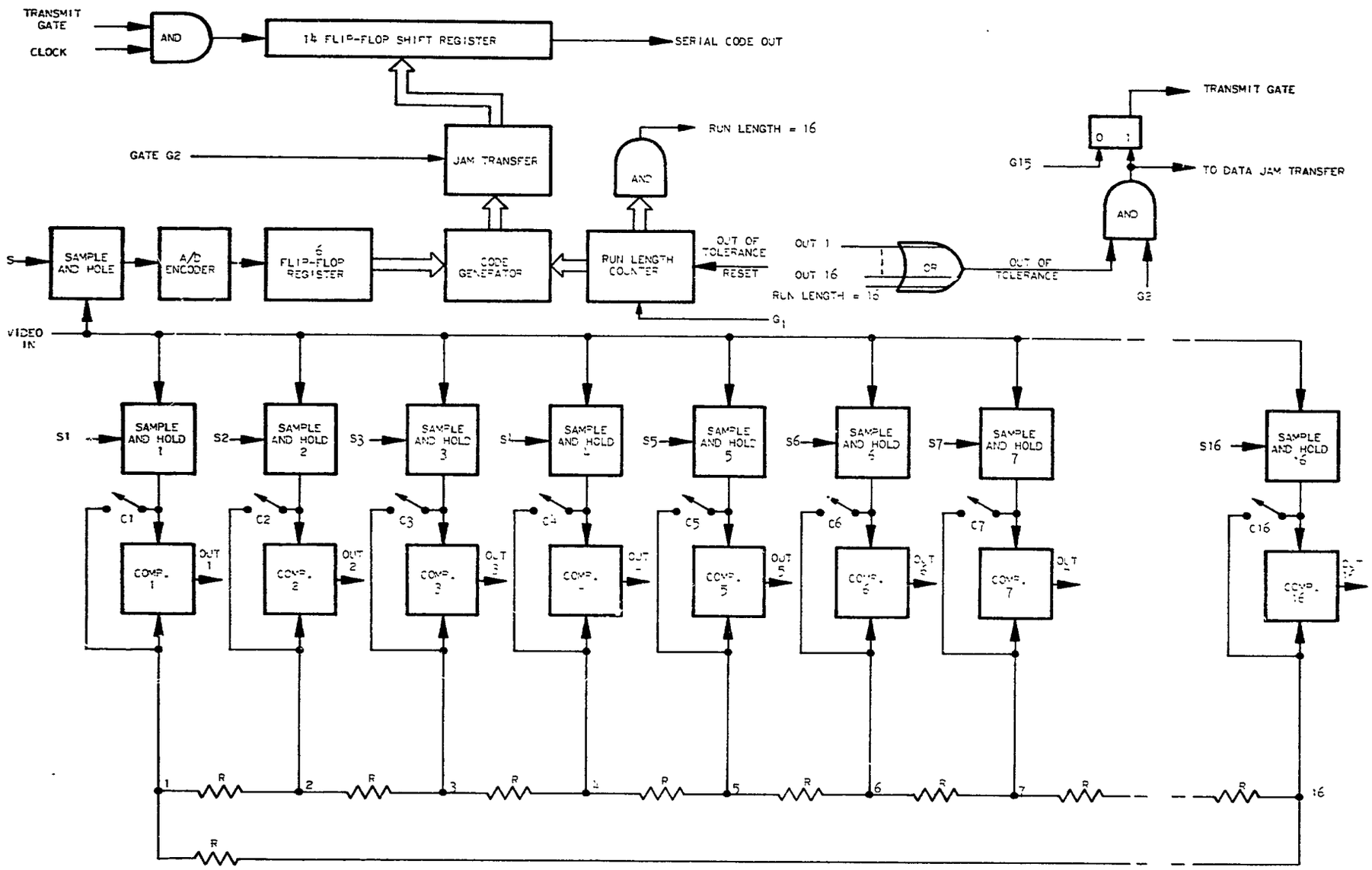

FIGURE F.2-1

LINEAR-APPROXIMATION ENCODER BLOCK DIAGRAM

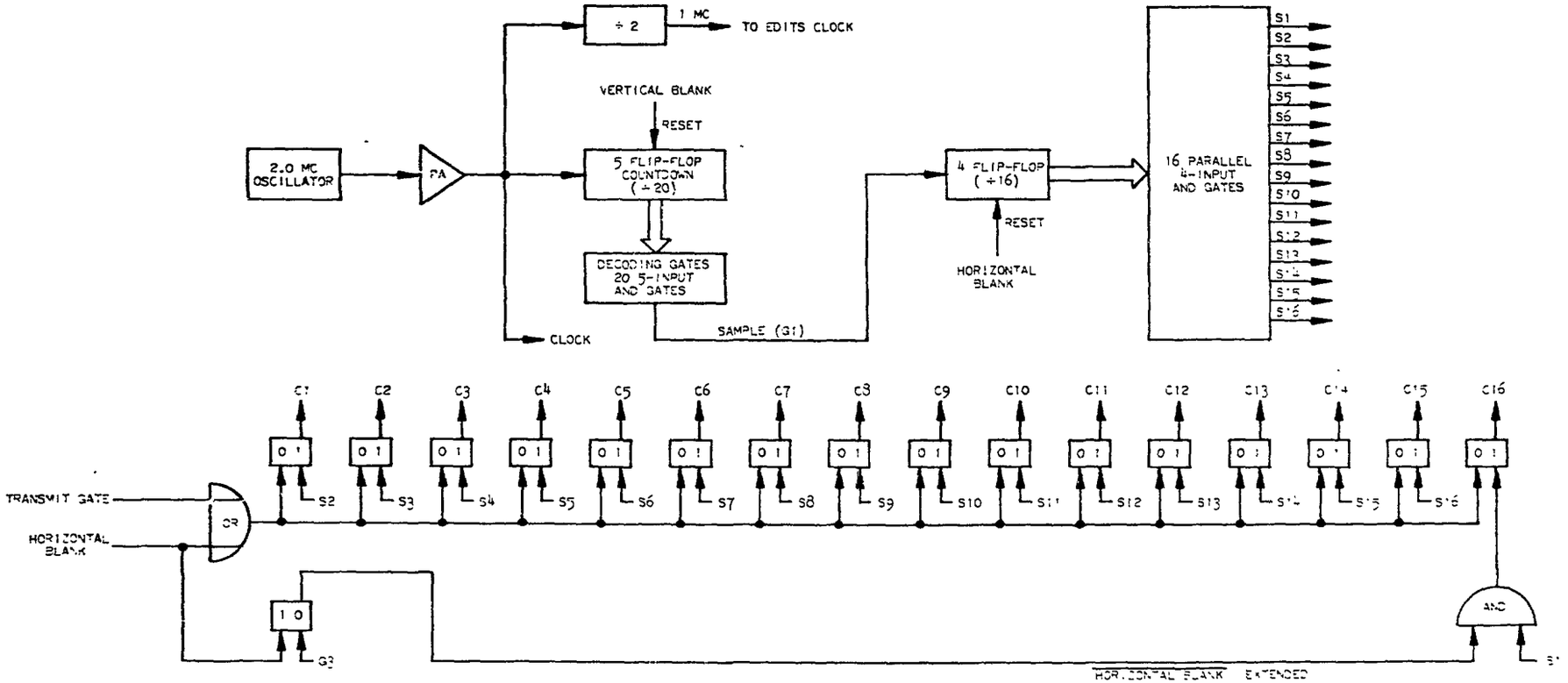

FIGURE F.2-2

LINEAR APPROXIMATION TIMING GENERATOR

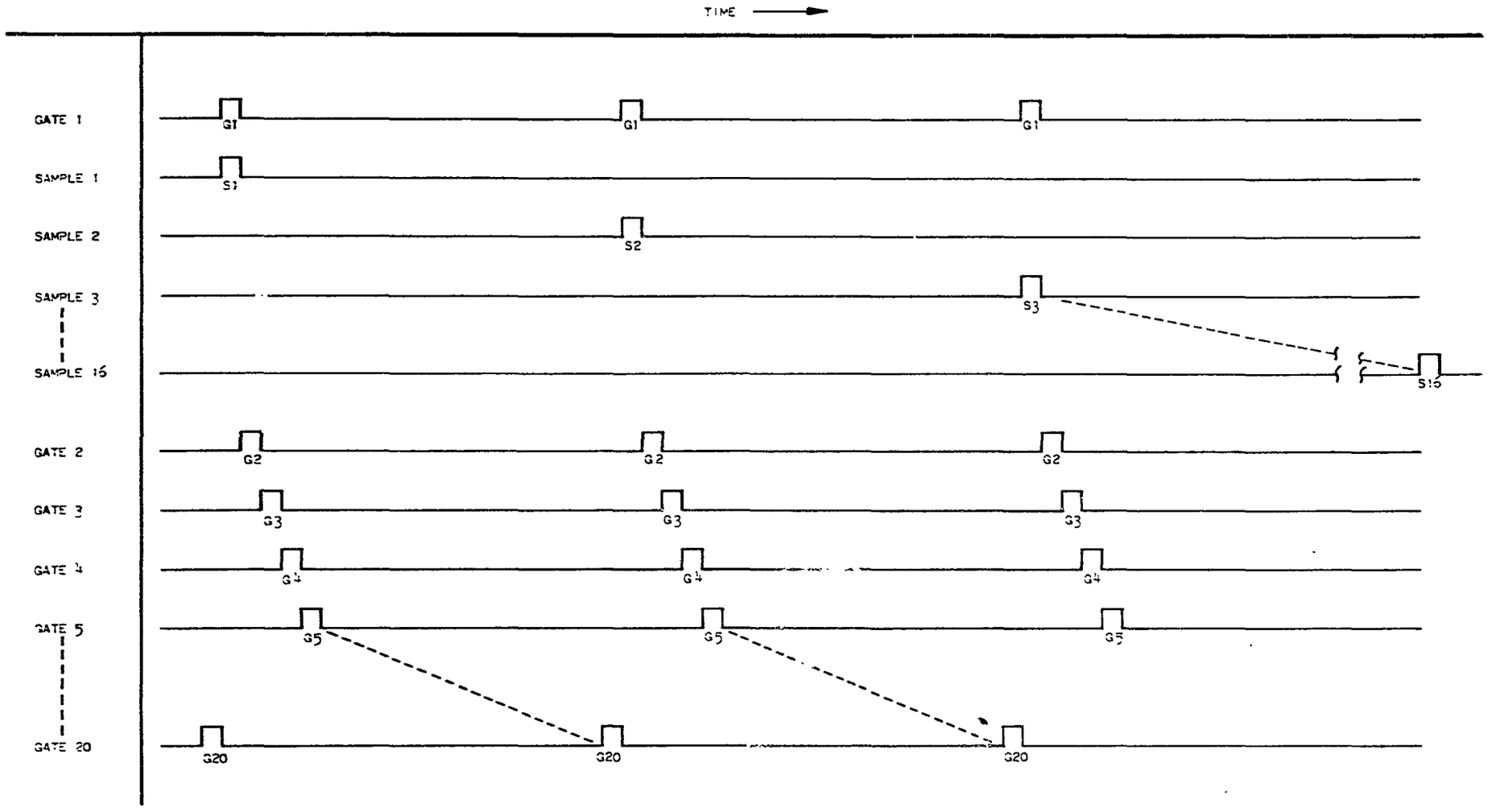

FIGURE F.2-3

LINEAR APPROXIMATION TIMING

The previous end-point amplitude coded to six bits is stored in a register in the code generator. Also the run-length count coded to four bits is fed into the code generator. The code generator combines these two digital words into one 10-bit word and generates a (14-10) Hamming word which is 14 bits in length. This coding technique is described in greater detail in Appendix B, Paragraph 5.4.